UNIVERSITÀ DEGLI STUDI DI MILANO

Dottorato di Ricerca in Scienze della Terra
Ciclo XXX

Soils evolution and treeline fluctuations on the southern side of the Alps under Holocene climate change

Ph.D. Thesis

Anna Masseroli
Matricola R10995

Tutor	**Academic Year**	*Coordinator*
Prof. Luca Trombino	**2016-2017**	**Prof. ssa Elisabetta Erba**

Index

Abstract

The climate in the Alps has been characterized, from the late 19th century until now, by an increase of the mean annual temperatures by about 2°C.

It is known that the climate plays an important role in the ecosystems, particularly in the Alps, where meteorological factors, combined with severe morphological conditions, often show extreme behaviours. The climate is a principal factor governing the natural environment of mountains on short-time scales, and it characterizes the location and the intensity of biological, physical and chemical processes.

Since mountains environments are susceptible to the impacts of a rapidly changing climate, they provide interesting locations for the early detection and the study of the signals of climate change and its impacts on the environmental systems.

Indeed, in mountain landscapes, biological and abiological responses to variations in climatic conditions are particularly noticeable. The main evidences concern the glacier shrinkage, characterized by a general reduction of glaciers, by a widening of proglacial areas followed by colonization of the vegetation, by the upward shift of the vegetation belts and, in particular, of the treeline.

Although altitudinal treelines are widely recognized as climatic boundaries, geomorphological processes and human activities can locally limit the treeline position, conditioning its altitude and dynamics. In fact, in mountain regions, trees establishment and growth at the highest altitudes may be greatly affected by geomorphological processes and/or local human impacts.

The aim of this PhD Project is the characterization of the maximum altitude of the treeline for the central part of the Italian Alps, the spatial and statistical investigations of the role of geomorphological processes and related landforms on the treeline position and, finally, the reconstruction of late Holocene soil evolution and environmental changes at the treeline in some sample areas.

In order to cover the central and the western part of the Italian Alps and also the northern part of Apennines, five different sample areas were selected: two in the Upper Valtellina (Mt. Confinale and proglacial area of Forni glacier), two in Aosta Valley (Becca di Viou and Saint Nicolas) and one in the Northern Apennines (Mt. Cusna).

In order to perform a more complete reconstruction of the environmental changes at the treeline a multidisciplinary approach was used. First, a detailed mapping of the treeline and the determination of the main factors (i. e., geomorphological constraints, climate and human impact) that limit the maximum altitude of the treeline by means of GIS software was performed to reconstruct the treeline position and to choose the sample areas.

Survey and sampling of soils was carried out in the sample areas, with the purpose of outlining the general characteristics of the soils and of searching for paleosols and other potential proxy archives. The analysis of the identified soil profiles took advantage of multiple laboratory and microscope techniques to provide both maximum accuracy of data and a wider overview of the aspects involved, with also new methods of analysis like the Rock-Eval pyrolysis and the stable carbon and nitrogen isotopes composition.

In addition, a detailed reconstruction of the treeline altitudinal dynamics using a dendrochronological approach and an analysis of climate-growth response using a dendroclimatic approach were performed. Whereas, in the sample areas with high geomorphological influence, the soil erosion rates was investigated using a dendrogeomorphological approach, sampling trees and related exposed roots.

From this multidisciplinary approach, the following results are emerged.

The treeline elevation in the Upper Valtellina region is primarily limited (82% of trees) by geomorphological constraints (treeline mean elevation 2355 m a.s.l.), whereas 15% of the analyzed trees belong to climatic treeline (treeline mean elevation 2530 m a.s.l.) and human impact influences only 3% of the analyzed trees (treeline mean elevation 2335 m a.s.l.).

The results also indicate that the current position of treelines is not only lowered by geomorphological constraints in general but, more specifically, can also be differently affected by different groups or types of geomorphological processes. In this study area, gravitational processes affect 87% of the treeline trees, running and/or channelized water affects 8% of trees, and ice affects only 5% of trees. Gravitational processes represent the most destructive processes of the treeline ecotone and tend to reduce the ecotone width, leading to coinciding treeline and timberline. Furthermore, the landforms related to gravitational processes can create considerable obstacles to the treeline upward shift, especially when they merge (e.g., merging talus cones).

As far as the site scale is concerned, in Mt. Confinale study area, the reconstruction of the altitudinal dynamics shows that the treeline elevation over time increased from 2505 m a.s.l. (period 1990–1999) to 2531 m a.s.l. (period 2000–2009) and, finally, to 2545 m a.s.l. (in 2013) with a rates of ongoing treeline upward shift for the period 2000–2009, of up to 2.6 m/y. On the Mt. Confinale study site the presence of geomorphological factors may combine with climatic ones to promote an upward shift in the treeline and also may influence the soil evolution, especially if active geomorphological processes are less intense. The soils, although showing a good degree of development, do not reach the characteristics of a typical forest soil. The presence of not particulary developed soil in the treeline ecotone suggests that the colonization of the *Pinus cembra,* favored by ecologic, microtopographic and microclimatic factors, is followed by the pedogenesis. The latter, in turn, may favor a more active colonization that could lead to a more marked shift to higher altitude of the vegetation belt.

In the proglacial area of the Forni glacier, the soil development fit quite well with the chronosequence approach, although not all pedological parameters seem to follow the age-related trend. In fact, even if these soils have a young age, in only 150 years of pedogenesis some transformations could be noticed. For example in the superficial horizons the organic carbon and total nitrogen content increased as well as the values of crystalline iron oxides, while the content of the amorphous iron oxides decreased according to the deglaciation time.

For what concerns the Becca di Viou study sites, the literature attests an upward shift of the treeline in the last century; the obtained pedological and the dendroclimatic data seem to stress a changing in treeline ecotone position, following by a possible shift of the timberline and also by a shift of the soil type. The pedological results also highlight that forest, in the past, could reach higher altitude than today.

In Saint Nicolas study area the soil analyses results underline the occurrence of colluvial events that influence the vegetation colonization and soil development. Moreover, the results show the great influence of water driven processes on the environmental evolution and also on soil erosion rates, the latter determined by means of trees roots exposure (local average erosion rates: 1.16 cm/year).

Instead, at Mt. Cusna study site, the soil analyses underline the presence of different pedogenetic phases: a first, strongly evident, phase leading to the formation of a brown soil under forest vegetation cover, which was interrupted by a colluvial event; a second phase characterized by the presence of a stable forest cover, which favored the formation of a brown soil, also interrupted by a colluvial events; the present day pedogenetic phase, associated to a vegetation change, in particular at higher altitude the presence of shrub as *Vaccinium myrtillus,* promoting the cryptopodzolization processes.

In conclusion, the multidisciplinary study of all examined sites enlightens the following common traits: the geomorphological processes and related landforms are the most important factor influencing the treeline position; in the areas with a climatic constraint (Mt. Confinale, Progracial area of the Forni glacier and Becca di Viou) an upward shift of vegetation belt and of the soil type has been observed; in the areas with geomorphological constraints (Saint Nicolas and Mt. Cusna) the vegetation and soil responses to climate change are masked by the effects of geomorphological processes, but a different response could be noted between Alpine and Apennine study case due to the slope dynamics and the climatic features.

Chapter 1

Introduction

Although the entire Holocene is characterized by climate variability with periods of significant rapid climate change, the current temperature variations are of maximum interest for the worldwide scientific community due to the rapidity of the change.

Not all the environments respond to climate change in the same way, in fact some studies underline (Theurillat et al., 1998; Halpin, 1994) that the trends may be more or less marked at local or global scale, in particular, the arid regions and the high-latitude and high-altitude areas are among the most sensitive to climate change.

In high altitude landscapes, biological and abiological responses to climate change are particularly evident (Evans & Clague, 1994). The glaciers shrinkage is characterized by a general reduction in glacier surface area (Frezzotti & Orombelli, 2014), and the retreat of the glacier tongues is followed by a progressive increase in supraglacial debris due to an increasing slope processes (e.g., Haeberli et al., 1997) and to an accelerated melting rate (Dyurgerov & Meier, 2000), by a widening of glacier forelands (Egli et al., 2006) and by new ecesis (Gravaglia et al., 2010). Moreover, debris covered glaciers represent a new habitat for animals and vegetation: when they are located below the treeline, their surface velocity is very low and the debris thickness is sufficient for trees to germinate and to grow (Pelfini et al., 2012; Burga, 1999). At the same time, valley slopes may experience an upward shift of the vegetation belts and, particularly, of the treeline.

The treeline ecotone, defined as the transition zone in mountain vegetation between the closed forest (timberline) and the alpine grasslands (Körner, 1999), is one of the most distinctive features of the mountain environments and it is widely considered a climatic boundary. By convention, treelines include trees taller than 2–3 m in height whose crowns are constantly exposed to atmospheric conditions during winter (Körner, 2003, 2012; Tinner & Theurillat, 2003).

Treeline fluctuations may be considered for the assessment of past and ongoing climatic and environmental changes. The altitudinal fluctuations of treelines caused by climate conditions are well documented by the retrieval of subfossil logs above current treeline elevations (e.g., Burga, 1991; Nicolussi et al., 2005; Pelfini et al., 2014; Porter & Orombelli, 1985; Schwörer et al., 2014). For example, many treelines lowered in elevation during the LIA after having stood at higher elevations during the Middle Ages (Helama et al., 2010; Kullman, 2001; Scapozza et al., 2010; Wick & Tinner, 1997). Treelines are sensitive to the rising temperatures, and upward shifts have been noted by several studies carried out in the European Alps (Gehrig-Fasel et al., 2007; Leonelli et al., 2011a; Vittoz et al., 2008),

in Scandinavia (Kullman, 2002; Kullman & Öberg, 2009), in North America (Beckage et al., 2008; Luckman & Kavanagh, 2000), and in the Central Greater Caucasus (Akhalkatsi et al., 2006; Hughes et al., 2009; Nakhutsrishvili, 2003). In other cases, the treeline response to changing climate has been characterized by an increase in forest density (Klasner, 2002; Mazepa, 2005; Shiyatov et al., 2005).

The ecological dynamics of the alpine treeline ecotone is mainly influenced by climate. In detail, several climatic parameters influence the maximum altitude of the treeline such as wind, duration of snow cover, frequency and intensity of precipitation, temperature (Holtmeier & Broll, 2005). Among these parameters, the temperature is the most important because it imposes a physiological limit to trees growth. Not only the air temperature but also the soil temperature is an important climatic parameter (Körner & Paulsen, 2004).

Although altitudinal treelines are widely recognized as climatic boundaries, climatic parameters are not the only factor that influence the treeline position (Malanson et al., 2007). In fact, the treeline altitude may be locally influenced by environmental factors, disturbances, and human activities (Zald et al., 2012; Holtmeier & Broll, 2007; Motta & Garbarino, 2003; Chauchard et al., 2007; Leonelli et al., 2009a). Especially in the European Alps, it is important to take into consideration the human impacts related to historic and also prehistoric practices of land and forest use (e.g., Barker, 1985; Milisauskas, 2002) that, modifying the natural distribution of trees, have caused a significant altitudinal depression of the treeline. On the contrary, in more recent times, the treeline position has also been influenced by the constant decline of pastoralism and the relevant human activities due to the land abandonment from the Industrial Revolution, making difficult to disentangle climate influence and human impacts (Motta & Nola 2001; Gehrig-Fasel et al. 2007; Chauchard et al. 2010).

At high altitude, geomorphic processes play a key role in conditioning treeline position (Holtmeier & Broll, 2012; Walsh et al., 1994). Tree germination and growth are affected by local topography (e.g., slope features, slope steepness, and bare rock walls) and by active surface processes shaping and reworking landforms, especially those due to gravitational processes, such as debris cones, talus, debris flow fans, avalanche fans. (Holtmeier & Broll, 2005). Moreover, water-driven erosional processes, such as rain wash, action of running water, etc., that form gullies and eroded surfaces as well as spectacular landforms such as calanchi and earth pyramids (Bollati et al., 2012; 2016) can play an ecological supportive role by conditioning the other components of the ecosystem (e.g., vegetation) via effects on tree growth and vegetation dynamics. Mass wasting is one of the most common, widespread, and complex processes acting in the Alpine environment (Haeberli et al., 1997). Seasonal debris falls, debris flows, landslides, and other events can, in conjunction with the effects of avalanches, generate a diffuse disturbance in the treeline dynamics. Indeed, treeline can be lowered in elevation well below the climate-controlled alpine treeline altitude (Butler et al., 2009; Leonelli et al., 2009a).

Nevertheless, at a local scale, geomorphological depositional processes and landforms can create favorable site conditions where tree seedlings may establish and survive (Butler et al., 2007; Virtanen et al, 2010; Resler, 2006).

The importance of site conditions and the interaction between biotic and abiotic factors in controlling tree establishment and recent treeline shifts have been often underlined (Stueve et al., 2011). Among abiotic factors, topography strongly modulates the climatic conditions, especially in high mountains where great differences in elevation, slope and aspect may occur at relatively low distances, and it is directly influencing both vegetation structures and geomorphological processes and features (Holtmeier, 2010). Elevation determines gradients of climatic conditions (e.g., of temperatures and of precipitation regimes) at the different altitudes. Slope and aspect are widely considered crucial in modulating site conditions for vegetation; however they are also very important in determining the geomorphological processes and in modulating their velocity (Derbyshire et al.,1979): e.g., soil formation and erosion, runoff, soil moisture, mass wasting and gravity processes in general are strongly influenced by slope; snow-cover persistence, soil temperature regimes, permafrost and rock weathering processes, are greatly influenced by aspect.

The substrate and hence the development of the soil can be decisive in the dynamics of colonization of new areas by trees, especially in the mountain areas, where the soil conditions change drastically with altitude. In fact, also small-scale factors such as grain size, moisture of the substrate seem to be crucial for the development of both vegetation and soil (Burga et al., 2010).

The interaction between soil and vegetation plays a key role in controlling soil development, especially in fast changing environments, like the mountain ones. In fact, vegetation can modulate the velocity and the intensity of soil development or erosion, but on the other hand, soil degradation processes may affect the normal development of shrubs and trees (Ballesteros-Cánovas et al., 2013). Consequently, a decrease in vegetation coverage causes a slowdown in soil formation and promotes further erosion (Thornes, 1985). The interplay between vegetation and water runoff becomes particularly meaningful where erosion rates are significant like in badlands area.

The soil could also be important for his function as archives, in fact like the other paleoenvironmental archives contains accurate information over large time intervals on Quaternary variations.

The soils are a valuable reservoir of information, since they are strongly influenced by the processes tuning the environmental balance and they can also record their effects in the form of permanent features, recognizable and quantifiable using appropriate analytical methods (Cremaschi and Rodolfi 1991; Trombino, 1998). Several studies show how the Holocene treeline fluctuations are also outlined by the soil data (Carnelli et al., 2004; Compostella et al., 2013).

Therefore, the treeline position is determined not only by climate conditions but also by the interaction among environmental conditions, geomorphological processes, soil development and evolution, and human impact.

For this reason, for the widespread presence of the treeline ecotone throughout the entire Alpine chain and at the highest altitudes of the Apennine, for treeline globally recognized role as climatic indicator, and its particular sensitivity to climate changes, the treeline ecotone has been chosen as the object of this research.

The aim of this PhD Project is the characterization of the maximum altitude of the treeline for the central part of the Italian Alps, spatially and statistically investigation of the role of geomorphological processes and related landforms on the treeline position and the reconstruction of late Holocene soil evolution and environmental changes at the treeline in some sample areas.

For the purpose of cover the central and the western part of the Italian Alps and also the northern part of Apennines, five different sample areas were chosen: two in Upper Valtellina (Mt. Confinale and proglacial area of Forni glacier), two in Aosta Valley (Becca di Viou and Saint Nicolas) and one in the Northern Apennines (Mt. Cusna).

For each sub-regional study area (Upper Valtellina, Aosta Valley and Northern Apennines), a chapter, containing an introduction, the overview of the study area, the results and the discussions, will be written; while the methods will be presented in the chapter 2 to avoid repetitions.

Chapter 2

Materials and methods

In order to do a more complete reconstruction of the environmental changes at the treeline a multidisciplinary approach was used. First, a detailed mapping of the treeline and the determination of the main factors (geomorphological constraints, climate and human impact) that limit the maximum altitude of the treeline by means of GIS software was performed to reconstruct the treeline position and choose the sample areas.

Survey and sampling of soils were carried out in the sample areas, with the purpose of outlining the general characteristics of the soils and searching for paleosols and other potential proxy archives. The analysis of the identified soil profiles took advantage of multiple laboratory and microscope techniques to provide both maximum accuracy of the data and a wider overview of the aspects involved, with also new methods of analysis like the Rock-Eval pyrolysis and the stable isotopes composition (carried out in collaboration with the University of Lausanne; Prof. Verrecchia and Dr. Sebag).

In addition, a detailed reconstruction of the treeline altitudinal dynamics using a dendrochronological approach and an analysis of climate-growth response using a dendroclimatic approach were performed (in collaboration with "Laboratorio di dendroclimatologia" at Department of Earth and Environmental Sciences of University of Milano-Bicocca; Dr. Leonelli). In the sample areas with high geomorphological influence, using a dendrogeomorphological approach, also the soil erosion rates was investigated, sampling trees and related exposed roots (in collaboration with "Laboratorio di Dendrogeomorfologia" at Earth Science Department of University of Milan; Prof. Pelfini and Dr. Bollati).

The soil analyses were done at the "Laboratorio di Sedimenti e Suoli" (Prof. Cremaschi, Dr. Compostella) and at the "Laboratorio di spettrofotometria di emissione al plasma"(Dr. Ferrari) of Earth Science Department of University of Milan except for the analysis of total nitrogen, which was executed at the "Laboratorio di Chimica del Suolo" of Agricultural and Environmental Sciences Departments - Production, Landscape, Agroenergy of University of Milan (Prof. Tambone and Dr. Bedussi). Moreover, the analyses of particle size distribution, pH and organic C content of the Mt. Confinale soil samples were done at "Laboratorio di pedologia" of Department of Earth and Environmental Sciences of University of Milano-Bicocca (Dr. Comolli).

While, the undisturbed samples were sent to an external laboratory (Servizi per la geologia, Piombino) for thin sections preparation.

2.1 Gis based approach: Upper Valtellina study area

2.1.1 Preliminary treeline position reconstruction with a Gis-based approach

At the sub-regional scale, the treeline elevation was estimated with a GIS-based approach for the whole administrative area of the Comunità Montana Alta Valtellina, corresponding to the upper Adda River catchment: 896 km^2 of total area. The orthophotos were used to locate the trees belonging to the treeline ecotone and growing at the highest elevations in the valleys. The analysis was performed with Quantum GIS software, and the orthophotos used were available from the National Geoportal (http://www.pcn.minambiente.it/GN/, WMS service) for the years 2006 and 2007. Treeline trees were mapped at an average of approximately every 200 m in each of the valleys, in order to have sufficient sampling intensity to understand even small environmental changes at the treeline. For approximately five trees per km, and by means of photointerpretation, the main environmental factors that could control an upward shift in the treeline was determined, distinguishing between geomorphological constraints, climate, and human impacts (Leonelli et al., 2016). Treelines controlled by geomorphological constraints are found where trees grow in areas subject to active geomorphological processes (such as gravitational processes related to slope instability, permafrost degradation, or avalanches), in areas characterized by various landforms (such as debris flow fans, talus cones, rock glaciers, and moraines), or where poor edaphic conditions are dominant (such as rock outcrops, screes, rock faces, rocky substrates, and bogs). Climate had the strongest influence on the highest treelines in the area (Körner & Paulsen, 2004), where trees in the upper forest belt grew on a regular slopes characterized by alpine grasslands with no evidence of active geomorphological processes or pasture disturbances (for example, cattle trails or the presence of barns). Human impacts were identified as an influence in all areas where anthropogenic artefacts existed (such as barns, ski runs and resorts) and where deforestation carried out for pastures was evident.

2.1.2 Gis-data statistical elaboration

To assess the association between the considered three main environmental factors (geomorphology, climate, and human impact) and the topographic variables, we derived elevation, slope, and aspect values for each tree from a 20-m DTM of Regione Lombardia (2014). The frequency distribution of the three topographic variables for treeline sites in the entire study area and for the sites under the three main environmental factors considered was calculated. Finally, chi-square ($\chi 2$) tests were performed to evaluate the relative importance of the three topographic variables and to assess the strength of their associations with the three main environmental factors influencing the treeline trees in the region, over the range of the considered classes. To compare the results obtained from chi-square tests, the three

topographic variables that were presenting different ranges were transformed into analogous ordinal data of 10 interval classes (tab. 2.1; Leonelli et al., 2016).

Class	Elevation interval (m a.s.l.)	Slope interval (°)	Aspect interval (° from North)	
1	1730 - 2150	0 - 10	342 - 18	N
2	2150 - 2200	10 - 15	18 - 54	NNE
3	2200 - 2250	15 - 20	54 - 90	NE-E
4	2250 - 2300	20 - 25	90 - 126	E-SE
5	2300 - 2350	25 - 30	126 - 162	SSE
6	2350 - 2400	30 - 35	162 - 198	S
7	2400 - 2450	35 - 40	198 - 234	SSW
8	2450 - 2500	40 - 45	234 - 270	SW-W
9	2500 - 2550	45 - 50	270 - 306	W-NW
10	2550 - 2640	50 - 90	306 - 342	NNW

Table 2.1. Class numbers and corresponding class intervals into which the three topographic variables were subdivided (from Leonelli et al., 2016).

2.1.3 Investigation about the role of geomorphological factors on the treeline position with a Gis-based approach

Being the treeline position and elevation had been already estimated on ortophotos (WMS service), by means of the Quantum GIS Software, in this portion of the study, only trees belonging to the "treelines with geomorphological constraints" were taken into account and analyzed. For each tree of this geomorphologically constrained group, the geomorphological process that prevents the treeline upward shift was detected using the combination of three different approaches (Masseroli et al., 2016): i) indirect observation of the environmental conditions of the areas where each tree grows, using ortophotos for the years 2006 and 2007 (http://www.pcn.minambiente.it/GN/, WMS service); ii) analysis of the thematic maps available on the Lombardy regional geoportal (http://www.geoportale.regione.lombardia.it/; tab. 2.2); iii) comparison with the previous geomorphological maps published and related to the Upper Valtellina (Pozzi et al., 1990; Bellotti et al., 1995). In order to disentangle the different effects of the various geomorphological processes on the treeline altitude and on the ecotone width, landforms interacting with the treeline upward shift and located at the treeline boundary were grouped according to their predominant genetic process. More in detail they were grouped into three classes: landforms mainly due to running and/or channelized waters (e.g., due to sheet erosion, rill and gully erosion), landforms mainly due to gravity processes (e.g., due to mass movements, rock falls, landslides, debris flows) and landforms mainly due to snow and ice actions (e.g., due to glacial and periglacial processes, avalanches; tab. 2.3) (Masseroli et al., 2016). The selected landforms due to running and/or channelized

waters include respectively erosional forms like rills and gullies and deposits as alluvial fans and/or mixed alluvial cones; these type of landforms were analyzed separately (tab. 2.3). In the study area, avalanches are very common phenomena: the two layers of the Lombardy Region (Avalanche sites by photo-interpretation and by survey; tab. 2.2) cover about the entire treeline ecotone. Given the widespread presence of this process, affecting almost the whole investigated area, avalanches were considered as a background noise. However, where avalanches impact is coupled with running waters action (i.e., rain wash erosion), the affected trees were grouped with trees constrained by gully erosion. Depositional landforms due to gravity processes were grouped into a unique category which includes scree slopes, rock screes, talus, debris cones, etc. In this group debris flow fans are also included for two reasons: i) gravity is the driving force of the process, ii) in most cases debris flows rework scree slope, debris cones etc. Moreover, the gravity landforms were classified as isolated landforms or merging landforms. This subdivision was done to better understand the role of gravity processes on the treeline position and the different impact that a merging landforms have on the treeline position. Finally, among the glacial and periglacial landforms only the rock glaciers were taken into account, because of the scale of observation. The glacial deposits have not been taken into account as distributed throughout the whole area and reworked over time by other geomorphological processes. In order to calculate the width of the treeline ecotone, the timberline position and elevation were estimated by mapping trees belonging to the timberline (timberline trees) with a spatial interval of 200 m. Where the timberline was discontinuous or interrupted, the elevation of the nearest timberline was considered. The elevation value of each mapped tree of timberline and treeline was extracted in the GIS from a 20-m DTM of Lombardy Region (Regione Lombardia, 2014; tab. 2.2). To evaluate if the effects of different landforms may cause differences in the frequency distribution of treeline trees (trees at the treeline) elevation, chi square tests were performed. The elevation variable was transformed into ordinal data of 10 interval classes (tab. 2.1). The tests were carried out both taking into account all the landforms and comparing only categories of landforms.

Shapefile name	Group of layers	Year	URL
Rock scree (Accumuli di frana)	Geoambientale	01/01/1987	http://www.cartografia.regione.lombardia.it/rlregisdownload/
Highly unstable areas (Aree ad elevata instabilità)	Geoambientale	01/01/1987	http://www.cartografia.regione.lombardia.it/rlregisdownload/
Areas exposed to channeled water erosion (Aree con erosione delle acque incanalate)	Geoambientale	01/01/1987	http://www.cartografia.regione.lombardia.it/rlregisdownload/
Areas exposed to water runoff and surface erosion (Aree di dilavamento e di erosione superficiale)	Geoambientale	01/01/1987	http://www.cartografia.regione.lombardia.it/rlregisdownload/
Geomorphic areas (Aree geomorfiche)	Geoambientale	01/01/1987	http://www.cartografia.regione.lombardia.it/rlregisdownload/
Potentially unstable areas (Aree potenzialmente instabili)	Geoambientale	01/01/1987	http://www.cartografia.regione.lombardia.it/rlregisdownload/
Alluvial fan (Conoidi di deiezione)	Geoambientale	01/01/1987	http://www.cartografia.regione.lombardia.it/rlregisdownload/
Scree slope and/or talus cone (Depositi detritici orientati)	Geoambientale	01/01/1987	http://www.cartografia.regione.lombardia.it/rlregisdownload/
Surface deposits (Depositi superficiali)	Geoambientale	01/01/1987	http://www.cartografia.regione.lombardia.it/rlregisdownload/
Punctual geomorphological features (Elementi geomorfologici puntuali)	Geoambientale	01/01/1987	http://www.cartografia.regione.lombardia.it/rlregisdownload/
Punctual elements of gravity and water runoff (Elementi puntiformi di gravità e dilavamento)	Geoambientale	01/01/1987	http://www.cartografia.regione.lombardia.it/rlregisdownload/
Fluvio-glacial erosion /melt water channel (Erosione incanalata scaricatore fluvioglaciale)	Geoambientale	01/01/1987	http://www.cartografia.regione.lombardia.it/rlregisdownload/
Glaciers and snowfields (Ghiacciai e nevai)	Geoambientale	01/01/1987	http://www.cartografia.regione.lombardia.it/rlregisdownload/
Landslide niches (Nicchie di frana)	Geoambientale	01/01/1987	http://www.cartografia.regione.lombardia.it/rlregisdownload/
Protalus rampart and Rocky crest-line (Nivomorena e cresta)	Geoambientale	01/01/1987	http://www.cartografia.regione.lombardia.it/rlregisdownload/
Rock glacier (Rock glacier)	Geoambientale	01/01/1987	http://www.cartografia.regione.lombardia.it/rlregisdownload/
Landslide areas (Aree franose)	GeoIFFI	05/02/2004	http://www.cartografia.regione.lombardia.it/rlregisdownload/
Areas subjected to rock fall, landslides, collapses (Aree soggette a crolli, franosità, sprofondamenti)	GeoIFFI	05/02/2004	http://www.cartografia.regione.lombardia.it/rlregisdownload/
Alluvial fans (Conoidi)	GeoIFFI	05/02/2004	http://www.cartografia.regione.lombardia.it/rlregisdownload/
Deep-seated gravitational slope deformation (Deformazioni gravitative profonde di versante)	GeoIFFI	05/02/2004	http://www.cartografia.regione.lombardia.it/rlregisdownload/
Linear landslides (Frane lineari)	GeoIFFI	05/02/2004	http://www.cartografia.regione.lombardia.it/rlregisdownload/
Avalanche sites by photo-interpretation (Siti valanghivi da fotointerpretazione)	Sistema Informativo Regionale Valanghe	13/05/2011	http://www.cartografia.regione.lombardia.it/rlregisdownload/
Avalanche sites by survey (Siti valanghivi da rilevamento)	Sistema Informativo	13/05/2011	http://www.cartografia.regione.lombardia.it/rlregisdownload/

	Regionale Valanghe		
Mountain community 2012 (Comunità montane 2012)	Limiti amministrativi 2012 agg.DBT/PGT	05/10/2012	http://www.cartografia.regione.lombardia.it/rlregisdownload/
Glaciers 2013 (Ghiacciai 2013)	Ghiacciai della Lombardia	16/07/2013	http://www.cartografia.regione.lombardia.it/rlregisdownload/
Isoipse (Curva di livello 10000 CT10)	Carta Tecnica Regionale 10000 vettoriale CT10	01/07/2006	http://www.cartografia.regione.lombardia.it/rlregisdownload/
Hydrographic network (Rete idrografica 10000 CT10)	Carta Tecnica Regionale 10000 vettoriale CT10	01/07/2006	http://www.cartografia.regione.lombardia.it/rlregisdownload/
DTM (Digital terrain model)	DTM	14/01/2014	http://www.geoportale.regione.lombardia.it/
2006 Color Ortophotos (Ortofoto a colori anno 2006 con relative date del volo)	WMS service	2007	http://www.pcn.minambiente.it/GN/ to_colore_06.map)

Table 2.2. Layers used for the characterization of geomorphologically constrained treelines and for the association of each geomorphologically constrained treeline tree with the process limiting its position. For each layer, the original shapefile name, the group where the layer is located in the regional geoportal, the year of the last update and the URL are specified (from Masseroli et al., 2016).

Type of landform	**Agents**	**Landforms**	**Classes**	**Classes of landforms used for the analysis**
Erosional	Gravity/Water/Snow	Avalanches channels, tracks	Landforms due to a combination of avalanches processes and running and/or channelized water	Gullies
Erosional	Water	Gullies	Landforms due to running and/or channelized water	Gullies
Erosional	Water	Rills		Rills
Depositional	Water	Alluvial fans		Alluvial fans
Depositional	Gravity/Water	Debris flow fans	Landforms due to gravity (mass movements)	Gravity deposits (isolated or merging)
Depositional	Gravity	Scree slopes, talus slopes, debris cones		
Depositional	Gravity	Deep-seated gravitational slope deformation		
Depositional	Gravity	Rock screes		
Depositional	Interstitial Ice	Rock glaciers	Cryogenic landforms	Rock glaciers

Table 2.3. Classification adopted for the different processes and related landforms limiting the position of treeline trees (from Masseroli et al., 2016).

2.2 Geopedological methods

2.2.1 Soil field description

The soils studied were all thoroughly described at the time of the opening of the profiles. The full section of the soil was observed, from field surface down to, where possible, the parent material at the base of the profile (Sanesi, 1977; Persicani, 1989; Cremaschi & Rodolfi, 1991; McRae, 1991; Sanesi, 2000). In none of the studied sites it was necessary to go beyond a depth of 2 m, thus remaining within the limits set by Soil Taxonomy (Soil Survey Staff, 2014).

Field description:

For each station were reported:

- location and elevation (acquisition of coordinates using GPS)
- slope and aspect of the relief
- substrate nature (lithology of the parent material by literature or direct observation)
- land use and vegetation
- surface features (outcroppings and coarse surface fragments, erosion, morphological environment, section type, etc.)

For each profile were reported:

- soil depth
- soil type (simple or compound)
- a listing of every soil horizons

A name was assigned to each horizon (provisional, subsequently modifiable according to the results of laboratory analyses and microscope observations) and were recorded:

- thickness and boundary depth (with distinctness and topography)
- moisture
- colour (according to Munsell Soil Color Charts: Munsell® Color, 1994)
- textural class of the fine earth fraction
- size, shape, frequency, and lithology of the coarse fraction
- size, shape and resistance of aggregates
- size and frequency of pores and roots
- possible presence of pedofeatures (clay coatings, nodules, mottles, etc.)

2.2.2. Soil sampling

Soil sampling was conducted with different methodologies, depending on whether or not they were samples for laboratory analyses, or undisturbed samples for the preparation of thin sections. In the first case, it was collected a homogeneous and representative sample for each horizon identified in the field, variable in weight between 0.5 and 1 kg. Sampling was always performed from the bottom to the top of the profile in order to avoid polluting the underlying horizons still to be sampled (Cremaschi & Rodolfi, 1991; Giordano, 1999). With regard to sampling for micro-morphological analysis, the use of Kubiena boxes allowed to take samples of undisturbed soil. Kubiena boxes are appropriate metal containers with removable lid and bottom which allow to extract and transport undisturbed soil samples; they are inserted in the profile and once extracted retain inside them a prism of undisturbed soil. On each Kubiena box was reported the original orientation of the sample, information needed in order to properly interpret the information derived from the observation of the corresponding thin section (Kubiena, 1953; Stoops, 2003).

2.2.3 Laboratory pre-treatments

All samples taken in the field have undergone a series of pretreatments before being subjected to the subsequent analysis. They were dried, weighed and sieved with a sieve with a square mesh of 2 mm, to separate the coarse fraction (retained in the sieve) from the fine earth. The coarse fraction was then thoroughly washed and weighed. Its weight was then expressed as a ratio to the total weight of the sample. The fine earth was used instead to perform all subsequent chemical, mineralogical and physical analyses (Avery & Bascomb, 1974; Gale & Hoare, 1991; Ministero per le Politiche Agricole, 1999).

2.2.4 Particle size distribution

The particle size distribution of a soil is the distribution of its mineral particles into size classes. It is a fundamental property on which depend many other chemical and physical properties of soils, and its determination is the basis of a correct classification of a soil (Ministero per le Politiche Agricole, 1999). Knowing the particle size, it is then possible to derive the texture of the sample, i.e. the proportion of the constituents of the earth end of the soil, grouped into size classes (McRae, 1991). For particle size analysis it was used the fine earth fraction in quantities of about 100 g. The portion to be subjected to analysis was obtained by one or more subsequent quartering, so arranged that the sub-sample was representative of the original sample. The obtained fraction was weighed and then pre-treated with hydrogen peroxide (H_2O_2, 130 volumes) in order to destroy organic matter, which, by favouring

aggregate formation, interferes with the analysis. Each sample was then analyzed using two distinct methodologies applied to different granulometric fractions: the distribution of sand (particles of diameter varying between 2 mm and 63 μm) was determined by sieving, the distribution of silt (particles of diameter varying between 63 and 2 μm) was determined by the Casagrande aerometer method (Avery & Bascomb, 1974; Gale & Hoare, 1991); the amount of clay was deduced by subtracting the sands and silts to the initial weight of the sample. Sand sieving was conducted on both wet and dry samples, using a column of 10 mesh sieves with decreasing values (1400, 1000, 710, 500, 355, 250, 180, 125, 90 and 63 μm). For the wet sieving it was used a stirrer under a constant stream of water to favour particle passage through the sieve; for dry sieving was used an intermittent mechanical stirrer, operated for 20 minutes. The sieves were then weighed in order to obtain the amount of sand fraction for every class. The fraction of the sample passing through the 63 μm sieve was collected in water tanks and left to settle for at least 24 hours; the volume of water has been progressively reduced by siphoning to obtain a total volume smaller than 1000 ml. The material thus obtained was analyzed by aerometry with the method of the Casagrande aerometer, into columns of 2 l volume after treatment with calgon (i.e. 3 g of sodium hexametaphosphate for each column). The aerometric analysis exploits Stokes law according to which settling velocity of a particle is proportional to its size. Density of the suspension thus tends to decrease with the passage of time and its variation depends on the size of the particles contained in the column. The measurement of density and temperature at standard intervals over 24 hours allows therefore to establish the amount of silt present in the sample. The data obtained by sieving and aerometry are then unified into frequency cumulative curves that allow an effective visualisation of the distribution of the constituents of the soil into dimensional classes.

2.2.5 pH

The pH was determined in water, using the sample sieved to 2 mm; 10 g of soil were added to 25 ml of solution (proportion soil/solution of 1/2.5); the suspension was placed on a shaker for twenty minutes and then left to stand for 24 hours. The pH measurement was carried out through the use of a dual point calibration automatic tester. The results were expressed as pH units to one decimal place.

2.2.6 Organic carbon (Walkley and Black method)

Organic carbon determination was obtained through the standard method by Walkley and Black (1934), which uses the reduction of potassium dichromate $K_2Cr_2O_7$ excess by organic matter and the subsequent determination of the remaining $K_2Cr_2O_7$ by oxide-reductive titration iron with a solution of iron

ammonium sulphate. The quantity of sample subjected to testing was often particularly low (approximately 0.250 g), given the high quantity of organic carbon content in the studied soils (the amount of sample must be such as to ensure that, at the end of the reaction, at least 3 ml of $K_2Cr_2O_7$ remain in excess). The organic matter is oxidized with 10 ml of $K_2Cr_2O_7$ and 20 ml of sulfuric acid (H_2SO_4). It is left to react inside a covered flask for 30 minutes. Then, 200 ml of water are added thus stopping the reaction and 5 ml of H_3PO_4 acid and 0.5 ml of acid 4-diphenilaminsulphonate sodium ($C_{12}H_{10}NaNO_3$) are added. The excess dichromate is titrated by the solution of ferric ammonium sulphate (Mohr salts) Fe $(NH_4)_2$ $(SO_4)_2$ x $6H_2O$. The titration is carried out on a magnetic stirrer.
The organic carbon content is expressed in g/kg with one decimal place; to obtain the corresponding value of organic matter starting from the organic carbon content was used a multiplication factor equal to 1.724 (Astori et al., 1994; Ministero per le Politiche Agricole, 1999).

2.2.7 Total nitrogen (Kjeldahl method)

In the method used the soil sample is mineralised with boiling sulphuric acid (H_2SO_4) 98% concentrated: 0.5 g - 1 g of soil sample is weighed and placed in a glass tube, 20 ml of sulfuric acid and selenium and copper oxide are added and brought to boiling. The mineralization is conducted inside a digester until the liquid turns light green (about 1 hour). At the end, it is allowed to cool for about 20 minutes and diluted with demineralized water. After mineralization, the solution is alkalised with 40% NaOH and then distilled for about 5 minutes and collected in 10 ml solution of 1% boric acid containing 5 drops of indicator (methyl red and bromocresol green). After all the ammonia has been distilled, the solution is titrated with 0.01N sulfuric acid.
Moreover, the C/N ratio was calculated.

2.2.8 Iron and aluminum extractable in ammonium oxalate acid

This method is used to determine the oxalate-extractable iron and aluminum, corresponding to amorphous or poorly crystalline iron and aluminum oxides. The ammonium oxalate acid solubilises the amorphous iron and aluminum oxides through a mechanism of complexation. High stability of the Fe-oxalate and Al-oxalate complexes causes the reagent to bring in solution also the iron and aluminum linked to the organic matter. Shaking needs to be carried out in the dark to avoid photo-degradation of the complex. After sieving of the sample with a mesh of 0.5 mm, 1 g is weighed and placed in a 50 ml tube, 40 ml of ammonium oxalate are added and this solution is shaken on a mechanical shaker for 2-3

hours in the dark. The reading of the amount of solubilized iron and aluminum in the supernatant is determined by means of a ICP-ES (model JY24 of Jobin-Yvon), after the appropriate dilutions.

2.2.9 Iron and aluminum extractable in dithionite-citrate-bicarbonate

This method, with steps similar to the above, is used for the determination of iron and aluminium extractable in a solution of sodium dithionite and sodium citrate, corresponding to free iron oxides (amorphous and crystalline). The method is based on solubilisation of the iron and aluminum oxides by the combined action of a reductant of Fe (III) and a complexing of Fe (II) and Fe (III). Bicarbonate is employed to buffer the solution. After sieving of the sample with a mesh of 0.5 mm, 1 g is weighed and placed in a 50 ml tube, 50 ml of a solution of citrate bicarbonate and 1.0 g of sodium dithionite are added and this solution is shaken on a mechanical shaker for 16 hours. The reading of the amount of solubilized iron and aluminum in the supernatant is determined by means of a ICP-ES (model JY24 of Jobin-Yvon), after the appropriate dilutions.

2.2.10 Iron and aluminum extractable in sodium pyrophosphate

This method, with steps similar to the two above, is used for the determination of iron and aluminium extractable in a solution of sodium pyrophosphate, corresponding to iron and aluminum bound to organic matter with covalent or partially polar bond. After sieving of the sample with a mesh of 0.5 mm, 1 g is weighed and placed in a 100 ml plastic container, 100 ml of a solution of sodium pyrophosphate are added and this solution is shaken on a mechanical shaker for 16 hours. The reading of the amount of solubilized iron and aluminum in the supernatant is determined by means of a ICP-ES (model JY24 of Jobin-Yvon), after the appropriate dilutions.

2.2.11 Iron and aluminum indices

In order to compare the results of the iron and aluminum extractions to the soil characteristics, the iron activity index (Feo/Fed) and the illuviation (podzolization) index (Alo+½Feo) were calculated. The iron activity index can be used as a measure of the crystallinity of free iron oxides and sometimes for estimating soil antiquity. This ratio, in fact, decreases with the increase of the soil alteration (e.g., Rhodes & Sutton, 1978; Magaldi et al., 1981; Arduino et al, 1984). The podzolization index is used as a diagnostic criteria to identify the spodic horizon, in fact a spodic horizon consists of mineral material and may has a subhorizon with an Alo + ½Feo value of ≥ 0.5% that is ≥ 2 times higher than the lowest Alo + ½Feo value of all the mineral horizons above the spodic horizon (FAO, 2014).

Moreover, the amount of crystalline iron oxides (Fed-Feo, fig. 2.1) was calculated for each horizons.

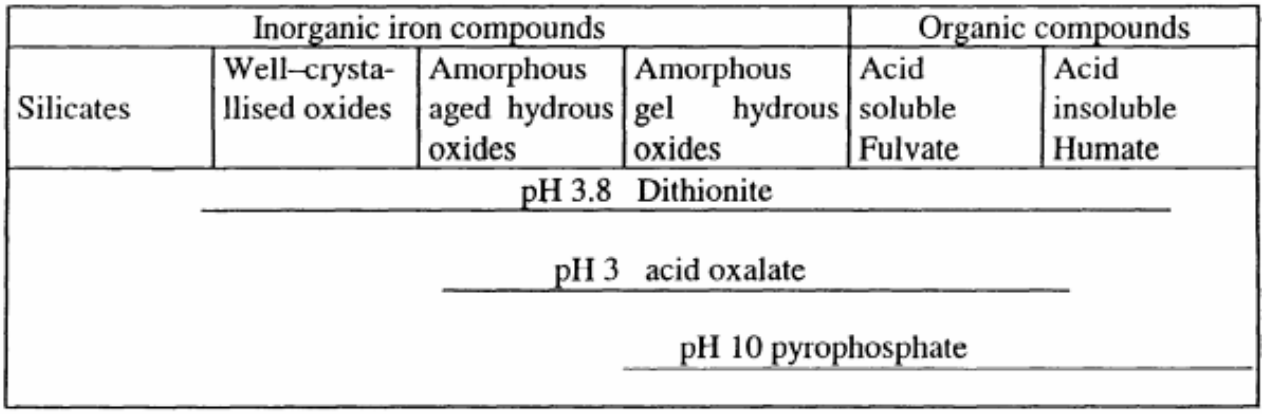

Figure 2.1. Solubility of Fe fractions in various solutions. Modified from Bascomb (1968). Al probably behaves in a similar way.

2.2.12 Rock-Eval analysis

Rock-Eval pyrolysis rapidly provides essential information on the amount and composition of SOM (Soil Organic Matter). In addition to the information on the abundance of SOM, Rock-Eval pyrolysis provides insight into the composition of SOM and even into its structure. Compositional information relies on the hydrogen and the oxygen index (HI and OI) values, related to the H and O content of SOM, respectively (Disnar et al., 2003). Structural information is less straightforward and relies on the shape of the S2 peak and on its ―Tpeak value(s). The method allows to follow the evolution of the humification process with increasing depth in soil profiles, i.e. the progressive disappearance of inherited biopolymers and the formation of humic substances.

In addition to the standard parameters (TpS2, HI, OI), new indices (I- and R-indices) reflecting the thermal stability of SOM rather than its bulk chemistry are computed. Their calculations are based on the contribution of four different areas (A1 to A4) integrated below the S2 pyrogram (amounts of released hydrocarbon compounds during the pyrolysis step). In particular, the I-index emphasizing the degree of transformation of the immature organic fraction (related to SOM stabilization), the R-index highlighting the contribution of the most refractory fraction or persistent SOM (related to pedogenic and inherited contributions) (Sebag et al., 2016). In addition, observing the I/R diagram, three linear trends are defined as humic, spodic and inherited organic matter trends (fig. 2.2); therefore plotting the Rock-Eval data on the I/R diagram a presence of one or more of these trends in our samples.

For each sampled horizon, about 60 mg of crushed material was analysed with a Turbo model Rock-Eval® 6 pyrolyser (manufactured by Vinci Technologies, Rueil-Malmaison, France) at the University of Lausanne.

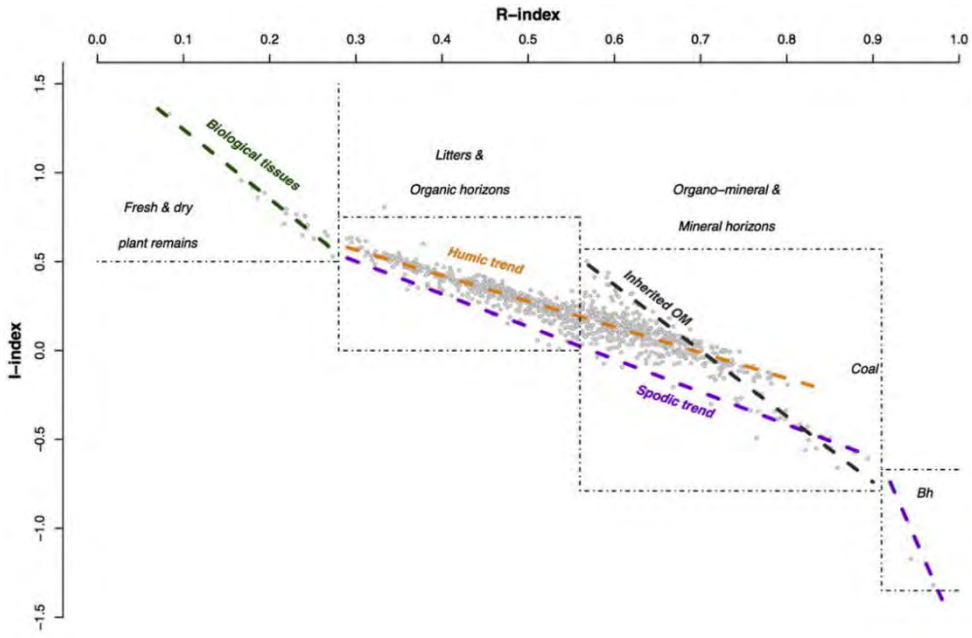

Figure 2.2. Rock-Eval I/R diagram and its interpretation. Boundaries of three different fields corresponding to biological tissue, litter and organic horizons, and organo-mineral and mineral samples, and finally, the specific domain of B humic horizons of podzols. In addition, three linear trends are defined as humic, spodic, and inherited organic matter trends (From Sebag et al., 2016).

2.2.13 Stable carbon and nitrogen isotopes analysis

For each sampled horizon, approximately 3-5g of crushed material was placed in a beaker with few ml of HCl and deionized water. The samples were shaken several times a day for three days, checking that the pH remained acid. This was followed by decanting the supernatant and care was taken not to lose any visible amount of sample. The beaker was then refilled with deionized water, and decanted 4 times at 12h intervals. After the final decant the beaker was placed in a drying cabinet at 50°C to evaporate the remaining water. Finally, the dry sample was removed from the beaker with a metal spatula.

About 5000 µg of sample were put in the capsule for the stable carbon isotope analysis, while for the stable nitrogen isotope analysis about 5000 µg (for the organic horizons) or 50000 µg (for the mineral horizons) of sample were put in the capsule.

The stable carbon and nitrogen isotope compositions of the samples were determined using Thermo Scientific Delta V, at the University of Lausanne.

The δ13C and δ15N values are reported relative to the Vienna Pee Dee Belemnite standard (VPDB) and air-N2, respectively. Laboratory standards were calibrated relative to international standards.

2.2.14 Soil micromorphology

Undisturbed samples were sent to an external laboratory for thin sections preparation. An initial drying for the total water removal is followed by the impregnation in epoxy resins (polystyrene); after a variable period of duration of some weeks, necessary for allowing the resin to harden, the sample was cut and polished, to obtain a thin section about 20-30 μm thick. The sections were then observed under a petrographic microscope (Leica Laborlux 18 POL), al parallel (PPL), cross-polarised (XPL) and oblique incident light (OIL), using different objectives of 1.6, 4, 10 and 25x. Sections were described according to Stoops (2003). The interpretation of thin sections was performed according Stoops et al. (2010).
For each section was followed a descriptive diagram which involved the observation of:
• Microstructure and porosity: type of microstructure, aggregate size and shape, void type, abundance, spatial arrangement, shape and size.
• Groundmass: c/f limit, ratio and relative distribution; nature, degree of weathering, size and frequency of coarse mineral and organic constituents; nature, colour, limpidity, interference colours and b-fabric of the groundmass.
• Organic matter (not part of the groundmass): nature, degree of weathering, size, frequency and spatial arrangement.
• Soil pedofeatures: nature, size, shape, variability, abundance and spatial arrangement of the different figures soil.
Compared to the standard guide of Stoops (2003), it was agreed that a number of changes should be done for reasons of tradition, of opportunities, and to facilitate the work of description.
• Frequencies related to voids should be given with respect to the total area occupied by the voids themselves. To facilitate frequency assignment, estimated through a comparison chart, it was preferred to use the whole area of the section as a reference instead.
• In the description of the coarse fraction two elements, phytoliths and charcoal, belonging to the category of inorganic material of biological or anthropogenic origin, were described instead as organic material. Phytoliths are opal bodies (composed of amorphous silica) formed within plant cells, whose shape changes depending on the type of plant and the organ from which it comes. They are therefore useful to indicate the presence of vegetation and, if possible, its type: therefore this change in classification. Charcoal was changed because of its origin: Stoops (2003) considers them belonging exclusively from human activity, so always sign of human influence. Since it is not possible in this area to assign charcoal fragments undoubtedly to human action, it was preferred to avoid this implication.

2.2.15 Soil classification

Since the aim of this work is not to classify the studied soils, for which reference is made to the literature, but to analyze the pedogenetic processes and their modifications that have taken place over time and space, only a genetic reference to ecological classification of Duchafour (1995) was carried out.

2.3 Dendrochronological approaches

Because of different purposes, different dendrochronological approaches were utilized in the various study sites: a dedrochronological approach was used to reconstruct the position of the treeline in the Mt. Confinale study site, a dendroclimatology approach was used at the Becca di Viou study site for the reconstruction of the climatic signal, and finally a dendrogeomorphological approach was used to study the evolution of the landforms due to running and channelized water in the Saint Nicolas study site.

2.3.1 Dendrochronological approach: Mt. Confinale study site

2.3.1.1 Tree sampling

The largest and oldest-looking trees located at various elevations, from approximately 2450 m to 2600 m a.s.l. were selected, and their coordinates were recorded using a GPS device. A total of 119 *Pinus cembra*, 7 *Picea abies* and 4 *Larix decidua* trees were analyzed at the Mt. Confinale site: for these trees, age, height, and stem diameter were determined.

2.3.1.2 Cores preparation

All wood increment cores were processed according to standard dendrochronological techniques and sanded with progressively finer grades of sandpaper to highlight annual rings.
The method of cores preparation is the same in each study site.

2.3.1.3 Tree-ring approach to age estimation

Tree age were estimated using a dendrochronological approach based on the cambial age of cores taken at different heights (Leonelli et al., 2016). The same tree ring approach to age estimation at different heights was used to reconstruct the altitudinal dynamics of the treeline, but for this calculation, the year in which each specimen reached 2 m in height was considered. This led to four age groups, from 1980–1989, 1990–1999, 2000–2009, and 2010–2013. For the two middle groups, a mean treeline position was

determined by averaging the elevation of those trees (maximum six per group) growing at the highest elevations, above the previous treeline position. The treeline in 1980–1989 was not estimated because only one tree reached 2 m in height in that time period and, for this reason, it was not possible to calculate an average elevation. In the period 2010–2013, above the position of the 2000–2009 treeline, only one tree reached 2 m in height; but, in order to depict the treeline condition up to 2013, the average elevation of the top 2-m trees growing at the highest elevations was calculated.

2.3.1.4 Estimation of potential treeline

To calculate the elevation of the potential treeline at the Mt. Confinale study site, a daily temperature series spanning the period from 1994 to 2013 from the Bormio weather station was used (approximately 10 km northwest of the Mt. Confinale study site, at an elevation of 1225 m a.s.l.; data from Maugeri et al., 2008; 1994–1995 data from ERSAF Lombardia, 1999–2013 data from ARPA Lombardia). The series was transformed using a gradient of −0.6 °C per 100 m up to the elevation of the potential treeline. The elevation of the potential treeline (PT20) was estimated with a thermal index defined by the altitude at which the air temperature is above 5 °C for at least 100 days (Ellenberg, 1963). To obtain a more representative value of potential treeline over a larger time period, the yearly data of potential treeline were averaged over the 20-year period from 1994–2013 (PT20) (Leonelli et al., 2016).

2.3.2 Dendroclimatology approach: Becca di Viou study site

2.3.2.1 Tree sampling

17 trees of European larch were sampled on the SW slope of Becca di Viou in a belt at about 2150 m a.s.l.. To minimize the possible effects of stand competition, only dominant *Larix decidua* specimens with undisturbed canopy were selected. An effort was made to avoid locations and trees affected by other non-climatic factors, e.g. human disturbance (grazing, tourism) and active geomorphological processes. Two or more increment cores, 5 mm diameter were extracted from each tree about 1.3 m above ground level, in a direction parallel to the contour lines.

2.3.2.2 Samples measuring and crossdating

The tree rings were first visually counted under the microscope and then measured using two different system. All samples were digitally scanned, and the annual ring width was measured using an image analysis software-based system (imageJ). In the samples with narrow and difficult to recognize rings, in

order to identify any missing and/or false double rings, a more detailed observation and measure were done using a LIN-TAB system.

All tree-ring measurements were visually and statistically crossdated to avoid potential dating errors and to test the quality of the data set. This procedure was performed with the TSAPWIN (Rinntech, Heidelberg, Germany) and COFECHA (Holmes et al., 1986; Grissino-Mayer, 2001) programs, and the data was then validated by selecting for further analysis only the ring-width series that correlated r> 0.5 with the site mean chronology (Hofgaard et al. 1999; Pelfini et al. 2006).

2.3.2.3 Site chronology construction

Site chronologies were built with the program winARSTAN (http://web.utk.edu) by detrending each ring-width series to remove long-term growth variations related to age and stand disturbances (Fritts, 1976; Cook et al., 1990). A first detrending was performed by fitting to the series with a spline of 100 year length (Cook et al., 1990). The standard chronology was computed by applying a robust biweight mean to the detrended indices, derived from autoregressive modelling (Cook & Briffa, 1990). Using residual chronologies from autoregressive modelling helps to remove the problem of biological persistence in the resulting series (Fritts, 1976).

The obtained site chronology was then truncated, discarding the periods showing an Expressed Population Signal (Wigley et al. 1984) EPS < 0.6.

2.3.2.4 Dendroclimatic analysis

For the dendroclimatic analysis we used data from 1848 to 2008 (160 years) comparing the chronology and the gridded mean monthly temperature (period 1842-2008) for the grid point 45° N, 7° E from the HISTALP dataset (Auer et al., 2007) and total monthly precipitation from Aosta Saint Cristophe weather station (period 1914-2007). For the monthly analysis, on the other hand, 15 variables were chosen, both for temperature and precipitation, from July of the year before growth (t−1) to September of the year of growth(t). For both seasonal and monthly analyses the program DENDROCLIM2002 (Biondi & Waikul, 2004) was used, computing correlation functions over the whole period and over 60-year periods with the moving correlation functions (MCF) approach.

In both the analyses, correlation coefficients were calculated with the bootstrapping method. With the MCF approach, correlation coefficients are calculated between tree-ring data and the climatic variables over fixed time periods (in our case 60 years).

The length of the calibration period (60 yr), twice the standard time length normally used in climatological studies, has previously been used in similar dendroclimatologic studies in the Ortles-Cevedale Group (Leonelli et al., 2009b, 2011b).

2.3.3 Dendrogeomorphology approach: Saint Nicolas study site

2.3.3.1 Tree sampling

In order to calculate the soil erosion rates of Saint Nicolas Badlands area, 10 exposed roots of *Larix decidua* were sampled. The root samples were taken using a Pressler increment borer or cutting disks with a hacksaw. The length of the exposed portion of the root and the distance from the ground, in multiple points, were also measured.

2.3.3.2 Samples preparation and measuring

Roots samples were sanded with progressively finer grades of sandpaper to highlight annual rings and then were observed under the microscope for the purpose of detecting and dating the year of exposure. The first year of response to soil erosion was determined by anatomical criteria.

2.3.3.3 Exposed roots analysis

For estimating the erosion rates, exposed roots were analyzed. In fact, roots exposure is useful for estimating the erosion rate derived mainly from water erosion (Stoffel et al., 2013). Morphometric analysis was performed on roots since the change in their micromorphology, from the production of root type wood to a trunk type wood, with the distinction in earlywood and latewood, is a consequence of the exposure (Gärtner, 2007; Stoffel et al., 2013; Pelfini & Santilli, 2006). The equation proposed by Hupp and Carey (1990) (E=D/A), allowing to obtain the erosion rate by dividing the distance (D) between the actual ground surface and the tree root top, by the age (A) of the micromorphologic change in root, is one of the most frequently used.
Recently Bodoque et al. (2015) refine the methodology, in the specific case of roots connected with the substratum, considering micromorphological issues due to secondary roots growth.
Local Erosion Rates (LERs), in correspondence of single trees, and Average Erosion Rates (AERs) over long periods (Bollati et al., 2012, 2016; Ballesteros-Cánovas et al., 2013) were calculated.

Chapter 3

Upper Valtellina study area

High-altitude areas in the European Alps have been widely investigated through time for reconstructing the Holocene climate fluctuations, by analyzing both biological and abiological indicators. In particular, altitudinal treelines characterize the uppermost forest limits in mountain ranges and globally represent an important biological indicator of climate conditions over entire regions from the Equator to temperate zones and poleward, where they tend to merge with the latitudinal treelines (Körner, 2003). At alpine treelines, trees grow in high-elevation environments that are very sensitive to climate change impacts (Körner, 2002; Nagy & Grabherr, 2009). Since the end of the Little Ice Age (LIA), the landscape in these environments has undergone rapid transformations that affect both biological and abiological systems (Anderson et al., 2011; Clague et al., 2004; Cunill et al., 2013; Wipf et al., 2013). Although altitudinal treelines are generally influenced by climatic conditions, geomorphological processes and human activities can locally limit the treeline position, conditioning its altitude and dynamics (Leonelli et al., 2009a). Indeed, in mountain regions, tree establishment and growth at the highest altitudes may be greatly affected by abiotic factors, like soil development and geomorphological processes, and/or human impacts.

Moreover, most of the debris-free glaciers are subjected to a generalized shrinkage due to the ongoing temperature increase. Therefore, the proglacial areas are increasingly widening since the end of the Little Ice Age. These newly deglacierized areas are being colonized by vegetation and soils have started to develop (D'amico et al., 2015; Egli et al., 2006). The increasing surface age with distance from the snout of a retreating glacier produces a soil chronosequence (Walker et al., 2010): a sequence of soils in which the dominant variable accounting for any physical, chemical and biological differences has been the duration in time over which the sequence has developed.

The aims of this first part of the study are: 1) determine the treeline elevation in Upper Valtellina based on three environmental factors (geomorphology, climate and human impact) that constrain the treeline elevation, with particular attention to the influences of the climate and geomorphological constraints; 2) investigate the role of geomorphological factors on treeline position and characterize the different types of landforms and geomorphological processes that influence the position of the treeline; 3) study the environmental changes at the treeline with a climatic constraint in the Mt. Confinale study site, reconstruct the altitudinal dynamics of the arboreal vegetation and the influence of climatic variations on it, predict the trend of arboreal vegetation upward shift, compare the climate trend with the arboreal

vegetation response to the ongoing climate change, determine the relationship between the development of the soil and the colonization by the vegetation; 4) investigate soil and environmental changes in the proglacial area of Forni glacier due to glacier retreat in relation to the climate change.

The sections 3.2.1, 3.2.2.1, 3.3.1 and a portion of 3.3.2 of this chapter were presented in two papers (i.e., Leonelli et al., 2016; Masseroli et al., 2016) published during my PhD.

3.1 Overview of the study area

3.1.1 Geography

The determination of the treeline maximum elevation, based on three main environmental factors (geomorphology, climate and human impacts) that constrain the treeline elevation and the study about the role of geomorphological factors on treeline position were carried out in the Central Italian Alps (fig. 3.1), specifically in Upper Valtellina (Ortles - Cevedale Group - Sondrio Province).
Upper Valtellina is located in the Rhaetian sector of the Alps and belong to the upper Adda River catchment.
The area is characterized by the presence of high peak like Cresta del Reit, Cristallo, Ortles, Gran Zebrù, Cevedale, Palon della Mare, Confinale, Sorbetta, Tresero and Gavia, with a height above 3000 m a.s.l..
A large part of the Upper Valtellina territory, even the two sample sites, is placed inside the Stelvio National Park, which is located between Lombardy, Trentino Alto Adige and Switzerland, born in 1935, with an extension of about 130000 hectares.

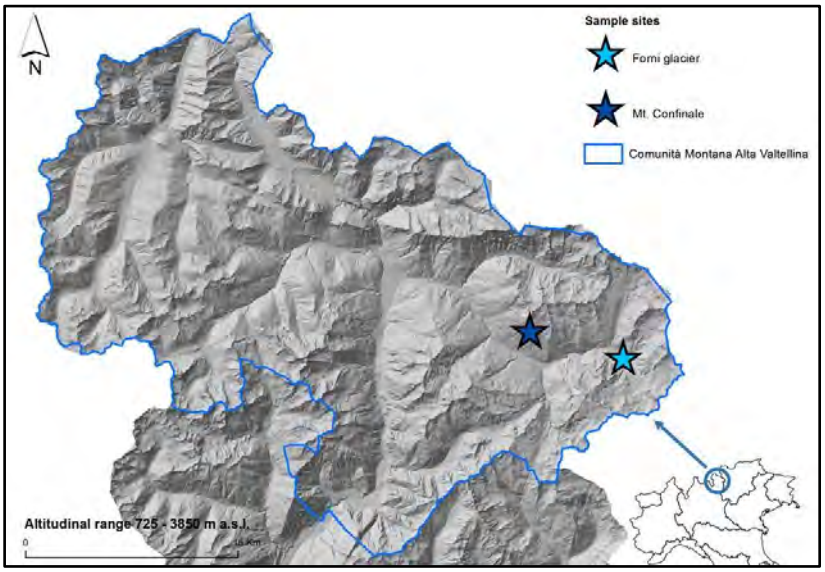

Figure 3.1. Upper Valtellina and sample sites location.

In the Upper Valtellina two samples sites were chosen. In particular, the study site where the altitudinal upward shift in the treeline and the soil studies were assessed is on the southwest-facing slope of Mt. Confinale, in Valfurva; while the investigation about the soil development on different depositional moraines was carried out in the proglacial area of Forni glacier, in Val di Forni (fig. 3.1).
Valfurva, is the most important and largest valley among the left tributary valley of Valtellina. Valfurva, crossed by the creek Frodolfo, left tributary of the Adda River, is delimited by the Ortles-Cevedale and the Gavia-Sorbetta groups. It begins east of Bormio and after receiving the valley of the Zebrù, it goes south-east to Santa Caterina, where it breaks in the Val di Forni-Val Cedec (Frodolfo torrent) and in the Gavia Valley.
Moreover, the Forni Glacier is included in the official "Geosites Inventory" of the Sondrio Province, Lombardy Region (Italy) and is located in areas identified as SICs (Sites of Community Importance) according to directive 92/43/CEE.

3.1.2 Geology

The history of the Alpine belt begins during Late Carboniferous after the end of the Hercinian orogeny, and the evolution of the Alps is closely related to the opening of the Neotethys ocean, splitting the Pangea supercontinent into the Laurasian and Gondwanan plates (Cavallin et al., 1997). The sedimentary successions deposited in the Alpine region record several different episods of rifting from Permian to Jurassic with predominant deposition of marine carbonatic successions (Cavallin et al., 1997). During Jurassic two E-W trending fracture zones split the Europa and Africa plates forming in between small microplates (Iberia, Adria-Apulia, Pelagonids-Menderes) separated by small oceans (i.e. Ligure-Piemontese ocean) (Cavallin et al., 1997). At the end of the Jurassic the paleogeographic domains of the area now forming the Alps were: the Helvetic-Delphines Domain, the Pennidic Domain, the Austroalpine Domain, the Southern Alps (Cavallin et al., 1997). At the end of the Jurassic, the inversion of the relative motion between Africa and Europa, due to the opening of the Atlantic Ocean, caused the closure of the Ligure-Piemontese ocean and the beginning of the Alpine orogeny (Cavallin et al., 1997). During Eocene, the Central Alps were affected by intensive regional metamorphism (Mesoalpine phase) related to the thermal Lepontine dome, caused by intensive crustal thickening following continental collision. Souht-vergent back-thrusting of the Central Alps with formation of antiformal structures (Cressim antiform in the Adula Nappe) and subsequent dextral strike-slip motion at shallow crustal levels during Miocene (Neoalpine phase) are generally recognized all along the Insubric Line (Cavallin et al., 1997). During Oligocene, large plutons intruded north (Masino-Bregaglia) and south (Adamello-Presanella) of the Insubric Line. At the end of the Oligocene, in the southern part of the Lombardian

sector, a foredeep basin, approximately corresponding with the area now occupied by the Northern Po Plain, was infilled by coarse turbiditic deposits of the Gonfolite Lombarda Group, attesting high rate of uplifting of the Central Alps (Cavallin et al., 1997). Up to the end of Tortonian, thrust embrication in the Southern Alps and dextral motion along the Insubric Line were active. During Tortonian also the Oligo-Miocene fore deep successions were stacked homeward leading to the formation of the Milano thrust belt, now buried below the Plio-Quaternary sediments of the Po Plain. During Messinian, the Alpine region was affected by deep erosion leading to the excavation of the major alpine valleys, due to the drying up of the Mediterranean basin (Cavallin et al., 1997). At the beginning of Pliocene, with the opening of Gibraltar and filling of the Mediterranean, the sea transgressed the lower part of the Southern Alps foothills, filling the Messinian canyons. From Late Pliocene probably starting the glaciations that added to the continuous uplift of the region caused a definitive regression of the sea from the Lombardian plane, which was subsequently covered by continental fluvial and fluvioglacial deposits. At present, the possible prosecution of tectonic activity at low strain rates is suggested by the presence of low seismicity, continuous uplifting, and isolated neotectonic evidences.

The area of two study sites belong to the Austroalpine Domain, which form the uppermost part of the Alpine belt, covering the Pennidic complexes (Cavallin et al., 1997). The Austroalpine of the Central Alps is formed by several polymetamorphic crystalline nappes with pre-alpine imprint, which did not undergo the HP-LT alpine metamorphism present in the Pennidic Nappes. In the northernmost part of upper Valtellina (north of Bormio) the Austroalpine includes a complex system of thick Mesozoic carbonatic successions.

The Austroalpine is generally divided in three main nappe complexes. In the two sample sites the founded geological formation belong to the middle Austroalpine units, which are represented by the Campo-Ortler Nappe, which comprises all the units located between the lower and the upper Austroalpine. This nappe includes marbles- and prasinite-bearing phyllites (Filladi di Bormio) and a lower paragneissic unit with augen-gneisses and amphibolites. Late-Hercinian granitic to granodioritic bodies are intruded into this unit as well as the stratified gabbric intrusions present around Sondalo (Gabbro di Sondalo) (Cavallin et al., 1997). The sedimentary units of the Middle Austroalpine Nappe form the Ortles-Quattervals nappe, stacked above the Filladi di Bormio along the north-dipping Zebrù Line. The Ortles-Quattervals Nappe is formed by several folded thrust sheets including a thick Permo-Mesozoic succession which forms the «dolomitic chain» present north of Bormio.

As for the detailed description of the Geological Units which characterize the sample sites (fig. 3.2), it is reported what is contained in the legend of the Italy Geological Map 1:50000, sheet 024 Bormio (Montrasio et al., 2012).

Falda Campo.

Peio Units.

Cristalline Basment (PRE-PERMIAN).

Ortogneiss (OOG): masses of considerable thickness or very elongated lenses with limited thickness of othogneiss, interpose in sericite and chlorite micaschists (OME) and in micashists or pragneiss (OMI). Generally, the orthogneiss are "occhiadini" or "listati", with two micas, with a granitic or granitic-granodioritic composition. The foliation is always planar.

Micascisti a clorite e sericite (OME): In these illustrative notes, these micascists correspond to the "Filladi di Bormio" formation of the 8-Bormio geological sheet in scale 1:100000 (Bonsignore et al., 1969, 1970). Micaschists and paragneiss with "varisico" metamorphism in anfibolytic facies. Rock with shiny silver to gray color, often with brownish-reddish surface patches due to hydroxides iron. The prevalent facies are given by rocks with a filladic structure and appearance, often with dark and light alternate bands, respectively formed by bands of sericite and chlorite rich in graphite and richer quartz bands. Locally, micaschist facies with large white mica plates, with biotites and porphyroclastic garnets are found. These facies are present especially in high Valfurva (particularly in Val Cedec), in Val Zebrù and sporadically on the Mt. Confinale.

Paragneiss a bande (OMP): generally inserted in the reverse micaschists, in variable thickness levels, typically several tens of meters. It is striped paragneiss, slightly foliated, grey or grey-brown, with medium-fine grain size, with biotite or two mica, with very small garnet.

Vein with uncertain age.

Andesiti e Basalti (fb): Andesite-basaltic veins, present in the crystalline basment of the Peio Unit (Falda Campo), on the north side of Valfurva (between Corna Rossa and Val Pisella), in the Forni Valley (Monte S. Giacomo) and in the Braulio Valley. Belong to Triassic - Lower Cretaceous.

Continental Quaternary deposits.

Sintema del Po (POI): all deposits (regardless of the deposition agent) originated behind the Peistocenic last glacial event; from the end of the Upper Pleistocene to all the Holocene.

Deposits surface and topographic surface coincide, characterized by absent to little-developed alteration (maximum depth 30-40 cm) and well preserved or still evolving landforms. Discordant limit with the substrate or units below. Very variable thickness: from 4-5 m of some ablation tills to 100 m in some landslide deposits.

Limited to glacial deposits and rock glaciers, includes the subunits of Ancient Postglacial (POI6), Postglacial Little Ice Age (POI7) and Recent Postglacial (POI8), distinguishable mainly on base of alteration profile and historical data (Upper Holocene). In particular, the POI6 subunit presents an alteration depth of 20 to 40 cm with continuous soil presence, while the POI7 subunit has an alteration profile depth less than 20 cm and a discontinuous to continuous soil. The POI8 subunit has not alteration, and is generally attributable, with regard to glacial deposits, to historically documented locations.

Slope deposits s.l. (a): massive diamicton and massive from coarse to fine gravel, sometimes with open-work structure, most commonly with clastic support or sandy matrix or absent to very abundant silty-clay matrix. Angular clasts coming from nearest rock walls, or sub-rounded with local or exotic provenience.

Landslide deposits (a1): massive diamicton, often with open-work structure, most commonly with clastic support or sandy matrix or absent to very abundant sandy-silt matrix. Angular to subangular clasts coming from local areas.

Alluvial deposits (b): stratified coarse to fine gravel, with a clastic support and absent to abundant sandy matrix. Subangular to rounded clasts; coarse to fine sands, often stratified with lamination or imbricates clasts. Massive to laminate silt.

Debris flow deposits (b4): massive diamicton, sometimes stratified with lamination or imbricates clasts, with a clastic support or with absent to very abundant sandy or silty-clay matrix, angular to subangular clasts, with local or exotic origin.

Ablation till (c5): massive diamicton with a clastic support or with sandy or silty-clay matrix. Subangular to rounded boulders and cobbles, often with characteristic shapes (“ferro da stiro”).

Glacial contact deposits (b5): complex depositits, characterized by juxtaposition and eterotropie among debris flow deposits, alluvial and lacustrine deposits.

Sintema di Cantù (LCN): glacial deposits, contact glacial deposits and fluvial deposits. The surface is characterized by well preserved landforms, even if sometimes subject to erosion or affected by slope movements when the surface and the topographic surface coincide. When the surface is buried by the postglacial deposits unit, the surface limit is discordant. The alteration profile, depending on the different

lithology prevailing in the valleys, is few evolved, but always with a thickness more than 40 cm, with continuous soil and generally with clasts and matrix oxidation in the deposits with high content of iron, partial sandstonized of schistose and intrusive clasts and rarely argillification of carbonate clasts. Discordant limit with the substrate. The thickness is variable and can reach 70 – 100 cm in the valley floor.

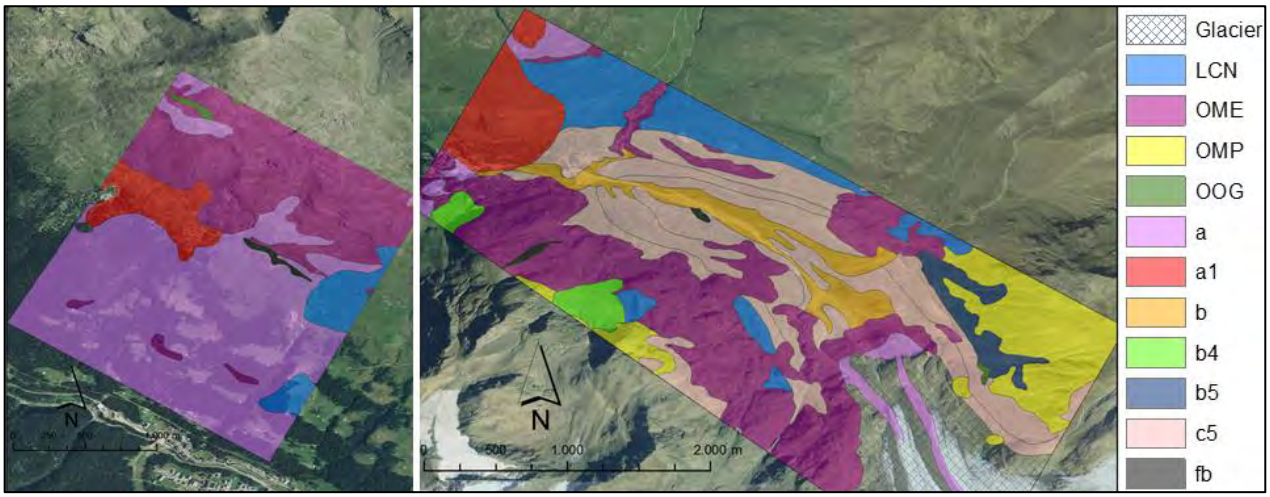

Figure 3.2. Geology of the study areas (taken from the sheet 24 Bormio, scale 1:50.000, Carta geologica d'Italia, ISPRA, 2012). On the right the Mt. Confinale study site and on the left the Forni glacier study site.
The orthophoto has been drawn from spatial data available at the National Geoportal.

3.1.3 Geomorphology

The central sector of the Italian Alps has typical aspects of alpine relief, characterised by high relief energy and glacial and periglacial erosion morphology (Cavallin et al., 1997; Montrasio et al., 2012). The complex morphology of Upper Valtellina is the result of both the lithological and structural aspects of the region, as well as the changes in type and/or frequency and intensity of geomorphological processes due to climatic changes. Glacial processes play a preeminent role, resulting in well-preserved typical landforms (e.g., U-shaped valleys, troughs, cirques, and moraine ridges) (Bellotti et al., 1995) and contributing to the local geoheritage (Pelfini & Gobbi 2005; Garavaglia et al., 2010). Due to the high altitude, the study area is characterized by periglacial processes and landforms, such as rock glaciers, protalus ramparts, and others (Scotti et al., 2013). Moreover, avalanche channels and cones are also common. The action of freeze-thaw cycles and the effects of gravity have contributed to the formation of debris slopes at the base of the cliffs (Bellotti et al., 1995). Gravity-related processes and landforms (e.g., talus cones, debris fans, debris flows and landslide deposits) are common in the study area, which is characterized by high-relief areas and high-elevation peaks, especially in the eastern part (i.e. Ortles-Cevedale Group; Pozzi et al., 1990). The morphogenetic role of water runoff is also locally

active: many gullies related to concentrated runoff are present, and they can be attributed to the current erosive action of running water. Evidence of sheet erosion is also common (Bellotti et al., 1995)
In particular, the SW slope of Mt. Confinale is affected by a relict DSGSD (deep-seated gravitational slope deformation) (GEOIFFI, Regione Lombardia, 2004). Above and in the treeline ecotone there are some inactive slope deposits, whereas the forested area is affected by soil creep and by the presence of relict landslides deposits.
While the Forni Glacier, one of the most important Italian glacier (ca. 11.36 km^2 of surface area; D'Agata et al., 2014) is widely debris-free, with only few occurrences of sparse, fine debris and dust at the ice melting surface (Diolaiuti & Smiraglia, 2010; Diolaiuti et al., 2012; Azzoni et al., 2014). It presents a north aspect and an elevation range between 2600 and 3670 m a.s.l. (Senese et al., 2014).
Moreover, the Forni glacier monitoring by the Italian Glaciological Committee (CGI) indicate that the glacier has experienced a strong decrease in area and length: it shranks from 17.80 km^2 at the end of the Little Ice Age (LIA; ~ 1860) to 11.36 km^2 in 2007 (−36.2 %), and at the same time its tongue has retreated about 2 km (Diolaiuti & Smiraglia, 2010; D'Agata et al., 2014). The ongoing rapid glacial retreat is creating a wide proglacial area while the major late Holocene advances are marked by frontal moraines dated to AD 1859, 1913-14, 1926 and 1980 (Pelfini, 1988).

3.1.4 Soils

In Upper Valtellina the most common type of soil is Leptosol (Carta pedologica 1:250000, Regione Lombardia, 2013), soils with a very shallow profile depth, and they often contain large amounts of gravel. Leptosols are approximately equally distributed among areas where soil formation is limited by severe climatic conditions. Because of continual wind or water erosion or shallow depth to hard bedrock, Leptosols show little or none of the horizonation, or layering, characteristic of other soils. Leptosols are related to the soils in the Entisol order of the U.S. Soil Taxonomy. The soil typology differs according to the parent material, so in the areas with calcareous parent material (near Cancano Lake) Calcaric or Rendzic Leptosol are found (Carta Ecopedologica d'Italia 1:250000, Geoportale Nazionale, 2013). While in the northwest and south part of Upper Valtelllina, characterized by acid parent material, Umbric and Lithic Leptosol are found, alternating with Umbrisol, especially in the northern part.
Umbrisol, are characterized by a surface layer that is rich in humus but not in calcium available to plants, owing to high rainfall and extensive leaching that lead to acidic conditions. They are found under forest cover in high-rainfall regions and are related to soils of the Inceptisol order of the U.S. Soil Taxonomy that form under coniferous forest vegetation.

The second most widespread type of soil is Podzol, developed, under forested landscapes, on coarse and high in quartz parent material. Podzols are closely similar to the Spodosol order of the U.S. Soil Taxonomy. In particularly, in one lateral valley of Valfurva (Valle del Gavia) also Podzol paleosols are found (Compostella, 2011).

In the south part of Upper Valtellina, as in the Mt. Confinale, there are also the presence of Regosols. They are characterized by shallow, medium to fine textured, unconsolidated parent material that may be of alluvial origin and by the lack of a significant soil horizon (layer) formation because of dry or cold climatic conditions. Regosols are similar to the soils in the Entisol order of the U.S. Soil Taxonomy.

In area with calcareous parent material Phaeozem and Cambisol are also found, while in the central sector of Upper Valtellina a Podzolic Cambisol are found (Carta Ecopedologica d'Italia 1:250000, Geoportale Nazionale, 2013).

3.1.5 Climate

The climate of the Upper Valtellina is alpine continental, with a typical high annual temperature excursions (minimum temperatures occur in January, and maximum temperatures occur in July). Rainfall is scarce in the valley bottom, with an annual average between 700 and 900 mm, which mainly occurs during the summer (Nigrelli, 2008). In particular, regarding the temperature trends recorded in Valtellina, observing the Bormio climograph (fig. 3.3), there is a winter minimum average temperature in December and January (-1.3°C) and a summer maximum average temperature in July (16.6°C), with an annual thermal excursion slightly lower 20°C.

The temperatures of Santa Caterina show a similar trend but with moderately lower temperatures (fig. 3.3), with a minimum average temperature in January (-8.0°C), a maximum average temperature in July (13°C), with a more marked annual thermal excursion (21.5°C). Average precipitation is scarce, concentrated in the summer months and with a minimum in February (762 mm annually for Bormio and 855 mm annually for Santa Caterina Valfurva).

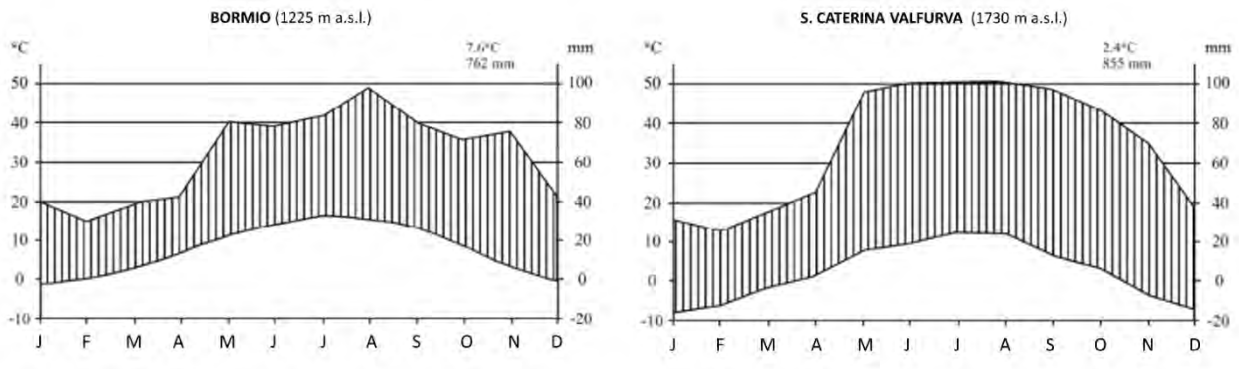

Figure 3.3. Climograph of Bormio and Santa Caterina Valfurva weather stations (modified from Compostella, 2011).

A marked and nearly constant increase in summer temperatures has been recorded in the region during two periods: 1915–1946 (fig. 3.4), with a local minimum at approximately 1935, and the late 1970s to the present (Leonelli et al., 2016).

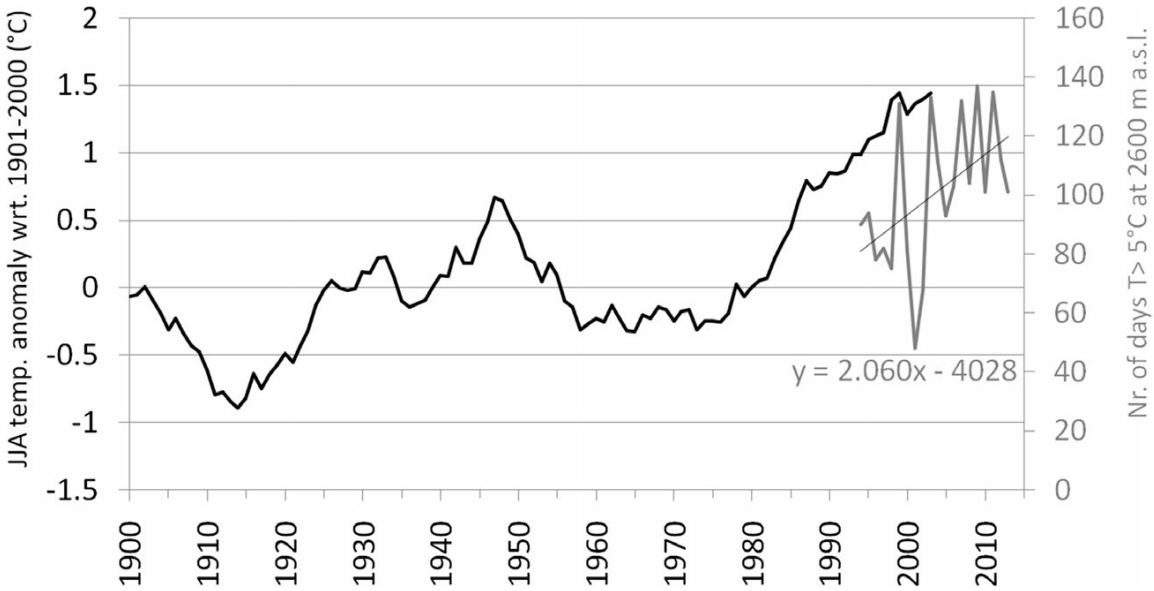

Figure 3.4. Jun–July–August temperature anomalies (Auer et al., 2007) expressed as an 11-year running mean from 1889–2008. The graphs also depict the number of days with air temperature ≥ 5 °C at 2600 m a.s.l. (i.e. at the elevation of the potential treeline PT20, see below) based on the daily series nfrom the Bormio weather station near the study site over the period 1994–2013 (from Leonelli et al., 2016).

Moreover, on the Forni Glacier an Automatic Weather Station Forni (AWS1 Forni) is set up on the ablation tongue at the base of the eastern icefall of Forni Glacier and the data from 1 October 2005 to 30 September 2009 were analysed in a study carried out in the 2012 by Senese et al.. The study show how over the 4-year period, an average air temperature of −1.3 °C was found, and the annual range was typically 7.4 °C. Regarding the extreme mean daily values, the AWS measured −22.9 °C in winter (29 December 2005) and +11.1 °C in summer (25 June 2008). The cumulative solid precipitation over the 4-year ranging from +0.6 m w.e. (2006-2007 hydrological year) to +0.8 m w.e. (2008-2009 hydrological year).

3.1.6 Vegetation

The determination of the treeline position was carried out in whole the Upper Valtellina region. Based on a map of the forest types of the Lombardy Region (Ente Regionale per i Servizi all'Agricoltura e alle Foreste [ERSAF], 2012), which species make up the forest in the valleys and the slopes and therefore which species most likely formed the treeline were determined. In the northwest part of the Upper

Valtellina, Swiss stone pine (*Pinus cembra* L.), European larch (*Larix decidua* Mill.), and isolated populations of *Pinus mugo* dominate the forests; whereas in the northeast (near Lake Cancano), the mountain pine (upright form) is the most common species, joined by sporadic larches and Swiss stone pines (Pelfini et al., 2006). Towards the south, closed forests of European larch and Swiss stone pine dominate the landscape. In some cases, such as in the Forni Valley, forests mainly consist of Swiss stone pine, while in other areas, the European larch prevails (such as Val Rezzalo). *Pinus mugo* is found only sporadically, and at lower elevations than the European larch and Swiss stone pine forests, near the bottom of valleys, Norway spruce (*Picea abies* Karst.) forests are usually found.

The study site of Mt. Confinale cover an altitudinal range from 1800 m a.s.l. to 2600 m a.s.l.. This area is characterized by different type of vegetation, subdivided in different vegetation belts.

In the first vegetation belt, from 1650 to 1950 m a.s.l., typical of crystalline substrate the *Picea abies* forest turn into a close subalpine forest dominated by *Pinus cembra* with *Picea abies* and *Larix decidua*. In the undergrowth *Vaccinium myrtillus*, *V. vitis-idaea*, *Lonicera coerulea* and *Juniperus nana* are found and the herbaceous vegetation dominated by *Calamagrostis villosa* with *Homogyne alpina*, *Linnaea borealis* (sporadic but observed in Valfurva), *Melampyrum sylvaticum*, *Luzula albida*, *L. luzulina*, *Moneses uniflora*, *Lycopodium annotinum* (Andreis et al., 2009).

In the second vegetation belt, from 1850 m a.s.l. to 2200 m a.s.l. and locally at higher altitude, the typical vegetation is the open forest composed of *Pinus cembra*, *Larix deciuda*, and *Picea abies*.The undergrowth is characterized by *Rhododendron ferrugineum, Lonicera coerulea, (Pinus mugo)*, *Sorbus aucuparia*, *Alnus viridis*, *Rubus idaeus*, *Vaccinium myrtillus*, *V. vitis-idaea* e *Juniperus nana*, *Calamagrostis villosa*, *Avenella flexuosa*, *Homogyne alpina*, *Luzula albida* e *Linnaea borealis* (Andreis et al., 2009).

The closed mixed forest, dominated by *Picea abies* Karst. and *Pinus cembra* L. at lower elevations, is replaced at the treeline by open *Pinus cembra* stands above 2200 m a.s.l. (Caccianiga et al., 2008). Above the treeline, the site is on a slope characterized by *Juniperus communis, Arctostaphilos uva-ursi, JuniperoArctostaphiletum* (Andreis et al., 2009), and by broad alpine grasslands that are interrupted by abundant rock outcrops, especially at the highest elevations.

The proglacial area altitudinal range, from the frontal morain of 1859 to the current glacial tongue, vary from 2140 m to 2600 m a.s.l., therefore the proglacial area belong to the subalpine vegetation belt (Pignatti, 1995). The subalpine vegetation belt includes a lower vegetation belt identified with boreal conifer forests and an upper vegetation belt, represented by bushes and shrubs, which reached the limit of the trees. The Forni Valley is characterized by the presence of a forest composed mainly of Swiss stone pine, while the proglacial area, considering the last 2 km that until the end of the PEG was covered by the Forni Glacier, is characterized by an arboreal coverage mainly represented by European larch

(*Larix decidua*, Mill.) and Norway spruce (*Picea abies*, L.) and less frequently by Swiss stone pine (*Pinus cembra*, L.), Mountain pine (*Pinus mugo*, Turra) and birch (*Betula pendula*, Roth), with a discrete density that gradually decreases moving close to glacial tongue, due to the time elapsed since the glacier retreat and thus the tree-settling (Bonetti, 2013). Near the glacier tongue only the European larch, the Norway spruce and rarely the beech are found (Bonetti, 2013).

3.1.7 Human presence

The proofs of human presence on the Alps are numerous throughout the Holocene. However, with the late Neolithic period and the beginning of the Bronze Age (between 4700 BC and 3500 BC), human impact begins to become important, as several studies have suggested in the Central and Western Alps (Gobet et al., 2003; Moe et al., 2007) and in the eastern Alps, the Prealps and Dolomites (Fedele, 1981, 1990). The human impact remains almost unchanged during the Iron Age and in Roman and Medieval epoch (Filippi et al., 2005; Moe et al., 2007). Near to the study site, at the Passo Gavia (2360 m a.s.l.), the presence of man is testified from the discovery of lithic artefacts (Angelucci et al. al., 1993). It is a site attributed to the mesolithic sauveterrian, based on the discovered lithic industry, which can be dated between the Preboreale and the Boreale; frequented by man at a time of strong glacial retreat (Orombelli & Porter, 1982) during a favourable climatic phase that would allow the penetration of mesolithic hunters up into the inner portion of the Alpine chain.

Moreover, during the XX century, the Forni Glacier was the scene of an important event in Italian history during the First World War, when battles were fought on the glacier surface and on the mountain ridges overlooking the glacier valley (Garavaglia et al., 2012); therefore the remains of the First World War fortifications and trenches can be observed.

Nowadays, the human impact in the Forni glacier area is mainly for tourism, whereas in the Mt. Confinale study site, the irregular conditions of the surface and the difficult accessibility probably prevented intensive exploitation of the area in previous centuries. However, at a distance of 1500 m east from the study site, there is a barn (2213 m a.s.l.) and an alpine pasture where cows graze during the summertime (Leonelli et al., 2016).

3.2 Results

3.2.1 Sub regional scale analysis

Overall, at the sub-regional scale the site conditions of 1814 trees along 360 km of treeline were analysed in the Upper Valtellina region. Based on the three main environmental factors (geomorphology, climate, and human impacts) affecting trees at the highest elevations, it was found that the treeline is mainly limited by geomorphological processes and features, and, to a lesser extent, by climate and human impacts (fig. 3.5). Out of a total of 1814 mapped trees, 1493 (82%) are influenced by geomorphological constraints, 271 (15%) by climate constraints and 50 by human impacts (3%; fig. 3.5).

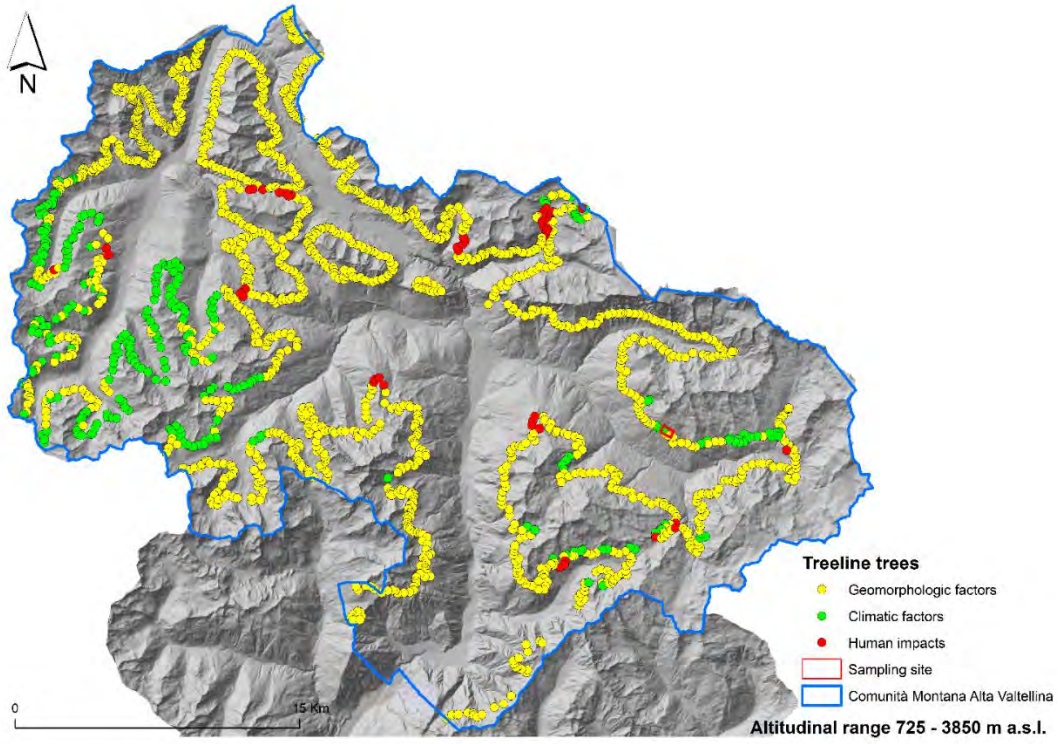

Figure 3.5. Treeline position in the Upper Valtellina region (inner portion of the Alpine range), differentiated by geomorphological constraints (yellow dots), climatic constraints (green dots) and human impacts (red dots) (see Methods section). The red rectangle corresponds to the sampling site of Mt. Confinale where the treeline altitudinal dynamics were assessed with a tree-ring based approach (from Leonelli et al., 2016).

Treelines with trees limited by geomorphological constraints are evenly distributed throughout the study area, with the exception of the western sector, and are mainly located in a belt between 2530 and 2175 m a.s.l., with an average elevation of 2355 m a.s.l. (fig. 3.5 and tab. 3.1). Treelines limited by climatic constraints are found at higher elevations, mainly on the west side of the Upper Valtellina and sparsely in the east side in a belt between 2605 and 2445 m a.s.l., with an average elevation of 2530 m a.s.l.. Treelines disturbed by human impacts are distributed through the whole study area, with a slightly higher

presence on the north side, and are located in a belt between 2500 and 2215 m a.s.l. with an average elevation of 2335 m a.s.l..

Frequency distributions of the three topographic variables (elevation, slope, and aspect) were obtained for the whole study area and in detail for the sites affected by the three considered main environmental factors (geomorphology, climate, and human impacts). For the elevation variable, geomorphological constraints had almost no effect on the frequency distribution of trees, as the distribution of elevations for trees affected by geomorphological constraints is almost symmetrical around the mean and is similar in shape to the distribution of elevations of all trees studied (fig. 3.6 a). In contrast, climatic constraints appear to strongly affect the shape of the frequency distribution, which is slightly negatively skewed and for which no trees below 2400 m a.s.l.were identified (fig. 3.6 a).

	Geomorphological constraints (m a.s.l.)	**Climatic constraints (m a.s.l.)**	**Human impacts (m a.s.l.)**
Mean elevation	2355 ± 100	2530 ± 50	2335 ± 80
Maximum elevation	2530 ± 30	2605 ± 10	2500 ± 65
Minimum elevation	2175 ± 55	2445 ± 20	2215 ± 10

Table 3.1. Mean elevation of the treelines limited by geomorphological constraints, climatic constraints and human impacts; maximum and minimum elevations were calculated as the average values of 10% of the trees at the highest and lowest elevations, respectively. Values are reported to the nearest 5 m with an error of 1 standard deviation (from Leonelli et al., 2016).

The frequency distributions for topographic variables at sites with human impacts appear to differ from those based on all sites in the study area, but there were only few cases to analyze. For the slope variable (fig. 3.6 b), only the geomorphological constraints show no effect on the frequency distribution of trees, while climatic constraints (and human impacts) have similar frequency distributions but only included trees growing on slopes with inclinations <45° (<40°, respectively). For the aspect variable (fig. 6 c), the more uniform (rectangular) shape of the frequency distribution over the study area is reflected in the distributions of aspects of the sites attributed to each of the three environmental factors, with differences in the modes only in some class intervals. The chi-square ($\chi 2$) tests, used to evaluate the association between the three topographic variables and the three environmental factors, are performed after subdividing the dataset into 10 class intervals (see methods section). The $\chi 2$ values obtained for the topographic variables are all significant at the $p < 0.005$ level; the $\chi 2$ value for elevation is 5.8 times greater than the value for slope and 15.9 times the value for aspect (tab. 3.2).

A high degree of association is found between elevation and the three environmental factors (Cramer's V = 0.49), and elevation is strongly associated with climatic constraints, as evidenced by the large separation of its cumulative curve compared to those for the other two environmental factors (fig. 3.7).

	χ^2
Elevation	855.31
Slope	147.56
Aspect	53.683

Table 3.2. Values of chi-square (χ^2) tests obtained by analyzing the association between the three topographic variables and the three environmental factors (χ^2 = 37.156; degrees of freedom = 18, p=0.005) (from Leonelli et al., 2016).

Under climatic constraints, 100% of trees grow at elevations above class 5 (>2400 m), while approximately half of trees under geomorphological constraints and 38% of trees affected by human impacts grow above the elevation defined by this class. The slope variable and the three environmental factors are less strongly associated (Cramer's V = 0.20), as reflected by the smaller separation in their cumulative curves. However, geomorphology shows a distinction with respect to the other two considered environmental factors, with up to 56.7% of trees growing on extreme slopes above class 5 (>30°). In contrast, only 29.1% of trees under climatic constraints grow on slopes >30°, and none above 45°; and only 20% of trees influenced by human impacts grow on slopes >30°, and none above 40°. Aspect shows the lowest association with the environmental factors (Cramer's V = 0.12) and is almost evenly distributed in all classes.

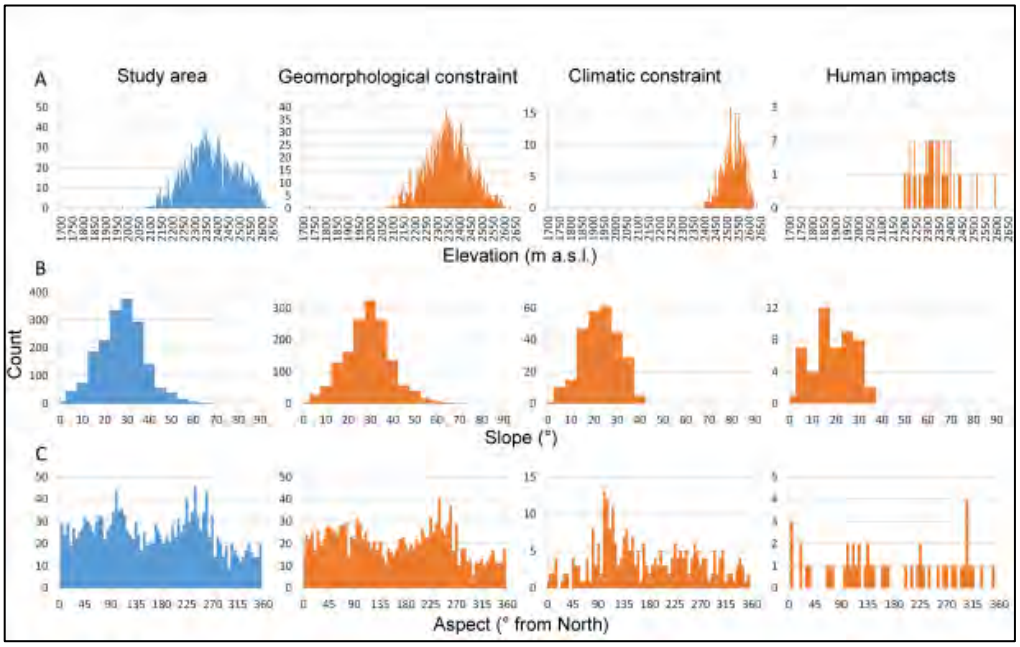

Figure 3.6. Frequency distribution of the three topographic variables (A) elevation, B) slope and C) aspect) for the analyzed treeline trees over the entire study area and subdivided by the three environmental factors limiting the treeline elevation (geomorphological constraints, climatic constraints and human impacts) (from Leonelli et al., 2016).

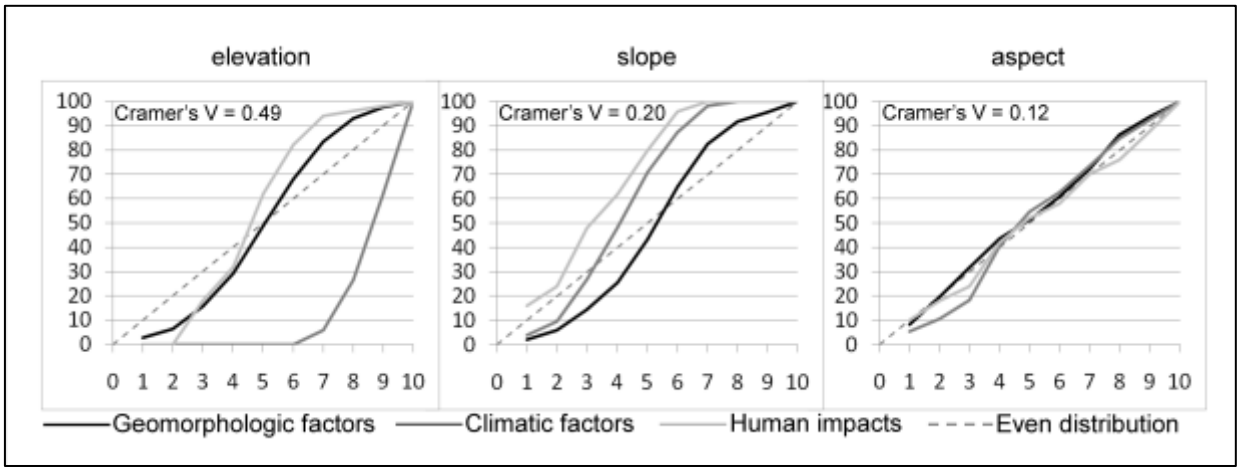

Figure 3.7. Cumulative percentages of the three topographic variables, elevation, slope and aspect, in the 10 classes into which treeline trees were subdivided (see methods). For each graph, the corresponding Cramer's V value derived from the chi-square analysis is also reported (ranging from 0 = no interrelation to 1 = perfect interrelation between the topographic variables and the distribution of treeline trees) (from Leonelli et al., 2016).

Overall, the influence of geomorphological processes on the position of 1493 treeline trees with geomorphological constraints were analyzed in the study area (fig. 3.8). The data obtained after the analysis of the correspondence between tree location, morphogenetic landforms and active geomorphological processes indicate, in general, that the treeline trees limited by geomorphological constraint are located at an average altitude lower than the treeline trees undisturbed by geomorphological processes (tab. 3.1).

The results highlight how different surface processes influence the treeline position and its altitudinal dynamics. Of the 1493 mapped trees belonging to the geomorphological treeline, 1301 (87%) are limited in their position by gravitational processes, 125 (8%) by processes due to running and/or channelized water and 67 (5%) by periglacial processes (fig. 3.8). Gravitational processes are the most important processes influencing the dynamics of geomorphologically constrained treelines. Active depositional landforms, such as debris cones, talus slopes, scree slopes, and debris flow deposits, represent the main disturbances causing a lower altitude of a geomorphologically constrained treeline.

In particular, the presence of merging deposits due to gravitational processes (e.g., merging talus cones and wide scree slopes) heavily limits the treeline altitude (mean elevation: 2300 m a.s.l.; tab. 3.3), whereas the presence of isolated depositional landforms seems to be less influential (mean elevation: 2389 m a.s.l.; tab. 3.3). Running water (e.g., rain wash and rill erosion) induces differentiated soil erosion, forming gullies and eroded slopes on which tree colonization may be very difficult. Rill erosion has less impact on the treeline (mean elevation: 2438 m a.s.l.) than gully erosion (mean elevation: 2376 m a.s.l.). Nevertheless, depositional landforms resulting from the action of water (i.e., small fans or mixed cones) are able to limit the treeline altitude (mean elevation: 2311 m a.s.l.; tab. 3.3). Periglacial

processes have a minor impact on the treeline. The presence of periglacial landforms, such as rock glaciers, has only a minor limiting factor (mean elevation: 2419 m a.s.l.; tab. 3.3).

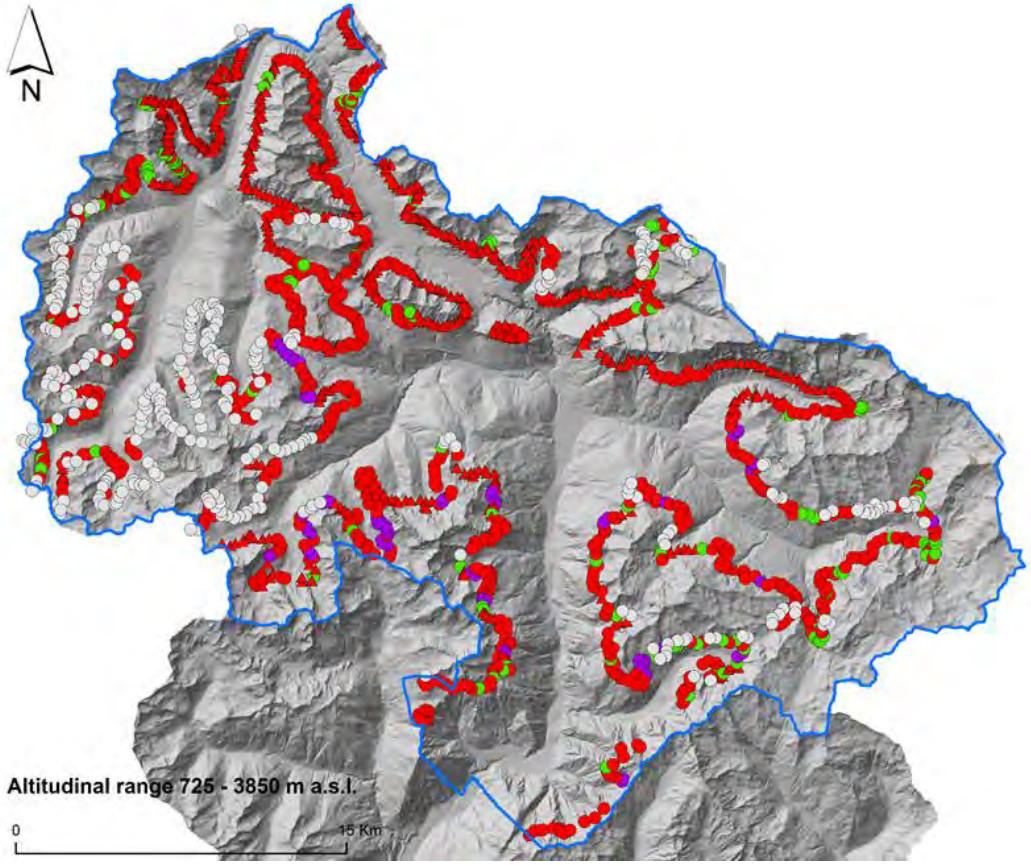

Figure 3.8. Treeline position in the Upper Valtellina region, differentiated according to the main processes influencing its position: surface areas affected by running and/or channelized water processes (green dots); isolated deposits due to gravitational processes (red dots); merging deposits due to gravitational processes (red triangles); and periglacial processes (violet dots). The grey dots depict the treelines limited by human impacts or the climatic treelines (modified from Masseroli et al., 2016).

	Isolated gravity deposits	Merging gravity deposits	Gullies	Rills	Alluvial fans	Rock Glaciers
Treeline mean elevation	2389 ± 87	2300 ± 97	2376 ± 84	2438 ± 63	2311 ± 87	2419 ± 73
Treeline ecotone mean width	183 ± 104	83 ± 94	177 ± 116	229 ± 50	155 ± 86	231 ± 78

Table 3.3. Mean elevation of the treeline trees limited by geomorphological factors and mean width of the treeline ecotone. The treeline trees are grouped according to the landforms modelled or built by the processes most effective in influencing the treeline position. Values (m a.s.l.) are reported with an error of ±1 standard deviation (from Masseroli et al., 2016).

Based on a comparison of the altitude of treeline trees in the analyzed portion of Upper Valtellina and the “disturbing factors”, it is evident that treeline trees limited by gravitational processes are the most

widespread (fig. 3.8). The treelines limited by isolated landforms due to gravitational processes are mainly located in an elevation belt between 2133 and 2634 m a.s.l.. Moreover, the treelines limited by merging deposits due to gravitational processes are mainly located in the northern portion of the study area and in an elevation belt between 1732 and 2587 m a.s.l. (fig. 3.9 a). In addition, the treelines affected by running and/or channelized water processes, although less common, are distributed throughout the entire study area. Treelines limited by gullies and by alluvial cones are located between 2185 and 2582 m a.s.l. and between 2142 and 2480 m a.s.l., respectively. Rill erosion influences only a few treelines and was found in a small altitudinal range (between 2339 and 2558 m a.s.l.) Rock glaciers affect the treelines located between 2276 and 2604 m a.s.l. mainly in the southern part of Upper Valtellina (fig. 3.9 a).

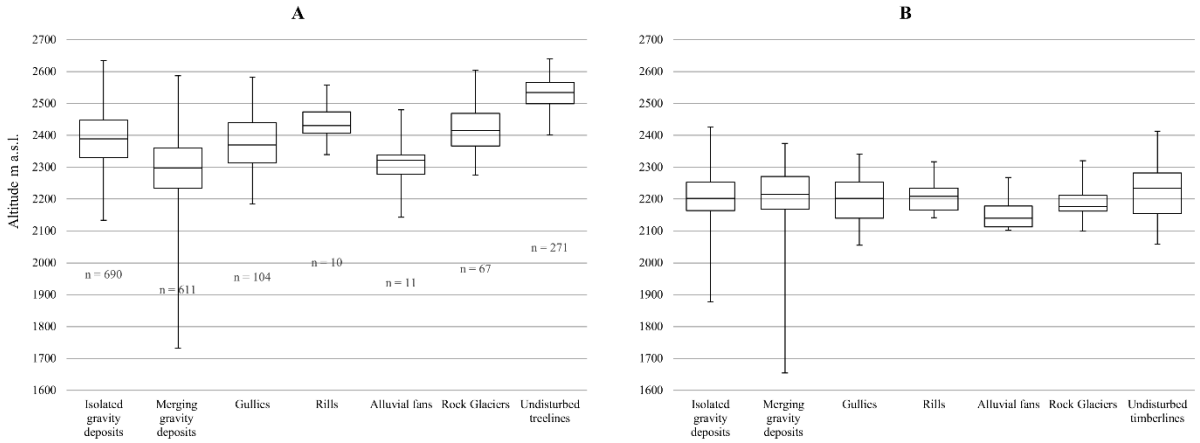

Figure 3.9. Distribution of treeline and timberline elevation. a) Treeline trees were grouped in relation to the different landforms and geomorphological processes responsible for their position. The data on undisturbed treeline elevation was taken and modified from Leonelli et al., (2016) (see "climatic treelines"). The whiskers of the boxplots correspond to minimum and maximum values. For each landform group, the number of affected trees is specified (n). b) Timberline trees were grouped in relation to the different landforms and geomorphological processes affecting the treeline ecotone. The whiskers of the box plots correspond to minimum and maximum values (from Masseroli et al., 2016).

Nevertheless, the altitude of the timberline trees limited by geomorphological processes is only slightly lower than that of the undisturbed timberline (fig. 3.9 b). Moreover, the type of geomorphological processes does not seem to affect the position of the timberline; in fact, the median altitude value of the distribution of the timberline trees is approximately the same for all the different classes of landforms. However, the distribution of timberline trees affected by gravitational processes (and related geomorphic evidence) show greater low-altitude variability than that of the landforms associated with running and/or channelized water or cryogenic landforms (as evidenced in fig. 3.9 b). Furthermore, only the altitude of timberlines associated with alluvial fans seems to be influenced by geomorphological processes. These observations show that, in most cases, geomorphological processes control the position of the treeline altitude (they prevent potential upward shifts) but not the position of the timberline altitude. Moreover,

the treeline ecotone influenced by geomorphic processes has a smaller width than does the undisturbed treeline ecotone (fig. 3.10). In fact, in areas where the treeline is limited by merging deposits due to gravitational processes, the treeline and the timberline altitudes are approximately the same (mean width of the ecotone: 83 m; tab. 3.3). In some cases, the width of the treeline ecotone is reduced to zero (fig. 3.10), and the treeline overlaps the timberline (fig. 3.10). In contrast, in areas where geomorphological processes have less of an impact on the position of the treeline, the treeline ecotone is wider. For example, in areas where the treeline altitude is limited by the presence of rock glaciers or rills, the treeline ecotone has a mean width of 231 m and 229 m a.s.l., respectively (tab. 3.3).

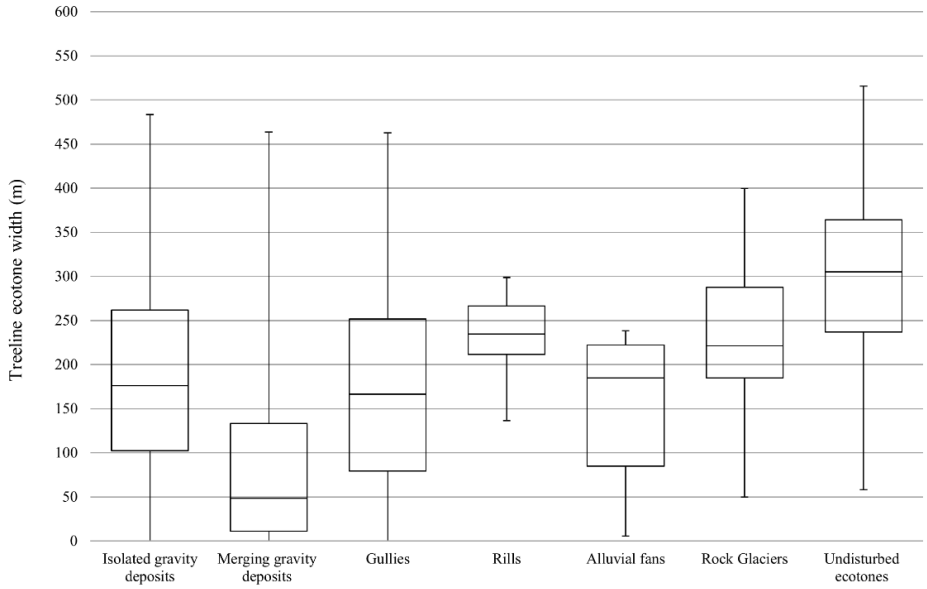

Figure 3.10. Distribution of treeline ecotone width, grouped according to the different landforms and geomorphological processes responsible for their positions, and the undisturbed ecotone. The whiskers of the box plots correspond to minimum and maximum values (from Masseroli et al., 2016).

Finally, the chi-square tests (tab. 3.4) show that the geomorphological processes may alter the frequency distribution of trees (fig. 3.11). The chi-square test that took into consideration the frequency distributions of all landform types and the different classes of landforms (landforms due to running and/or channelized water, landforms due to gravity and landforms due to cryogenic processes) is significant at the $p<0.005$ level (tab. 3.4). The chi-square value obtained for the comparison of the elevation of the trees limited by the merging and isolated gravity deposits is also significant at the $p<0.005$ level (tab. 3.4). On the contrary, the value of the frequency distribution of landforms due to running and/or channelized waters (gullies, rills and alluvial cones) from the chi-square test is not significant at the $p<0.005$ level (tab. 3.4).

	χ^2	d.f.	P	χ^2 Critical values
All the landforms	363	45	0,005	73
All the classes	52	18	0,005	37
Landforms due to running and/or channelized water	36	18	0,005	37
Merging and isolated gravity deposits	276	9	0,005	24

Table 3.4. Values of chi-square tests obtained by analysing the association between the landforms due to different processes that limit the treeline position and the elevation (from Masseroli et al., 2016).

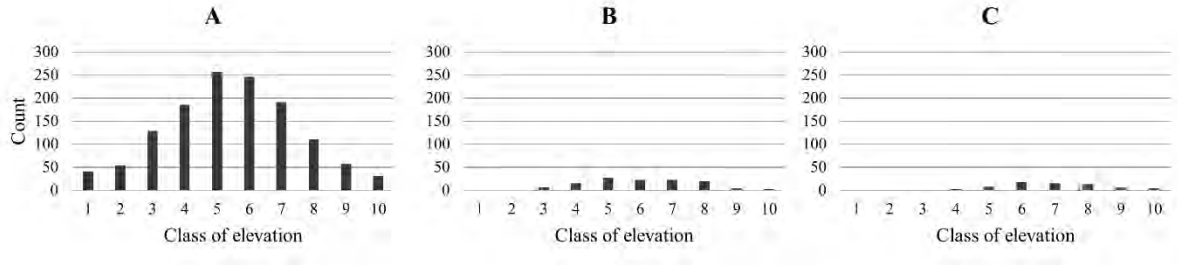

Figure 3.11. Distribution of the elevation variable for the analysed treeline trees subdivided by the three classes of landforms limiting the treeline elevation: (A) landforms due to gravity, (B) landforms due to running and/or channelized water, and (C) cryogenic landforms (from Masseroli et al., 2016).

3.2.2 Site scale analysis: Mt. Confinale study case

3.2.2.1 Reconstruction of treeline position on Mt. Confinale

At the local scale, at the Mt. Confinale site, the upward shift through time in the treeline elevation was assessed by analyzing tree age distribution on the slope (fig. 3.12 a). Trees are clustered at elevations above 2545 m a.s.l., which reflects the typical distribution of *P. cembra* in groups growing in small niches on rocky substrates, where fine debris accumulates and initial soils may develop. Interestingly, areas with alpine grass at the same elevations do not have any trees. The treeline elevation over time (based on the years in which the trees reached 2 m in height) increased from 2505 m a.s.l. (period 1990–1999) to 2531 m a.s.l. (period 2000–2009) to 2545 m a.s.l. (in 2013) (fig. 3.12 b). The species line for *P. cembra* at this site is found at 2605 m a.s.l., as determined by saplings and seedlings growing at the highest elevations (fig. 3.12). This elevation is similar to the modelled elevation of the potential treeline PT20 (2600 m a.s.l.) based on an average of 100 days/year with temperatures above 5 °C for the period from 1994 to 2013. The number of days with a temperature above 5 °C has markedly increased over

time at the PT20 elevation, going from approximately 80 days in 1994 to approximately 120 days in 2013 (fig. 3.4).

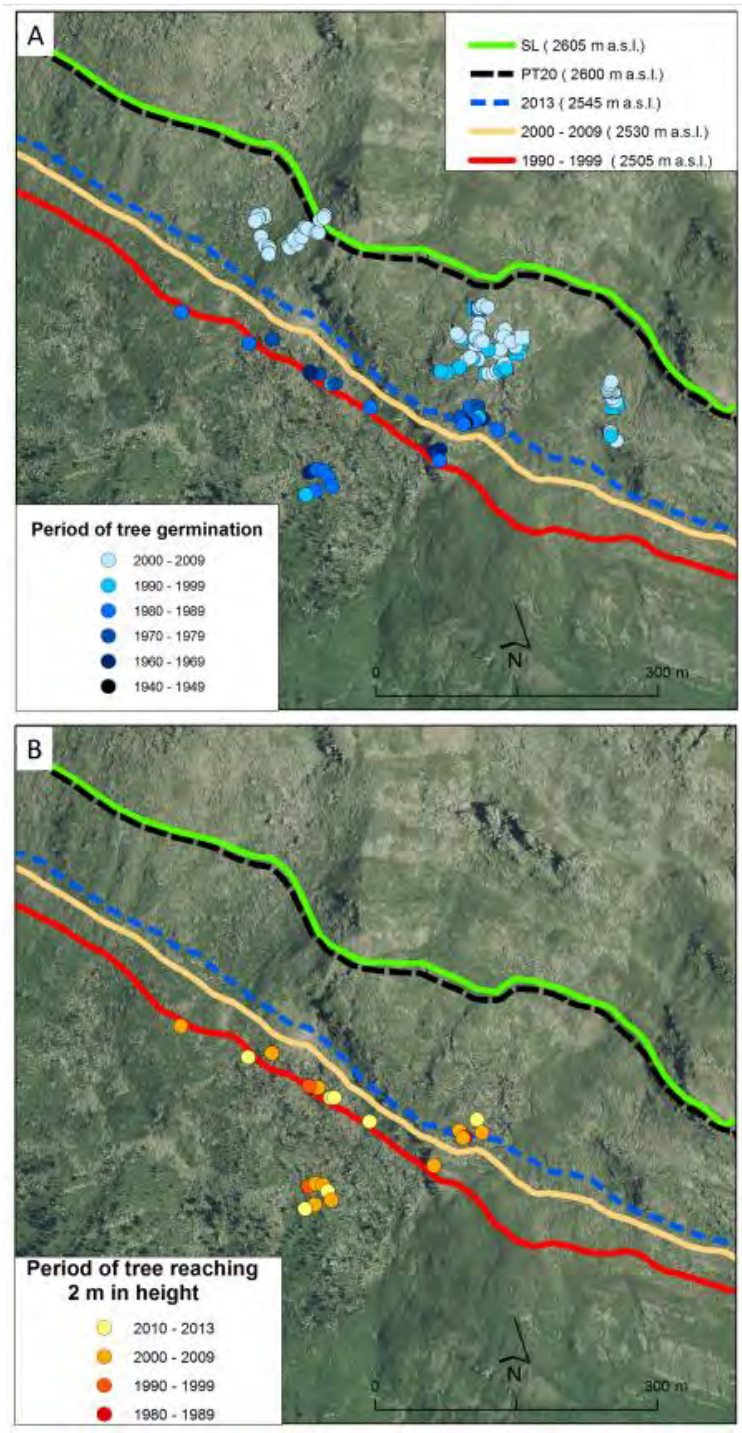

Figure 3.12. The figure depicts the treeline elevations for the periods from 1990-1999, 2000-2009 and in 2013, as well as the Potential Treeline 20 (PT20) and the Species Line (SL) in 2013. The ortophoto has been drawn up from spatial data available at the National Geoportal website www.pcn.minambiente.it. a) Distribution and periods of germination for the sampled trees at the treeline in the Mt. Confinale study site. The colors refer to the germination periods, subdivided into 10-year classes since 1940. Circles refer to Pinus cembra specimens (n = 119), triangles to Larix decidua (n = 4, not visible) and the squares to Picea abies (n = 7). b) Distribution of the sampled trees and periods when reaching 2 m in height, subdivided into 10-year classes since 1980 (from Leonelli et al., 2016)

3.2.2.2 Results of geopedological analysis at Mt. Confinale study site

A field and laboratory characterization of a transect of nine soil profiles developing at an altitude ranging from 1800 m a.s.l. (closed forest) to 2600 m a.s.l. (species line) were performed, in order to understand the relationship between colonization by arboreal vegetation and soil development (fig. 3.13).

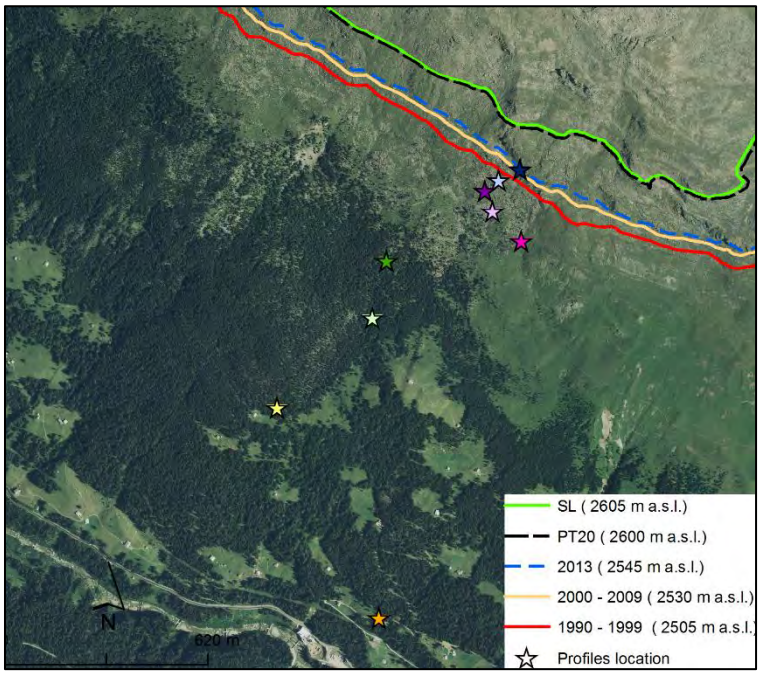

Figure 3.13. Profiles location and treeline position.
The orthophoto has been drawn from spatial data available at the National Geoportal.

3.2.2.2.1 Field data

The first five soil profiles (C15/01, C15/02, C15/03, C15/04 and C15/05) are located in the treeline ecotone, while the other four profile (CF 01, CF 02, CF 03 and CF 04) are placed in the forested area. All the soil profiles have the same parent material characterized by micaschists (OME). From the geomorphology point of view, all the profiles are located in an area with morenic and gravity deposits (fig. 3.13, tab. 3.5).

Profile thickness assumes variable values (usually 0.3 to 1 m) depending on the altitude range and vegetation cover. In fact, maximum thickness is found in correspondence of soils evolved in forested area and the minimum thickness is found in correspondence of soil evolved in the treeline ecotone.

The colour of the horizons belong the soil developed in forest area shows a clear uniformity in the area, particularly as regards the hue values, that is never different from 10 YR or 2.5 Y. Instead the colour of the horizons belong to the soil developed in the treeline ecotone have higher variability in the hue values.

Soil structure is moderately expressed, at the treeline ecotone the soil are mainly characterized by granular aggregates while the soil developed in forest are characterized by subangular blocky aggregates (Appendix 1).

Profile	Elevation (m a.s.l.)	Inclination (°)	Slope exposure	Profile exposure	Parent Material	Geomorphology	Vegetation
C15/01	2537	5	SW	N	Micaschists (morenic deposits)	Slope deposits and relict DSGSD	Treeline ecotone composed of open *Pinus cembra* stands
C15/02	2485	5	SW	W	Micaschists (morenic deposits)	Slope deposits and relict DSGSD	Treeline ecotone composed of open *Pinus cembra* stands
C15/03	2460	29	S-SW	S	Micaschists (morenic deposits)	Slope deposits and relict DSGSD	Treeline ecotone composed of open *Pinus cembra* stands
C15/04	2440	5	S-SW	S	Micaschists (morenic deposits)	Slope deposits and relict DSGSD	Treeline ecotone composed of open *Pinus cembra* stands
C15/05	2413	22	S-SW	S	Micaschists (morenic deposits)	Slope deposits and relict DSGSD	Treeline ecotone composed of open *Pinus cembra* stands
CF01	2300	35	W	W	Micaschists (morenic deposits)	Slope deposits and relict DSGSD	Forest
CF02	2170	40	W	W	Micaschists (morenic deposits)	Slope deposits and relict DSGSD	Forest
CF03	2030	10	SW	E	Micaschists (morenic deposits)	Slope deposits and relict DSGSD	Forest
CF04	1802	30	W	W	Micaschists (morenic deposits)	Slope deposits and relict DSGSD	Forest

Table 3.5. Station descriptions for the studied profiles.

3.2.2.2.2 Particle size analysis

Examining the relative percentages of particle size distribution in the analyzed soil profiles it can be seen that there is a common trend. First, the gravel and the sand content are higher compared to the silt and clay content. In fact, the amount of gravel and sand reach the 50% on total weight (fig. 3.14). In all soil samples, gravel and sand are the predominant fractions, while the amount of silt and clay is more variable. The silt rarely exceed 35% on the total weight, while clay never exceed 25%. In deeper

horizons, the percentages of gravel and sand tend to increase to the detriment of the clay component (fig. 3.14). In no profiles, trend anomalies are found.

In the C15/02 and CF01 profiles, the content of coarse fraction has a visible increasing trend with depth, as well as a progressive decreasing trend of the clay. The main anomaly is represented by the superficial horizons, which contains a lot of sand. The deepest horizons show a lower sand content than the above horizons (fig. 3.14), and the fine fractions has a slight increase.

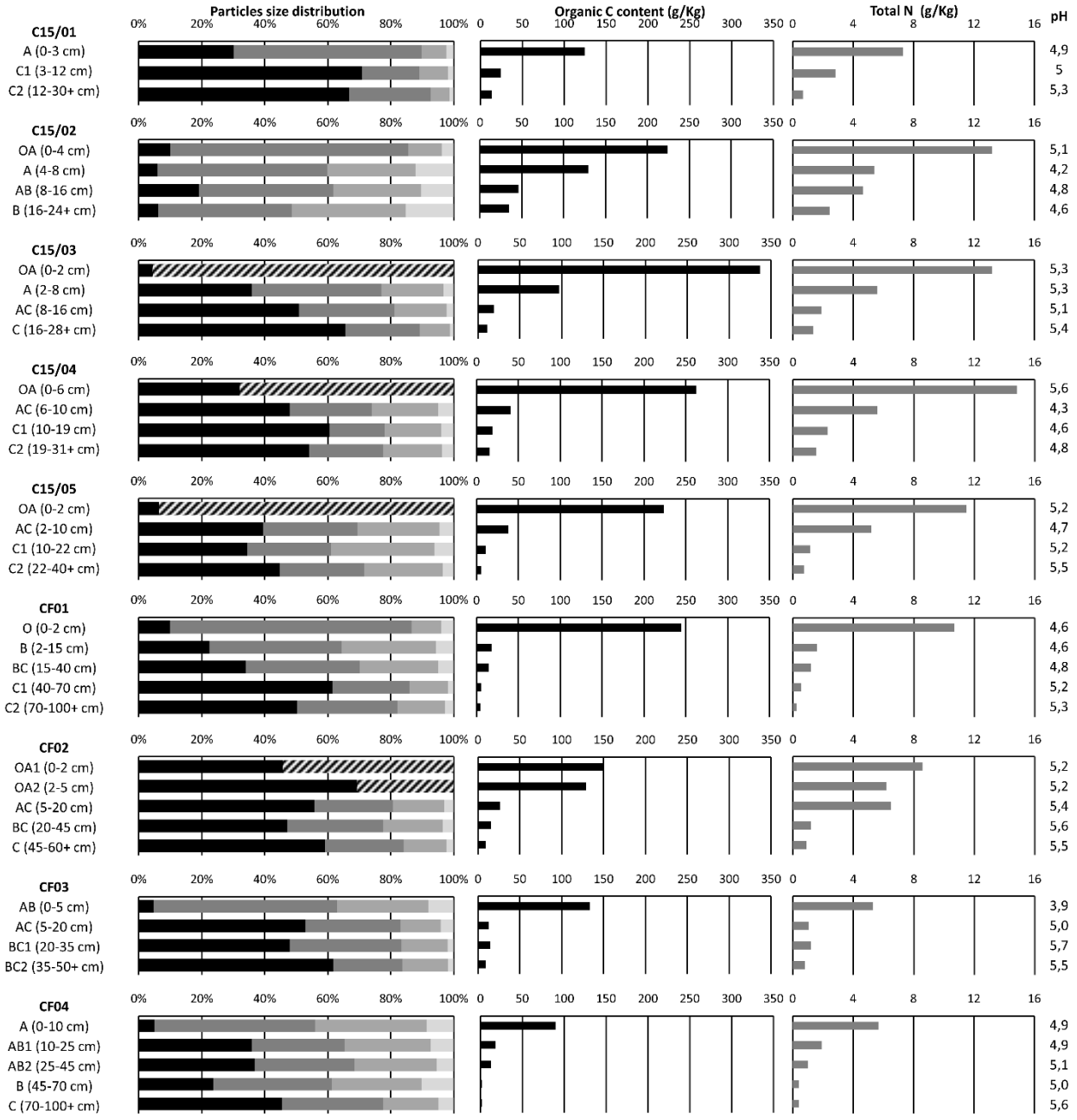

Figure 3.14. Particle size distribution, Organic C content, total Nitrogen content and pH values in the studied profiles. For the particle size distribution plot: in black is depict the gravel content, in dark grey the sand content, in grey the silt content. in light grey the clay content and in black strips the n.d..

3.2.2.2.3 Organic Carbon Content

The absolute quantities of organic carbon are very variable depending on the type of profile and depth (fig. 3.14). In surface horizons, values ranging between 89 g/Kg (CF O4) and over 300 g/kg (C 15/03) are found. Usually, the C organic values decrease with depth: the general trend is therefore represented by a decrease of organic carbon content as horizons get deeper. This decrease can be more or less gradual, as in profile C15/02, or concentrated as a rapid loss at the transition from the uppermost horizon to the ones those below, such as in the profiles C15/05 and CF01.
All the profiles show the same trend, characterized by a decreasing in C content with depth, except the CF03 profile. In this profile the AB horizon shows a greater C organic content then the above horizon (A), while in the underlying horizon the value return to decrease.

3.2.2.2.4 Total Nitrogen

The total nitrogen contents have the same trend of the organic C content (fig. 3.14), but with significantly lower values (not exceeding 15 g/Kg). In almost all the studied profiles the total nitrogen content decreases with depth along the profile, but two exceptions are found (CF02 and CF03). The decrease is concentrated as a rapid loss at the transition from the uppermost horizon to the ones those below, while in the underlying horizons the decrease is more gradual.
Among the organic horizons, those belong to the C15/02, C15/03 and C15/04 have the highest N content (about 13-14 g/Kg), while the lowest values are recorded in CF03 (about 5.3 g /Kg). Similar trend anomalies may also be recognized to those underlined for organic C content in the CF03 profile.
Finally, the C/N ratio have a high values (over 15 g/Kg) in the superficial horizons. Generally decrease with depth, except in the C15/01 and CF01 profiles, where the last horizon have approximately the same C/N ratio than the superficial horizon (fig. 3.15).

3.2.2.2.5 pH

All the soil horizons analyzed have a tendency to acidity, the pH in H_2O never reaches the neutrality and the values of pH in H_2O ranging between 3.9 and 5.7 (fig. 3.14). In particular, the superficial horizons belong to soil developed in forest have low values of pH than the superficial horizons belong to soil developed in the treeline ecotone.
Although, the pH values measured in H_2O neither get large variations between successive horizons nor within the entire depth of profile, in most of the analysed profile the pH values progressively increase with the profile depth, approaching to the parent material. In many cases, this variation seems to be very

moderate; being rarely more than 1 pH unit and for the profile under forest vegetation the variation is more pronounced than for the profile located in the treeline ecotone. In the C15/05 profile the most superficial horizons showing a lower acidity than the immediately below horizons, with pH values greater than 5.

However, in the C 15/02 and C15/04, the pH values seem to oscillate independently of the depth, and no well-defined pattern can be recognized.

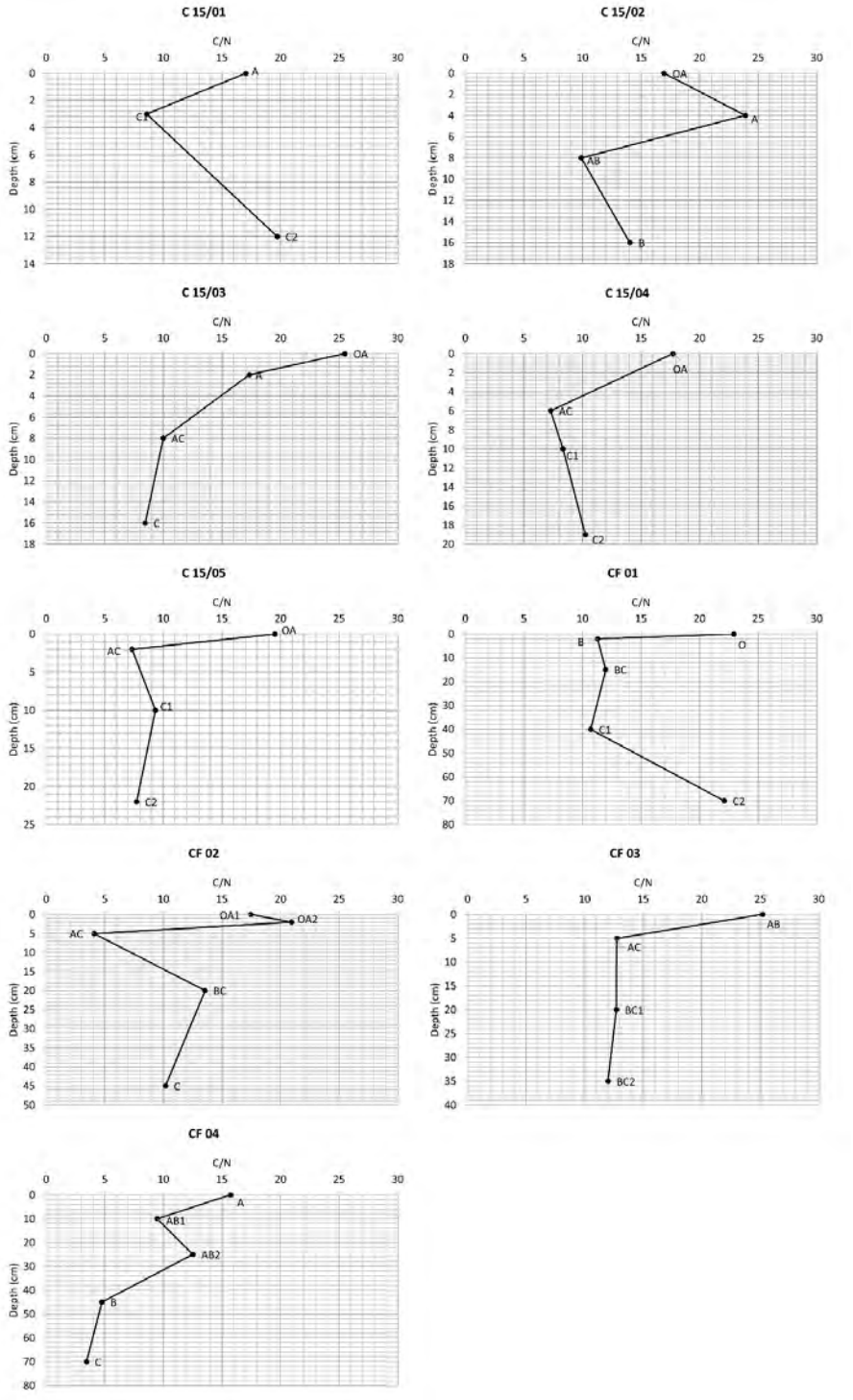

Figure 3.15. C/N ratio in the studied profiles.

3.2.2.2.6 Alluminum and Iron extractions

The total content of free iron oxides (Fed) in one horizon (CF03 AC) reaches 52 g/Kg but generally ranging between 10 and 30 g/Kg (fig. 3.16). The values of amorphous iron oxides (Feo) tend to be lower, between 1.5 and 13 g/Kg, as well as iron bound with the organic matter (Fep). For all three of these parameters, particularly high values are observed in CF03 AC, CF03 BC1, CF02 C, CF02 AC, CF04 AB1 and C15/03 OA horizons (fig. 3.16).

As regards the aluminum oxides content, the quantities tend to be inferior to those of iron oxides. Free aluminum oxides (Ald) reaches values between 1 to 10 g/Kg, aluminum amorphous oxides (Alo) between 1 and 8 g/Kg, and the aluminum bound with the organic matter (Alp) between 1 and 7 g/Kg.

Similarly to what has been observed for iron, different types of aluminum show similar trends and similar peaks along the profiles.

The crystalline iron oxides (Fed - Feo) are mainly concentrated in the C 15/03 A, CF02 AC, CF02C, CF03 AC, CF03 BC1 and CF 03 BC2 horizons (tab. 3.6). Instead, the OA horizons have lowest value of crystalline iron oxides. On average, the profiles excavated in forested area (CF) have higher quantity of crystalline iron oxides than the profile excavated in the treeline ecotone (C 15).

The iron activity ratio (Feo/Fed index) ranging between 0.07 and 0.54, values above 0.5 are observed at C15/01 C1, C15/04 C2, C15/05 OA, C15/05 AC and CF 01 B. Very low values of iron activity index are found in the profile CF04 B and CF04 C (tab. 3.6). Finally, the results of the podzolization index Alo + ½ Feo meet the conditions of podzolization processes only in the cases of A and AC horizons of C 15/03 and CF03 AB and AC horizons (FAO, 2014).

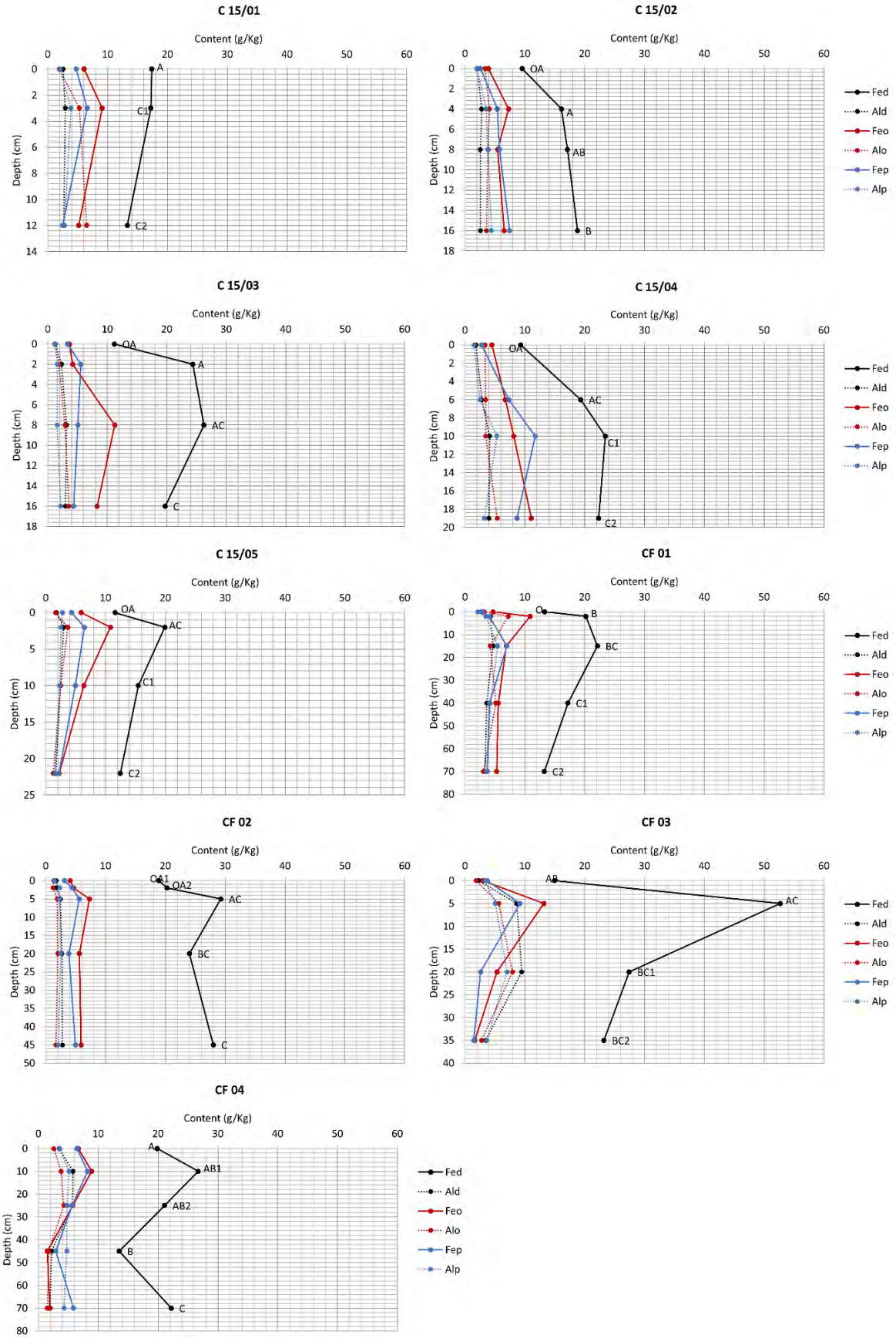

Figure 3.16. Free (Fed), amorphous (Feo) and bound to the organic matter (Fep) iron content, free (Ald), amorphous (Alo) and bound to the organic matter (Alp) aluminum content of the studied profiles The horizons name are close to the Fed curves.

Profile	Horizon	Depth (cm)	Fed-Feo (g/Kg)	Feo/Fed	Alo+1/2Feo (%)
C15/01	A	0-3	11.3	0.35	0.50
C15/01	C1	3-12	8.1	0.53	0.98
C15/01	C2	12-30+	8.1	0.39	0.91
C15/02	OA	0-4	5.6	0.41	0.53
C15/02	A	4-8	8.8	0.45	0.77
C15/02	AB	8-16	11.7	0.32	0.66
C15/02	B	16-24+	12.2	0.35	0.69
C15/03	OA	0-2	7.6	0.32	0.30
C15/03	A	2-8	20.2	0.17	0.40
C15/03	AC	8-16	15.0	0.43	0.85
C15/03	C	16-28+	11.4	0.42	0.77
C15/04	OA	0-6	4.8	0.48	0.56
C15/04	AC	6-10	12.6	0.35	0.68
C15/04	C1	10-19	15.3	0.35	0.75
C15/04	C2	19-31+	11.3	0.50	1.09
C15/05	OA	0-2	5.7	0.51	0.46
C15/05	AC	2-10	9.1	0.54	0.91
C15/05	C1	10-22	9.1	0.41	0.57
C15/05	C2	22-40+	10.2	0.18	0.24
CF01	O	0-2	8.6	0.35	0.55
CF01	B	2-15	9.3	0.54	1.27
CF01	BC	15-40	15.2	0.31	0.77
CF01	C1	40-70	11.6	0.32	0.79
CF01	C2	70-100+	7.9	0.40	0.57
CF02	OA1	0-2	14.8	0.22	0.34
CF02	OA2	2-5	15.6	0.23	0.36
CF02	AC	5-20	21.9	0.25	0.56
CF02	BC	20-45	18.4	0.23	0.48
CF02	C	45-60+	22.1	0.21	0.46
CF03	AB	0-5	12.0	0.20	0.34
CF03	AC	5-20	39.5	0.25	1.22
CF03	BC1	20-35	22.1	0.20	1.06
CF03	BC2	35-50+	21.6	0.07	0.36
CF04	A	0-10	13.2	0.34	0.59
CF04	AB1	10-25	17.8	0.33	0.82
CF04	AB2	25-45	15.3	0.27	0.71
CF04	B	45-70	12.0	0.11	0.24
CF04	C	70-100+	20.3	0.09	0.24

Table 3.6. Iron and aluminum indeces. Crystalline iron oxides (Fed-Feo), activity iron index (Feo/Fed) and podsolization index (Alo+1/2Feo).

3.2.2.2.7 Rock Eval data

In the I/R diagram the organic horizons have I-index values between 0.3 and 0.5 and a R-index between 0.35 and 0.5. While the B and C horizons have I-index values between -0.1 and 0.2 and a R-index between 0.5 and 0.7 (fig. 3.17). The CF04 B and C horizons slightly deviate from the trend of other B and C horizons and have a I-index values of about 0.3 and a R-index between 0.65 and 0.7.

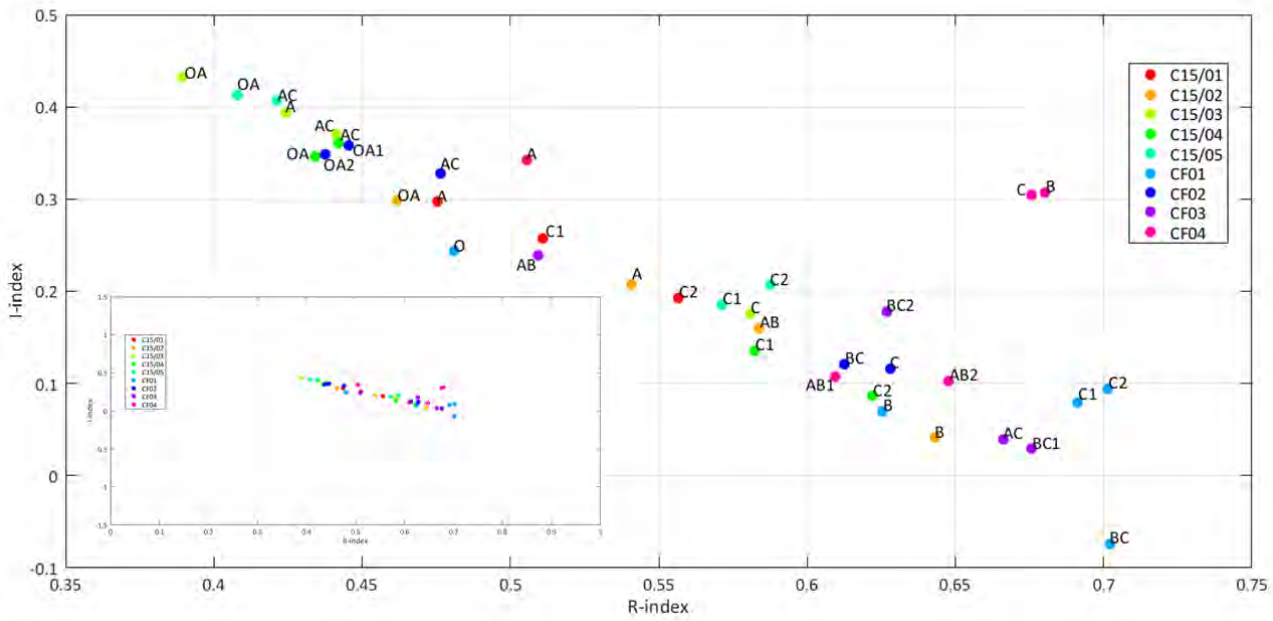

Figure 3.17. I-index/R-index. On the bottom left the data are plotted using the grid values from Sebag et al., 2016 in order to better visualize the trends.

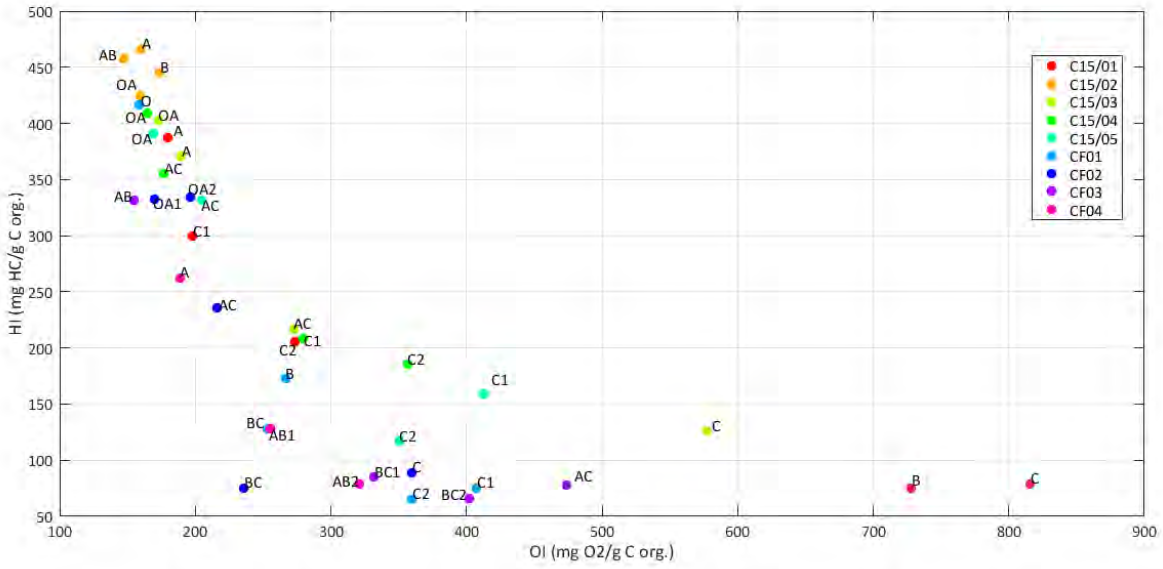

Figure 3.18. HI/OI diagram.

The HI/OI index shows different values in different horizons typology (fig. 3.18). In fact the O and A horizons show a high HI values and low OI values, while the B and C horizons show high OI values and

low HI values, in particular the CF04 B and CF04 C have high values of OI. Finally the AC and AB horizons have an intermediate values.

3.2.3 Site scale analysis: Proglacial area of Forni glacier study case

3.2.3.1 Results of geopedological analysis at Forni proglacial area study site

Aiming to explore the geo-ecological succession in the proglacial area of the Forni glacier, the soils developed on different regression moraines were investigated. At the Forni Glacier, the ongoing rapid glacial retreat is creating a wide proglacial area while the major late Holocene advances are marked by frontal moraines dated to AD 1859, 1913-14, 1926 and 1980 (fig. 3.19). Two or three soil profiles for each regression moraine are excavated and sampled, in order to understand the effects of time and vegetation primary succession on soil development.

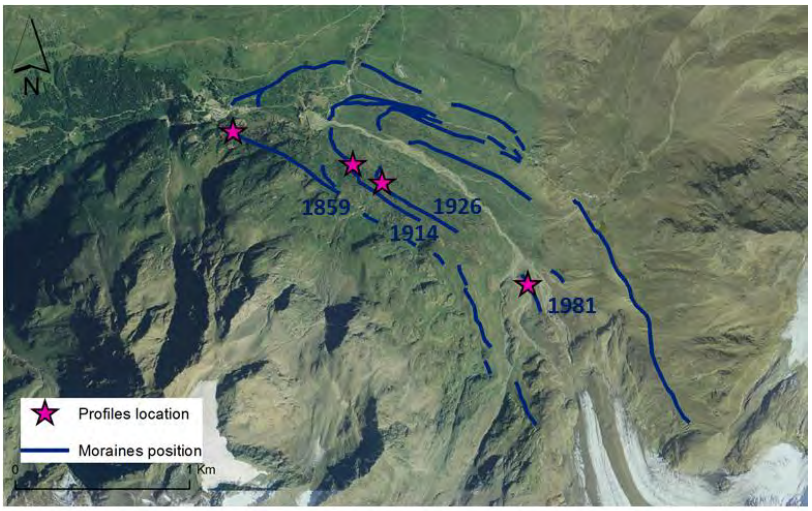

Figure 3.19. Regression moraines position and approximate profiles position on different moraines. The orthophoto has been drawn from spatial data available at the National Geoportal.

3.2.3.1.1 Field data

The profiles are excavated in different portion of different regression moraines. In particular the P01, P02, P03 and P05 profiles are located respectively in the ridge, internal portion, terrace and external portion of 1926 regression moraine; the P06 and P07 profiles are located respectively in the ridge and internal portion of 1913-14 regression moraine; P08 and P09 profiles are located respectively in the internal portion and ridge of 1981 regression moraine; the PEGe, PEGd and PEGi profiles are located respectively in the external portion, ridge and internal portion of the 1859 regression moraine.

Therefore, all the soil profiles are placed on a moraine deposits and have the same parent material characterized by micaschists (OME) (fig. 3.2, tab. 3.7).

Profile thickness is little and assumes, generally, the same values in all the profiles and ranging between 0.16 to 0.50 m.

The colour of the sampled horizons shows a clear uniformity in the area, particularly as regards the hue values, that is never different from 10 YR, 2.5 Y or 5 Y.

Soil structure is weakly expressed and when present is mainly characterized by granular aggregates (Appendix 2).

Profile	Elevation (m a.s.l.)	Moraine deposition year	Inclination (°)	Slope exposure	Profile exposure	Profile location on the moraine	Parent Material	Vegetation
P01	2200	1926	5	N	SE	Ridge	Phyllades and micaschists	Shrubby
P02	2200	1926	5	N	E	Internal portion	Phyllades and micaschists	Shrubby
P03	2210	1926	5	N	E	Internal portion (terrace)	Phyllades and micaschists	Shrubby
P05	2200	1926	10	N		External portion	Phyllades and micaschists	Shrubby
P06	2210	1913-1914	10	NW		Ridge	Phyllades and micaschists	Shrubby
P07	2200	1913-1914	10	NW	W-NW	Internal portion	Phyllades and micaschists	Shrubby
P08	2335	1981	10	N-NW		Internal portion	Phyllades and micaschists	Grassland
P09	2335	1981	10	N-NW		Ridge	Phyllades and micaschists	Grassland
PEGe	2180	1859	30	NE	NE	Esternal portion	Phyllades and micaschists	Shrubby
PEGd	2180	1859	10	N	SW	Ridge	Phyllades and micaschists	Shrubby
PEGi	2180	1859	10	N	NE	Internal portion	Phyllades and micaschists	Shrubby

Table 3.7. Station descriptions for the studied profiles.

3.2.3.1.2 Particle size analysis

The relative percentages of particle size distribution in the analyzed soil profiles show a common trend. First, the gravel and the sand content are higher compared to the silt and clay content. In fact, the amount of gravel and sand reach more than 50% on total weight, except for the P05 2A and P03 O. The amount of silt and clay is more variable. The silt only in seven horizons (P03 O, P05 2A, P07 AC1, P08 C2, PEGe A, PEGe AC and PEGd AC) exceed 20% of the total weight, while clay exceed 10% only in two horizons (P03 O and P05 2A).

In all the analyzed soil profiles (except the P05) particle size distribution shows a standard trend, in fact in the deeper horizons the percentages of gravel and sand tend to increase to the detriment of the clay component (fig. 3.20, 3.21). Instead, in the P08 profile, although the content of coarse fraction has a visible decreasing trend with depth, as well as a progressive increasing trend of the clay, there is a trend anomaly represented by the superficial horizon, which contains lower content of silt and clay then the deeper horizons.

Analyzing the soil profile P05 it is noticed that coarse material (sand and gravel) increases with depth to the horizon AC, where it reaches about 75% of the sample total weight. Below the AC horizon, the sand and gravel have again very low values (horizon 2A, about 28%), that grow with depth: the coarse material in the deeper horizon (2C) represents approximately the 85% of the material. Moreover, silt and clay show a content peak (61.3 and 11.5% respectively) in the 2A horizon and tend to decrease in 2C deeper horizon, where they reach 12.9% and 3% respectively on the soil total weight.

Observing the cumulative curves of this profile (fig. 3.20), a granulometric discontinuity is highlighted. Curves related to 2A horizon show lower values of sand than the AC horizon above. It is therefore possible to detect a discontinuity in the granulometry trend within the profile located at the transition between AC and 2A horizons.

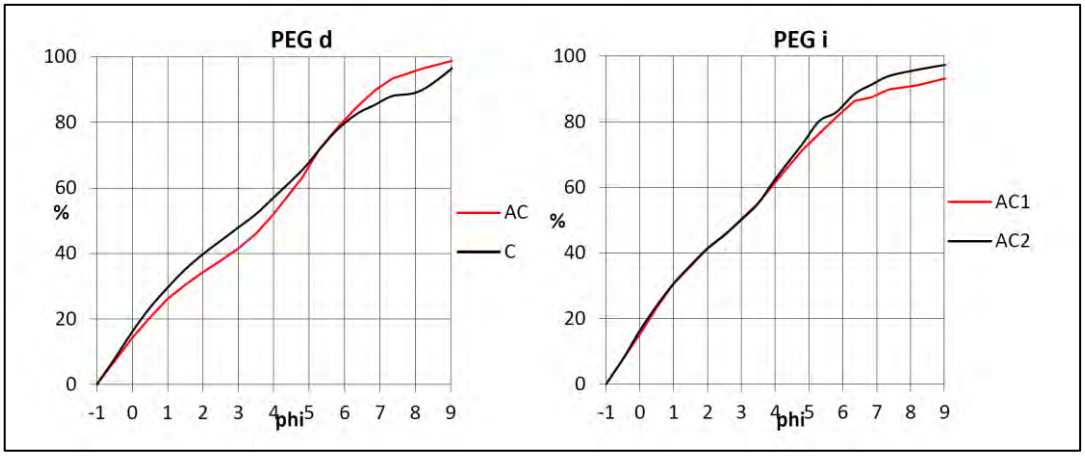

Figure 3.20. Cumulative curves of grain size distribution in the studied profiles (to be continued).

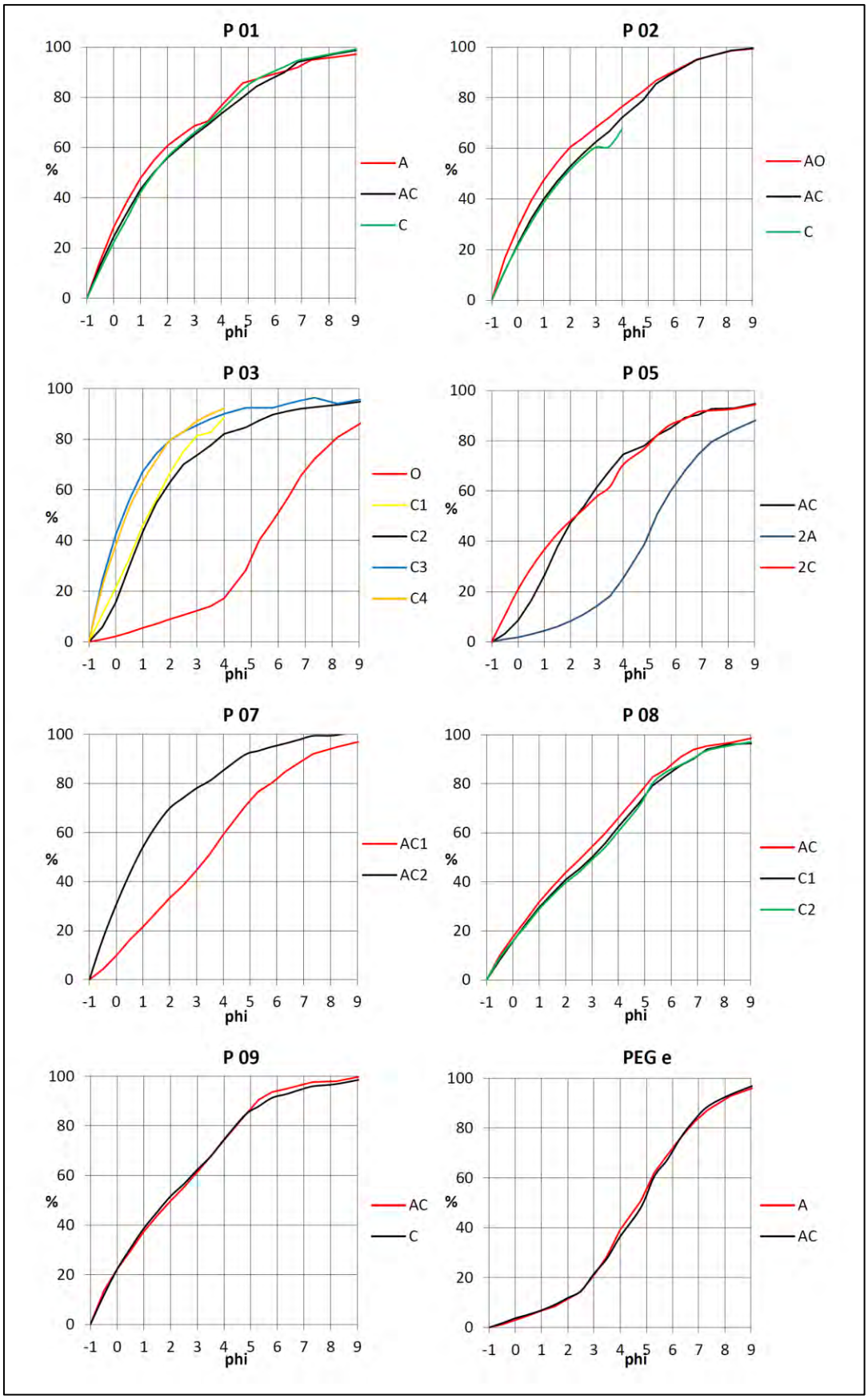

Figure 3.20. Cumulative curves of grain size distribution in the studied profiles.The P06 profile does not have the graph of cumulative curves because for two horizons is not possible do the particles size analysis for insufficient sample quantity.

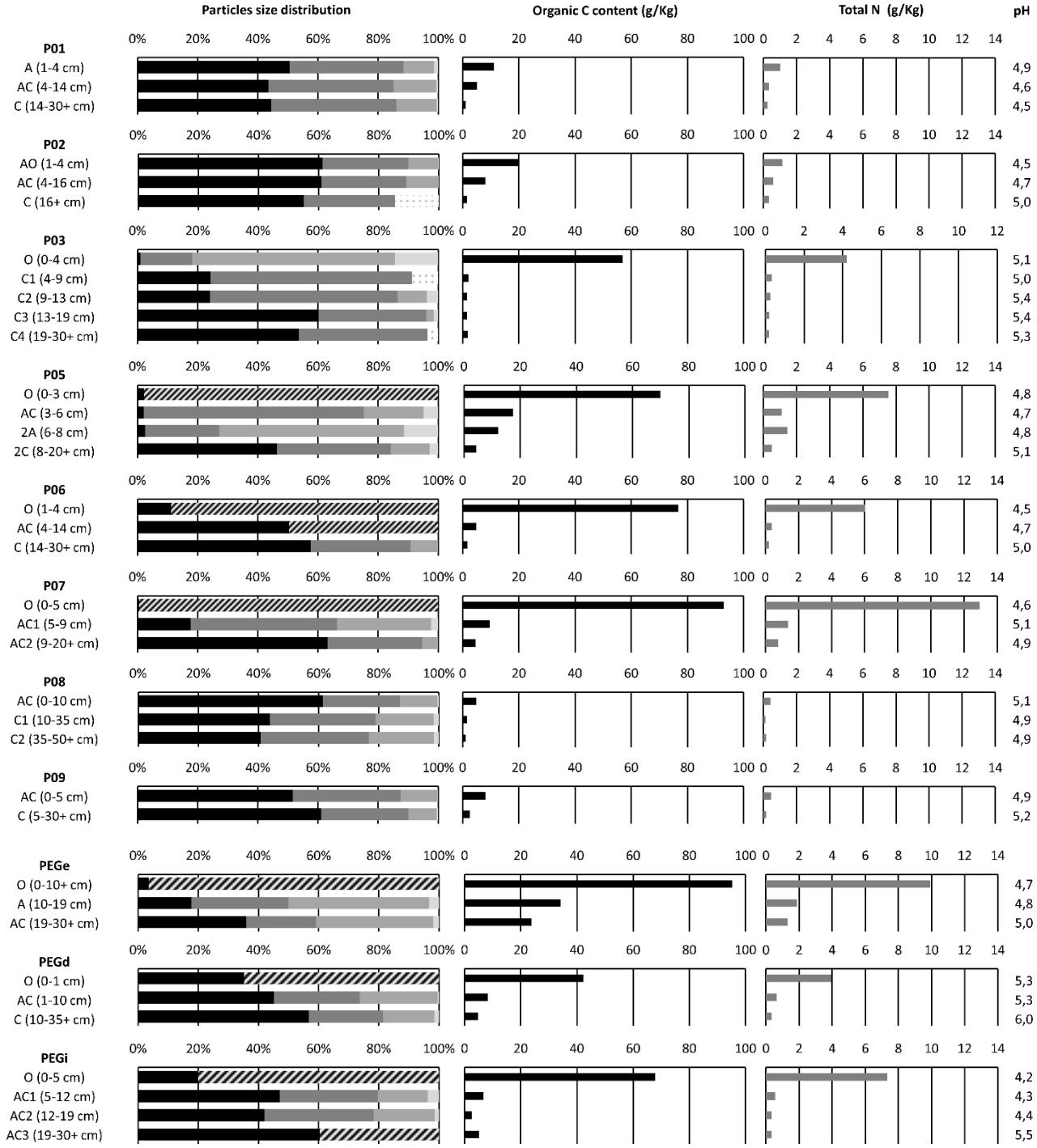

Figure 3.21. Particle size distribution, Organic C content, total Nitrogen content and pH values in the studied profiles. For the particle size distribution plot: in black is depict the gravel content, in dark grey the sand content, in grey the silt content. in light grey the clay content, in black strips the n.d and in white and black dots the silt plus clay content..

3.2.3.1.3 Organic Carbon Content

The absolute quantities of organic carbon are very variable depending on the type of profile and depth (fig. 3.21). In surface horizons, values ranging between 5 (P08) and over 95 g/kg (PEGe) are found. In

particular, the PEGe, P07 and P06 are the soil profile with highest content of organic C, while the P08 and P09 profiles have the lowest content of organic C.

Usually, the C organic values decrease with depth: the general trend is therefore represented by a decrease of organic carbon content, as horizons get deeper. This decrease can be more or less gradual, as in profiles P01 and PEGe, or concentrated as a rapid loss at the transition from the uppermost horizon to the ones those below, such as in the profiles P06 and PEGi.

All the profiles show the same trend, characterized by a decreasing in C content with depth, except P03 and PEGi profiles. In these profiles the C4 (P03) and AC3 (PEGi) horizons show a little bit more C organic content then the above horizons C3 and AC2.

3.2.3.1.4 Total Nitrogen

The total nitrogen contents have the same trend of the organic C content (fig. 3.21), but with significantly lower values (not exceeding 14 g/Kg). In almost all the studied profiles the total nitrogen content decreases with depth along the profile, but two exceptions are found (P05 and P08). The decrease is concentrated as a rapid loss at the transition from the uppermost horizon to the ones those below, while in the underlying horizons the decrease is more gradual.

Among the organic horizons, those belong to the PEGe, PEGi and P05 have the highest N content (about 7-9 g/Kg), while the lowest values are recorded in P08 and P09 (about 0.4 g/Kg).

Finally, the C/N ratio have a values ranging between 7 and 17 g/Kg in the superficial horizons. Generally decrease with depth (fig. 3.22), except in the PEG profiles, where the last horizon have approximately the same C/N ratio than the superficial horizon (fig. 3.22).

3.2.3.1.5 pH

All the soil horizons analyzed have a tendency to acidity, the values of pH in H_2O ranging between 4.2 and 6.0 (fig. 21). Although, the pH values measured in H_2O neither gets large variations between successive horizons nor within the entire depth of profile, in almost all the profile the pH values progressively increase with the profile depth, approaching to the parent material. In many cases this variation seems very moderate, being rarely more than 1 pH unit and for the P05 and P03 profiles the most superficial horizons showing a lower acidity than the immediately underlying horizons, with pH values greater than 5.

However, in the P01 and P07 profiles, the pH values seem to oscillate independently of the depth, and no well-defined pattern can be recognized. Besides, in the P08 profile the pH values range along the profile of only 0.2 points.

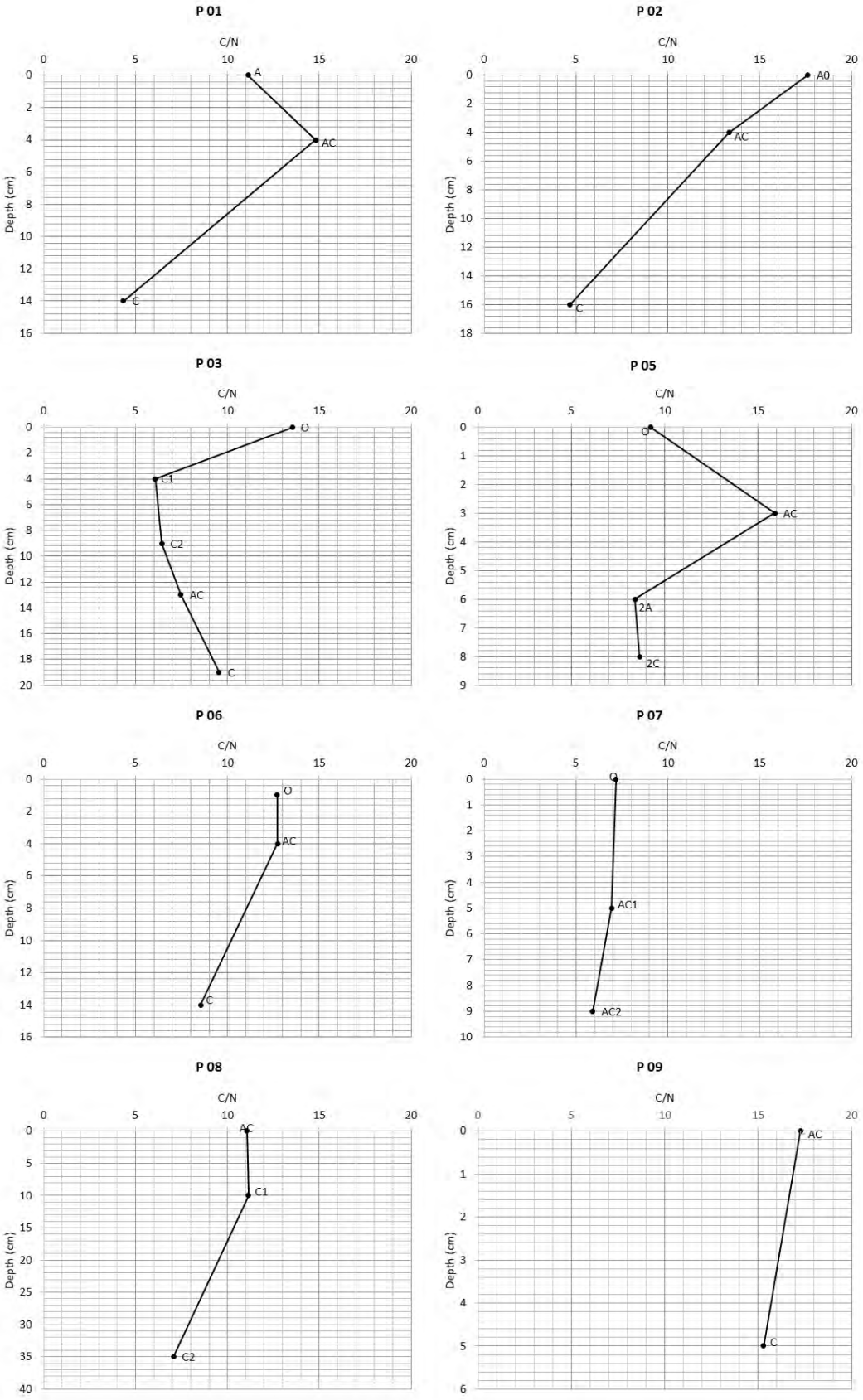

Figure 3.22. C/N ratio in the studied profiles(to be continued).

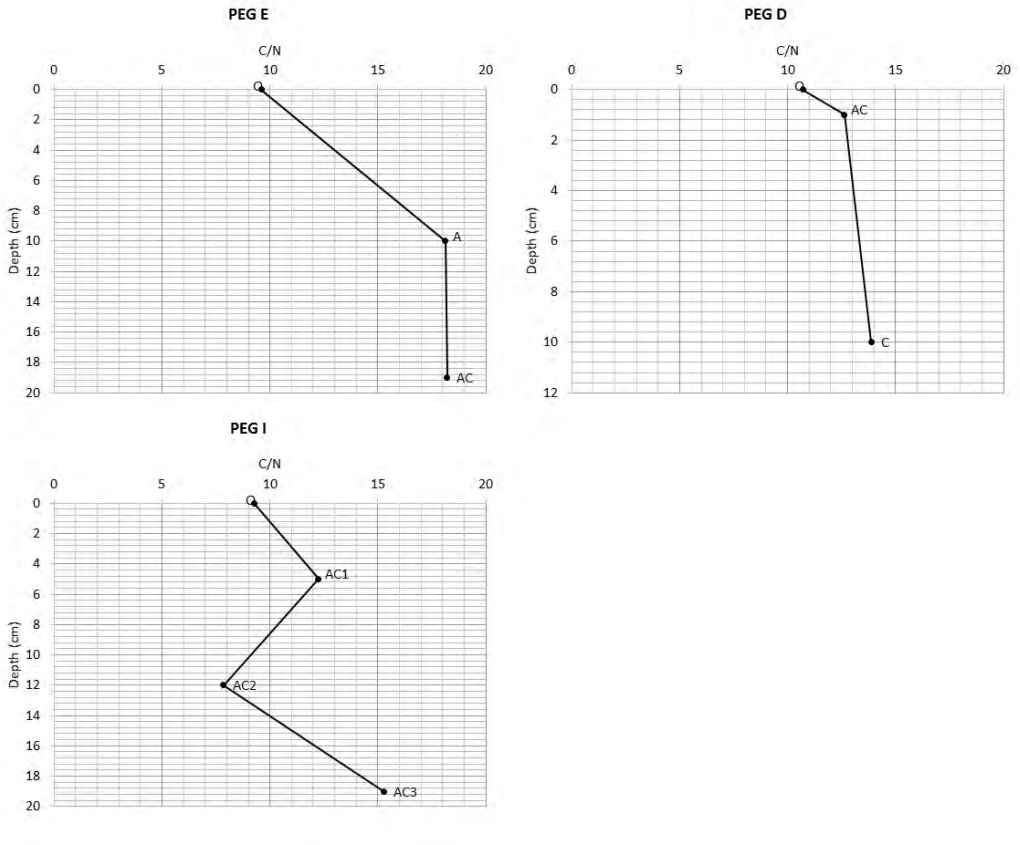

Figure 3.22. C/N ratio in the studied profiles.

3.2.3.1.6 Alluminum and Iron extractions

The total content of free iron oxides (Fed) don't exceed the 16 g/Kg but generally ranging between 8 and 13 g/Kg. Also, the values of amorphous iron oxides (Feo) are generally between 8 and 12 g/Kg. While the iron bound with the organic matter (Fep) has lower values, between 0.5 and 5 g/Kg. For all three of these parameters, particularly high values are observed in P01 AC, P03 O, P09 AC, PEGd AC, PEGi AC2 horizons (fig. 3.23).

As regards the aluminum content, the quantities tend to be inferior to those of iron, and less variable. Free aluminium oxides (Ald) reaches values between 0.6 to 3 g/Kg, amorphous aluminium oxides (Alo) between 0.8 and 3 g/Kg, and the aluminium bound with the organic matter (Alp) between 0.2 and 3 g/Kg.

Both the iron and aluminum show similar trends and similar peaks along the profiles.

On average, the crystalline iron oxides content is very variable and not high. In particular, the crystalline iron oxides are mainly concentrated in the superficial horizons (tab. 3.8), in fact the highest values are found in the PEGd AC (10.8 g/Kg), also in the buried horizon P05 2A the crystalline iron oxides content

is higher (6.8 g/Kg) than the other horizons. In some case the crystalline iron oxides values are negative (P01 AC, P05 2C, P06 AC and P07 AC1).

The Feo/Fed index has value close to the unit, in particular only two horizons (PEGd O and PEGd AC). have an iron activity index smaller than 0.5. (tab. 3.8). Finally, the results of the podzolization index Alo + ½ Feo meet the conditions of podzolization processes only in the case of 2A and 2C horizons of P05 (FAO, 2014).

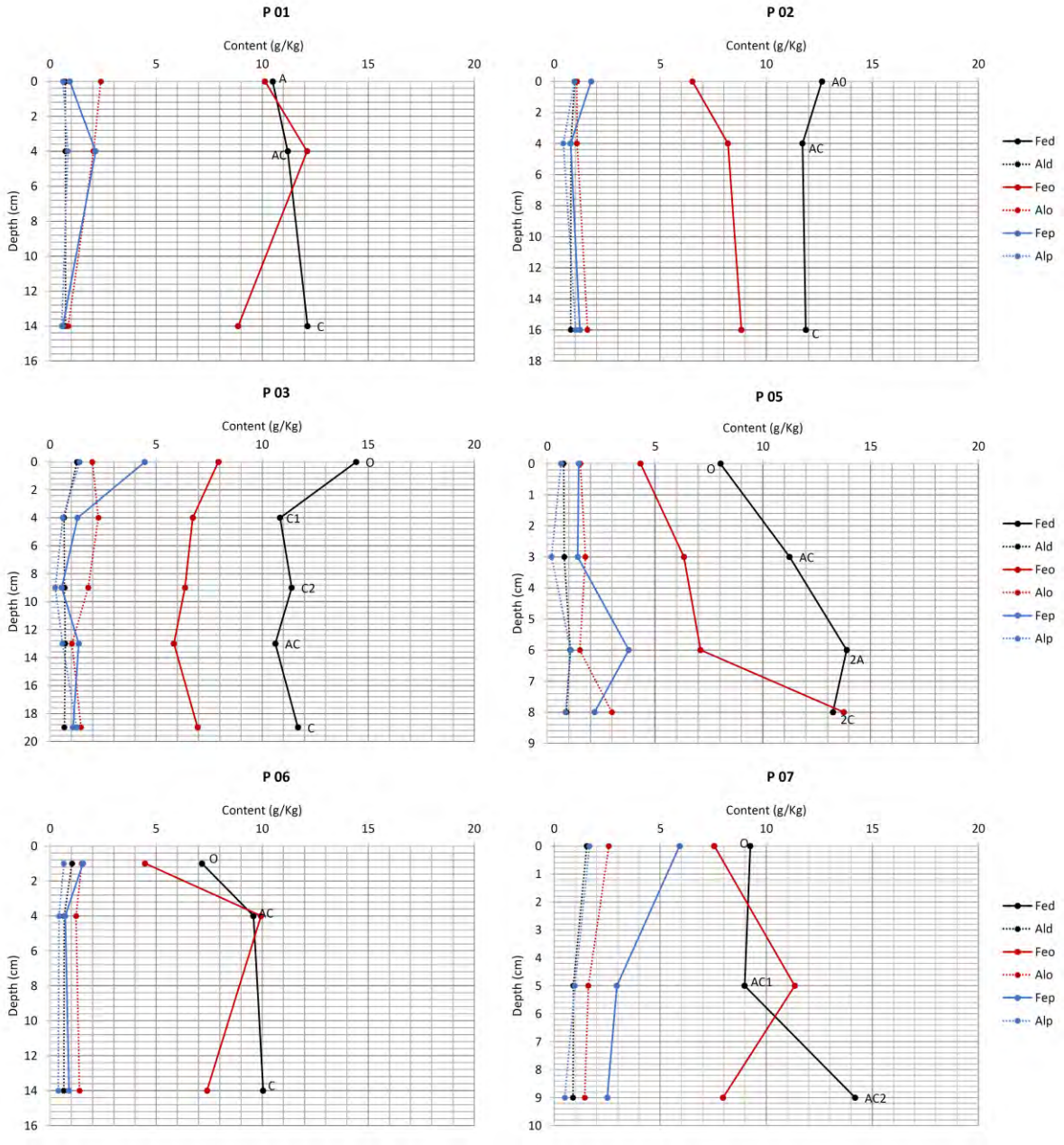

Figure 3.23. Free iron oxides (Fed), amorphous iron oxides (Feo) and iron bound to the organic matter (Fep) content, free aluminum oxides (Ald), amorphous aluminum oxides (Alo) and aluminum bound to the organic matter (Alp) content of the studied profiles The horizons name are close to the Fed curves (to be continued).

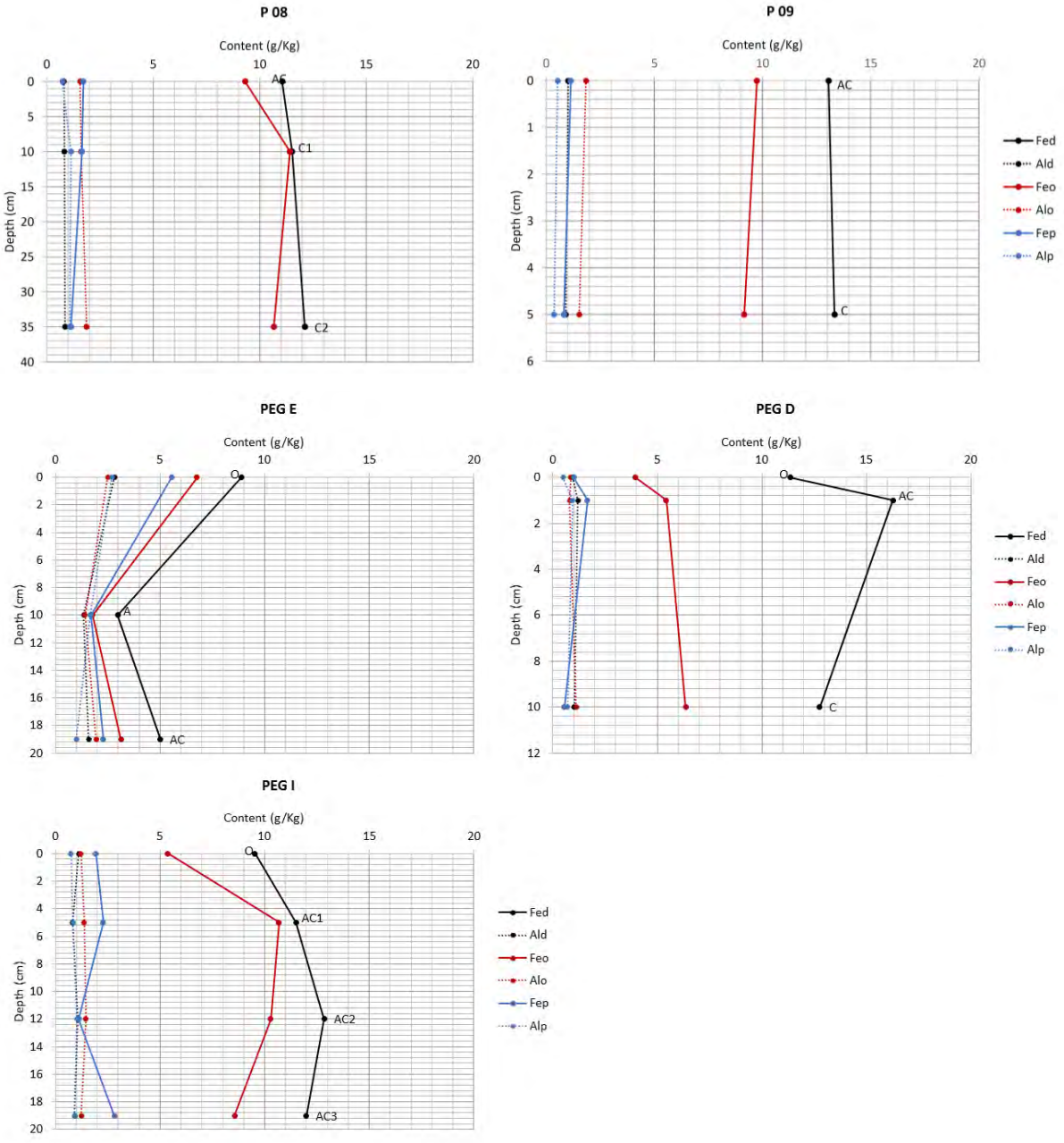

Figure 3.23. Free iron oxides (Fed), amorphous iron oxides (Feo) and iron bound to the organic matter (Fep) content, free aluminum oxides (Ald), amorphous aluminum oxides (Alo) and aluminum bound to the organic matter (Alp) content of the studied profiles The horizons name are close to the Fed curves.

Profile	Horizon	Depth (cm)	Fed-Feo (g/Kg)	Feo/Fed	Alo+1/2Feo (%)
P01	A	1-4	0.4	0.97	0.75
P01	AC	4-14	-0.9	1.08	0.81
P01	C	14-30+	3.3	0.73	0.53
P02	AO	1-4	6.1	0.52	0.43
P02	AC	4-16	3.5	0.70	0.52
P02	C	16+	3.0	0.74	0.60
P03	O	0-4	6.5	0.55	0.60
P03	C1	4-9	4.1	0.62	0.56
P03	C2	9-13	5.0	0.56	0.50
P03	C3	13-19	4.8	0.55	0.39
P03	C4	19-30+	4.7	0.60	0.49
P05	O	0-3	3.7	0.54	0.37
P05	AC	3-6	4.9	0.56	0.49
P05	2A	6-8	6.8	0.51	0.51
P05	2C	8-20+	-0.5	1.04	0.99
P06	O	1-4	2.7	0.63	0.37
P06	AC	4-14	-0.4	1.04	0.62
P06	C	14-30+	2.7	0.74	0.51
P07	O	0-5	1.7	0.82	0.64
P07	AC1	5-9	-2.4	1.26	0.73
P07	AC2	9-20+	6.2	0.56	0.54
P08	AC	0-10	1.7	0.84	0.62
P08	C1	10-35	0.1	0.99	0.73
P08	C2	35-50+	1.5	0.88	0.72
P09	AC	0-5	3.3	0.75	0.67
P09	C	5-30+	4.2	0.69	0.61
PEG e	O	0-10	2.1	0.76	0.59
PEG e	A	10-19	1.2	0.59	0.23
PEG e	AC	19-30+	1.9	0.63	0.35
PEG d	O	0-1	7.4	0.35	0.28
PEG d	AC	1-10	10.8	0.33	0.35
PEG d	C	10-35+	6.4	0.50	0.43
PEG i	O	0-5	4.2	0.56	0.39
PEG i	AC1	5-12	0.8	0.93	0.67
PEG i	AC2	12-19	2.6	0.80	0.66
PEG i	AC3	19-30+	3.4	0.71	0.55

Table 3.8. Iron and aluminum indeces. Crystalline iron oxides (Fed-Feo), activity iron index (Feo/Fed) and podsolization index (Alo+1/2Feo).

3.2.3.1.7 Rock-Eval data

In the I/R diagram the organic horizons have I-index values between 0.25 and 0.5 and a R-index between 0.3 and 0.5. While the C horizons have I-index values between 0.1 and 0.55 and a R-index between 0.5 and 0.65 (fig. 3.24).

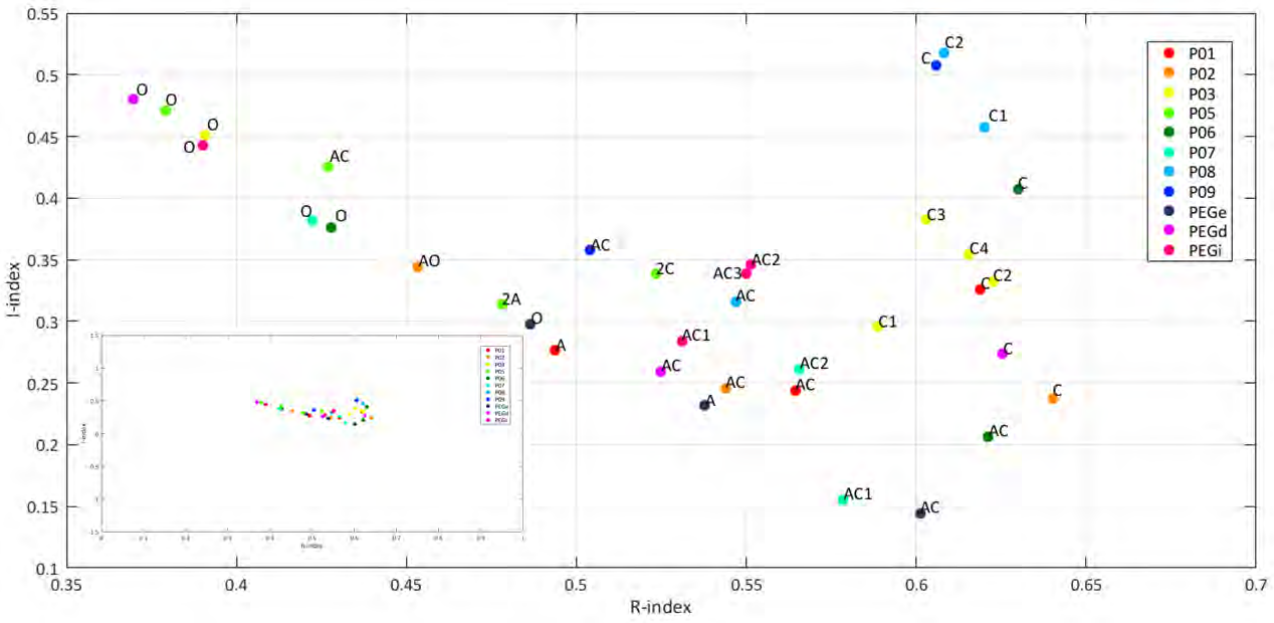

Figure 3.24. I-index/R-index. On the bottom left the data are plotted using the grid values from Sebag et al., 2016 in order to better visualize the trends.

The HI/OI index shows different values in different horizons typology (fig. 3.25). In fact, the O and A horizons show a high HI values and low OI values, while the C horizons show high OI values and low HI values, in particular the P03 C2, P03 C3, P03 C4 and P06 C have high values of OI. Finally the AC horizons have an intermediate values.

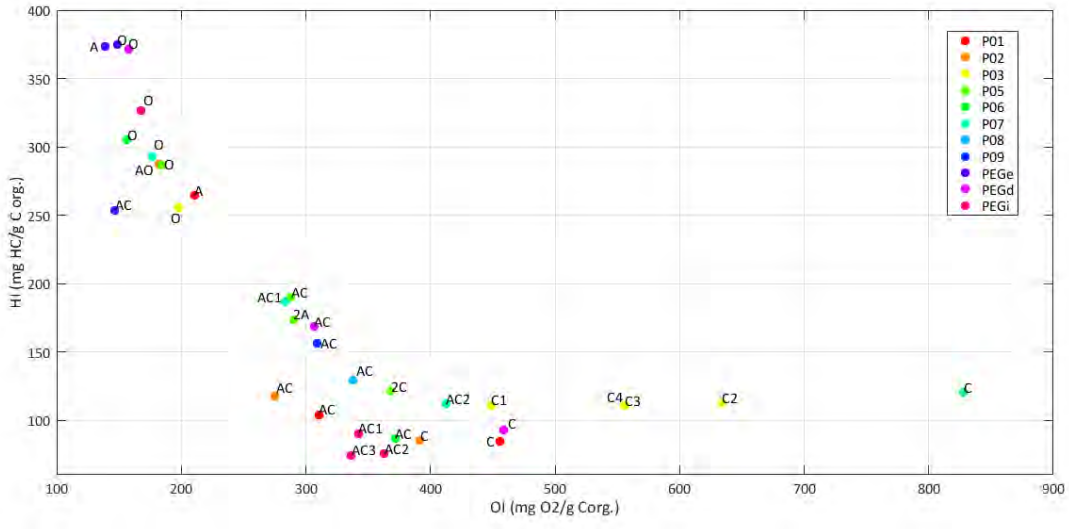

Figure 3.25. HI/OI diagram. The P08 C1, P08 C2 and P09 C horizons are not plotted due to their out of range values.

3.3 Discussion

3.3.1 Sub regional scale analysis

In the first part, this study analyzes the treeline within a region in the central Italian Alps (the Upper Valtellina) based on the identification of three main environmental factors – geomorphology, climate, and human impacts – influencing the treeline elevation. The degree of association between these environmental factors and three topographic variables (elevation, slope and aspect) are assessed. Overall, the treeline elevation in the Upper Valtellina region is primarily limited by geomorphological constraints, that is, by active surface processes and landforms that strongly affect the treeline position at a regional scale in mountainous areas (fig. 3.5). Altitudinal treelines (as well as latitudinal ones) are widely recognized as sensitive proxies for climate conditions over entire regions. Treeline altitudinal fluctuations have occurred in the past and demonstrate the importance of climatic factors in modulating the altitudinal ranges of trees. The results of this study show that elevation is the topographic variable that mostly distinguished climatic treelines from treelines limited by geomorphological constraints and by human impacts in the study region, whereas slope inclination is more strongly associated with treelines influenced by geomorphological constraints. Many studies have emphasized that, in addition to climate (and particularly soil temperature; Körner & Paulsen, 2004), treeline elevation at the local and regional scale is also strongly influenced by topography, landforms, and geomorphological processes occurring at high elevations (Butler et al., 2003; Butler & Walsh, 1994; Holtmeier & Broll, 2012; Malanson et al., 2011; Resler, 2006). Where treelines are limited by geomorphological constraints, these factors may be more important than climate in determining treeline elevation because they directly control tree establishment and growth (e.g., Butler et al., 2007; Leonelli et al., 2011a; Macias-Fauria & Johnson, 2013). Clear evidence of the importance of geomorphological constraints can be found in areas marked by avalanche paths, drainage channels, scree, rock outcrops and rock faces, debris flow channels, and debris flow deposits (Pelfini & Santilli, 2008). These factors mostly occur in areas with high slope angles (>45° in the study area), where repeated high-energy geomorphic events are likely. Treelines under geomorphic control are commonly found at lower elevations than climatic treelines (Leonelli et al., 2016, 2009a) and also on less steeply inclined slopes. Despite rising air temperatures, these treelines are likely driven by the dynamics imposed by geomorphological constraints rather than climate. In particular, where geomorphological processes are dominant, it is their response to climatic triggers that will drive the possibility of tree establishment at any elevation. Rising air temperatures are already enhancing tree growth in treeline belts at a global scale (e.g. Briffa et al., 2008; Qi et al., 2015; Salzer et al., 2009), promoting an increase in forest density (Klasner, 2002; Mazepa, 2005; Shiyatov et al., 2005)

and an upward shift of treelines. As treelines tend to move upward along the slopes when less limited by climate, trees grow at higher elevations, even where slope inclinations are typically higher and gravitational geomorphological processes and soil degradation (Holtmeier, 2010) are more intense. According to the predicted trends in temperature rise (e.g., Beniston, 2006), the influence of geomorphological constraints on treeline will likely increase in the next decades. As the results demonstrate, treelines at the highest elevations (> 2400 m in the study area) where non-extreme slopes (<45°) occur, likely will undergo a climate-driven upward shift (fig. 3.6). However, treeline elevation anomalies suggest that site-specific factors can either constrain or facilitate these shifts (Case & Duncan, 2014; Grafius et al., 2012). Thus, upward altitudinal shifts in the treeline can also be detected where geomorphological factors are dominant. In this study, the aspect variable is not associated with any of the three environmental factors controlling treeline elevation. This suggests that treeline elevation in the region is not influenced by the different radiative warming regimes that typically occur on slopes with different aspects. This result is consistent with the conclusions of Wang et al. (2013), who did not find any slope exposure effect on treelines in southwestern China and proposed that treelines there are mainly influenced by atmospheric circulation. Also Paulsen and Körner (2001) found no slope exposure effect on climatic treelines in the Swiss Alps. However, the role of aspect may be more important when considering the treeline structure and its response to climate: in the Southern Rocky Mountains of the U.S., Elliott and Kipfmueller (2010) found that significantly younger trees comprised the treeline ecotone on north-facing slopes at various spatial scales. Human impact is another factor that is often not fully considered. Especially in the European Alps, land abandonment and the decline in traditional cattle grazing has decreased the pressure on high-elevation forest ecosystems (e.g. Motta & Nola, 2001), thus masking climatic effects and improving forest regeneration (e.g., Gehrig-Fasel et al., 2007). As results demonstrate, the treelines controlled by human impacts occur on gentle slopes (80% of the trees in this class grow on slopes <40°) that are more easily accessed by humans and cattle (fig. 3.6).

Moreover, a comparison of the treeline elevation in this study was performed with previous studies conducted by Leonelli et al. (2009a) in Valle d'Aosta, western Italian Alps, where the treeline is mainly formed by *Larix decidua* Mill. trees. Both sites are located in the inner regions of the Alps, but although the Upper Valtellina region has a lower orography, we found that here the climatic treelines and the treelines constrained by human impacts reached higher elevations than in the Valle d'Aosta (+30 m and +55 m, respectively), whereas treelines limited by geomorphological constraints were found at almost the same elevation (−10 m) (fig. 3.26).

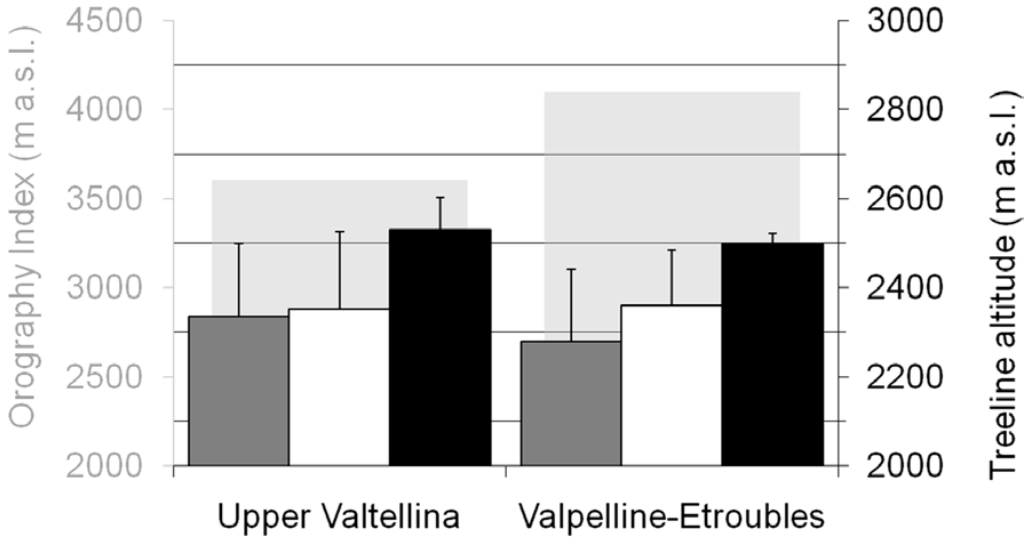

Figure 3.26. Treeline mean elevation in the Upper Valtellina and in the Valle d'Aosta (from Leonelli et al., 2009a) divided into human impacts (gray bars), geomorphological constraints (white), and climatic constraints (black). Positive error bars indicate the maximum elevation reached by 10% of the highest-elevation trees for each type of treeline. The graph also depicts the Orography Index (light gray bars), calculated as the mean elevation of the three highest peaks surrounding each valley (from Leonelli et al, 2016).

In the second part of this study, the relevance of the different geomorphological constraints on treeline were statistically and spatially analyzed and quantified in detail for the first time. Different studies have shown that the altitudinal treelines, besides responding to climate (Holtmeier & Broll, 2007; Gehrig-Fasel et al., 2008; Körner & Paulsen, 2004; MacDonald et al., 2008), are also influenced by topography, landforms and related geomorphological processes occurring at high elevations (Butler et al., 2007; Holtmeier & Broll 2012; Zald et al., 2012; Leonelli et al., 2016). The treelines limited by landforms and geomorphological processes are located at lower elevations than treelines constrained solely by climate (Leonelli et al., 2009a; 2011a). In fact, the undisturbed treeline ("climatic treeline") is located at a higher altitude than the treelines limited by geomorphological processes (tab. 3.1) (Leonelli et al., 2016). The analysis on geomorphological constraints reveals that different geomorphological processes and related landforms may have different impacts on the treeline dynamics (fig. 3.9 a). Mass movements and deposits due to gravitational processes are the most common in the Alpine environment (fig. 3.8). Therefore, instability phenomena and erosional and/or depositional processes related to gravity, as documented by the degree of landform activity, may be considered the most important controlling factors on the treeline position. Therefore, treelines affected by geomorphic processes can act as indicator of climate change. The treeline trees affected by gravitational processes are located at lower altitudes than the trees limited by other processes (fig. 3.9 a and tab. 3.3). Moreover, merging landforms derived from gravitational processes have a greater impact on treeline position than isolated landforms as they tend to eliminate free stable space for tree colonization. In areas where large portions of the valley slopes are

covered by a continuous debris/block layer, a lower treeline altitude has been recorded. This means that the treeline altitude is differently affected not only by different geomorphological processes but also by the array of factors associated with landforms, such as size and rates of change (e.g., rock gelivity, fractures, precipitation, and time). While isolated deposits due to gravitational processes allow trees to colonize the surrounding areas and avoid the individual landforms, merging deposits influence the treeline altitude and reduce the treeline ecotone width, making recolonization more difficult. Moreover, the merging deposits due to gravitational processes affect larger areas than the isolated ones and can in some cases also damage the forest, thereby depressing the timberline altitude (fig. 3.9 b). On the contrary, gully erosion has little impact on the treeline trees, firstly because the gullies in the examined ecotone are scattered and not continuous, allowing trees to colonize the neighboring areas at the same altitude, and secondly because these processes generally do not affect the timberline (fig. 3.9 b). Rill erosion, even if only a few cases were available for analysis, represents a negligible factor in terms of the influence on the treeline position in the studied area because this geomorphological process can damage trees but does not seem to prevent their growth. Nevertheless, the lack of statistical difference in elevation distributions among the landforms due to running and/or channelized water is attributable mainly to the small number of trees limited by rills and small alluvial fans (tab. 3.4). More data are likely necessary to assess the role of periglacial processes in the treeline ecotone. In the investigated area, such processes do not seem to be effective in lowering the treeline (fig. 3.9 a). Moreover, rock glaciers may also represent an opportunity for tree germination and growth if they are inactive or relict. The stability of inactive rock glaciers and the presence of fine-grained soil material occurring in small pockets at the edge and at the front of active rock glaciers favor tree colonization (Burga et al., 2004). The results suggest that the timberline position is less influenced than the treeline position by geomorphological processes; this involves a reduction in the treeline ecotone width (fig. 3.10). Moreover, the analysis of the ecotone width reveals that the most impactful processes greatly reduce the width and that the treeline in most cases coincides with the timberline. The timberline altitude seems to be lowered only in some cases of extreme events associated with gravitational processes and in areas affected by alluvial cones. In the first case, there is evidence of the destructive role of mass transport, while in the second case, the lowest position of the timberline seems most influenced by the presence of alluvial cones at low altitudes. At the regional spatial scale, as in the case of this research, the destructive effects of geomorphological processes on the treeline are prevalent. Nevertheless, other studies carried out at the local scale show that geomorphological processes and landforms can also facilitate upward shifts in the treeline (Butler et al., 2007; Resler, 2006). For example, the presence of boulders may moderate the temperature in close proximity to the block, providing plants with protection from severe weather and wind, may influence soil conditions, and may serve as seed traps (Resler et al., 2005; Zald et al., 2012). Finally, the analysis

of geomorphological factors can add more information about treeline response to climate change. Future upward shifts in treeline might be severely limited by geomorphic processes, which could become even more effective than at present in determining the distribution of trees at the highest elevations. In fact, if the temperature continues to increase, the upward shift in treeline will encounter harsher geomorphic environments that are not suitable for trees colonization (Macias Fauria & Johnson, 2013). Moreover, warmer temperature conditions will not cause an advance to higher elevations as long as mass wasting, landslides, and similar processes occur (Holtmeier & Broll, 2005).

In conclusion, climate conditions related to the rise in air temperatures since the end of the LIA are expected to enhance the upward shift in the treeline in the Upper Valtellina region of the European Alps. This increase will occur especially at high elevations (>2400 m) and on non-extreme slopes (<45°), where trees form high-elevation climatic treelines. In areas with more extreme slopes and thus with more intense geomorphological processes, trees tend to grow at lower elevations, and treelines are primarily affected by the presence of active landforms and active geomorphological processes rather than by climate (up to 8.3% of trees in this class grow on slopes with inclinations between 45° and 72°). The results also indicate that the current positions of treelines are not only lowered by geomorphological constraints in general, as recently demonstrated (Leonelli et al., 2016), but can also be differently affected by different groups or types of geomorphological processes. In the study area, gravitational processes affect 87% of the treeline trees, running and/or channelized water affects 8%, and ice affects only 5%. The landforms related to gravitational processes can create considerable obstacles to the upward shift in treeline, especially when they merge (e.g., merging talus cones). Gravitational processes represent the most destructive processes of the treeline ecotone and tend to reduce the ecotone width, leading to coinciding treeline and timberline.

3.3.2 Site scale analysis: Mt. Confinale study case

At Mt. Confinale study site, the altitudinal dynamics are favoured on convex and well-exposed rock outcrops where geomorphic gravitational processes are less intense and sporadic, while no trees grow on the alpine grassland at the same elevation. Of course, ecologic and microtopographic factors are also important, and the tree species forming the treeline is also a key factor in modulating the magnitude of treeline shifts among Europe in response to the ongoing warming (Rabasa et al., 2013). At Mt Confinale study site, the zoochorous seeds of the Swiss stone pine establish at higher elevations because nutcrackers (*Nucifraga caryocatactes* L.) often abandon some of their seed caches (e.g., Holtmeier, 2010). Thus, germination and growth are mainly controlled by the microclimatic conditions of rock niches and by shorter periods of snow cover with respect to alpine grassland. As a result, treeline advance

is typically clustered (fig. 3.12). The treeline position estimates in the European Alps based on meteorological indices evidence treeline elevations that range from approximately 1850 m a.s.l. in the peripheral regions characterized by oceanic climate conditions, to 2200–2500 m a.s.l. in the inner regions characterized by continental climate conditions (Caccianiga et al., 2008; Ellenberg, 1963). A comparison of the treeline altitudinal shift in the Mt. Confinale study area was performed with previous studies conducted on Becca di Viou in Valle d'Aosta (western Italian Alps) where the treeline is mainly formed by *Larix decidua* Mill trees (Leonelli et al., 2011a). The overall upward shift in the treeline over the period from 2000 to 2009 was an increase of 2.6 m/year: 1.35 m/yr higher than in the site in the western Alps over a similar period (fig. 3.27 and tab. 3.9). The lower rates of treeline upward shift found in the western Alps (1.25 m/yr over the period 2000–2008) could be related to talus slopes and active gravitational processes that control and hamper the altitudinal dynamics of the treeline. Although the treeline was at the same elevation at both sites from 1999 to 2000 (2505 m a.s.l.), by 2008–2009 the treeline at Mt. Confinale was 15 m higher (at 2530 m a.s.l.) than at the Becca di Viou site, and in 2013, it was at 2545 m a.s.l.. If similar height-growth rates of the treeline trees persist in the future, the treeline at Mt. Confinale should reach 2570 m a.s.l. by 2023.

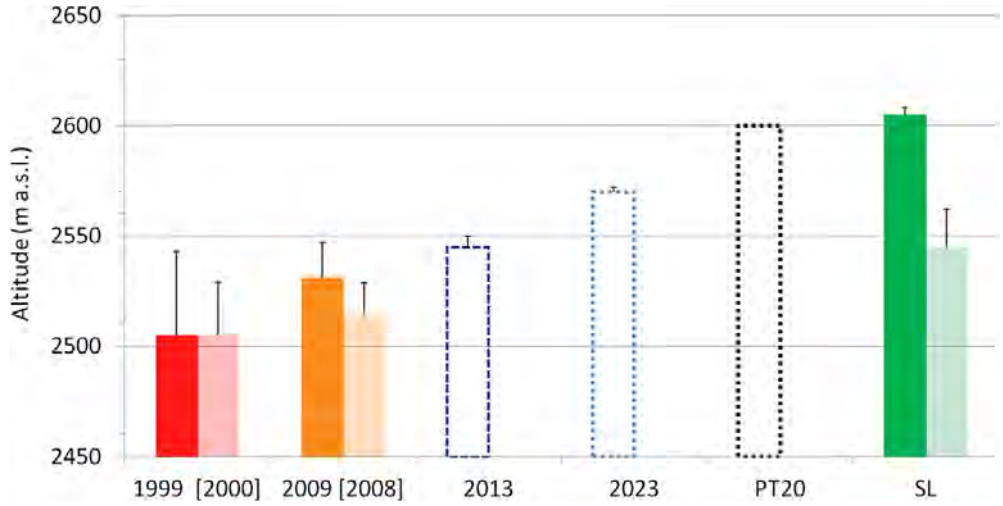

Figure 3.27. The mean treeline elevation at the Mt. Confinale study site for the 10-year time periods ending in 1999 and 2009 and for the year 2013. The treeline altitude for the year 2023, the potential treeline (PT20) and the Species Line (SL) elevation are also shown. Faded bars refer to data from the Becca di Viou site in the Valle d'Aosta (Leonelli et al., 2011a) and the corresponding years are reported in square brackets. The error bars correspond to ±1 standard deviation (from Leonelli et al, 2016).

	Mt. Confinale: 2000-2009 (2010-2013)	**Becca di Viou: 2000-2008**
Upward shift	2.6 m/year	1.25 m/year
	(3.5 m/year)	-

Table 3.9. Rates of the upward shift in the treeline for the Mt. Confinale (this study) and the Becca di Viou (Leonelli et al., 2011a) study sites (from Leonelli et al, 2016).

In the Mt. Confinale study site the profile thickness of the investigated soil clearly shows a gradient with altitude, at higher altitudes the soil profile are shallower. This tendency is typical for Alpine soil (Merkli et al., 2009). Although the soils are deep, observing the particle size distributions analysis (fig. 3.14) is evident that the coarse material is predominant, given by a strong parent material influence. Moreover, the particles size distribution shows the classical trend in all samples. In fact, the particles size increases with the depth, so there is no evidence of buried paleosurfaces.

Even the analysis of the amount of organic carbon and total nitrogen does not show any anomalies. Indeed, in all the profiles, except for the CF03 profile, we have a decrease of the content of nitrogen and organic matter with the depth. In the CF03 profile the organic C and total N content show a peak along the profile, in the BC1 horizon. This anomaly is may be due to the contribution of colluvial upslope materials, incorporated along the profile. The C/N ratio values allow to identify two types of humus in the studied profiles: Moder and Mull (Duchafour, 1983). The first is an evolved type of humus, characterized by a higher degree of humification and is typical of coniferous forests. While the second is a type of evolved humus with stable clay-humic complexes and poor litter, typical of the broadleaf forest or herbaceous vegetation (as in the study area)(Cremaschi, 2000). This means that degradation and decomposition of organic matter is good, most likely due to a good microbiological activity. The values are also coherent with the literature ones for the profile on south facing slopes in the Alps (Egli et al., 2009).

The pH does not have great variations in the different profiles and does not seem to have a marked trend. On average, the pH decreases moving close to the parent material, although it remains acid. In the profiles located in forest, surface horizons tend to be more acid due to the acidification of the coniferous forest litter.

The content of oxides of iron and aluminum within the horizons analyzed shows a good correlation with the results of other study carried out in the Alps (Merkli et al., 2009; Egli et al., 2009). The content of crystalline iron oxides increases in the well developed horizons (e.g. B horizons) and in particular in the profile located under forest vegetation. Indeed, according to Remaury et al. (2002), the crystalline Fe oxides (Fed–Feo) in Bs horizons are the product of in situ weathering of Fe-bearing primary minerals.

The iron activity index has low values and rarely exceed 0.5 (tab. 3.6); this indicates the presence of developed soil and supposedly ancient. In fact, assuming that the iron activity index can be used as measure of soil antiquity, decreasing with the soil maturity and alteration degree (Cremaschi & Rodolfi, 1991). In this study site the more developed horizons have a lower iron activity index. Moreover, very low values are found in the CF03 BC2, CF04 B and CF04 C, which belong to the soil under forest coverage with a higher degree of development than the soil located in the treeline ecotone. With respect to the Alo + ½ Feo index, the values obtained at profiles C15/03 and CF03 appear to indicate the presence

in this profile of a weakly podzolization, or better a cryptopodzolization (Do Nascimento et al., 2008; FAO, 2014). In fact, the podsolization conditions are not so expressed as in other studies (Waroszewski et al., 2013).

Analyzing the Rock-Eval data (fig. 3.17) it was possible to divide the analyzed horizons into several boxes (Sebag et al., 2016). In particular, the O horizons are placed in the range of the box "Litters and Organic Horizons" while the other horizons show three different trends (Sebag et al., 2016). Indeed, the B and C horizons are located in the box of "Organo mineral & Mineral horizons", and are placed along three different linear trends: most of the horizons follow the humic trend whereas the CF01 BC are close to the Spodic trend and the CF04 B and C are close to the inherited OM trend. Therefore, the Rock-Eval I/R indeces support the hypothesis that the study area is characterized by a moderate developed soil. Especially in the area covered by forest vegetation the soil developed is marked, but the high incline and the instability of the slope influence the linear development of the soil, bringing colluvial material. The continuous contributiom of material is also observed by the presence of coarse materials even in the most developed horizons. As evidenced by other studies (e.g., D'Amico et al., 2009), the morphology of the relief and active geomorphologic processes are therefore the factors that most influence pedogenesis in the mountain environments.

The Rock-Eval data also provide more information of the organic matter maturity. In the HI/OI diagram (fig. 3.18) the horizons are grouped by typology, in fact starting from the top left we find the O horizons, then the OA/A, the B and so on. At the bottom right the CF04 B and C horizons are found, that belong to the deeper and developed soil.

On the Mt. Confinale study site, the presence of geomorphological factors, especially where active processes are less intense, may combine with climatic factors to promote an upward shift in the treeline, which is located at an altitude of 2545 m a.s.l. and, if similar height-growth rates of the treeline trees persist in the future, the should reach 2570 m a.s.l. by 2023.

The geomorphological processes and the slope dynamics also influence the soil evolution, which, although showing a good degree of development, does not reach the characteristic of a typical forest soil. Specifically, the soils of Mt. Confinale can be attributed to the class of "Sols humifères désaturés" (Duchafour, 1995); in particular the soils developed under forest is identifiable as "Ranker cryptopodzolique" while the soils located at the treeline ecotone is identifiable as "Ranker alpin" (Duchafour, 1995).

The presence of soil, although not particularly developed in the treeline ecotone, suggests that the colonization of the *Pinus cembra,* favored by ecologic, microtopographic and microclimatic factors, is then followed by the development of the soil. Which in turn favors a more active colonization that could lead to a more marked shift to higher altitude of the vegetation belt.

3.3.3 Site scale analysis: Proglacial area of Forni glacier study case

In the Forni study site a chronosequence approach was used in order to investigate the different characteristics of soil with different age, covering a time span of deglaciation of about 150 years (time since the end of the "Little Ice Age" in the 1850s). Firstly, the profile thickness of the investigated soil does not show a gradient with age: all the profiles have more or less the same thickness and the same number of horizons. Even the Munsell colour do not show any trend.

In these soils a high proportion of soil skeleton is found, in fact the soil skeleton varies from 0% up to 60% of the mass of the investigated soils. It should be stressed that the skeleton proportion in the soil may, furthermore, vary within short distances, then the sampled skeleton may not always be representative to the variability of skeleton content. The fine earth of all soils of the investigation area is very sandy and contains partially some silt (fig. 3.21). The P03 O and P05 2A horizons have higher silt content. The silt mainly have an aeloian attribution or is produced by grinding due to fluvial transport (Egli et al., 2006).

In contrast to Righi et al. 1999 but in agreement with Egli et al., 2001, no significant trends of higher clay contents with increasing age could be found for the investigated soils in Forni study site.

Moreover, the particles size distribution shows the classical trend in almost all samples, in fact, the particles size increases with the depth. Instead, in the profile P05 between the AC and 2A horizons there is a granulometric discontinuity due to the presence of buried paleosurfaces. This discontinuity is also underlined by a peak of total nitrogen content in the 2A horizons.

The soil profiles have a standard trend of organic C and total N content decreasing with depth; except the P05 and P08 deeper horizon that have a little organic C peak. These anomalies cannot be attributed to the presence of buried surfaces as there is no evidence in the other analyses (fig 3.21).

As in other studies (Egli et al., 2001, 2006; Kabala & Zapart, 2012), in the Forni study site, the organic C and the total N content of surficial horizons seem to depend on the soil age: starting from the younger soil (P08 and P09) developed on the 1980's moraine to the older soil (PEGi, PEGe and PEGd) developed on the 1859's moraine the organic C content and the total N content varies from about 5-8 to 42-95 g/Kg and from about 0.4-0.5 to 4-10 g/Kg respectively.

In the studied profiles, based on the C/N ratio values the humus is Mull (Duchafour, 1983), type of evolved humus with stable clay-humic complexes and poor litter, typical of herbaceous vegetation as in the case of the study area (Cremaschi, 2000) characterized by alpine grassland and small trees mainly represented by European larch and Norway spruce and birch, with a discrete density that gradually decreases moving close to glacial tongue (Bonetti, 2013).

The pH values don't show any trend with both profile age and depth.

The content of free oxides of iron and aluminum within the horizons analyzed shows a good correlation with the results of the other study carried out in other proglacial area with a similar time span of deglaciation (Kabala & Zapart, 2012). While the amorphous iron oxides have greater values in the analyzed profile than in literature. Especially in the profiles developed on the most recent moraines, amorphous iron oxides reach high amounts, perhaps due to biochemical alteration in the area. Moreover, it is possible that the iron bound to the organic matter, which is extracted also in the oxalate and dithionite extractions, has created interference. In fact, the amount of iron bound to organic matter is not negligible (see Fep values, Appendix 2) and would also explain the appearance of some negative values in crystalline iron (Fed-Feo).

On the contrary, the content of crystalline iron oxides increases in the most developed and older soil (PEGd, P05 and P03). The iron activity index has high values and rarely is lower than 0.5 (tab. 3.8), except for the profile PEGd. This indicates the presence of younger and not developed soil. In fact, assuming that the iron activity index can be used as measure of soil antiquity, decreasing with the soil maturity and alteration degree (Cremaschi & Rodolfi, 1991). In this study site only the soil profile PEGd results to be enough developed, in fact this profile is one of the oldest among the studied profiles.

With respect to the Alo + ½ Feo index, the values obtained at the profile PO5 (2A and 2C horizons) appear to indicate the presence of a very weakly podsolization, or better criptopodzolization (FAO, 2014).

The Rock-Eval analysis (tab 3.24) allows to define two different trends in the distribution of the analyzed horizons (Sebag et al., 2016). In particular, the O horizons are placed in the range of the box "Litters and Organic Horizons" while the other horizons show two different trends (Sebag et al., 2016). Indeed, the C horizons are located in the box of "Organo mineral & Mineral horizons", and are placed along two different linear trends: most of the horizons follow the humic trend whereas the P03 C2, C3 and C4, P08 C2 and C1, P09 C, P06 C, P01 C, P02 C, PEGd C, PEGi C are close to the inherited OM trend. Therefore, the Rock-Eval I/R index supports the hypothesis that the study area is characterized by a weakly developed soil characterized by a humic trend but also affected by the input of the older organic material, maybe transported by wind or gravity.

In the HI/OI diagram (fig. 3.25) the horizons are grouped by typology, in fact starting from the top left we find the O horizons, then the OA/A and at the bottom right the C horizons. It does not seem to be an age-related distribution. Maybe for the presence of not so older soil.

Even if soils of the proglacial area of Forni glacier have a young age, in only 150 years of soil development some transformation trends could be noted. After deglaciation, transformation of chemical soil properties started: in the superficial horizons the organic carbon and total nitrogen content are

increased as the values of crystalline iron oxides, while the content of the amorphous iron oxides is decreased with the rise of deglaciation time.

For a classification point of view the younger soils developed on the more recent moraines can be attributed to the class of "Sols peu évolués sur matériaux récents" (Duchafour, 1995), whereas the soils developed on older moraines is identifiable as "Sols humifères désaturés" and precisely "Ranker alpin" (Duchafour, 1995).

In conclusion, although not all parameters seem to follow the age-related trend, the soils developed in the proglacial area of Forni glacier fit quite well with the chronosequence approach. Moreover, if the climatic trend does not change and given the presence of vegetation also close to the glacier tongue, it is possible to assume a more pronounced development of the soil in the future.

Chapter 4

Central Valle d'Aosta study area

The treeline ecotone, defined as the transition belt in mountain vegetation between the closed forest (timberline) and the alpine grasslands, is one of the most distinctive features of mountain environments and it is widely considered as a climatic boundary. Treeline altitudinal fluctuations may be considered to assess past and ongoing climatic and environmental changes. Although the ecological dynamics of the alpine treeline ecotone is mainly influenced by climate, especially by soil temperature, climatic parameters are not the only factors that influence the treeline position. In fact, the treeline altitude may be locally influenced by environmental factors, geomorphological processes, soil development, and human activities.

The importance of site conditions and the interaction between biotic and abiotic factors in controlling tree establishment and recent treeline shifts have been often underlined (Stueve et al., 2011).

Among the biotic factors, the geomorphological is one of the most important. In particular, water driven erosional processes, such as rain wash, running water action etc., can affect tree growth and vegetation dynamic shaping gullies, eroded surfaces etc. (Bollati et al., 2012). In badlands area the erosion rates are significant, therefore the interplay between vegetation and water runoff become particularly meaningful. The vegetation coverage, especially trees, may control the modalities of the runoff processes but, at the same time, trees are able to record, in their growth rings, both the climatic signals and the environmental changes (Schweingruber, 1988). In fact arboreal vegetation responds to the stress induced by climate variations and geomorphical processes, recording disturbance events through growth anomalies, abrupt growth changes, compression wood, etc. (e.g. Alestalo 1971; Guida et al. 2008) or through exposure of roots (e.g., Hupp & Carey, 1990; Pelfini & Santilli, 2006; Ballesteros-Cánovas et al., 2013; Stoffel et al., 2013).

Moreover, the substrate and hence the development of the soil can be decisive in the dynamics of colonization of new areas by trees. The soil could also be important for his function as archives, in fact like the other palaeoenvironmental archives containing accurate information over large time intervals on Quaternary variations.

Anthropic factors can also influence the maximum altitude of the treeline. Humans have always used high altitude areas to make room for cattle grazing or, more recently, for tourist facilities. This has caused a significant altitudinal depression of the treeline, thus modifying the natural distribution of trees.

Moreover, the abandonment of these areas has caused the re-colonization of these territories by the forest, but this process is not attributable to a climate change (Gehering-Fasel et al., 2007).
The aims of this second part of the study are: 1) reconstruct the environmental changes at the treeline with a climatic constraint in the Becca di Viou study site and in particular compare the climate trend with the arboreal vegetation response to the ongoing climate change, determine the relationship between the soil development and the colonization by the vegetation; 2) reconstruct the environmental changes at the treeline with both geomorphological constraints (landforms due to running and channelized water) and human impact (pasture) in Saint Nicolas study site, in particular study the badlands recent history and the role of vegetation and soil in badlands evolution.

4.1 Overview of the study area

4.1.1 Geography

The two study sites are located in Valle d'Aosta, a region, in the north of Italy, characterized by a predominantly mountainous territory, with a minimum altitude of 345 m a.s.l. (Pont-Saint-Martin) and a maximum altitude of 4810 m a.s.l. (Mt. Bianco). The Valle d'Aosta region is surrounded by the highest peaks in the European Alps: the Mt. Bianco (4810m a.s.l.) in the west, the Mt. Rosa (4634 m a.s.l.) and the Mt. Cervino (4478 m a.s.l.) in the north east, the Gran Paradiso (4061 m a.s.l.) in the south and the Gran Combin (4314 m a.s.l.) in the north part of the region.
Most of the current total glacial coverage, consists of 192 glaciers, equal to about 5% of the total area (about 160 km^2), is located in correspondence of the main massifs (Smiraglia et al., 2015).
In particular, the upward shift of the treeline was assessed on the SW slope of the Becca di Viou Mountain, few kilometers to the northeast of Aosta, in the municipality of Roisan (fig. 4.1).
The study area of the environmental changes at the treeline with both geomorphological and human constraints is located on the southern facing slope between Mount Fallére (3061 m a.s.l.) and Punta Leysser (2770 m a.s.l.). The sample sites are located in the Saint Nicolas and Saint Pierre municipality at an altitude range between 1300 and 2400 m a.s.l., about 10 km to the west of Aosta (fig.4.1).
In particular, the study concerned the badland areas of Saint Nicolas, the S slope of Punta Leysser and a flat area on the S slope of Mt. Fallére.
Moreover, the badlands of Saint Nicolas is included in the official "Geosites Inventory" of the Valle d'Aosta Region (Italy).

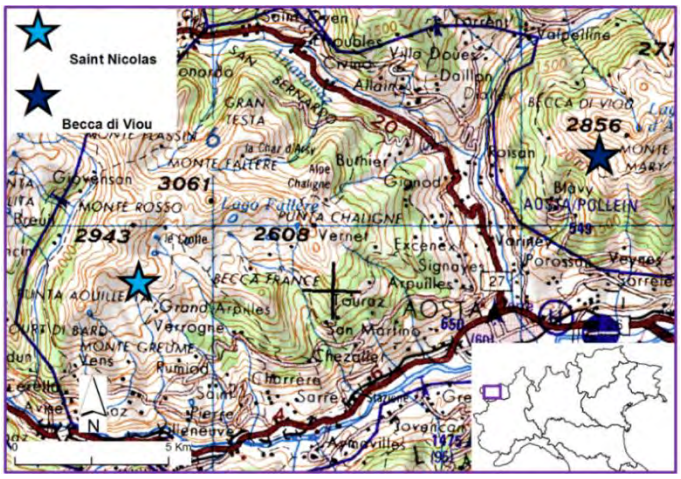

Figure 4.1. Saint Nicolas and Becca di Viou study sites location. The figure has been drawn from spatial data available at the National Geoportal.

4.1.2 Geology

The Aosta valley is the main axial depression of the western Alps, situated between the Duomo of Ossola-Ticino and the culmination of the Gran Paradiso (Elter 1960; Dal Piaz et al. 2003; De Giusti et al., 2003).

It displays a complete section of the Austroalpine-Penninic orogenic prism. The orogenic prism extends from the Canavese Line to the Penninic Front and is composed of the Austroalpine system, the Piemontese Zone with calceshists plus greenstones and of the Penninic Zone. It is an important area of the Italian north-western Alps which is dominated by the upper and inner part of the collisional orogenic wedge, a fossil subduction complex here represented by a stack of continental (Austroalpine, i.e. Adria-derived) and ophiolitic (Piedmont ocean) nappes (Dal Piaz et al., 2010). From top to bottom the nappe stack consists of: i) the Austroalpine Sesia-Lanzo inlier and the upper Austroalpine outliers (Dent Blanche-Mt. Mary-Pillonet thrust system) and the underlying ophiolitic Combin unit which includes, near its base, the southern tail of the Pancherot-Cime Bianche continental cover unit; ii) the lower Austroalpine outliers (Mt. Emilius, Glacier- Rafray, Chatillon and minor basement slices) and other ophiolitic units (Zermatt-Saas, Grivola-Urtier) (Dal Piaz et al., 2010). The former group is eclogite-free and displays blueschist facies relics of Late Cretaceous age (Dal Piaz et al., 2010). The latter is characterized by an eclogitic imprint of lower-middle Eocene age and includes toward the bottom a decollement continental cover unit (Cogne) and a blueschist facies, Combin-type ophiolitic unit (Aouilletta) (Dal Piaz et al., 2010).

The Becca di Viou study site is located in the Austroalpine domain, composed of a large inlier element (Sesia-Lanzo Zone) and numerous outliers flaps, originally assembled in Dent Blanche stratum.

Within the stratum of the Dent Blanche, two groups of Austroalpine units can be distinguished: the upper (non-eclogitic) flaps, located on the top of the Piedmont Zone (Dent Blanche-M Mary, outcropping in

the study area-Pillonet); the lower flaps (eclogitic), tectonically intertwined within the ophiolitic Piedmont sequences, in the north (Etirol-Levaz) and in the south (M. Emilius, Glacier Rafray, Tour Ponton, Santanel Acque Rosse) of Graben Aosta-Ranzola or in the inner of Graben (Chatillon-St. Vincent) (Dal Piaz et al., 2010). The upper flaps (Pillonet, M. Mary, Dent Blanche), located to the north of the Dora, are made of various type of paragneiss, intercalated with ancient marbles and basic masses, and/or metagranodiorites, orthogneiss (Gneiss d'Arolla) and metagabbers derived from Permian protolites (Dal Piaz et al., 2010).

The Mont Fallère area is located in the axial sector of the Western Alps along the contact between the Middle Penninic (northern sector) and Piedmont Zone (southern sector). The Middle Penninic is represented by the Palaeozoic basement of the Gran San Bernard Nappe. This area consists of garnet micaschist and albitic paragneiss, with some minor bodies of metabasite, and is covered by discontinuous lower Mesozoic dolomitic metabreccia and marble (Forno et al., 2016). The overlying Piedmont Zone, which is represented by the Upper Tectono Metamorphic Units (as defined by Forno et al., 2012), consists of prevailing carbonate calcschist that alternates with decimetric marble layers. This marble contains many centimetric layers of quartzite, which were probably derived from original chert. Few discontinuous layers of meta-rudstone locally occur and consist of marble and dolomite clasts in a calcite matrix. All the rocks in this area were strongly deformed under blueschist metamorphic conditions, followed by widespread recrystallization under greenschist facies metamorphism (Forno et al., 2016).

As for the detailed description of the Geological Units which characterize the sample sites (fig. 4.2, 4.3), it is reported what is contained in the legend of the Italy Geological Map 1:50000, sheet 091 Chatillon (Dal Piaz et al., 2010) for Becca di Viou study site and sheet 090 Aosta (Polino et al., 2015) for Saint Nicolas study site.

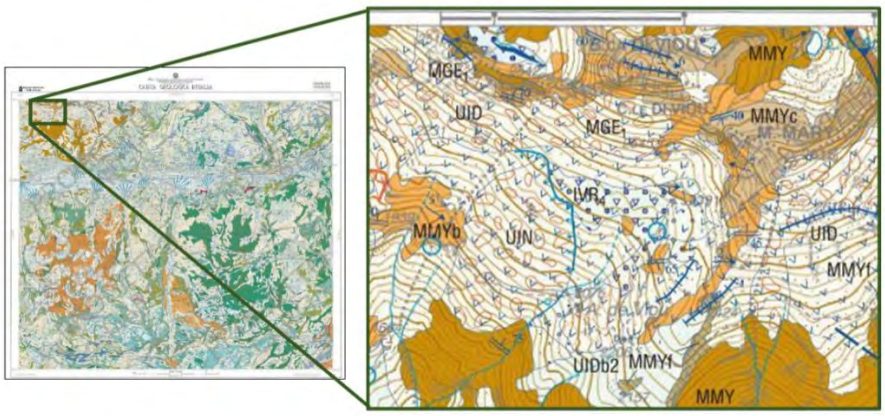

Figure 4.2. Geology of the Becca di Viou study area (taken from the sheet Chatillon, scale 1:50.000, Carta geologica d'Italia, ISPRA, 2010).

Austroalpine Domain

Lembi superiori

Mont Mary

Unità inferiore (PRE-TRIASSIC)

Extended portion of top-middle crust of prealpine age with from moderate to pervasive tecto-metamorphic alpine with green schist facies re-elaboration.

Complesso polimetamorfico indifferenziato (MMY)

The predominant lithotype is a paragneiss with chloritized biotite, light colored mica, porphyroblastic albite, epidotes, and rare garnet porphyroclasts. The paragneiss, with a well-preserved pre-alpine mark, have brown-reddish color and discontinuous band texture, alternating with rich biotite bedrocks and granoblastic domain with quartz and feldspats. Such textures recall facies of anatettica origin. Prealpine relict paragenesis consists of biotite-muscovite-plagioclase + - K-feldspate and garnet, which is sometimes associated with relict of andalusite, kyanite or staurolite. In some cases there are from centimeteric to decimetric vein of pegmatite that cut the Prealpine foliation.

Pegmatiti e loro derivati alpini (MMYb): the paraschists located at the top of the unit contain various intercalation of leucocratic rocks derived from pre-Alpine pegmatites. They have a very variable thickness, from m to hm. The major ones are located north of Chamerod and in the southern side of the Becca di Viou. The dominant type is a leucocratic gneiss with greenschists facies, with a highly schistic fabric and foliation underlined by thin layers of fengitic mica.

Parascisti a bande (MMYc): portion of polimetamorphic basement characterized by thin and repeated alternation of paraschists and gneissic pegmatite. The rocks has a from schistic-laminated to mylonitic fabric, are transposed along the alpine regional schistosity and, at least partly, are perhaps attributable to migmatites of varisic age or older.

Miloniti alpine (MMYf): extremely tectonized and retrograde varieties, with dark color and from m to dam thickness, rich in quartz, sericite and chlorite, derived from the paraschists of crystalline basement.

Quaternary Units.

Sintema di Ivrea

Includes deposits and landforms linked to the hydrographic and glacial grid, dating to the last great glacial expansion of the Upper Pleistocene, in particular at its retreat stages.

Subsintema di Pileo (IVR 4): Deposits belong to the last LGM and late-glacial period, composed of flaps located at the base of the principal tributary valleys. Their distribution varies with the morphology of the valleys and the retreat way of each glacier. Undifferentiated till, ablation and lodgment till; landslide deposits redistributed by ice flow, loose "skeletal" till, ice-contact deposits, glaciolacustrine and glaciofluvial deposits along the thalweg of tributary valleys.

Sintema del Miage (MGE) (POST-GLACIAL UNITS).
Local name of the Postglacial unit which includes the glacial and alluvial deposits laid down after the last glacial episode.

Subsintema del Chateau Blanc (MGE 1): ablation till and lodgment till, landslide deposits redistributed by ice flow and undifferentiated till, related to Little Ice Age or older Holocene-age glacial episodes, in moraines at the head of tributary valleys; alluvial terrace deposits.
The unit groups glacial and alluvial deposits linked to the Dora Baltea basin and is currently not in formation. The most recent and morphologically evident part of the glacial deposits, present only in the tributary valleys, is related to the last multi-century expansion period, known as PEG. Since recent formation, PEG's glacial deposits have a well-preserved morphologic expression, with moraines (lateral and frontal) and well-defined and continuous ridges, and poor or absent vegetation cover. In the area, all the moraine systems PEG-related are linked to modest size glaciers, which have now reduced their extension to about half that reached at the peak of the expansion phase, or which are currently reduced to glacierets. These deposits often appear as flow of large blocks that, due to subsequent periglacial deformations, do not follow the shape of the old glacier front.

Unità ubiquitarie (PLEISTOCENE SUP. – PRESENT).
Depositi completamente formati (UIN): Ancient landslides deposits, big blocks deposits and polygenic deposits; peat bog deposits.

Unità in formazione (UID): talus and landslide deposits, big blocks deposits, debris flow and polygenic deposits; peat bog deposits.

Prodotti detritico-colluviali indifferenziati (coltre detritico colluviale) (UID-b2): colluvial deposits derived from degraded bedrock and gravitational accumulates mainly due to sheet and rill erosion and soil slip. The colluvial deposits can almost completely cover the rock outcrops and the various types of deposits, with usually modest and variable thickness (from a few dm to a few meters). It consists of a

sandy-gravel non-thickened diamicton, formed by etherometric clasts, angular, in a slightly silty sandy matrix, if derived directly or indirectly from the rocky substrate. If is linked the re-elaboration of glacial deposits is made up of gravel-sandy materials, with boulders and pebbles of glacial transport and non-thickened sandy or sandy-silty matrix.

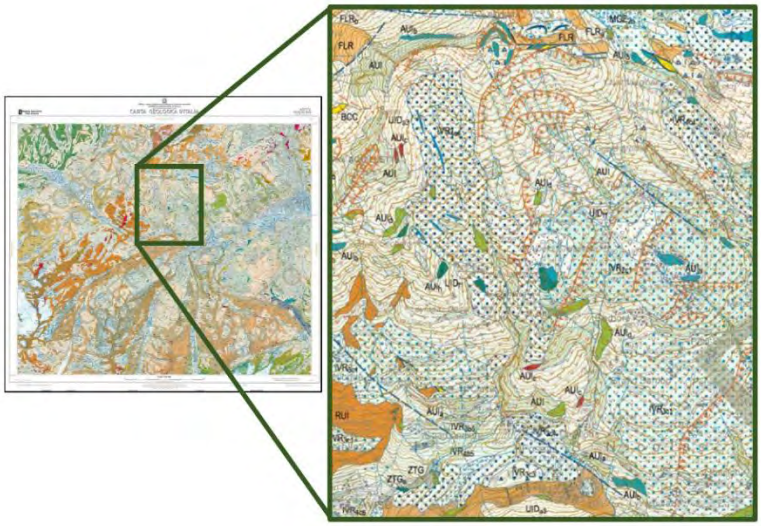

Figure 4.3. Geology of the Saint Nicolas study area (taken from the sheet Aosta, scale 1:50.000, Carta geologica d'Italia, ISPRA, 2015).

Unità di Crosta continentale.

Unità del Ruitor (PALEOZOIC)

Complesso del Ruitor (RUI): chloritoid-garnet-bearing paragneisses and micaschists, and biotitemuscovite-bearing paragneisses with alpine-age epidote-blueschist facies reequilibration.

Unità del Fallère-Métailler (falda del Mont Fort) (CARBONIFEROUS-PERMIAN)

Complesso del Fallère

Micascisti e paragneiss albitico-cloritici (FLR): reddish and locally porphyroblastic chlorite-albite micaschists and paragneisses, quartz-rich gneisses and minor chloritoid-bearing quartzites.

Prasiniti, ovarditi, metabasiti a glaucofane e granato e glaucofaniti a granato (FLRa): epidote-albite-actinolite-chlorite metamafites, glaucophane-garnet-bearing metamafites, and garnet-bearing glaucophane-rich metamafic rocks.

Micascisti a granato ± Na-anfibolo (FLRb): glaucophane-garnet-bearing micaschists.

Unità Ofiolitiche

Unità dell'Aouiletta (MESOZOIC)

Calcescisti indefferenziati

Calcescisti indifferenziati in facies scisti blu (AUI): are the most widespread part of the Unity. The prevalent litofacies are carbonate calceschists which contain variable quantity of quartz and white mica, chlorite and albite. There are sometimes intercalations from centimeters to meters of impure marbles (ridge between Punta Aouilletta and Punta Leisser), micaceous-cloritic marbles with ochre alteration coat (southern slope of Mount Fallere).

Alternanze di scisti fillonitici e marmi grigi (AUIa): main alternations of phyllonitic schists and greyish marbles.

Marmi dolomitici (AUIb): gray or white marbles, more or less dolomitic, with local levels of breccia with calcareous and dolomite elemtes. Mainly located in the northern margin of the Unit, near the contact with the Fallere-Métailler Unit.

Quarziti micacee e micascisti quarzosi (AUIc): micaceous quartzites and quartz-rich micaschists. Small outcrops are found within the deep-seated slope gravitational deformation of Punta Leisser.

Metabasiti e gneissparasinitici in facies scisti blu (AUId): metabasites and blueschist-facies mesocratic gneisses.

Zone di Taglio e Melanges tettonici
Predominantly composed of calc-micaschists, calcschists and phyllitic schists, historically attributed to the Piedmontese Zone, which include not only metabasite flakes, but also triassic shells and pretriassic basement.

Calcescisti, calcescisti marmorei, calcemicascisti e scisti filladici neri (ZTG): Calcschists, micaceous marbles, calc-micaschists and black phyllitic pelites.

Serpentiniti, serepentinoscisti e talcoscisti (ZTGa): serpentinites, serpentine-schists and talc-schists.

Brecce a cemento carbonatico (BCC): carbonate tectonic breccias with fragments of calcitic and dolomitic marbles and minor calcschists and micaschists, exposed along major shear zones and high-angle faults (*Carniole Auct.*)

Quaternary deposits.
Sintema di Ivrea (IVR): includes deposits and landforms linked to the hydrographic and glacial grid, dating to the last great glacial expansion of the Upper Pleistocene, in particular at its retreat stages.

Subsintema di Nissod (IVR1): dissected remnants of undifferentiated till, at elevation greater than 1700 m a.s.l. on both sides of the main valley, related to the maximum development of the glacial network.

Subsintema di Colle San Carlo (IVR2): undifferentiated till, lodgment till and loose 'skeletal' till at intermediate to high elevation on the slopes of the main valley, or in small dissected remnants at high elevation in tributary valleys. It includes deposits left by glaciers, belong to Dora Baltea basin, during the second phase of LGM. The most extensive glacier deposits attributable to the Subsistema di Colle San Carlo are preserved within the area of Punta Leisser DGPV, and in particular at Vetan and around Verrogne. Clast supported glacial deposits, dominated by local lithologies (calcschists and marbles) angular clasts with granites, gneiss, serpentinites and prasinite, in sandy-gravel matrix (50%), prevail (IVR2c1).

Subsintema di Excenex (IVR3): undifferentiated till, ablation till, lodgement till, landslide deposits redistributed by ice flow, ice-contact deposits, glaciolacustrine and glaciofluvial deposits, in dissected remnants at low-to-intermediate elevation in the main valley and in the Buthier and Grisenche valleys.

Subsintema di Pileo (IVR4): undifferentiated till, ablation till and lodgement till; landslide deposits redistributed by ice flow, loose 'skeletal' till, ice-contact deposits, glaciolacustrine and glaciofluvial deposits along the thalweg of tributary valleys or in dissected remnants at low elevation in the main valley.

Sintema del Miage (MGE): local name of the Postglacial unit which includes the glacial and alluvial deposits laid down after the last glacial episode.

Subsintema di Les Iles (MGE2): fluvial deposits related to present-day activity of river channels or preserved in lowermost fluvial terraces; lodgement till deposited by present-day glaciers.

Unità ubiquitarie in formazione (UID) (PLEISTOCENE SUP. – PRESENT).

Depositi detritici di falda e di conoide (UID a3): gravity deposits located at the base of the mountainside, due to detachment, fall and accumulation of rock fragments. The deposits are composed of hetherometric coarse and angular clasts, with scarce matrix and open to clasts supported texture.

Travertino e agglomerati detritici a cemento travertinoso (UIDf1): travertines are genetically linked to the presence of carbonate formations (calcschists and marbles) deeply and intensely fractured.
The greatest concentration of travertine masses is found in the area of the Punta Leisser DGPV, particularly along the incisions of Isolettaz and Vétan streams between the villages of Vetan and the Grand Arpilles alpine pasture, and also in the incisions of T. Verrogne (between 1830 and 1870 m a.s.l.), T. Méod (1600 m a.s.l.), on the right of T. Gaboé (from 1280 m to 1370 m a.s.l.), at Alpe Leytanaz-Damon, 200 m east of Verrogne and finally along the road to St. Nicolas between the villages of Ferrère and Gratillon.

4.1.3 Geomorphology

The Valle d'Aosta region is characterized by glacial, alluvial and gravity deposits mainly generated during the retreat of the maximum glacial expansion. Quaternary deposits has been largely influenced by alpine glacier modelling during glaciations; the expansion of Dora Baltea glacier has repeatedly affected the entire main valley (Gianotti et al., 2008). Sediments linked to glacial activity, such as undifferentiated till, ablation till and lodging till, are very widespread. PEG-related moraine systems are also observed, in the area are linked to modest size glaciers, which have now reduced their extension to about half that reached at peak of the expansion phase or which are currently reduced to glacierets. Moreover, large gravitational slope deformations, rock falls and debris flows are a characteristic feature of the study area (Dal Piaz et al., 2010).
In particular, the study area of Becca di Viou is characterized by the presence of extensive talus slopes and rockfall deposits above the forest line. The study area is mainly dominated by mass wasting and gravity processes. Glaciers are absent in the present day and deposits due to mass wasting dominate the landscape. Detachment zones related to rock falls and rock avalanches are present on the higher slope. Unconsolidated and coarse deposits characterize the whole site (Leonelli et al., 2011a). The debris cover is represented by many debris cones and, in the central belt, by a continuous talus slope. Several debris-flow channels and deposits cross this talus slope. Between the talus area and the rocky area the debris is partially stabilized, while below the talus area, the soil slopes are more stable (Leonelli et al., 2011a).
The Saint Nicolas study site is located in an area now completely free of glaciers but largely shaped by the wide Clusellaz Glacier during the Last Glacial Maximum (LGM) and Lateglacial (Forno et al., 2013).

This glacier previously drained through the Clusellaz Valley, only subsequently shaping the Verrogne Valley. In the glacial valley floor and in the low slopes many rocky rounded reliefs and associated depressions, linked to subglacial erosion, are found. Subglacial sediments and glacial marginal deposits, which form short and low lateral moraines, locally cover these landforms (Forno et al., 2016). The same glacial valley floor and the low slopes also locally conserve horizontal surfaces, which consist of shallow lacustrine and peat sediments from the Lateglacial to the Holocene in age (Forno et al., 2016). Debris, colluvial, avalanche and torrential sediments, formed during the Holocene, widely cover the bedrock and the more ancient Quaternary sequences. Bedrock, Quaternary cover and landforms have also been fractured, loosened and dislocated by DSGSD structures (Forno et al., 2016). The Punta Leisser DSGSD is one of the largest in the Valle d'Aosta (23 km^2 of surface area), it is complex and consists of zones with varying degrees of deformation and with different movement directions; is characterized by a more deformed central sector, extending for about 9 km^2 and morphologically similar to a landslide cone (Polino et al., 2015). This area is moved (about 1 km according to the morphological evidence) to the valley bottom, causing the shrinkage (Polino et al., 2015). Moreover, the presence of particularly rugged rock predisposes the evolution of various size landslides. In addition, karst corrosion phenomena, in deep horizons of carbonate or sulphatic rocks, have been hypothesized as the main cause of some DSGSD (Carraro in Dal Piaz, 1992) and as a concomitant cause. In the Saint Nicolas study area the presence of DSGSD conditions the water erosion processes, in fact the water erosion acts selectively on impluvium, influenced by the structural conditions. In particular the study area is affected by running and concentrated water run off processes that shaping badlands. The area subject to erosion due to water driven processes is changing in space and time (fig. 4.4), nowadays they have progressively reduced. Moreover, the badlands stabilization favors and is favored by the vegetation colonization.

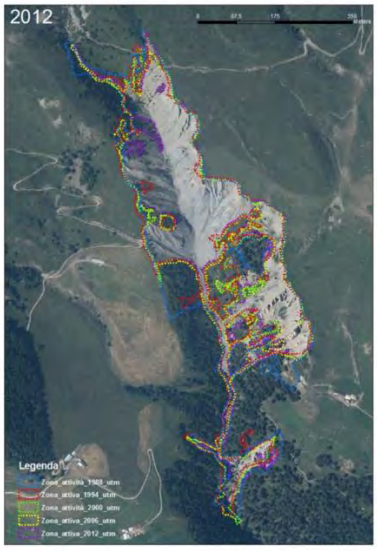

Figure 4.4. Area variation of the zone affected by erosion and scarp recession in the period 1988-2002. (Modified from Cattaneo, 2014)

4.1.4 Soils

The two study area are characterized by the presence of different type of soil (Carta Ecopedologica d'Italia 1:250000, Geoportale Nazionale, 2013). In particular, the Becca di Viou study area is characterized by the presence of two ecopedological units. Both units have the same parent material, as micaschists, paragneiss, phyllites and marbles, and are typified by thin and not well developed soil, with a lot of coarse component, characteristic of high mountain areas, like Leptosol and Regosol. In the unit at lower altitude, Umbrisols are also found.

Also in the Saint Nicolas study area, two different ecopedological units are found (Carta Ecopedologica d'Italia 1:250000, Geoportale Nazionale, 2013). The first unit is located in the portion at higher altitude with micaschist, paragneiss, phyllites and marbles as parent material, in this unit a thin soil (Leptosol) and a soil characterized by surface layer rich in humus (Umbrisol) are found. The second unit is placed at lower altitude and has a metamorphic limestones and marls as parent material. In this unit, there are three typology of soils: from very thin (Leptosol) or not well developed soil (Regosol) to a soil with properties, aggregate structure, colour, clay content, carbonate content, that give some evidence of soil-forming processes (Cambisol).

4.1.5 Climate

The climate in the region has a semi-continental temperature regime, with a monthly temperature range of about 20°C. Precipitation is scarce (about 680 mm in the main valley) with 70% of the land receiving less than 1000 mm per year (Mercalli et al. 2003). In particular, regarding the temperature trends recorded in Aosta, observing the Aosta (Saint Christophe) climogram (fig. 4.5), there is a winter minimum average temperature in January (-0.1°C) and a summer maximum average temperature in July (19.2°C), with an annual thermal excursion slightly lower 20°C. Average precipitation is scarce, concentrated in the summer months and with a minimum in January (805 mm annually).

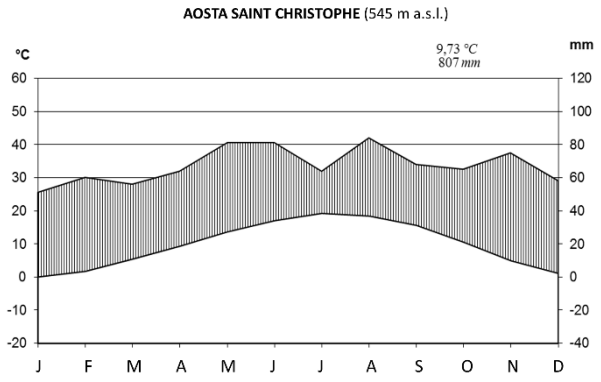

Figure 4.5. Climograph of Aosta weather stations (modified from Pellegrini, 2016).

Analyzing the mean annual temperature of the period 1974 to 2017 (fig. 4.6) a period of marked temperature increase is evident starting from 2000 to nowadays.

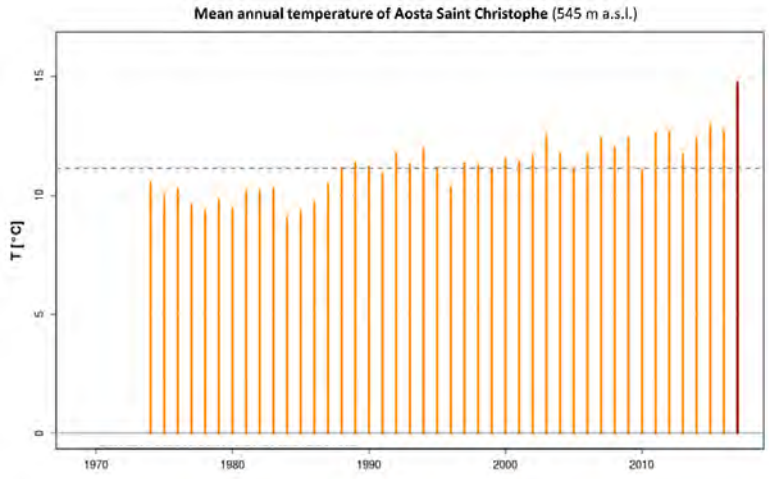

Figure 4.6. Mean annual temperature of Aosta weather stations, in orange the mean annual temperature, in red the 2017 mean anuual temperature and in grey the mean annual temperature for the period 1981-2010 (Centro Funzionale della Valle d'Aosta, 2017).

4.1.6 Vegetation

The broad altitudinal range of the two study sites, ranging from 1300 m to 2400 m a.s.l., determines a strong variability of ecological conditions that affect the type of vegetation cover.

In the Becca di Viou study area *Picea abies* and *Pinus sylvestris* forest dominate the belt under 1900 m a.s.l., whereas the closed mixed forest dominated by *Larix decidua* and *Pinus cembra* reaches higher altitude (about 2300 m a.s.l.) (Forestazione-foreste di protezione, Geoportale Valle d'Aosta, 2013). In 2008 the treeline was located at an average altitude of 2515 m a.s.l, while the species line for the European larch at this site, determined by living specimens, was found at 2545 m a.s.l. (Leonelli et al., 2011a). Up to high altitudes there are several sparse portions of alpine grassland and shrubs. Past timber harvesting may have altered the distribution of trees, especially on the southernmost side of the area. However, the forest in its highest portion and at the treeline ecotone presents semi-natural conditions, with some old trees in the open forest at the lower treeline and progressively younger trees at the upper treeline. Some small trees, stunted and deformed trees (krummholz), dead trees and saplings are sparsely present at the species line (Leonelli et al., 2011a).

At Saint Nicolas study site, the montane zone, from 1300 to 1500 m a.s.l., is characterized by *Pinus Sylvestris* and Black Pine (*Pinus nigra*). Due to the favorable exposure and climate conditions of the area, the limit of broadleaf (such as poplars, oaks and locust tree) rises at higher altitude. The subalpine zone, between 1500 m a.s.l. and 2100 m a.s.l., is dominated by *Larix decidua* and *Picea abies*, but locally other trees such as *Betula* sp., *Salix* sp., *Alnus viridis* are found. Above the limit of the arboreal

vegetation, the upper alpine zone, between 2100 m and 2400 m a.s.l., is characterized by the alpine grasslands and shrubs (*Juniperus* sp. and *Rhododendron* sp.).

4.1.7 Human presence

Especially in the study area of Saint Nicolas the man presence is attested from the Mesolithic period. In fact a palynological study (Pini et al., 2012) carried out in a peatland, not far from the sampling site, found higher frequency of fire probably associated with hunting camps. The same study shows that since the Copper Age, high altitude forests were severely damaged by cutting and fire: the free areas were used as alpine pastures for seasonal and alpine transhumance activities. And until the Bronze Age there is a deforestation and spread of fertilized alpine pastures and nitrophile vegetation. Anthropic deforestation on Mt. Fallère, begun in the IV millennium BC, continues until the transition of the Age of Copper - Bronze Age, and at the beginning of the Roman Age a further expansion of pastures areas is identified. Nowadays the area is mainly used for grazing.

In the Becca di Viou study area, the irregular conditions of the surface prevented an intensive exploitation of the area in the past centuries. South-west of the study area, about 200 m below the forest treeline boundary, instead, there is barn (at 2080 m a.s.l.) and an alpine pasture where cows graze during summertime (Leonelli et al., 2011a).

4.2 Results

4.2.1 Becca di Viou study case

4.2.1.1 Results of geopedological analysis

Field and laboratory characterizations have been performed along two transects of seven soil profiles developing at an altitude ranging from 2100 m a.s.l. (closed forest) to 2400 m a.s.l. (treeline ecotone), in order to understand the relationships between colonization by trees and soil development under the ongoing climate change and also to search the evidence of buried paleosurfaces (fig. 4.7).

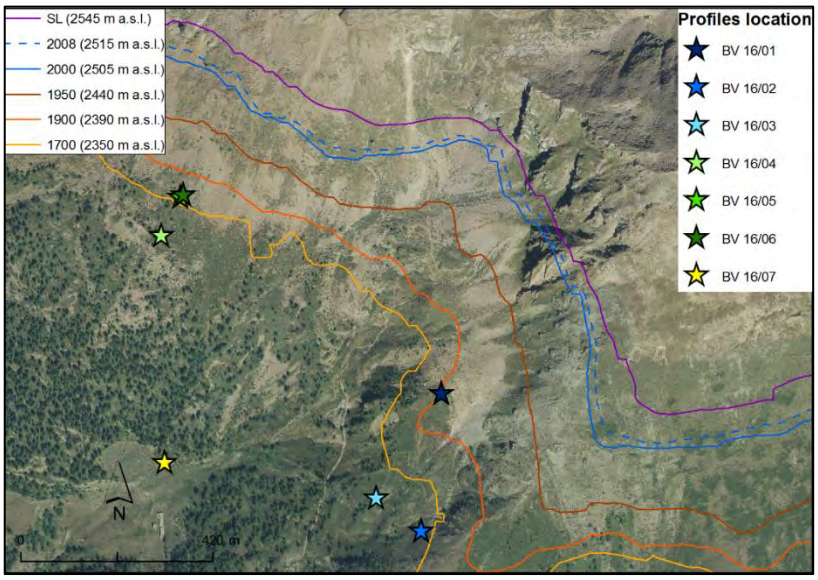

Figure 4.7. Profiles location and treeline position.
The orthophoto has been drawn from spatial data available at the National Geoportal.

4.2.1.1.1 Field data

Three soil profiles (BV16/01, BV16/02 and BV16/03) are located on the right portion of SW slope of Becca di Viou, while other three soil profiles (BV16/04, BV16/05 and BV16/06) are placed on the left portion of SW slope of Becca di Viou. (fig. 4.7, tab. 4.1). As comparison, one soil profile (BV 16/07) was done in forested area (fig.4.7).

Profiles thickness assumes variable values (usually 0.3 to 0.6 m) depending on the altitude range and vegetation cover. In fact, on average maximum thickness is found in correspondence of soils evolved in forested area and the minimum thickness is found in correspondence of soil evolved in the treeline ecotone. The profile BV 16/02, even if is located in the treeline ecotone, has a high thickness.

The colour of the horizons shows a clear uniformity in the area, particularly as regards the hue values, that is never different from 10 YR or 2.5 Y. Soil structure is moderately expressed, both at the treeline ecotone and in forested area the soil are mainly characterized by granular aggregates (Appendix 3).

Profile	Elevation (m a.s.l.)	Slope (°)	Slppe exposure	Profile exposure	Parent Material	Geomorphology	Vegetation
BV16/01	2400	10	N	N	Gneis and Shists	slope deposits	treeline ecotone composed of open *Larix decidua* stands
BV16/02	2340	20	NW	NW	Gneis and Shists	slope deposits	treeline ecotone composed of open *Larix decidua* stands
BV16/03	2300	30	W-SW	W-SW	Gneis and Shists	slope deposits	treeline ecotone composed of open *Larix decidua* stands
BV16/04	2325	15	SW-W	SW-W	Gneis and Shists	slope deposits	treeline ecotone composed of open *Larix decidua* stands
BV16/05	2365	25	S-SW	S-SW	Gneis and Shists	slope deposits	treeline ecotone composed of open *Larix decidua* stands
BV16/06	2370	25	S-SW	S-SW	Gneis and Shists	slope deposits	treeline ecotone composed of open *Larix decidua* stands
BV16/07	2110	20	S-SW	S-SW	Gneis and Shists	slope deposits	Open forest

Table 4.1. Station descriptions for the studied profiles.

4.2.1.1.2 Particle size analysis

Examining the relative percentages of particle size distribution in the analyzed soil profiles it can be seen that there is a common trend. First, the gravel is on average in large quantities and varies between 5% to 60%.

The silt content is higher compared to the sand and clay content. In fact, the amount of silt ranging between 15% and 60% on total weight (fig. 4.8, 4.9), whereas the amount of sand and clay ranging between 8-40% and 0.2- 16% respectively. In almost all soil samples, gravel and silt are the predominant fractions, while the amount of clay is more variable. In deeper horizons, the percentages of gravel tend to increase to the detriment of the fine earth component (fig. 4.9). In no profiles, trend anomalies are found.

In the BV 16/02 profiles, the content of coarse fraction has a visible increasing trend with depth, as well as a progressive decreasing trend of the clay. However, observing the cumulative curves (fig. 4.8) is clear that in BV 16/02 profile there are two distinct families of curves. One includes the superficial horizons (O and AC) and one includes the deeper horizons (2AC, 3Bs and 3BC).

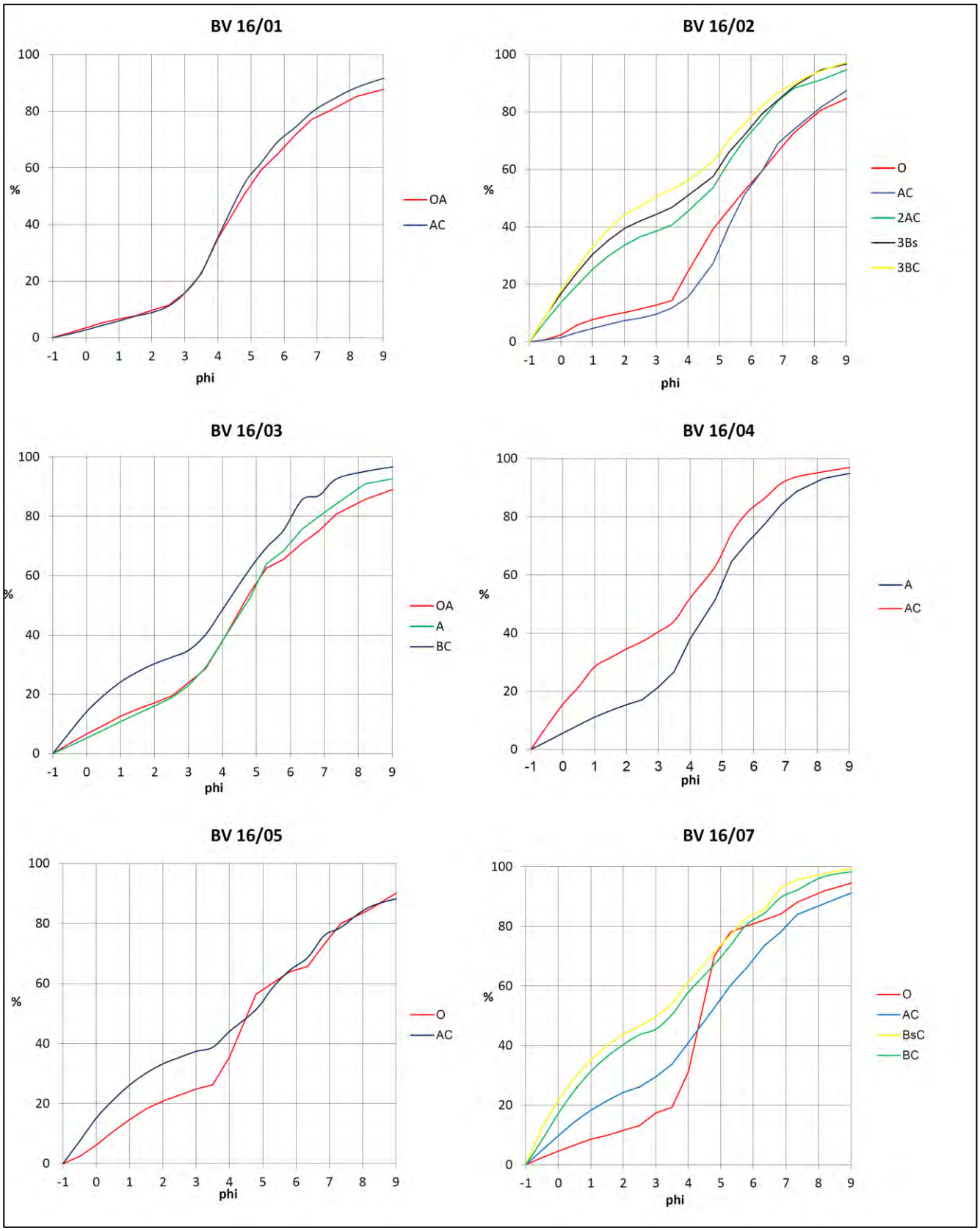

Figure 4.8. Cumulative curves of grain size distribution in the studied profiles.

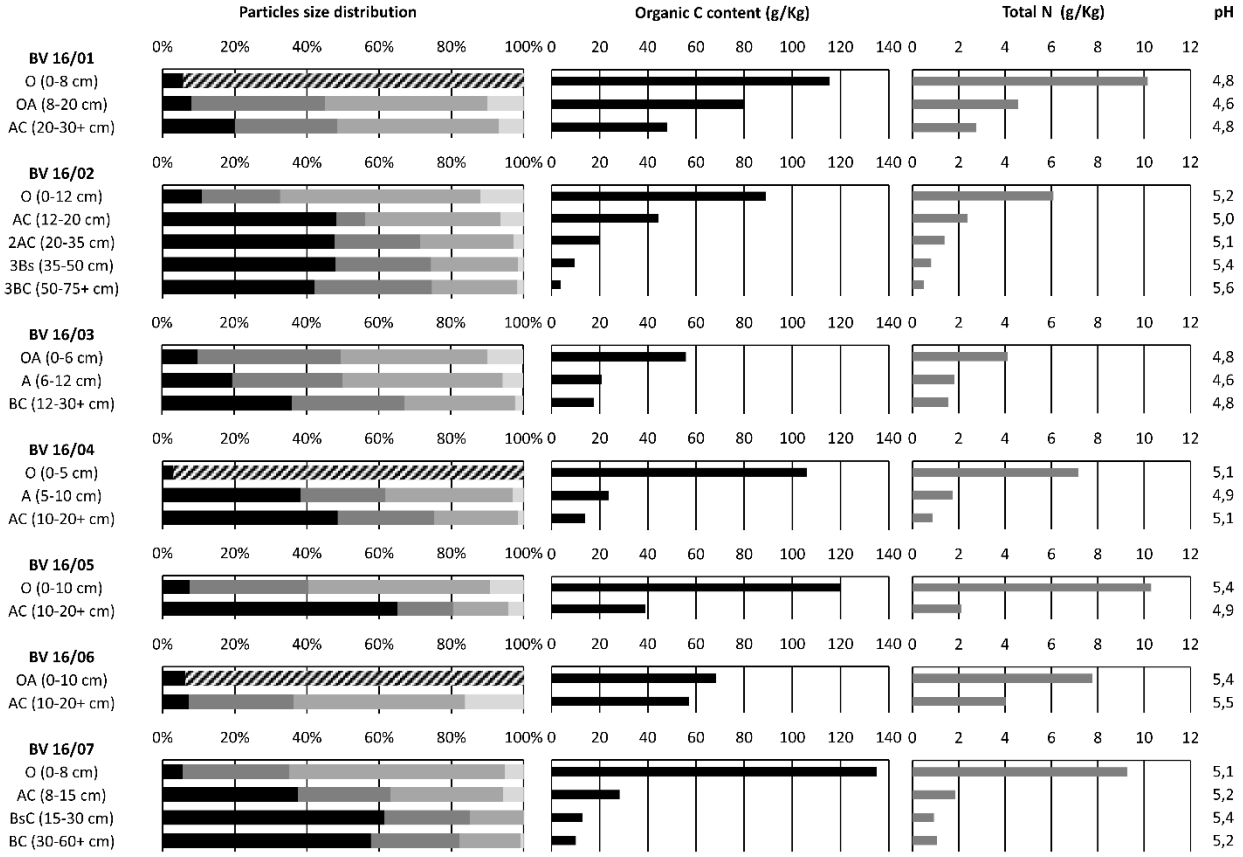

Figure 4.9. Particle size distribution, Organic C content, total Nitrogen content and pH values in the studied profiles. For the particle size distribution plot: in black is depict the gravel content, in dark grey the sand content, in grey the silt content. in light grey the clay content and in black strips the n.d..

4.2.1.1.3 Organic Carbon Content

The absolute quantities of organic carbon are very variable depending on the type of profile and depth (fig. 4.9). In surface horizons, values ranging between 55.8 (BV 16/03) and 135 g/kg (BV 16/07) are found. Usually, the C organic values decrease with depth: the general trend is therefore represented by a decrease of organic carbon content as horizons get deeper. This decrease can be more or less gradual, as in profile BV 16/01, or concentrated as a rapid loss at the transition from the uppermost horizon to the ones those below, such as in the profile BV 16/07.

All the profiles show the same trend, characterized by a decreasing in C content with depth.

4.2.1.1.4 Total Nitrogen

The total nitrogen contents have the same trend of the organic C content (fig. 4.9), but with significantly lower values (not exceeding 11 g/Kg). The total nitrogen content decrease with depth along the profile

and the decrease is concentrated as a rapid loss at the transition from the uppermost horizon to the ones those below, while in the underlying horizons the decrease is more gradual.

The highest content of total N are found in the superficial horizons and, in particular, the BV16/01 and BV16/05 have the greatest values. Whereas, the lowest values are recorded in BV 16/02 3BC (about 0.5 g /Kg).

Finally, the C/N ratio have values ranging between 14.8 and 8.8 g/Kg in the superficial horizons. In the profile BV 16/03 the C/N ratio decreases with depth, while in the BV16/01, BV 16/04, BV16/05 and BV 16/06 profiles increases with depth. In the profiles BV 16/02 and BV 16/07 the C/N ratio tend to decrease with depth, with exception of the horizon below the superficial one, where there is a peak of C/N ratio (fig. 4.10).

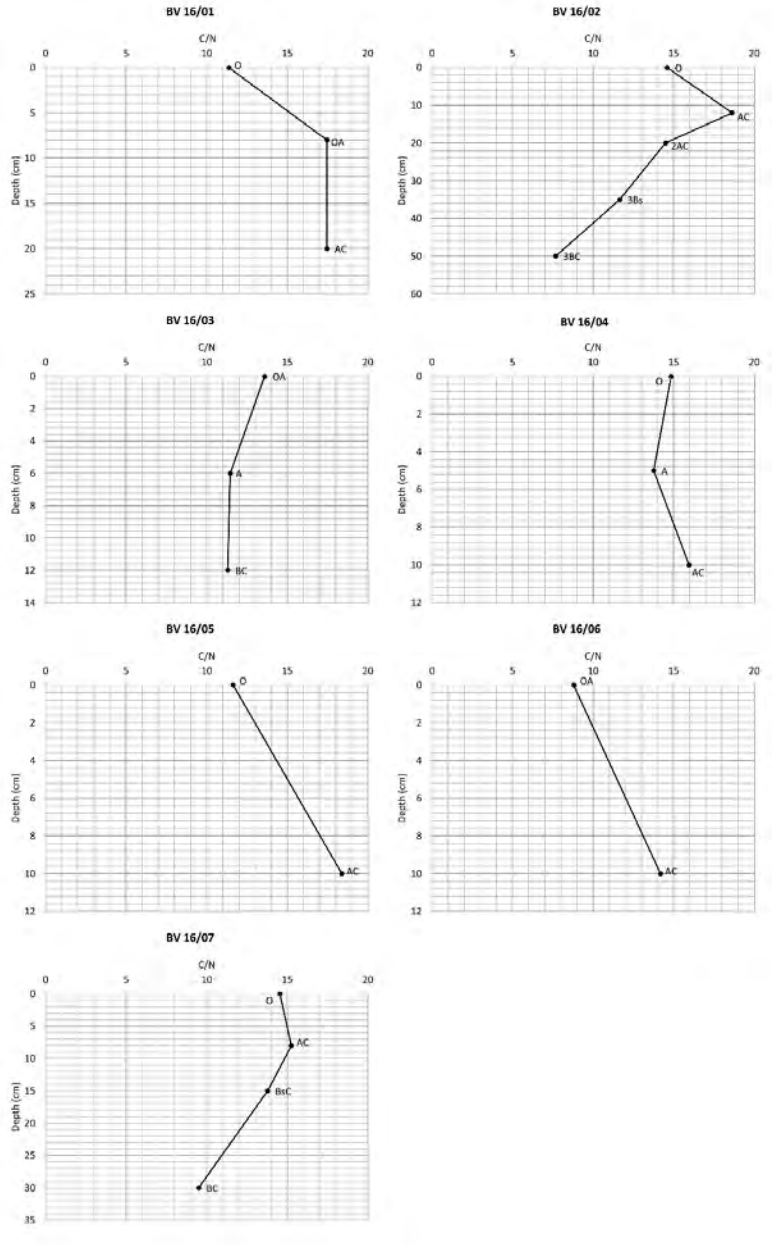

Figure 4.10. C/N ratio in the studied profiles.

4.2.1.1.5 pH

All the soil horizons analyzed have a tendency to acidity, the values of pH in H_2O ranging between 4.6 and 5.6 (fig. 4.9). Although, the pH values measured in H_2O neither gets large variations between successive horizons nor within the entire depth of profile, in almost all the profile the pH values progressively increase with the profile depth, approaching to the parent material. In many cases this variation seems very moderate, being rarely more than 1 pH unit and for almost all the profiles (except for the profile BV 16/07) the most superficial horizons showing a lower acidity than the immediately underlying horizons.

However, since the pH values varies only from few point along the profile (for almost all the profiles the pH values varies by less than 0.5), a well-defined pattern cannot be recognized.

4.2.1.1.6 Alluminum and Iron extractions

The total content of free iron oxides (Fed) do not exceed the 16 g/Kg and ranging between 3.2 and 15.3 g/Kg. The values of amorphous iron oxides (Feo) are slightly lower and ranging between 0.9 and 13.6 g/Kg, as the iron bound with the organic matter (Fep) that ranging between 1.3 and 10.8 g/Kg. For all three of these parameters, particularly high values are observed in BV 16/02 2AC and BV 16/03 BC horizons (fig. 4.11).

As regards the aluminum content, the quantities tend to be inferior to those of iron, and less variable. Free aluminium oxides (Ald) reaches values between 1 to 4.4 g/Kg, amorphous aluminium oxides (Alo) between 0.6 and 6 g/Kg, while the aluminium bound with the organic matter (Alp) has greater values (between 2.4 and 29.3 g/Kg).

Both the iron and aluminum show similar trends and similar peaks along the profiles.

On average, the crystalline iron oxides content is very variable. In particular, the crystalline iron oxides are mainly concentrated in the superficial and in B horizons (tab. 4.2). The highest values are found in the BV 16/04 AC (11.2 g/Kg). The buried horizons BV16/02 3Bs and 3BC have values similar to the BV 16/07 BsC horizon.

The Feo/Fed index has low values, in particular only two horizons (BV 16/02 AC and BV 16/03 BC) have an iron activity index higher than 0.8. (tab. 4.2). Finally, the results of the podzolization index Alo + ½ Feo meet the conditions of podzolization processes in the BV 16/02, BV 16/03 and BV 16/07 profiles (FAO, 2014).

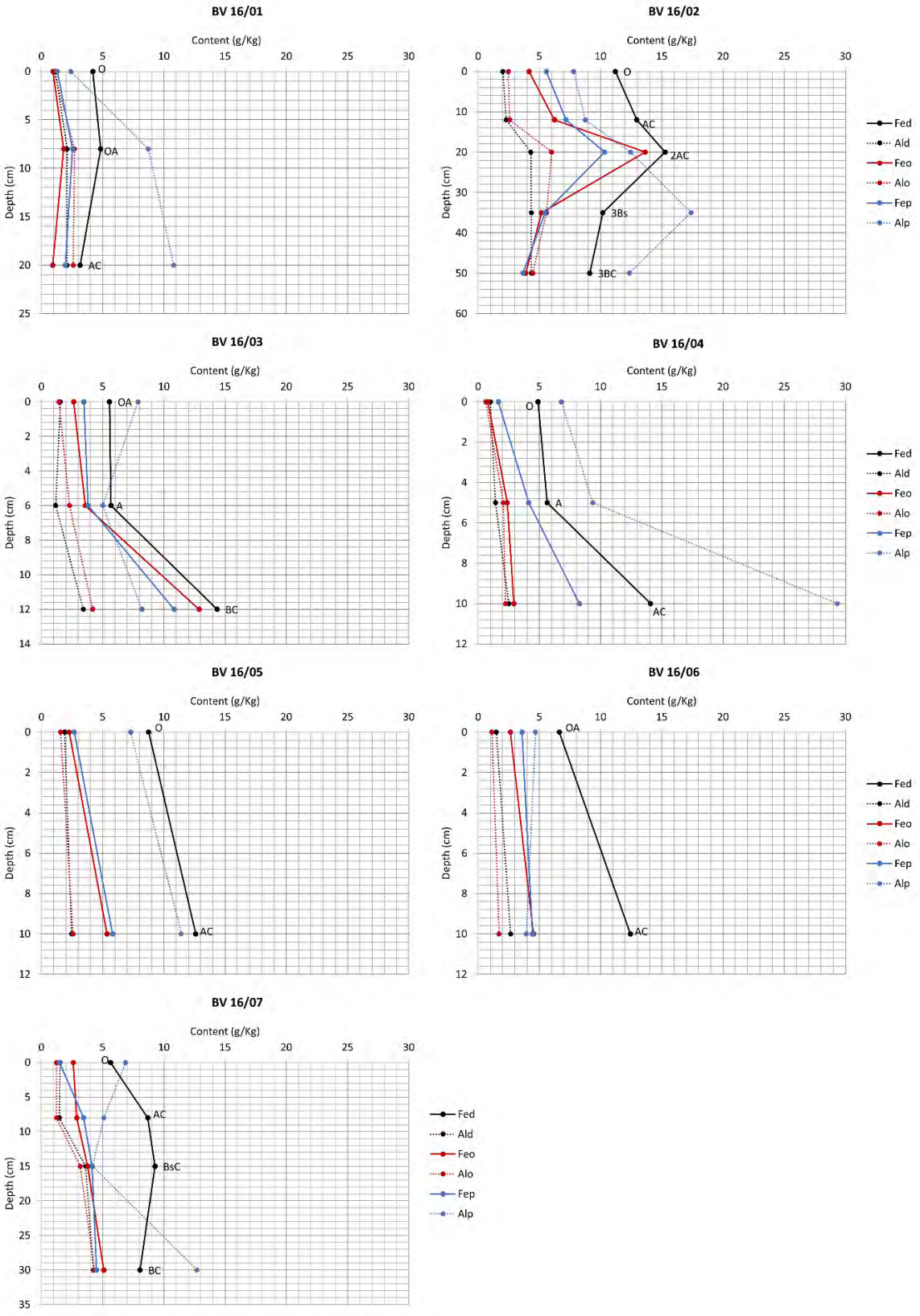

Figure 4.11. Free iron oxides (Fed), amorphous iron oxides (Feo) and iron bound to the organic matter (Fep) content, free aluminum oxides (Ald), amorphous aluminum oxides (Alo) and aluminum bound to the organic matter (Alp) content of the studied profiles The horizons name are close to the Fed curves.

Profile	Horizons	Depth (cm)	Fed-Feo (g/Kg)	Feo/Fed	Alo+1/2Feo (%)
BV 16/01	O	0-8	3.3	0.23	0.15
BV 16/01	OA	8-20	3.0	0.38	0.36
BV 16/01	AC	20-30+	2.2	0.29	0.31
BV 16/02	O	0-12	7.0	0.37	0.45
BV 16/02	AC	12-20	6.7	0.48	0.57
BV 16/02	2AC	20-35	1.6	0.89	1.28
BV 16/02	3Bs	35-50	5.0	0.51	0.82
BV 16/02	3BC	50-75+	5.2	0.43	0.64
BV 16/03	OA	0-6	2.9	0.47	0.27
BV 16/03	A	6-12	2.1	0.63	0.41
BV 16/03	BC	12-30+	1.5	0.90	1.06
BV 16/04	O	0-5	4.1	0.16	0.10
BV 16/04	A	5-10	3.3	0.42	0.32
BV 16/04	AC	10-20+	11.2	0.21	0.37
BV 16/05	O	0-10	6.5	0.26	0.27
BV 16/05	AC	10-20+	7.2	0.43	0.53
BV 16/06	OA	0-10	4.0	0.40	0.24
BV 16/06	AC	10-20+	7.9	0.36	0.40
BV 16/07	O	0-8	3.0	0.46	0.25
BV 16/07	AC	8-15	5.8	0.33	0.27
BV 16/07	BsC	15-30	5.5	0.41	0.51
BV 16/07	BC	30-60+	3.0	0.63	0.69

Table 4.2. Iron and aluminum indeces. Crystalline iron oxides (Fed-Feo), activity iron index (Feo/Fed) and podsolization index (Alo+1/2Feo).

4.2.1.1.7 Rock-Eval data

In the I/R diagram the organic horizons have I-index values between 0.2 and 0.5 and R-index between 0.35 and 0.55. While the B and C horizons have I-index values between 0.1 and 0.3 and R-index between 0.5 and 0.65 (fig. 4.12). Whereas the BV 16/02 2AC, 3BC and 3Bs horizons have I-index values between -0.1 and 0 and R-index between 0.7 and 0.75.

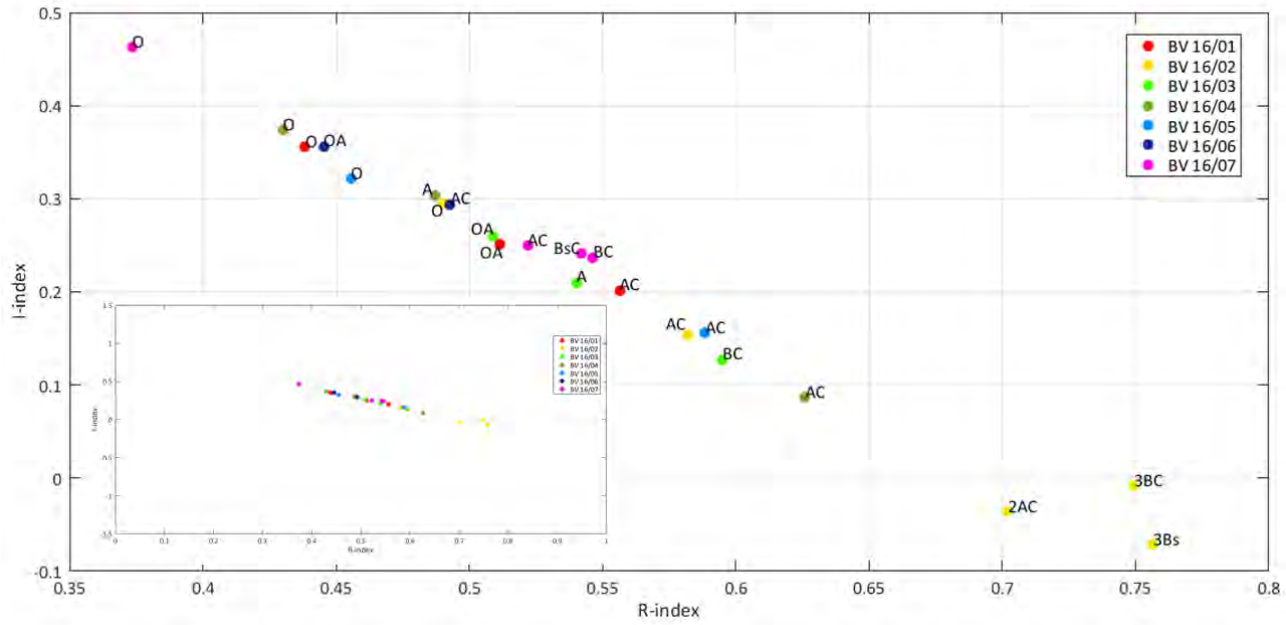

Figure 4.12. I-index/R-index. On the bottom left the data are plotted using the grid values from Sebag et al., 2016 in order to better visualize the trends.

The HI/OI index show different values in different horizons typology (fig. 4.13). In fact, the O and A horizons show a high HI values and low OI values, while the B and C horizons show high OI values and low HI values. The 3Bs and 3BC horizons have the highest OI values and the lowest HI values.

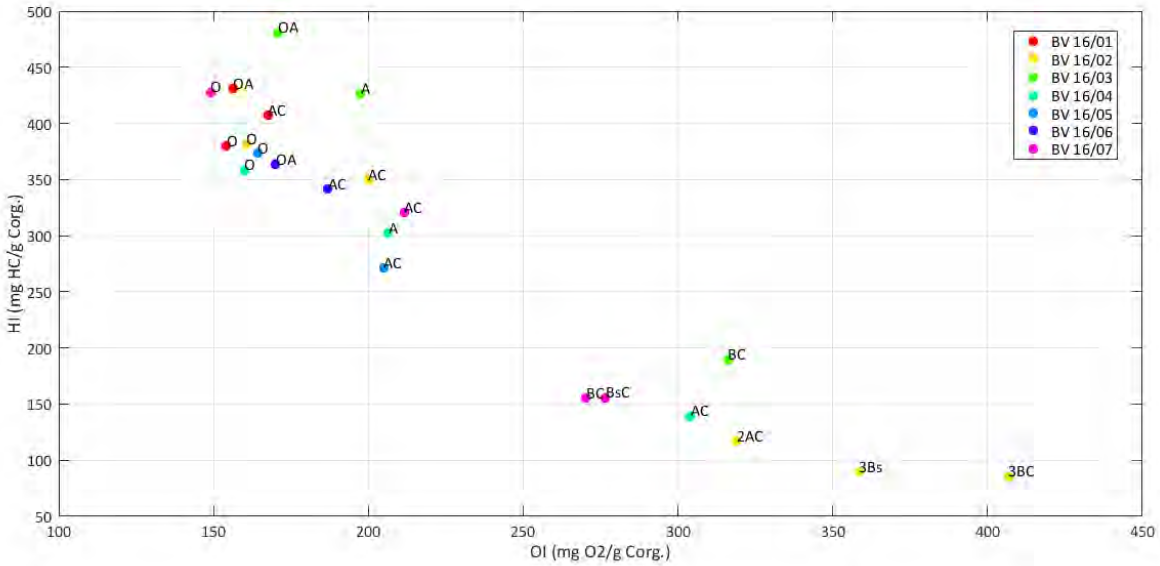

Figure 4.13. HI/OI diagram.

4.2.1.1.8 Results of Isotope analysis

The $\delta^{15}N$ ranging from -2 to 7 (‰), and almost in all the profiles the $\delta^{15}N$ increase with depth (fig. 4.14). In the profile BV 16/02 a negative peak is found, in fact the horizons 2AC, 3Bs and 3BC are characterized by $\delta^{15}N$ lower than the overlying horizons. The $\delta^{13}C$ ranging from -28 to -25 (‰) (fig. 4.15). In the profiles BV16/03, BV16/04 and BV16/06 $\delta^{13}C$ increase with depth. Whereas, in the profiles BV 16/01, BV 16/02, BV 16/05 and BV 16/07 a trend inversion is found.

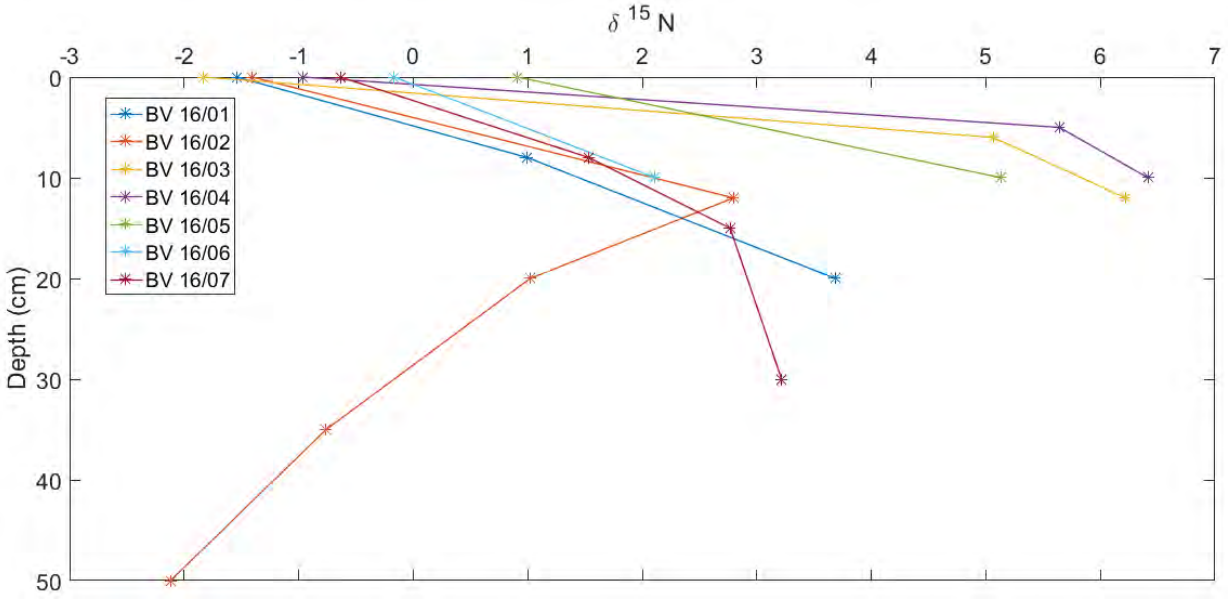

Figure 4.14. $\delta^{15}N$ (‰) content of the studied profiles.

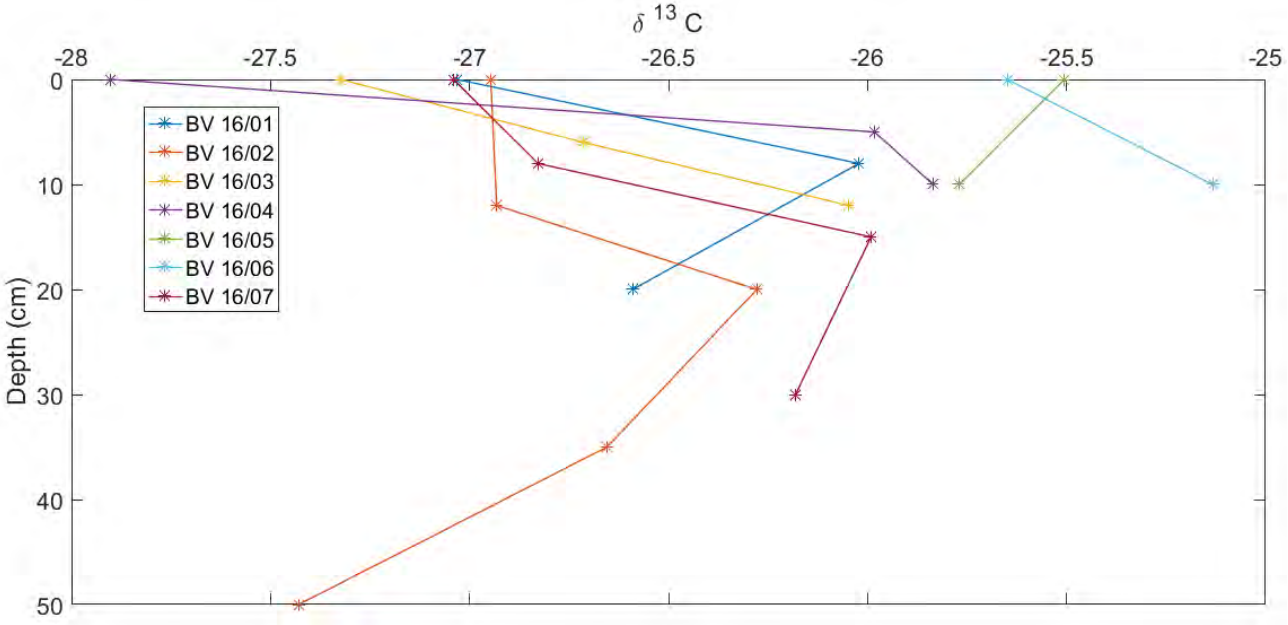

Figure 4.15. $\delta^{13}C$ (‰) content of the studied profiles.

Moreover, in the plots showing the isotopic enrichment for each profile with reference to the first horizon (fig. 4.16, 4.17) the BV 16/02 show a marked inversion of the trend and is the only profile to have a negative Δδ, along the profile, for both ^{13}C and ^{15}N.

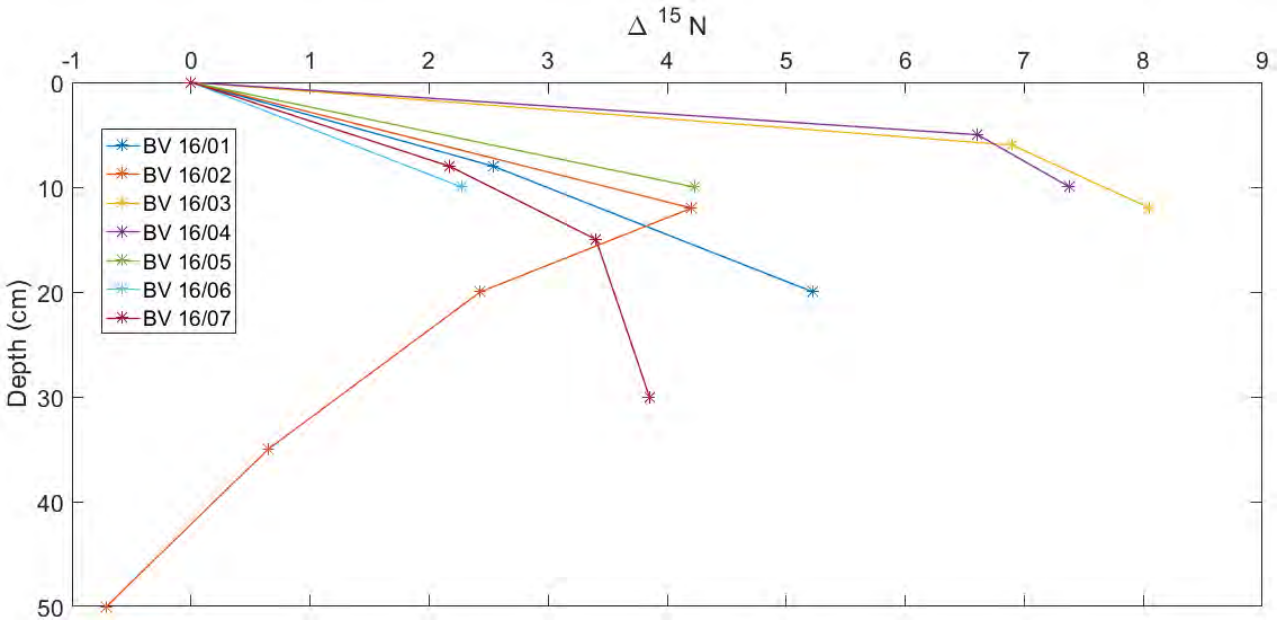

Figure 4.16. Δδ ^{15}N (‰) content of the studied profiles, isotopic enrichment with reference to the first horizon.

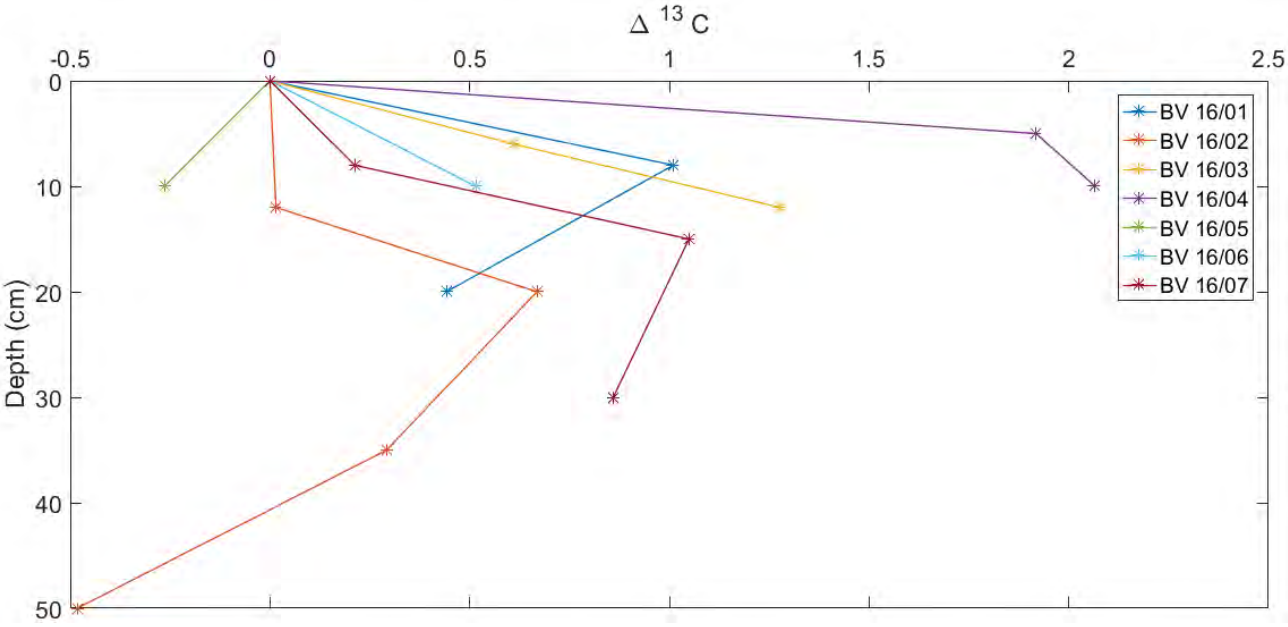

Figure 4.17. Δδ ^{13}C (‰) content of the studied profiles, isotopic enrichment with reference to the first horizon.

4.2.1.2 Dendroclimatic analysis

The moving correlation function (MCF) analysis confirms the predominant influence of early summer mean temperatures on tree growth but shows that the climate/growth relationship has varied over time. In fact, the larch chronology shows a non stationary climate-growth response, particularly for May and June mean temperatures.

The MCF analysis performed with May mean temperatures shows a long-term increasing trend in the correlation coefficient values (fig. 4.18). This trend is most evident for the period 1925–1960. A slight decrease started in the 1960s and was followed by a renewed increase in the correlation coefficient values for the latest years of the analysis. Since 1988, the correlation coefficient alternates between little increment and little reduction. However, the long-term trend show a correlation coefficient increase. The correlation coefficient is significant only for a few portion of the analysis.

The MCF analysis performed with the June mean temperatures (fig. 4.18) shows that the correlation coefficient values have a synchronous decreasing trend that begins in the 1960s. Moreover, the correlation coefficient is significant for almost the whole period analyzed.

The MCF computed with the July mean temperatures (fig. 4.18) reveals a slight decreasing trend in the correlation coefficient values, which is significant for almost the entire period.

The same trend is found analyzing the MCF computed with the September mean temperatures, but in this case the correlation coefficient is significant only for 1974-2005 period.

The MCF analysis computed over the entire period of analysis with August and October mean temperatures (fig. 4.18) shows a stationary trends, but the correlation coefficient is significant only for the period 1908-1932 for the analysis with August mean temperature, while is not significant for the analysis with October mean temperature.

As regards the MCF analysis performed with total precipitation, significant correlation coefficient values are found only for the mean precipitation of April and of June of the current year (fig. 4.19). In particular, the correlation coefficient values computed with April precipitation show an increasing trend but are significant only for a portion of the analyzed period, while the coefficient correlation values computed with June precipitation are significant for almost all the period and show a generally stationary trend.

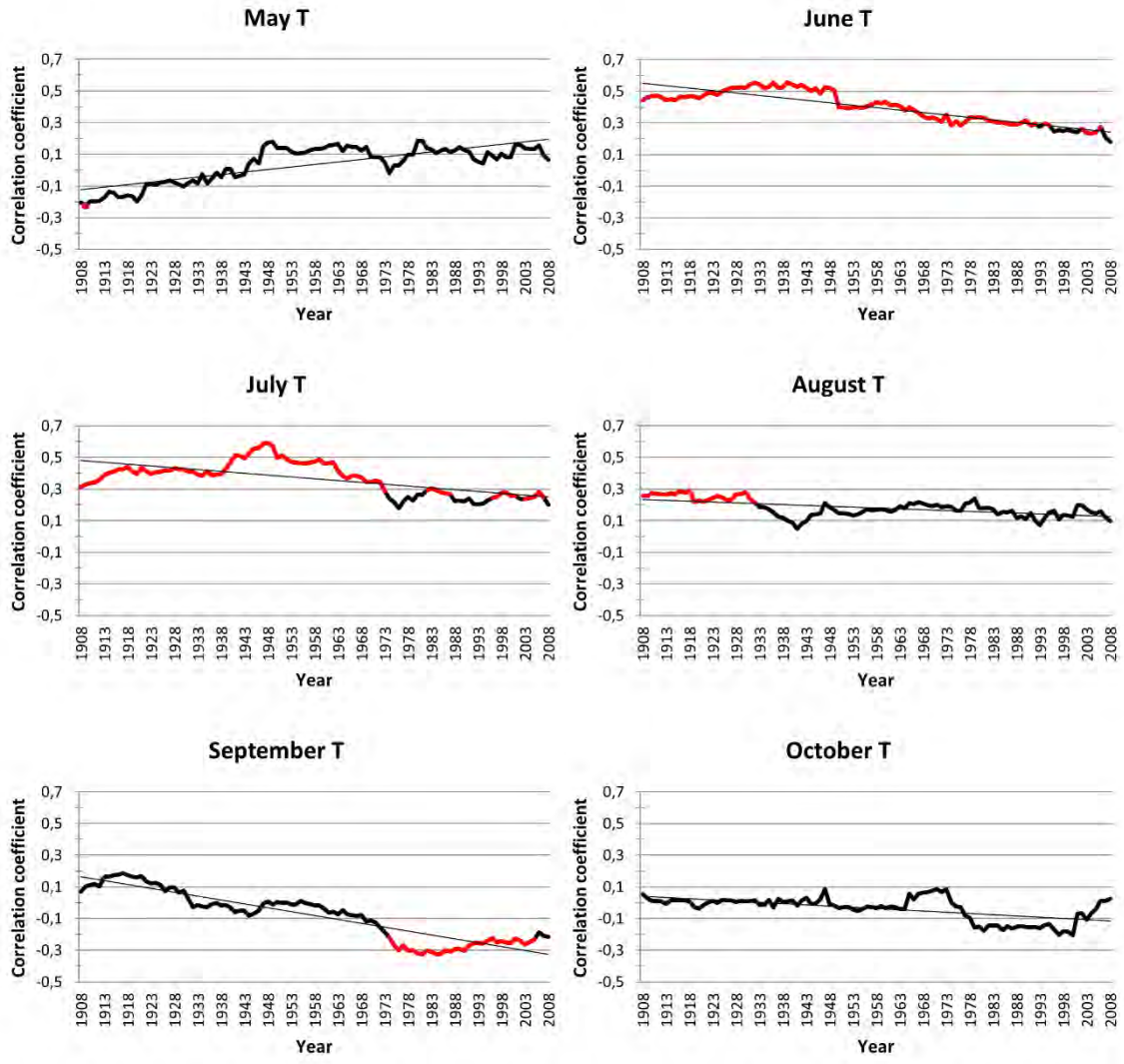

Figure 4.18. Moving correlation function analysis computed on the standard chronology. The linear regression lines are plotted and the curves are in red where the correlation coefficient is significant (significance test: 95% percentile range, $p<0.05$).

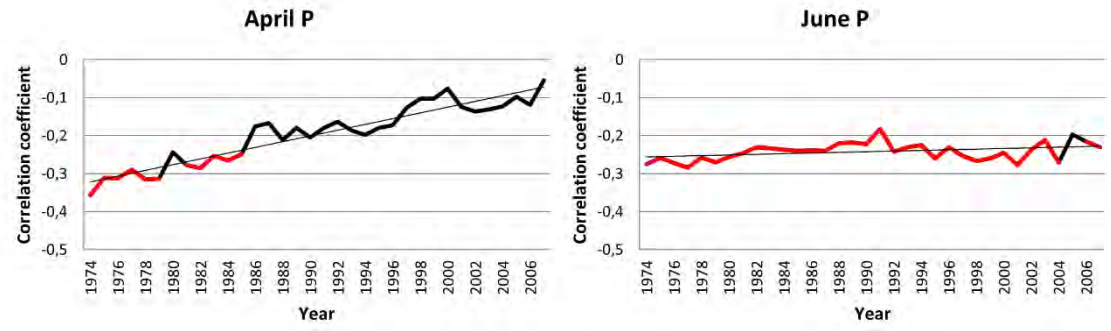

Figure 4.19. Moving correlation function analysis computed on the standard chronology. The linear regression lines are plotted and the curves are in red where the correlation coefficient is significant (significance test: 95% percentile range, $p<0.05$).

4.2.2 Saint Nicolas study case

4.2.2.1 Results of geopedological analysis

Field and laboratory characterizations have been performed for six soil profiles located in different portion of the study area. Two profiles (SN01 and SN05) were excavated on the southern slope of Monte Fallére in order to observe the slope dynamics; two profiles (SN03 and SNA16/01) are located on the edge of two badlands in order to understand the dynamics of soil erosion due to the action of water driven process; finally, two profiles (SNA 16/02 and SNA 16/03) were selected in a flat and stable area, in order to observe soil development in a more stable geomorphological context than in the previous ones (fig.4.20).

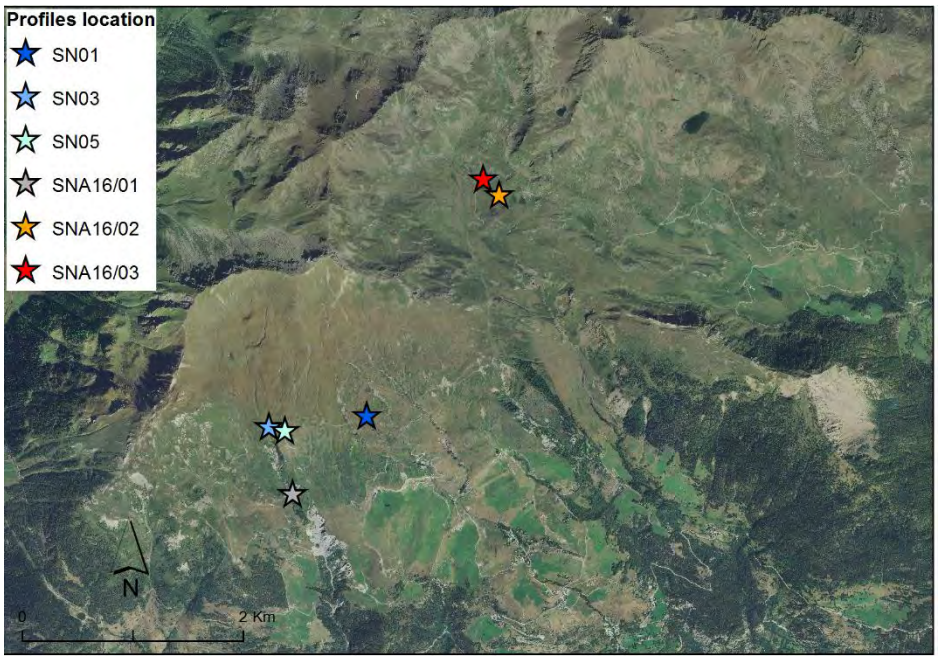

Figure 4.20. Profiles location and treeline position.
The orthophoto has been drawn from spatial data available at the National Geoportal.

4.2.2.1.1 Field data

The profiles SNA 16/01 and SN 03 are placed at the edge of badlands area at an altitude of 2093 m a.s.l. and 2298 m a.s.l. respectively. The profiles SN01 and SN05 are situated on the colluvial slopes at about 2250 m a.s.l. (tab. 4.3). The profiles SNA 16/02 and SNA16/03 are located in a flat and stable area at about 2360 m a.s.l..

All the profiles have the same parent material characterized by metamorphic limestones and marls. The profiles thickness assumes variable values, ranging between 0.5 to 2 m. The profiles located in the flat and stable area show the highest thickness. The profiles were excavated taking advantage to the presence of a natural scarp, except for the profile SN16/02 where an excavator was used.

The colour of the horizons shows a clear uniformity in the area, particularly as regards the hue values, that is different from 10 YR only in one case. Soil structure is moderately expressed and are mainly characterized by granular or sub angular blocky aggregates (Appendix 4).

Profile	Elevation (m a.s.l.)	Inclination (°)	Slope expossure	Profile exposure	Parent Material	Geomorphology	Vegetation
SN 01	2215	20	S	S	Metamorphic limestones and marls	Colluvial deposits	Shrubby
SN 03	2298	30	S	S	Metamorphic limestones and marls	Badlands edge	Grassland
SN 05	2254	20	S	SW	Metamorphic limestones and marls	Colluvial deposits	Shrubby
SNA 16/01	2093	40	SE	SE	Metamorphic limestones and marls	Badlands edge	Grassland
SNA 16/02	2363	5	S-SE	S-SE	Metamorphic limestones and marls	Glacial deposits	Grassland
SNA 16/03	2382	20	SW	SW	Metamorphic limestones and marls	Glacial deposits	Grassland

Table 4.3. Station descriptions for the studied profiles.

4.2.2.1.2 Particle size analysis

The particle size distribution, in the analyzed soil profiles, shows that the gravel and the sand are the most represented granulometric classes (fig. 4.21, 4.22); in fact, the sand content varies between 16 and 57% and the content of gravel varies between 6 and 79%. The silt content is more variable, in the horizons SNA16/03 AO and SN01 2A it reaches 38 and 34% respectively, while in other profiles it is below 30%. While clay content is limited and always below 10%.

Generally, the percentages of gravel tend to increase, along the profile, to the detriment of silt and clay components, as in the case of the profiles SN05, SNA16/01 and SNA16/03 (fig. 4.22).

In the profile SN01 in the horizon 2AC there is an increment of silt and clay content compared to the above horizon; moreover the gravel content decrease, whereas the sand content remains roughly constant (fig. 4.22).

A granulometric trend anomaly is found also in the profile SN03, where sand, silt and clay content increases in the 2AC horizons, accompanied by a decrease of gravel content, compared to the above horizon (fig. 4.22).

In the profile SNA 16/02 silt and clay content decreases along the profiles, and the coarse material tend to increase; but in the superficial horizon the gravel content increases compared to the below horizon.

Also observing the cumulative curves of grain size distribution of this profile the AC horizon show a very different trend from other horizons (fig. 4.21).

Except for profiles located in more stable areas (SNA16/02 and SNA16/03), the cumulative curves show a linear trend without mode, which highlights a not selective distribution of fine material with a predominant sand presence (fig. 4.21).

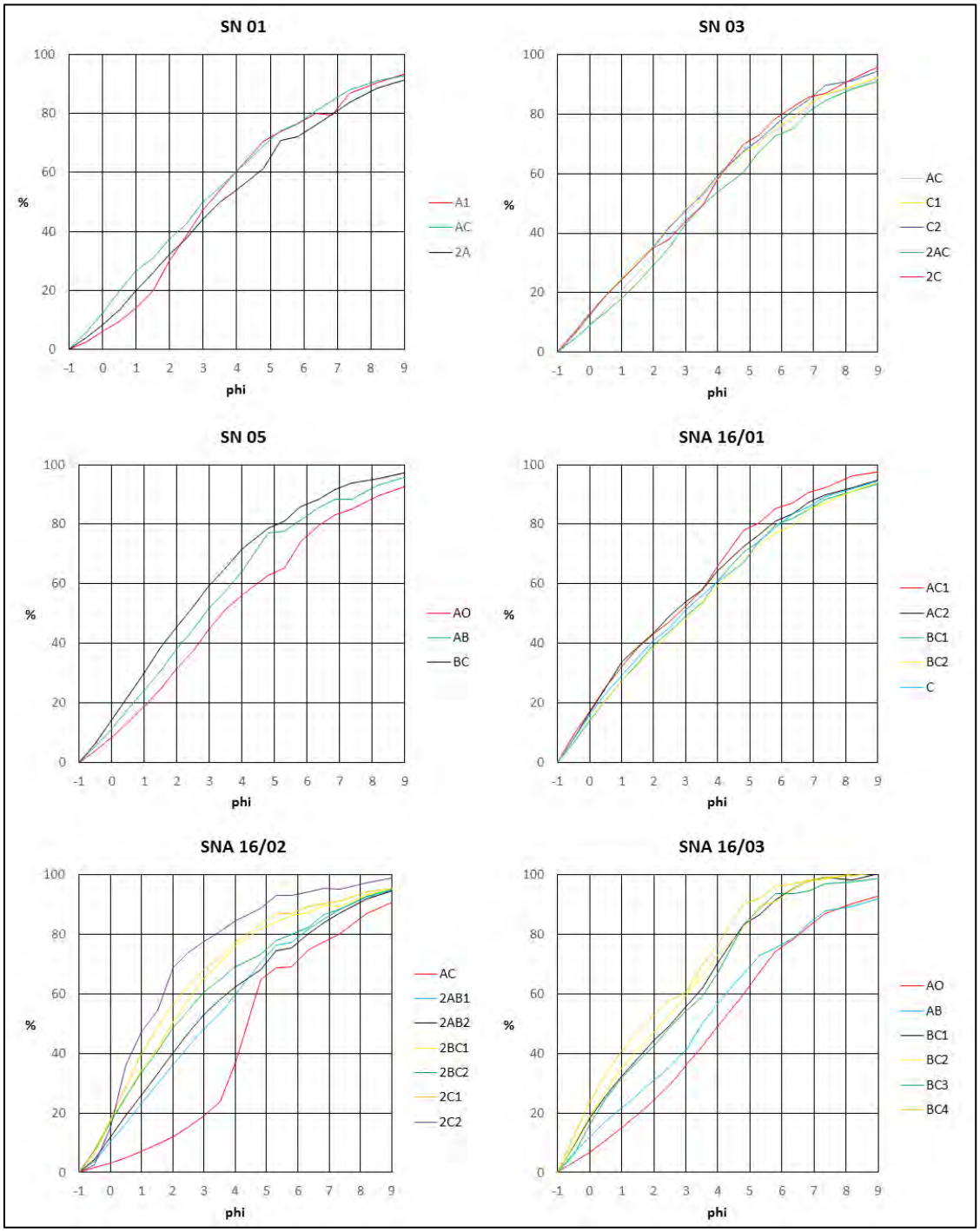

Figure 4.21. Cumulative curves of grain size distribution in the studied profiles.

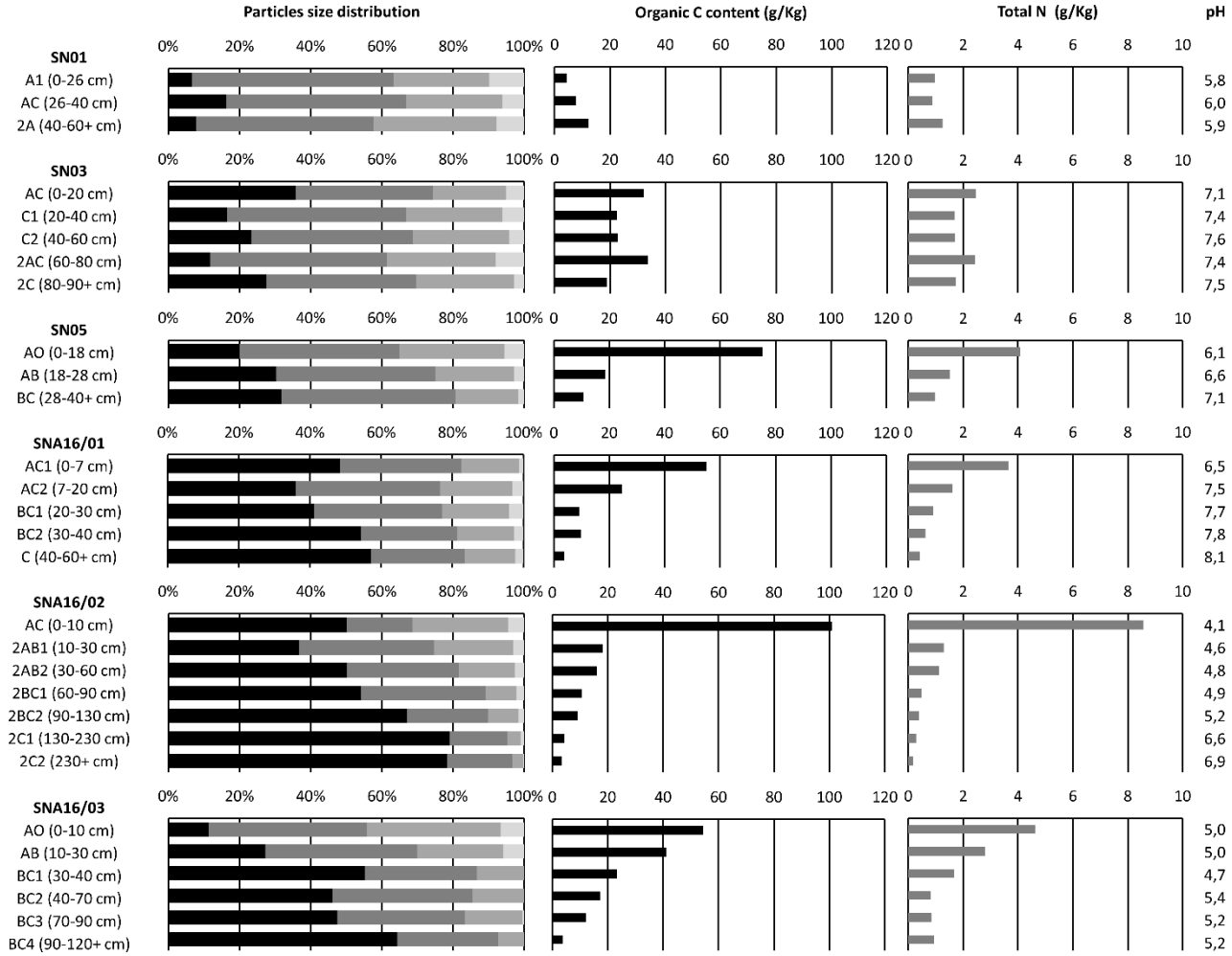

Figure 4.22. Particle size distribution, Organic C content, total Nitrogen content and pH values in the studied profiles. For the particle size distribution plot: in black is depict the gravel content, in dark grey the sand content, in grey the silt content. and in light grey the clay content.

4.2.2.1.3 Organic Carbon Content

The absolute quantities of organic carbon varies between 3.8 and 100.9 g/Kg (fig. 4.22). Except for the profile SN01 and SN03 the superficial horizons have the highest quantities of organic C. Usually, the C organic values decrease with depth: the general trend is therefore represented by a decreasing of organic carbon content as horizons get deeper. This decrease can be more or less gradual, as in profile SNA 16/03, or concentrated as a rapid loss at the transition from the uppermost horizon to the ones those below, such as in the profile SN 05 (fig. 4.22).

However, not all the profiles show the same trend, characterized by a decreasing in C content with depth. In particular, in the profile SN01 the organic C content increases along the profile reaching the maximum value in the deepest horizon (2A); while in the profile SN03 the C organic content shows a peak in the horizon 2AC, in this horizon the C organic content is more than the superficial horizon C organic content (fig. 4.22).

4.2.2.1.4 Total Nitrogen

The total nitrogen contents have the same trend of the organic C content (fig. 4.22), but with significantly lower values (not exceeding 8.6 g/Kg). The total nitrogen content decrease with depth along the profile and the decrease is concentrated as a rapid loss at the transition from the uppermost horizon to the ones those below, while in the underlying horizons the decrease is more gradual.

The highest content of total N are found in the superficial horizons and in particular, the SNA16/02 AC has the greatest values. Whereas, the lowest values are recorded in SNA16/02 2C2 (about 0.2 g /Kg).

Finally, the C/N ratio have values ranging between 4.7 and 18.4 g/Kg in the superficial horizons. The C/N ratio does not show a clear ad unique trend, in fact in the profile SN01 increases with depth, instead in the profile SN05 the C/N ratio decreases with depth, while in other profiles there seems to be no trend (fig. 4.23).

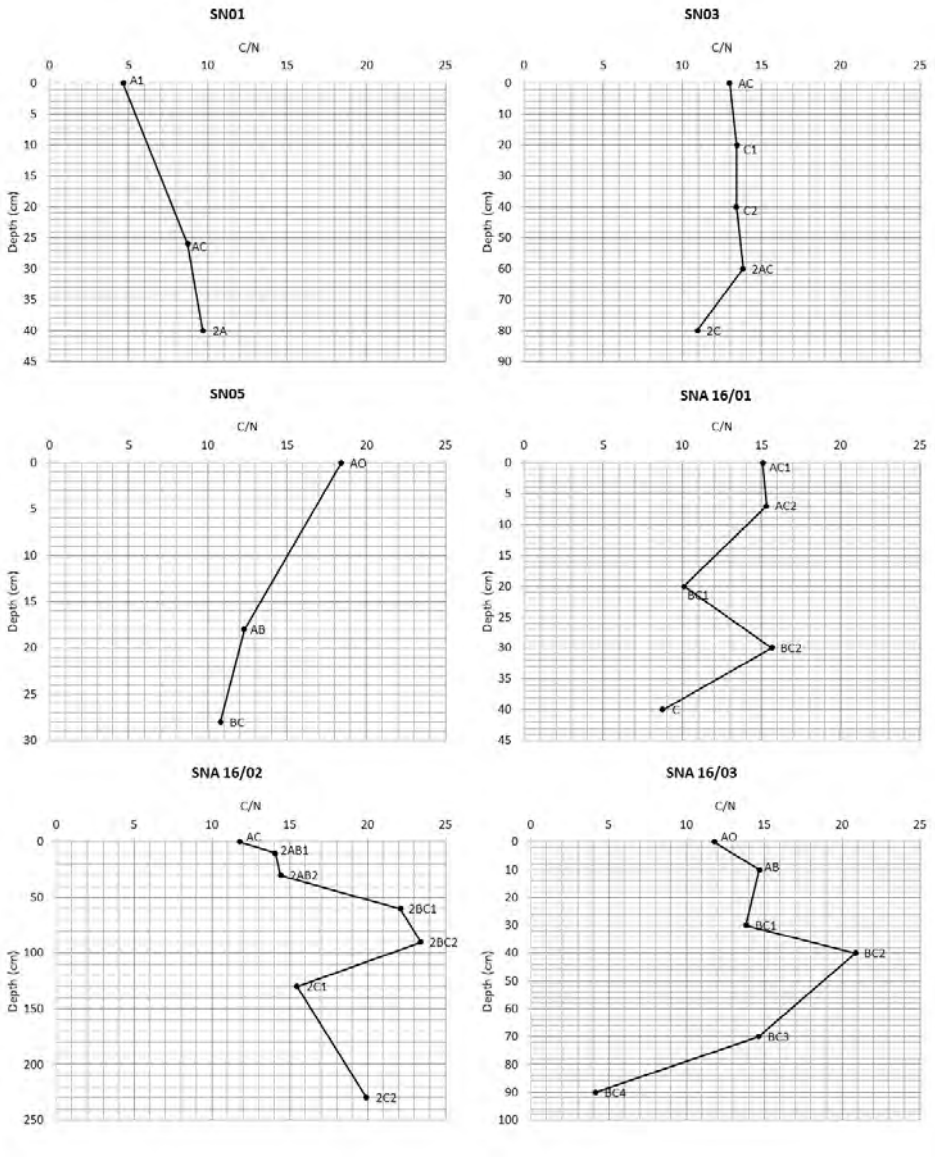

Figure 4.23. C/N ratio in the studied profiles.

4.2.2.1.5 pH

The pH values in H_2O ranging between 4.1 and 8.1 (fig. 4.22). On average, the superficial horizons are the more acid. In particular, the profiles SNA16/02 and SNA16/03 show the most acid values. More or less, in all the profiles the pH increases along the profile, approaching to the parent material; but in some case the trend in not linear. In the profile SNA16/02 the pH increments 2 units along the profile, while in the profile SN03 the pH variation seems very moderate, increasing only by 0.5

4.2.2.1.6 Alluminum and Iron extractions

The total content of free iron oxides (Fed) ranging between 8 and 32 g/Kg. The values of amorphous iron oxides (Feo) are lower and ranging between 0.4 and 14 g/Kg, as the iron bound with the organic matter (Fep) that ranging between 0.2 and 13 g/Kg. For all three of these parameters, particularly high values are observed in SNA16/03 AB and SNA16/03 BC1 horizons (fig. 4.24).

As regards the aluminium oxides content, the quantities tend to be inferior to those of iron, and less variable. Free aluminium oxides (Ald) has values between 0.7 to 9.5 g/Kg, amorphous aluminium oxides (Alo) between 0.2 and 6.7 g/Kg, aluminium bound with the organic matter (Alp) has values ranging between 0.6 and 8.8 g/Kg.

Both the iron and aluminium show similar trends and similar peaks along the profiles, for what concern the same extractions.

On average, the crystalline iron oxides content is quite high and ranging between 7.2 and 29.5 (tab. 4.4). The highest value is found in the SN03 2C, while the lowest value is found in the SNA16/02 2C2.

The Feo/Fed index has very low values, in particular only one horizon (SNA16/03 2AB1) has an iron activity index higher than 0.5. (tab. 4.4). Lastly, the results of the podzolization index Alo + ½ Feo do not meet the conditions of podzolization processes (FAO, 2014).

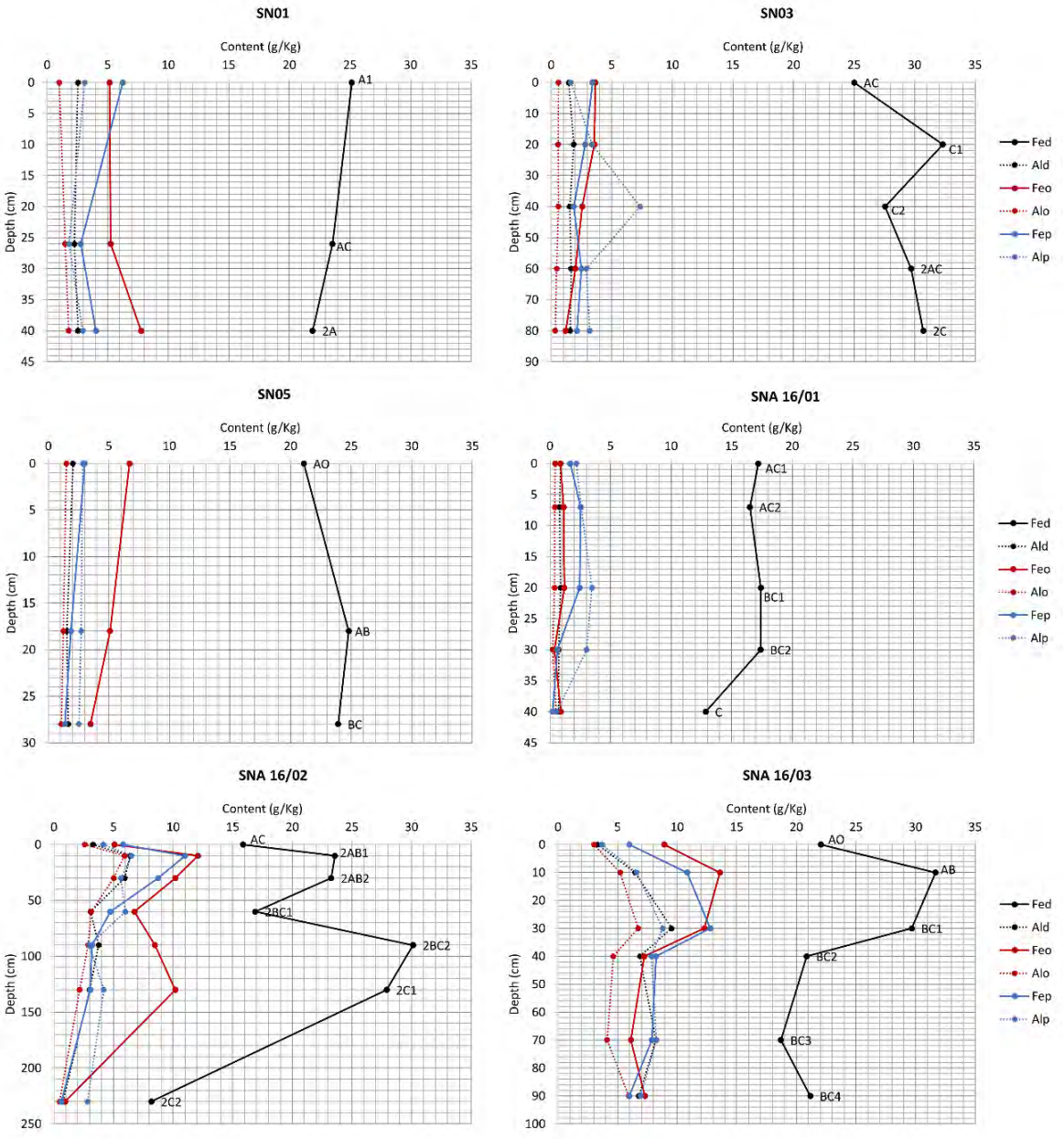

Figure 4.24. Free iron oxides (Fed), amorphous iron oxides (Feo) and iron bound to the organic matter (Fep) content, free aluminum oxides (Ald), amorphous aluminum oxides (Alo) and aluminum bound to the organic matter (Alp) content of the studied profiles The horizons name are close to the Fed curves.

Profile	Horizon	Depth (cm)	Fed- Feo (g/Kg)	Feo/Fed	Alo+1/2Feo (%)
SN 01	A1	0-26	20.0	0.21	0.36
SN 01	AC	26-40	18.3	0.22	0.41
SN 01	2°	40-60	14.2	0.35	0.57
SN 03	AC	0-20	21.4	0.15	0.24
SN 03	C1	20-40	28.8	0.11	0.24
SN 03	C2	40-60	25.0	0.09	0.19
SN 03	2AC	60-80	27.7	0.07	0.15
SN 03	2C	80-90	29.5	0.04	0.09
SN 05	AO	0-18	14.4	0.32	0.48
SN 05	AB	18-28	19.7	0.21	0.38
SN 05	BC	28-40	20.4	0.15	0.28
SNA 16/01	AC1	0-7	16.3	0.05	0.09
SNA 16/01	AC2	7-20	15.4	0.07	0.10
SNA 16/01	BC1	20-30	16.2	0.07	0.10
SNA 16/01	BC2	30-40	17.0	0.02	0.04
SNA 16/01	C	40-60+	12.0	0.07	0.09
SNA 16/02	AC	0-10	10.8	0.32	0.51
SNA 16/02	2AB1	10-30	11.5	0.51	1.20
SNA 16/02	2AB2	30-60	13.1	0.44	1.01
SNA 16/02	2BC1	60-90	10.1	0.40	0.65
SNA 16/02	2BC2	90-130	21.6	0.28	0.71
SNA 16/02	2C1	130-230	17.7	0.36	0.73
SNA 16/02	2C2	230+C	7.2	0.12	0.10
SNA 16/03	AO	0-10	13.1	0.40	0.75
SNA 16/03	AB	10-30	18.1	0.43	1.20
SNA 16/03	BC1	30-40	17.4	0.41	1.29
SNA 16/03	BC2	40-70	13.6	0.35	0.83
SNA 16/03	BC3	70-90	12.6	0.33	0.72
SNA 16/03	BC4	90-120+	13.9	0.34	0.96

Table 4.4. Iron and aluminum index. Crystalline iron oxides (Fed-Feo), activity iron index (Feo/Fed) and podsolization index (Alo+1/2Feo).

4.2.2.1.7 Rock-Eval data

In the I/R diagram the organic horizons have I-index values between 0.2 and 0.4 and R-index between 0.45 and 0.55. While the B and C horizons have I-index values between -0.1 and 0.3 and R-index between 0.55 and 0.8 (fig. 4.25). The profiles SNA16/02 and SNA16/03 have the lowest values in I-index and the highest values in R-Index.

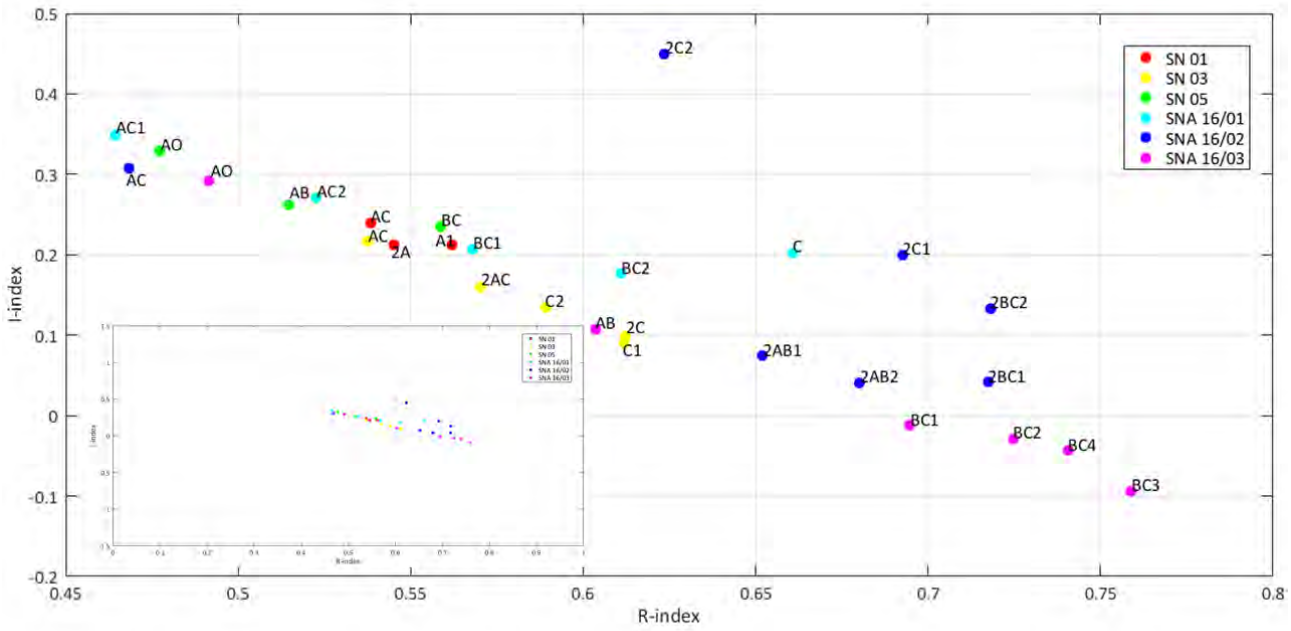

Figure 4.25. I-index/R-index. On the bottom left the data are plotted using the grid values from Sebag et al., 2016 in order to better visualize the trends.

The HI/OI index shows different values in different horizons typology (fig. 4.26). In fact, the O and A horizons show a high HI values and low OI values, while the B and C horizons show high OI values and low HI values.

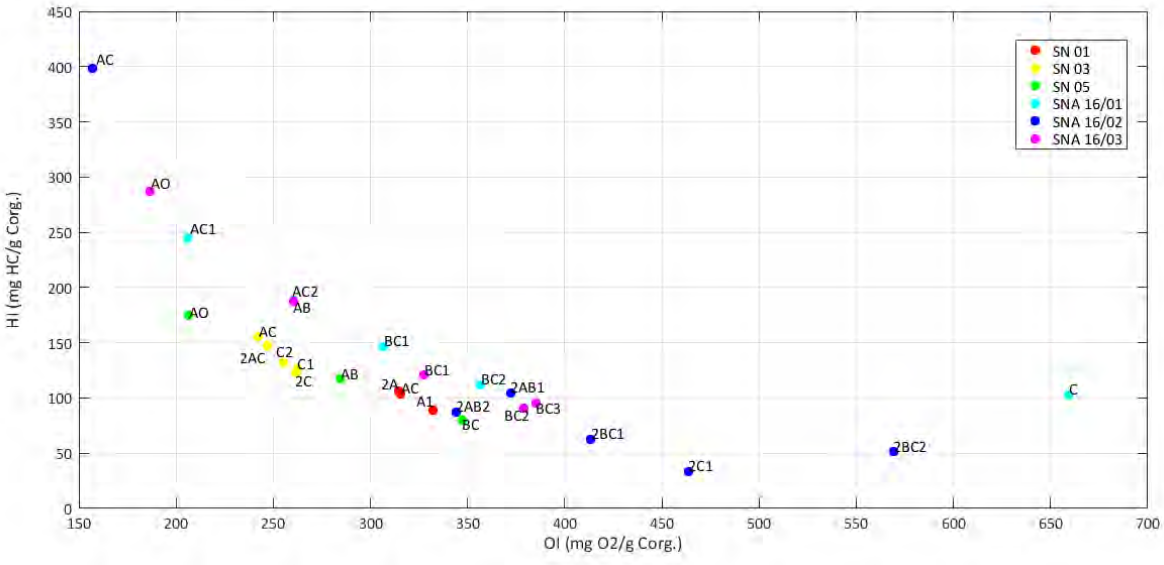

Figure 4.26. HI/OI diagram. The SNA16/02 2C2 and SNA16/03 BC4 horizons are not plotted due to their out of range values.

4.2.2.2 Dendrogeomorphological analysis: soil erosion rates

In the Saint Nicolas study site the roots belonging to 3 trees were sampled: 2 trees (SN 20 and SN 21) are located on the west edge of the degradation scarp (red area in fig. 4.27) and 1 (SN 14) is placed along the slope in the inner portion of the badlands (yellow area in fig. 4.27). No other trees to sample exposed roots were found in the area.

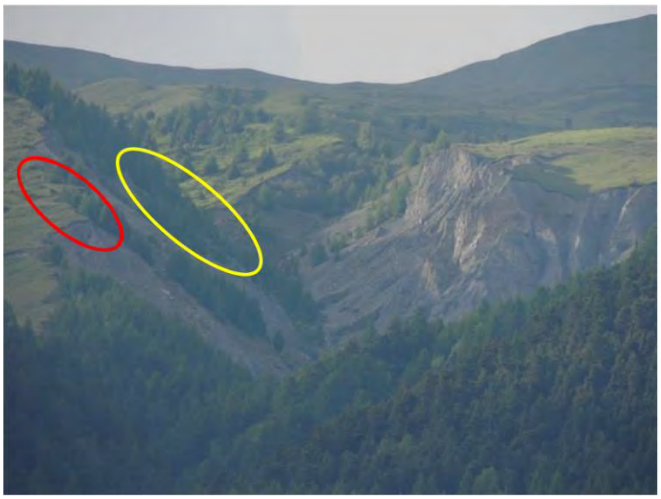

Figure 4.27. Location of roots sampled.

Tree	Root	Sampling year	Year of exposure	Time interval * (years)	Removed sediment thickness (cm)	LDR (cm/year)
14	1_1	2016	1998	17	6.5	0.36
14	1_2	2016	1993	22	6.5	0.30
20	1	2016	1991	24	26	1.08
20	2_1	2016	2004	11	21.5	1.95
20	2_2	2016	2006	9	21.5	2.39
20	3	2016	1989	26	26.5	1.02
21	1	2016	2013	2	8	4
21	2	2016	1958	57	30.8	0,54
21	3_1	2016	1981	34	54	1.59
21	3 _1	2016	1988	27	55	2.00

Table 4.5. Calculated local denudation rates of Saint Nicolas study site. Ten samples of exposed roots are available and provide an estimate erosion rates for the area close to the trees to which sampled roots belong (Modified from Pellegrini, 2016). * The time interval is calculated taking into consideration the last complete ring, in this case the ring belong to 2015; as the sampling took place in mid-2016.

The roots of trees "14", located in the inner portion of the badlands and close to a forested area, show lowest erosion rates. On the contrary, the tree "20" and "21", located at the edge of degradation scarp, has a great number of exposed roots and higher rates of erosion (tab. 4.5).

In the Saint Nicolas study sites the average erosion rates, calculated from the most representative local rates, is equal to 1.16 cm/year.

4.3 Discussion

4.3.1 Becca di Viou study case

In the Becca di Viou study site the analyzed soil profiles show a clear relation between altitude and profile thickness, in fact, like in other alpine soil (Merkli et al., 2009) at higher altitudes the soil profile are shallower.

In the Becca di Viou study site the profile thickness varies also related to the soil position on the slope. Indeed, the soil profiles belong to the transect done on the right portion of the slope reach higher depth than the soil profiles located on the left portion of the slope; these differences seem to be attributable to the different degree of stability of the slope, which affects the evolution of the soil, too.

The analysis of particle size distribution underlines the preponderant presence of coarse material and therefore a strong parent material influence. Moreover, the influence of parent material on soil development is also evident taking into consideration the pH analysis that show an acid pH, characterized by little variations, in all the profiles. The pH acidity seems to be influenced by the parent material rather than by pedogenetic processes, since the more superficial horizons are not characterized by the typical acidity increase.

The examination of studied soil granulometry highlight also the higher content of silt in the fine earth component, probably the silt have an aeolian attribution (Stahr et al., 1989; Küfmann, 2003).

In all the studied profiles the particle size distribution shows the standard trend: in fact, the particles size increases with the depth. Besides the Organic C content and the total N content don't show any discontinuity/peak along the profile, and in all the profiles have a decrease with the depth (fig. 4.9).

Although these data suggest that there are no buried surfaces, observing the cumulative curves of profile BV 16/02 two families of curves are visible: one grouping the superficial horizons (O and AC), while the other grouping the deep horizons (2AC, 3Bs and 3BC). In addition, on the field between the AC and 2AC horizons a stone line was observed. It is therefore possible that in the profile BV 16/02 there are two paleosurfaces, identified by two discontinuities between AC-2AC and 2AC-3Bs (see below for further observations).

Starting from the C/N ratio values, a humus Mull (Duchafour, 1983) is found: a type of evolved humus with stable clay-humic complexes and poor litter, typical of the broadleaf forest or herbaceous vegetation (Cremaschi, 2000). The values are coherent with the literature ones for what concern the soil profile located in the treeline ecotone (Merkli et al., 2009); while in the forested area a higher C/N ratio was expected, this discrepancy may be due to the location, under an open and not closed forest, of the BV16/06 profile.

The content of oxides of iron and aluminum within the horizons analyzed shows a good correlation with the results of other study carried out in the Alps (Catoni et al., 2016). The content of crystalline iron oxides increases in the well developed horizons (e.g., B horizons) and in particular, in the profile located under forest vegetation. Indeed, according to Remaury et al. (2002), the crystalline Fe oxides (Fed–Feo) in Bs horizons are the product of in situ weathering of Fe-bearing primary minerals (tab 4.2).

The iron activity index has low values and rarely exceed 0.5; this indicates the presence of developed soil in fact, the decrease of the Feo/Fed index within the more mature horizons (Bs, BC) is highlighted, and can be related to the greater alteration of the material and to the translocation of iron from the above horizons.

With respect to the Alo + ½ Feo index, the values obtained at profiles BV16/02, BV16/03 and BV16/07 appear to indicate the presence in this profile of a weakly podzolization, or better a cryptopodzolization (Do Nascimento et al., 2008; FAO, 2014) because the podzolization conditions are not so expressed as in other studies (Waroszewski et al., 2013).

It is interesting to note that the profiles affect by criptopodzolization are located in the forested area (BV16/07) and in the right and more stable portion of the slope (BV16/02 and BV16/03).

Anyway, the podzolization index of the profile BV16/02 is not easy to interpret because is located over the two discontinuity.

Analyzing the Rock-Eval data (fig. 4.12) it was possible to divide the analyzed horizons into several boxes (Sebag et al., 2016). In particular, the O horizons are placed in the range of the box "Litters and Organic Horizons" while the other horizons show two different trends (Sebag et al., 2016). Indeed, the B and C horizons are located in the box of "Organo mineral & Mineral horizons", but are placed along two different linear trends: most of the horizons follow the humic trend whereas the BV16/02 2AC, 3BC and 3Bs are close to the inherited OM trend. Therefore, the Rock-Eval I/R index support the hypothesis that the study area is characterized by a moderate developed soil, in fact none of the analyzed soils shows a spodic trend; and support also the hypothesis of the presence of a paleosols in the BV16/02, indeed the BV16/02 2AC, 3BC and 3Bs horizons follow the "Inherited OM trend" (Sebag et al., 2016).

The possible presence of a discontinuity in the BV16/02 profile is also underlined by the isotopic composition analysis: normally, the increase in $\delta\ ^{13}C$ with depth in mineral horizons occur in all soil under C3 vegetation (Balesdent et al., 1993), while in the BV16 / 02 profile there is a marked inversion of both $\delta\ ^{15}N$ and $\delta\ ^{13}C$ trends.

In fact, starting from the BV16/02 2AC horizon the $\delta^{15}N$ and $\delta^{13}C$ trends instead of continuing to increase start to decrease, and in the BV16/02 3Bs horizon the $\delta^{15}N$ and $\delta^{13}C$ values are almost the same to those of the surface horizon (BV16/02 O).

This variation could be attributed to the presence of a buried surface covered by a colluvial event that isolated the underlying portion of the profile.

Trend inversions, just for $\delta\,^{13}C$, are also found in the BV16/01, BV16/05 and BV16/07 profiles; for the first two profiles the trend inversion may be due to the reduced thickness of the profile, while for the BV16/07 profile the trend inversion is not particularly marked and therefore attributable to a natural variation.

The Rock-Eval data (fig. 4.13) also provide to have more information the organic matter maturity. In the HI/OI diagram the horizons are grouped by typology, in fact starting from the top left we find the O horizons, then the A/AC, the B and so on. At the bottom right the horizons (2AC, 3Bs and 3BC) belong to paleosols (BV 16/02) are found, near to these, the B horizons (BC and BsC) belong to the profile excavated in forest and the deepest horizons of the two profiles close to the timberline (BV16/03 BC and BV16/04 AC) are found.

These results emphasize the similarity between the paleosol and the present soil developed under forest cover, as well as the ongoing development trend of the soils located in the lower part of the treeline ecotone, which shows increasingly similar features to the soil developed under forest.

Therefore, the presence at the treeline ecotone of paleosols, similar to the soil developed nowadays under forest cover, it could attest that in the past the timberline could be located at higher altitudes then today.

The soil of the Becca di Viou study site can be attributed to the class of "Sols humifères désaturés" (Duchafour, 1995); in particular the soil developed under forest is identifiable as "Ranker cryptopodzolique" while the soils located at the treeline ecotone is identifiable as "Ranker alpin" (Duchafour, 1995).

The dendroclimatic study carried out on the Becca di Viou slope shows that the temperature, rather than precipitation, exerts the primary control on the radial growth of larch at the treeline. In particular, the response of larch to climate is driven primarily by the June mean temperature. However, the MCF analysis revealed that climate parameters primarily involved in larch growth at the treeline have significant unstable response and substantial variability over time; as also reported by Carrer and Urbinati (2006).

In fact, the MCF analysis computed with June mean temperature shows a decreasing trend in the correlation coefficient values (fig. 4.19). A similar decreasing trends are also obtained by other studies carried out on *Pinus cembra* and *Larix decidua* in the Alpine treeline ecotone (Leonelli et al., 2009b; Coppola et al., 2012).

In the studied larch chronology, the loss of the June mean temperature signal is evident from the beginning of 1960s. Instead, contrary to what has been found in other studies (Leonelli et al., 2009b;

Coppola et al., 2012), the MCF analysis performed with June precipitation doesn't show any trend change over time.

However, an increasing trend is observed in the correlation coefficient computed between the standard chronology and the May mean temperatures. Conversely, an increasing trend in the coefficient correlation values computed between the chronologies and the August mean temperatures is not ascertained.

Therefore, the decreasing trend in the correlation values found with the June monthly temperature and the increasing trend in the correlation values found with the May monthly temperature can be attributed to the prolongation of the growing season. Numerous studies have reported an extension of the growing season in Europe due to the recent temperature increase (Menzel & Fabian, 1999; Sparks & Menzel, 2002; Walther et al., 2002; Menzel et al., 2006). It is probable that the effects of a prolonged growing season on tree-ring growth are particularly important at sites where temperatures represent the main limiting factor as in our study area.

Moreover, the study underlines that precipitation exerts less control on tree-ring growth than does temperature.

In conclusion, at the Becca di Viou study site the pedological data and the dendrcoclimatic data, combined with the literature data that attest an upward shift of the treeline in the last century (Leonelli et al., 2011a), seems to stress a changing in treeline ecotone position, following by a possible shift of the timberline and also by a shift of soil type. The pedological data also highlights that forest, in the past, could reach higher altitude.

4.3.2 Saint Nicolas study case

In all the studied soil profiles at Saint Nicolas study site the analysis of particle size distribution underlines the preponderant presence of coarse material typical of less developed soils and of soils subject to frequent colluvial events. Moreover, the influence of parent material on soil characteristic is also evident taking into consideration the pH analysis, that show a neutral - slightly alkaline pH in all the profiles. However, the pH has more acid values in the more superficial horizons, due to the presence of organic matter (D'amico et al., 2009), and in better developed profiles (SNA16/02 and SNA16/03). The latter two profiles have a greater development degree and a greater thickness because are located in a more stable portion of the slope.

In the soil profiles SN05, SNA16/02and SNA16/03, the particles size distribution shows the standard trend: in fact, the particles size increases with the depth (fig 4.22). Besides the Organic C content and

the total N content do not show any discontinuity/peak along the profile, and have a decrease with the depth.

Although, in the profile SNA 16/02 the superficial horizon (AC) shows an increase in gravel content, probably caused by an upslope material transport.

In the profiles located close to the badlands (SN03) and along the slope (SN01) a granulometric discontinuity are found, due to the presence of buried paleosurfaces. This discontinuity is also underlined by a peak of total nitrogen and organic carbon content in the SN03 2AC and SN01 2A horizons.

While the profile SNA16/01 and SN05, even though they are located near the badlands and along the slope respectively, are probably less disturbed by colluvial depositional events, as it is placed on an upland, in fact they not show any trend anomalies in particle size distribution, C organic content and total N content.

The C/N ratio values allow to identify a humus Mull (Duchafour, 1983): a type of evolved humus with stable clay-humic complexes and poor litter, typical of the broadleaf forest or herbaceous vegetation (Cremaschi, 2000). The values are coherent with the literature ones for what concern the soil profile located in the treeline ecotone (Merkli et al., 2009).

The content of oxides of iron and aluminum, within the analyzed horizons, shows a good correlation with the results of other study carried out in the Alps (Merkli et al., 2009; Catoni et al., 2016). The high content of crystalline iron oxides, as they are the product of in situ weathering of Fe-bearing primary minerals and as they decrease along profile, it may indicate only passive enrichment due to the leaching of carbonates (Merkli et al., 2009). The iron activity index has very low values and rarely exceed 0.5 (tab. 4.4); this should indicate the presence of developed soil, but in the case of the profiles SNA 16/01 and SN03 the low iron activity index may be caused by the presence of colluvial material already pedogenized into the profile or be due to the type of parent material. Moreover, lower iron activity ratio in BC horizons has been observed in Bw horizons of Cambisols developed from crystalline rock in Sudeten Mountains (Waroszewski et al., 2013).

With respect to the Alo + ½ Feo index, in none of the studied profiles the podsolization index meet the conditions of podzolization processes (FAO, 2014). Anyway, in the profile SNA16/02 the podzolization index meet the conditions of podzolization processes (FAO, 2014) but is not easy to interpret because is located over the discontinuity.

Analyzing the Rock-Eval data (fig. 4.25), it was possible to divide the analyzed horizons into several boxes (Sebag et al., 2016). In particular, the O horizons are placed in the range of the box "Litters and Organic Horizons" while the other horizons show two different trends (Sebag et al., 2016). Indeed, the B and C horizons are located in the box of "Organo mineral & Mineral horizons", but are placed along two different linear trends: most of the horizons follow the humic trend whereas the SNA16/02 2C2,

2C1, 2BC2 and 2BC1 are close to the inherited OM trend. Therefore, the Rock-Eval I/R index support the hypothesis that the study area is characterized by a moderate developed soil, in fact none of the analyzed soils shows a spodic trend; and support also the hypothesis of the presence of a buried soil in the SNA16/02, indeed the horizons follow the the SNA16/02 2C2, 2C1, 2BC2 and 2BC1 "Inherited OM trend" (Sebag et al., 2016).

The Rock-Eval data (fig. 4.26) also provide to have more information the organic matter maturity. In the HI/OI diagram the horizons are grouped by typology, in fact starting from the top left we find the A horizons, then the A/AC, the B and so on. At the bottom right the horizons (2BC1, 2C1, 2BC2) belong to a buried soil (SNA16/02) and the SNA 16/01 C are found, underlining the highest SOM maturity degree in the deep horizons.

Starting from the analysis and field observations the soils of the Saint Nicolas can be divided into two groups: the SNA 16/01, SN01, SN03, and SN05 profiles are less developed soils, subject to continuous sedimentation/erosion phases due to colluvial events and water driven processes, therefore can be defined as "Sols peu évolués sur matériaux récents" (Duchafour, 1995); whereas the soil profiles located in stable and flat area near the Mt Fallere (SNA 16/02 SNA16/03) are better developed, and are identifiable as "Sols Brunifiés"(Duchafour, 1995).

For the erosion of the soil, the average erosion rate of this study site is 1.16 cm/year, which indicates the presence of erosional action due to water driven processes. The average value obtained in the study site is similar to those in the literature (Bodoque et al., 2011; Bollati et al., 2012; Stoffel et al., 2013). It is important to underline that the erosion rate values obtained through dendrochronology investigations include the resolution of the entire period of exposure and, as a consequence, they provide a mean value over the investigated period (relatively long term ERs), not recording the single peak events.

The presence of these erosional and depositional processes affecting the slope can be caused to the presence of a DGPV (Carraro in Dal Piaz, 1992) extending from the ridges to the main valley of Dora Baltea (Forno et al, 2012), in fact, the badlands are located in an incision, in which the Torrente Gaboè flows, along the western margin of the DGPV.

In addition to the geomorphological factor, in this area, the dynamics of vegetation is also influenced by the human presence that colonizes the area from the Mesolithic period (Pini et al., 2012). The anthropic deforestation, carried out since the IV millennium BC (Pini et al., 2012) on Mt. Fallère to use the area as alpine pasture, has in fact favored the instability of the slope and the soil erosion.

The evolution of the area, albeit influenced by the geomorphological constraint, remains mainly linked to the human presence, which acting on the vegetation preventing the colonization of the slope and the soil development, favors the erosion due to water driven processes and the formation of badlands.

Chapter 5

Febbio study area

The interaction between soil and vegetation plays a key role in controlling erosion rates, especially in fast changing environments, like the mountain ones. In fact, vegetation can modulate the velocity and the intensity of soil development or erosion, but on the other hand, soil degradation processes may affect the normal development of shrubs and trees (Ballesteros-Cánovas et al., 2013). Consequently, a decrease in vegetation coverage causes a slowdown in soil formation and promotes further erosion (Thornes, 1985). The interplay between vegetation and water runoff becomes particularly meaningful where erosion rates are significant like in badlands area. Therefore, the third part of the study aims to reconstruct soil erosion and environmental changes in an area, below the treeline, affected by diffuse and concentrated water runoff, on the northwest slope of Mt. Cusna (Febbio, Emilia Romagna) located in the Northern Apennines.

5.1 Overview of the study area

5.1.1 Geography

The study area is located in the territory of Febbio (RE) in the Northern Apennines, inside the "Parco Nazionale dell'Appennino Tosco-Emiliano" (Tuscan-Emilian Apennine National Park). In particular, the study site is located on the northwest slope of Mt. Cusna (fig. 5.1), the second highest peak of the Tosco-Emiliano Apennine (2120 m a.s.l.), which develops in the NO-SE direction along the border between Emilia Romagna and Tuscany regions, about 50 km south of Reggio Emilia.

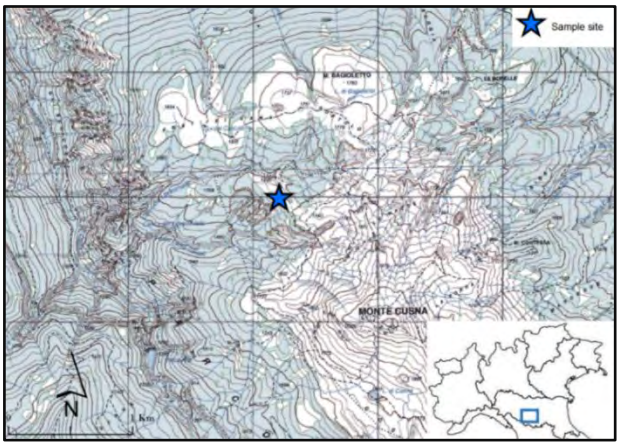

Figure 5.1. Febbio and sample site location on Mt. Cusna. The figure has been drawn from spatial data available at the National Geoportal.

Specifically, this study take into consideration a defined area of the north-western slope of Mt. Cusna, located between 1600 and 1700 m a.s.l., at SE of the Prati di Sara.

5.1.2 Geology

The Northern Apennines originated during the Late Cretaceous to Present convergence between the European and Africa plates (Boccaletti et al., 1971; Kligfield, 1979; Vai & Martini, 2001). They currently extend from NW to SE bearing a vergence towards NE between two major tectonic features represented by the Sestri-Voltaggio line in the north and the Ancona-Anzio line in the south. Both features are interpreted as large structures with a large transcurrent component.
The overall structural framework results from the middle Eocene-Pliocene thrusting of oceanic and continental allochthonous units (Ligurian and Subligurian units overlain by the Epiligurian wedge-top Succession) over Oligocene-Miocene foredeep turbidite units (Ricci Lucchi, 1986; Pini, 1999).
These units have been displaced even hundreds of kilometers from their point of origin (Bortolotti, 1992). The study area can be fully framed within the Tuscan Domain, characterized by a Triassic basal clastic section, first continental and then of shallow sea (not outcropping in the Reggian Apennines), followed in succession by evaporite deposits, by Jurassic carbonate platform deposits and by pelagic limestone and siliceous sediments, then by a terrigenous Cretaceous clay-carbonate deposition and by debris with the beginning stages of tectonic compression; Oligocene begins with the deposition of turbiditic siliciclastic sediments (Bortolotti, 1992). From the early Miocene, the orogenic wedge was affected by widespread thrusting and folding, as well as extensional tectonics (e.g., Carlini et al 2013, Clemenzi et al., 2014). Since the late Miocene-late Pliocene its western part was subjected to a progressive exhumation process (Balestrieri et al., 2003, Fellin et al., 2007; Thomson et al., 2010; Carlini et al., 2013) which rate almost doubled during middle-late Pleistocene (Bartolini et al., 1982).

As for the detailed description of the Geological Units which characterize the study area (fig. 5.2), it is reported what is contained in the legend of the 235090 "Monte Cusna" geological map (1: 10000, Geological, Seismic and Soil Service of the Emilia Romagna Region, 2007) and, of the Italy Geological map 1:50000 sheet 235 "Pievepelago" (Plesi et al., 2002).

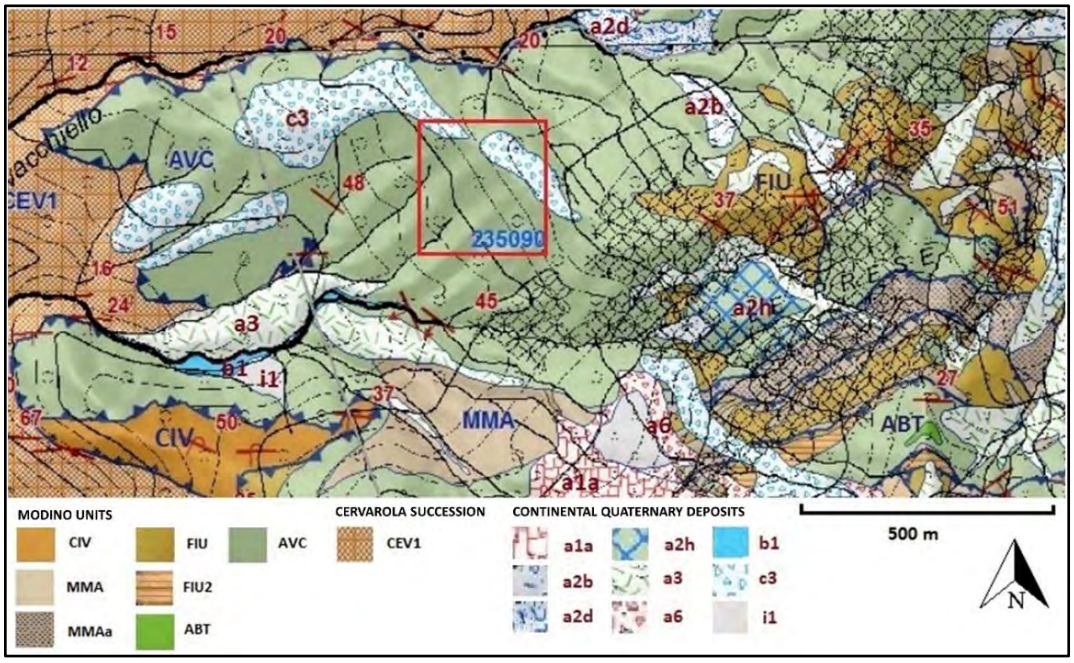

Figure 5.2. Geology of the study area (modified from the sheet 235090, scala 1:10.000, Servizio Geologico, Sismico e dei Suoli della Regione Emilia Romagna, 2007). The red square is the location of the sample site.

Modino Units (CREATCEOUS-MIOCENE)

Argilliti Variegate con Calcari (AVC): brown and green clays, rarely Varicolori, with greybrown limestone layers with reddish hue, graded siltstones and marl layers. Clay-limestone breccia with prevalent type "palombini" limestone clasts. Lead-grey clays with thin and average bluish-grey limestone layers. Deep marine environment deposit. Bottom tectonic contact with Sorba flysch, in neighbouring areas. The microfaunas found (Praeglobotrincana delrioensis, Ticinella roberti, Thalmanninella ticinensis, *Apennine rotalipora*, *Planomalina buxtorfi*, *Globigerina* sp.) seem to indicate for this formation an age between upper Albiano and lower Cenomaniano. However, given the uncertainty of the chronological settling of some levels, the entire formation was attributed to the Hauterivian – lower Cenomanian chronological interval.

Formazione dell'Abetina Reale (ABT): calcilutitic or grey calcareous matrix turbidites, passing to whitish calcareous marls, in thin to very thick layers, alternating with fine sandy and silty matrix turbidites and dark-grey clay roof in thin and average layers. Local interbedded layers of graded siliciclastic and ophiolitic sandstones. *Inoceramus* traces and remains. Continuous passage to the formation below. The formation of Abetina Reale was attributed, through the analysis of calcareous nano-fossils, to the Upper Campanian.

Argille di Fiumalbo (FIU) in the lower part greenish or red shales intercalated with thin calcarenitic/marly layers often gathered in thick decimetric sequences and with chondrites and fucoids bioturbation in the marl intervals. In the upper part-ash grey marl shales with interbedded siltstones and fine sandstones in thin layers. Discordant stratigraphic contact with the successions below. Maximum thickness of 200-300 m. Given the presence of *C. grandis*, *D. barbadiensis*, *C. formosus*, *H. compacta*, *R. umbilicus*, *S. predistentus*, *S. distentus* the Argille di Fiumalbo belong to Bartonian-Rupelian p.p.

Argille di Fiumalbo - Membro del Rio Acquicciola (FIU2): calcareous cemented sandstones in sometimes thick layers. Intercalated in the upper part of the Fiumalbo Clays, perhaps in more levels. Maximum thickness of some tens of meters. The calcareous nano-fossils analyzed belong to the Priabonian-Rupelian p.p.

Marne di Marmoreto (MMA): marls, grey silty marls with poorly visible stratification with rare interbedded siltstones and fine clear-grey sandstones, weathering to yellowish, also of volcanoclastic origin. In the basal part are interbedded clay and limestone breccias. Discordant bottom contact on FIU. Escarpment deposit. Maximum thickness of about 100 m. Numerous biostratigraphic analyses have revealed the presence of nano-fossil-rich associations belonged to the Rupelian p.p.-Chattian p.p.

Marne di Marmoreto - Litofacies a brecce del Rifugio Battisti (MMAa): coarse breccia mostly matrix-supported, metric or decametric thick, originated from debris flows sometimes coarsely stratified. Clay and limestone clasts, in sizes up to decimetric, of Ligurian-Subligurian origin. The founded fossil associations belong to Chattian p.p.

Marne di Civago (CIV): ash grey marls, often silty, with poorly distinguishable stratification. Locally levels of black flint. Interbedded with thin discontinuous sandstone layers also from volcanoclastic origin, with coarse sand levels of marly matrix with abundant redeposited glauconite. The presence of *C. abisectus*, *D. bisectus, H. carteri* and *S. disbelemnos* led to the attribution of the Marne of Civago to the Aquitanian.

Cervarola Succession (MIOCENE)

Arenarie di Monte Cervarola - Membro del Torrente Dardagna (CEV1): coarse turbidites in thick and very thick strata alternating with finer turbidites and with slumping levels even several meters thick, and pebbly sandstone. The presence of *S. conicus, S. disbelemnos, S. belemnos* and *H. carteri* allow to assign the CEV1 at Burdigalian p.p..

Continental Quaternary deposits

Active landslide deposit (a1): gravitational deposit with evidence of current or recent movements, consisting of heterogeneous, rarely monogenic, rock types of different size composition, more or less chaotic. The texture of the deposits is conditioned by the substrate lithology and type of prevailing movement. Most of the landslide deposits in the Apennine area are complex and the result of more types of movement superimposed in space and time (typically slides/flows). The prevalent texture is constituted by clasts of variable size immersed in an abundant clayey and/or sandy matrix.

Fall/topple deposit active (a1a): originated from detachment of rocks by a steep slope and put in place by free fall, bouncing and rolling of pebbles and boulders. The accumulation of debris consists of heterogeneous material of different size composition with lithoid fragments ranging in size from a few cm^3 and dozens of m^3, with no or sandy-pelitic matrix, in places weathered and pedogenized.

Quiescent landslide deposit (a2): gravitational deposit with no evidence of current or recent movements but with the possibility of reactivation, consisting of heterogeneous, rarely monogenic, rock types of different size composition, more or less chaotic. The texture of the deposits is conditioned by the substrate lithology and type of prevailing movement. Most of the landslide deposits in the Apennine area are complex and the result of more types of movement superimposed in space and time (typically slides/flows). The prevalent texture is constituted by clasts of variable size immersed in an abundant clayey and/or sandy matrix.

Slide deposit (a2b): deposit originated from the movement towards the base of the slope of a mass of soil or rock, which occurs in large part along a rupture surface or within a band, relatively thin, of intense shear deformation.

Flow deposit (a2d): deposited by a continuously distributed movement within the moving mass. The cutting surfaces within this mass are multiple, temporary and generally not preserved. The materials involved are mostly cohesive. The most frequent deposits consist mainly of a clayey and/or clayey-sandy matrix including clasts of varying sizes.

Block slide deposit or DSGSD (deep-seated gravitational slope deformation) (a2h): complex and deep gravitational mass movement that affects large rock masses, sometimes with its related surface cover, and is conducted through a deformation mostly slow and progressive of the rock mass, without a well determinable sliding surface.

Slope deposit S.L. (a3): deposit consisting of heterogeneous lithologies of different size composition, more or less chaotic. Frequently the deposit shows a texture formed by clasts of variable size immersed and supported by a clayey and/or sandy matrix (which can be weathered by oxidation and soil formation), in places stratified and/or cemented. The genesis can be tentatively gravitational, by surface runoff and/or solifluction.

Scree (a6): accumulation of debris consisting of heterogeneous material of different size composition, usually at high or very high altitudes, with lithoid fragments ranging in size from a few cm^3 to dozens of m^3, with no or sandy-clayey matrix weathered and pedogenized, of gravitational origin frequently at the foot of escarpments and along the steeper slopes.

Evolving alluvial deposits (b1): gravels, sometimes imbricate, clayey sands and silts of fluvial origin, currently subject to variations due to fluvial dynamics; generally incoherent and chaotic debris, consisting of heterogeneous, sometimes rounded clasts of different size composition with sandy matrix, at the mouth of watersheds and secondary valleys.

Skeletal spread moraine deposit (c3): incoherent detrital deposits in a chaotic structure made of materials of different size composition embedded in silty-sandy matrix. Locally frequent erratic blocks.

Evolving colluvial fan (i1): alluvial deposits, mostly fan-shaped gravel open towards the valley, at the mouth of valleys transversal to the main waterways where slope decrease causes sedimentation of the material transported by water, subject to evolution with the water dynamics.

5.1.3 Geomorphology

The study area was modelled in the past by glacial and periglacial processes, while slope and fluvial processes acted with a stronger influence in more recent times together with human activity (Panizza et al., 1982). The slopes of Mt. Cusna were diffusely subject to glacial activity during the last glacial period (Losacco, 1949), with the formation of various cirques on the North-eastern slopes between 2100 and 1900 m a.s.l. (Mariani, 2015). These have been strongly remodelled by recent erosive phenomena, but their shape and dimensions can still be reconstructed. Another effect of glacial activity during the last glacial phase is the deposition of wide till deposits. It has been argued that the lowest and biggest glacial tongues reached between 850 and m a.s.l. and where related to the Last Glacial Maximum (Panizza et

al., 1982); other successive events were consequently related to later periods. A second generation of moraine arcs, located around 1100-1300 m a.s.l. was associated to the Pleniglacial, while a third at 1400-1600 m a.s.l., to the Tardiglacial.

Periglacial morphologies are numerous in variety and quantity. A great part of the gentle morphology of this area is probably the consequence of the great influence of Periglacial activity, which allowed the formation of great quantities of debris through gelifraction from such erodible rocks (Mariani, 2015). This debris, mobilised by slope movements (gelifluction and flows) and the action of water, has covered during time the roughness of the landscape. In the Mt. Cusna area have also been found rock glaciers (Panizza et al., 1982; Mariani, 2015). Gelifluction phenomena are regaining strength in recent times thanks to the deforestation produced by human activity leaving barren soils better available to frost activity during the winter (Panizza et al., 1982).

Gravitational processes are among the most widespread processes in the study area; in fact, all slopes are affected by landslides of different nature and size (Panizza et al., 1982). Among the erosional landforms due to gravitational processes the linear elements are prevalent such as flow debris channels. They affect both substrate and deposits of incoherent material (gravitational or glacial / periglacial origin) and in most cases are active landforms (Mariani, 2015). Among the depositional landforms due to gravitational processes, debris flow cones and talus cones can be observed. Also the DSGSD, complex and deep gravitational mass movement that affects large rock masses caused mainly by post-glacial or tectonic phenomena (Mariani, 2015), are common.

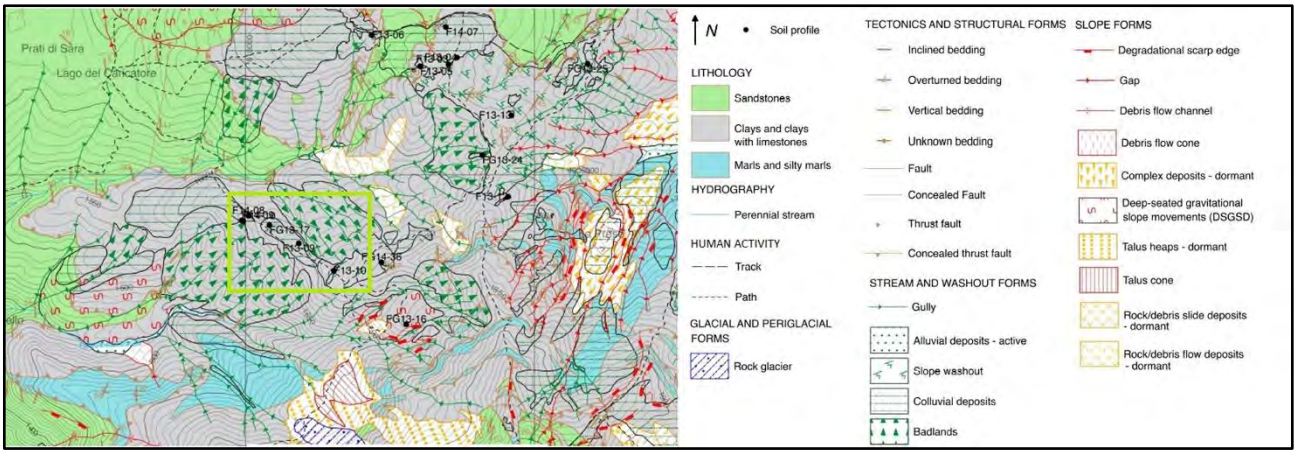

Figure 5.3. Monte Cusna geomorphological map 1:10000. In green the sample area (modified from Mariani, 2015). The grid square sides size is 100 m.

Moreover, the presence of running or channelized water has an important role shaping the landforms widespread in the area. The different substrate can modulate the response. In fact, although generally fractured due to tectonic stresses related to orogeny, the lithologies of the area have different degrees of permeability (Mariani, 2015). Sandstones and incoherent deposits of coarse material, which are semi-

permeable, allow rapid water infiltration into the soil: the surfaces with these lithotypes are not affected by sheet erosion. Instead, in areas with claystone and marl outcrops there is an intense erosion due to water runoff, which causes the removal of large quantities of material (Mariani, 2015). In many cases, the water runoff tends to channelize in rills and gullies, shaping particular landforms: the Badlands.
These processes are presently active and the human impact only gave them more force through forest clearing which progressively left ample portions of territory without a sufficient forest cover to prevent soil erosion (Panizza et al., 1982). In fact, the dynamic of Badlands formation is strongly hindered by the presence of a stable vegetable cover, which protects the substrate from erosion.
Even if, the study area is depicted as colluvial deposit in the geomorphological map (Mariani, 2015), it is also affected by running and channelized water processes (fig. 5.3).

5.1.4 Soils

The pedogenesis in the study area started after the last glacial retreat, therefore, all studied soils (including paleosols) belong to the Holocene (Mariani, 2015). The traces of soil formation prior to the glacial times completely disappeared during the glaciations (Panizza et al., 1982, Compostella et al., 2013) as the direct and indirect result of glacier action.
A study carried out by Panizza et al. (1982) giving a broad characterization of the Mt. Cusna soils, using Soil Taxonomy (Soil Survey Staff, 1975) as reference. They established three altitudinal belts characterized by the interaction of several factors such as substrate and soil temperature regime. Soil moisture regime is not considered among these factors since it is mainly characterized as udic (dry for more than 90 or 45 consecutive days in total in normal years) and does not change among the different altitudinal belts.
The first altitudinal belt, located below 1300 m a.s.l., has a mean annual temperature between 8°C and 15°C, with a mean difference in summer and winter of more than 6°C (mesic temperature regime). The strong presence of partially dynamic clays, inherited from the parent material, and the high content of carbonates cause soil cracking, which in slope topography results in a continuous rejuvenation by erosion. Soil formation is recent and forms Entisols and Inceptisols; locally, in areas where clays produce areas less permeable to water, soils with hydromorphic features are found (Mariani, 2015).
The second altitudinal belt, located between 1300 and 1900 m a.s.l., has a more frigid temperature regime, with temperatures between 0°C and 8°C. This altitudinal belt is affected by the majority of degradation processes, leaving substantial amounts of material. For that reason, Inceptisols developed on colluvial deposits are frequent. Beneath these deposits are traces of older soil formation, in the form

of relict or buried paleosols; the most important are associated to the paleosurface located on the northern slope of Mt. Cusna (Panizza et al., 1982; Mariani, 2015).

The third altitudinal belt, located above 1900 m a.s.l., has a cryic temperature regime (similar to frigid, but with a more limited mean summer temperature). The substrate is composed primarily by sandstone and on average more draining. This increases greatly organic matter and acidity, which in combination tend to form Spodosols. However, the most common type of soil is Entisols, since the harsh climate heavily impairs soil formation.

Moreover, the geopoedology map (Carta Ecopedologica d'Italia, Geoportale Nazionale, 2013) characterizes, using the FAO classification as reference (FAO, 2014), the soils of the study area as Cambisols or Regosols.

Whereas, the soils belong to the paleosurface have been described as Taptho-Luvisols (Mariani, 2015; Compostella et al., 2014; Krasilnikov & Calderón, 2006): these are more mature soils, subject to illuviation and with well differentiated horizons.

5.1.5 Climate

Two different meteorological stations are taken as reference for the area in exam: Ligonchio weather station located at 928 m a.s.l and Mt Cimone weather station located at 2165 m a.s.l.. For both stations, the data were elaborated in a previous study (Compostella, 2011) and the observation period is 1961–1990. The nearest is located in Ligonchio, at a lower quota compared to the area of study (928 m a.sl.). Observing the climograph (fig. 5.4) it can be recognised the typical Apennine rainfall regime, with a maximum of rainfall in November and a well marked minimum in July, though without the incurrence of dry conditions. Mean rainfall is quite abundant (mean value: 2000 mm per year). The mean annual temperature is 8.8°C.

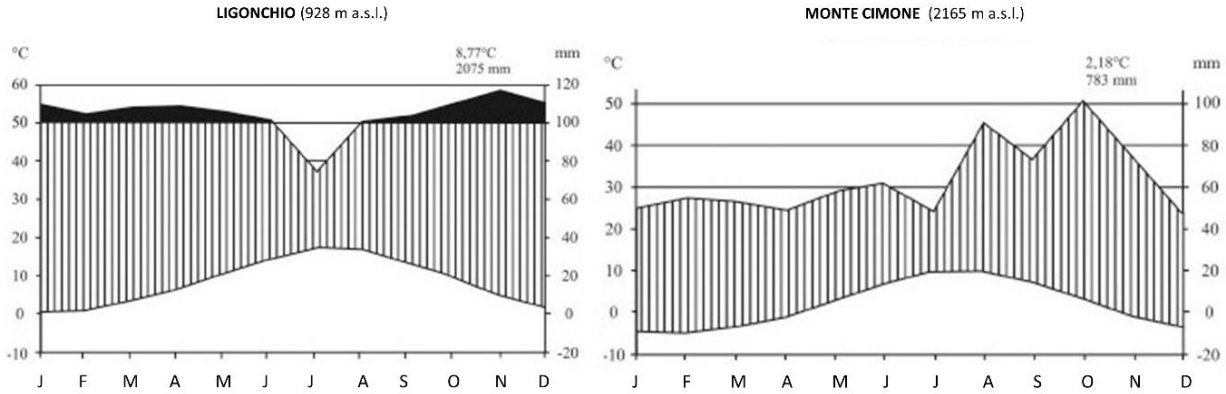

Figure 5.4. Climograph of Ligonchio and Monte Cimone weather stations (modified from Compostella, 2011).

The meteorological station that can best represent climatic conditions on the Mt. Cusna ridge is the Mt. Cimone one (2165 m a.s.l.), 50 m higher than Mt. Cusna. Here the recorded mean annual temperature is of 2.2°C with a February minimum (-4.6°C) and an August maximum (10.6°C). Rain is distributed quite irregularly during the year, with low values (783 mm) due both to its quota and its geographic position. Compared to Mt. Cusna and in general to the part of the chain NW to it, Mt. Cimone is less subject to the influence of the Tyrrhenian Sea and the moist air currents coming from it: this implies less rainfall, determining a subcontinental climate regime (Bertolani Marchetti et al., 1994; Tomaselli, 1994; Tomaselli et al., 1994).

5.1.6 Vegetation

The northern Apennines stand on the southern limit of the medioeuropean phytogeographical zone in contact with the mediterranean phytogeographical zone (Pignatti, 1979). In its highest part, it can be divided in a series of vegetation belts. Recent studies have produced a vegetation map of the northern area of Mt. Cusna (Redondi, 2009).

The montane zone is located between 800-1000 m a.s.l. and 1600-1750 m a.s.l. and this is occupied prevalently by beech (*Fagus sylvatica*) forests. The ample distribution of beech gives an apparent uniformity to these forests even if in this part of the Apennines are present different types of beech forest (Tomaselli, 1997). In particular, in the study area a vegetation dominated by *Fagus sylvatica*, monospecific in the tree zone, with an undergrowth composed by species such as *Vaccinium myrtillus*, *Luzula nivea*, *Hieracium sylvaticum*, *Oxalis acetosella*, *Saxifraga rotundifolia*, *Solidago virgaurea*, *Myosotys sylvestris* and *Galium odoratum* (Redondi, 2009).

Nearest to the tree line, about 1730 m a.s.l., the beech forest becomes open with a tree cover composed by *Fagus sylvatica*, and *Sorbus aucuparia*. In some areas a low shrub cover develops, dominated by *Juniperus nana*, and characterized by sparse *Laburnum alpinum* trees, which is a rare species in the Apennines (Redondi, 2009).

Above the natural tree line, up to 1800-1900 m a.s.l., can be found a shrub cover with a prevalence of *Vaccinium myrtillus* and *V. gaultherioides.,* whereas *V. vitis-idaea* is not always present. Two varieties of *Vaccinium* shrub cover can be recognised (Tomaselli, 1997): one with the presence of *Empetrum hermaphrodithum* and a high cover and frequency of *V. gaultherioides*, more related to steeper slopes and convex forms of relief where the snow cover stays no more than six months per year (Rossi, 1989). The second variety is located on more gentle slopes and on concave morphologies, which permit to the snow cover to stay for more than six months per year. It is characterized by the presence of *Hypericum richeri* and the predominance of *V. myrtillus*, by the absence of *Empetrum* and by stronger importance

of grassland species (*Nardus stricta, Avenella flexuosa*, *Hypericum richeri*, *Carex sempervirens*, *Meum athamanticum*, *Geum montanum*, *Festuca nigrescens*, *Luzula gr. sylvatica*, *Leontodon helveticus*, *Homogyne alpina*, *Anthoxanthum alpinum*) (Redondi, 2009).

From 1800-1900 m a.s.l. to around 2000 m. a.s.l., the high-altitude grasslands, differentiated by substrate typology, prevailed. Neutrophilous and calcicole grasslands are developed on soils on marlstones or limestones, and can be divided in terrace vegetations with *Anemone narcissiflora* and *Aquilegia alpina* and in pastures with *Festuca puccinellii* and *Trifolium thalii*. The latter, on slope screes steeper than 35°, is characterized by discontinuous vegetation with *T. thalii*, *Alchemilla alpina*, *A. saxatilis* and *Cirsium bertolonii* (Tomaselli, 1997). Primary acidic grasslands are typical of sandstones and claystones and are characterized by *Trifolium alpinum*, *Plantago alpina*, *Silene acaulis*, *Luzula spicata*. On the steepest slopes exposed to SW another grassland type appears which has as dominant species *Festuca robustifolia*, an Apennine endemism (Tomaselli, 1997). Secondary acidic grasslands (pasture associations) are the most diffused grassland in the area of study. They can be divided into two types. One is dominated by *Nardus stricta*, which is an index of pasture degradation, and are characterized by the presence of species such as *Geum montanum*, *Potentilla aurea*, *Gentiana kochiana*, *Leontodon helveticus*, *Centaurea nervosa*, *Festuca nigrescens*, *Antennaria dioica, Luzula multiflora*, *Potentilla erecta* (Tomaselli, 1997). *Brachypodium genuense* dominated grasslands and to developing correspondence of the steepest slopes exposed south. They also have a dryer microclimate and a quite heterogeneous floristic composition. *Brachypodium genuense* itself is an Apennine endemism (Tomaselli, 1997). These grasslands tend to evolve with time into *Vaccinium* shrub cover, but exposition to south, slope steepness and pasture activity can stop or anyway slow this process (Tomaselli, 1997).

In particular, the study area is located between 1600-1700 m a.s.l., slightly below the current treeline position (1750 m a.s.l., Compostella et al., 2013). In fact, the arboreal cover gradually becomes more discontinuous at higher altitude, where the beech leaves more space for the herbaceous and shrubbery component, composed mainly of *Vaccinium myrtillus*, *Juniperus nana*, *Thymus* sp, and *Laburnum alpinum*.

5.1.7 Human presence

The analysis of the anthropic influence on the landscape is very important in a paleo-environmental study. In fact, since prehistory, man has been able to adapt any colonized environment to his needs, modifying it more or less directly.

The first traces of human presence in this area of Mt. Cusna goes back to the Mesolithic. In the study area are present the two sites of Bagioletto and Lama Lite in which have been found both lithic artefacts

and traces of fireplaces, together with the remains of campsite structures (Castelletti et al., 1976; Panizza et al., 1982; Cremaschi et al., 1984). Later on, only scattered frequentation traces have been found, indicated by remains from the late Iron Age and Roman Age (Panizza et al., 1982; Cremaschi et al., 1984); from the Subatlantic period onwards there is a gradual return towards a more intense exploitation of the forest (Castelletti et al., 1976). Historical sources show progressive colonisation of the area from the High Mediaeval Times, with communities surviving on livestock and forest exploitation. Agriculture plays a minor role and is limited to small patches nearest to settled villages (Panizza et al., 1982). It is in this phase that human impact, above all the forest use, could ever had an important role in increasing slope instability by erasing the tree cover and favouring colluvial deposition in the study area.

In present times, farming grows up to 1000-1300 m a.s.l., while pasture reaches even greater heights. In addition to these activities forested areas have been destroyed to derive ski slopes and parking for tourist activities.

5.2 Results

Along the Mt. Cusna downslope a transect of five soil profiles was performed in the area affected by running water erosion. A spot sampling was done along the slope, at highest topographic points, preserved by erosion. Many profiles have been dug using the preexisting erosion scarps. As comparison, one soil profile (FC 16/04) was done in forested area (fig. 5.5).

Figure 5.5. Profiles location. The orthophoto has been drawn from spatial data available at the National Geoportal.

5.2.1 Field data

All the soil profiles are located between 1600 and 1700 m a.s.l. and have the same parent material (Argilliti con Calcari Variegate, AVC). From the geomorphology point of view, all the profiles are located in an area with colluvial deposits (Mariani, 2015), five soil profiles (FC 16/01; FC 16/02; FC 16/03; FC 16/05; FC 16/06) are also located in area affected by running water erosion. The vegetation cover is shrubby in all the profiles area, excluding the profile FC 16/04 characterized by beech forest (tab. 5.1).

Profile thickness assumes variable values (usually 0.5 to 2 m) depending on the morphology. In fact, maximum thickness is found in correspondence of soils evolved in forested area or in the case of superimposed sequences of soil developed on claystones. In this specific case, more than half of the profile thickness consists of one or more colluvial layers covering a paleosol.

The colour of the soil horizons, as well, shows a clear uniformity in the area, particularly as regards the hue values. In fact, when comparing all the described soils, the hue is never different from 10 YR or 2.5 Y. Soil structure is moderately expressed, and a well separated angular structure is described mostly related to buried horizons. In general, granular or subangular blocky structures are found (Appendix 5).

Profile	Elevation (m a.s.l.)	Inclination (°)	Slope exposure	Profile exposure	Parent Material	Geomorphology	Vegetation
FC 16/01	1675 m	10	NE	SW	Claystones	Colluvial deposits affected by running water erosion	Shrubby
FC 16/02	1678 m	2	N-NW	SW	Claystones	Colluvial deposits affected by running water erosion	Shrubby
FC 16/03	1670 m	4	NW	N	Claystones	Colluvial deposits affected by running water erosion	Shrubby
FC 16/04	1665 m	11	NW	N-NE	Claystones	Colluvial deposits affected by running water erosion	Forest
FC 16/05	1660 m	10	NW	N-NE	Claystones	Colluvial deposits affected by running water erosion	Shrubby
FC 16/06	1665 m	22	S-SE	SW	Claystones	Colluvial deposits	Shrubby

Table 5.1. Station descriptions for the studied profiles.

5.2.2 Particle size analysis

Examining the relative percentages of particle size distribution in the analyzed soil profiles it can be seen that there is a common trend. First, the gravel and the sand content are less compared to the silt and clay content. In fact, gravels never exceed 5% on the total weight, while sands rarely exceed 20%.

In all soil samples, the silts are the predominant fraction, ranging from about 44 to about 65%, while the amount of clay is more variable. In deeper horizons, the percentages of gravel and sand tend to increase to the detriment of the clay component (fig. 5.6, 5.7).

Analyzing the soil profile FC 16/01 it is noticed that coarse material (sand and gravel) increases with depth to the horizon BC, where it reaches about 15% of the sample total weight. Below the BC horizon, the sand and gravel have again very low values (horizon 2AB1), to gradually grow with depth: the coarse material in the two deeper horizons (2BC1 and 2BC2) represents approximately the 20% of the material. While the silt assumes very variable values within the profile, the clay tends to decrease in deeper horizons (2BC1 and 2BC2), where they reach 20% on the soil total weight.

Observing the cumulative curves of this profile (fig. 5.6), a granulometric discontinuity is highlighted. Curves related to 2AB horizons show lower values of sand than the BC horizon above. In the lower horizons, the amount of sand returns to rise, to reach the maximum value in the deep 2BC horizons. It is therefore possible to detect a discontinuity in the granulometry trend within the profile located at the transition between BC and 2AB1 horizons.

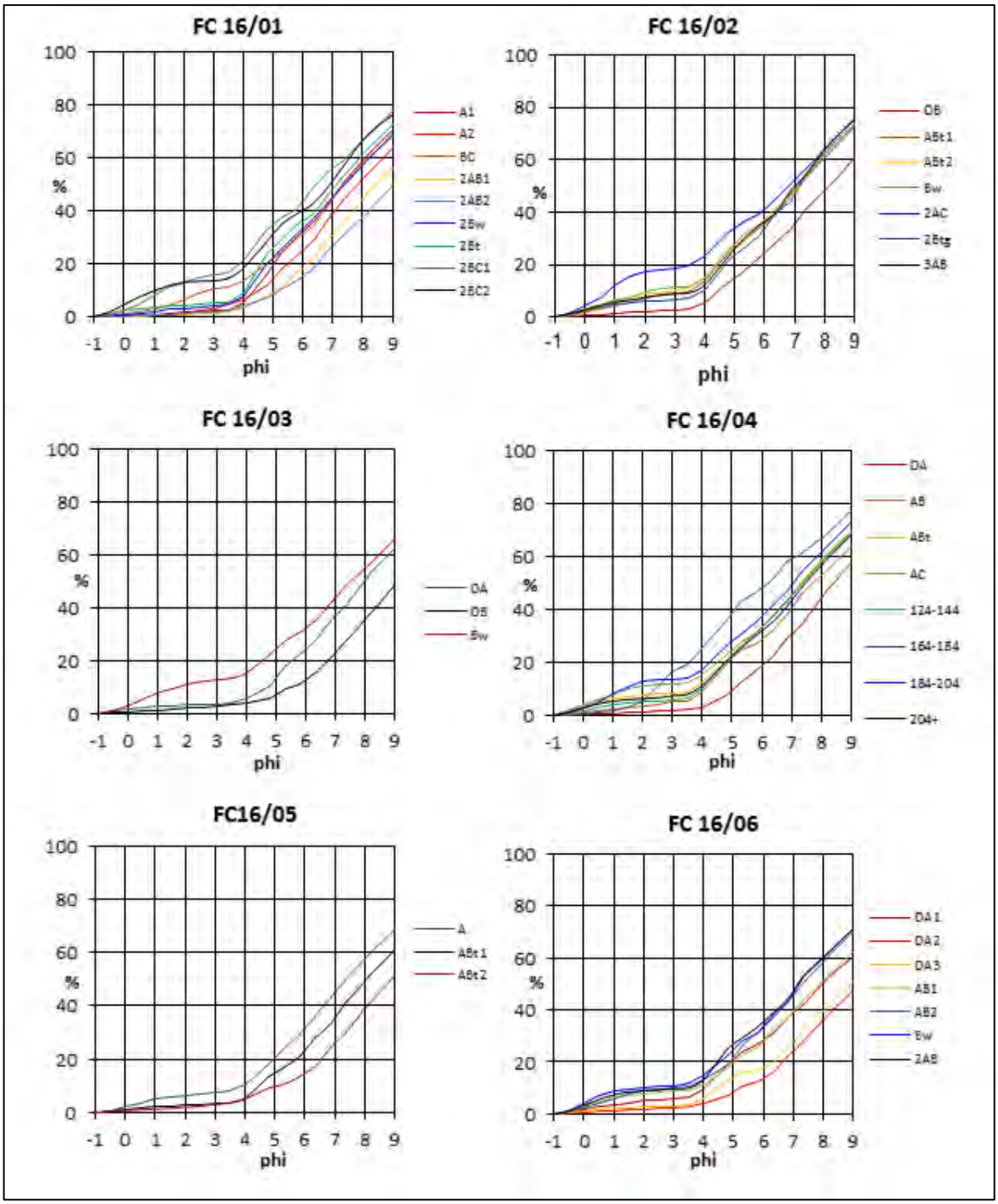

Figure 5.6. Cumulative curves of grain size distribution in the studied profiles.

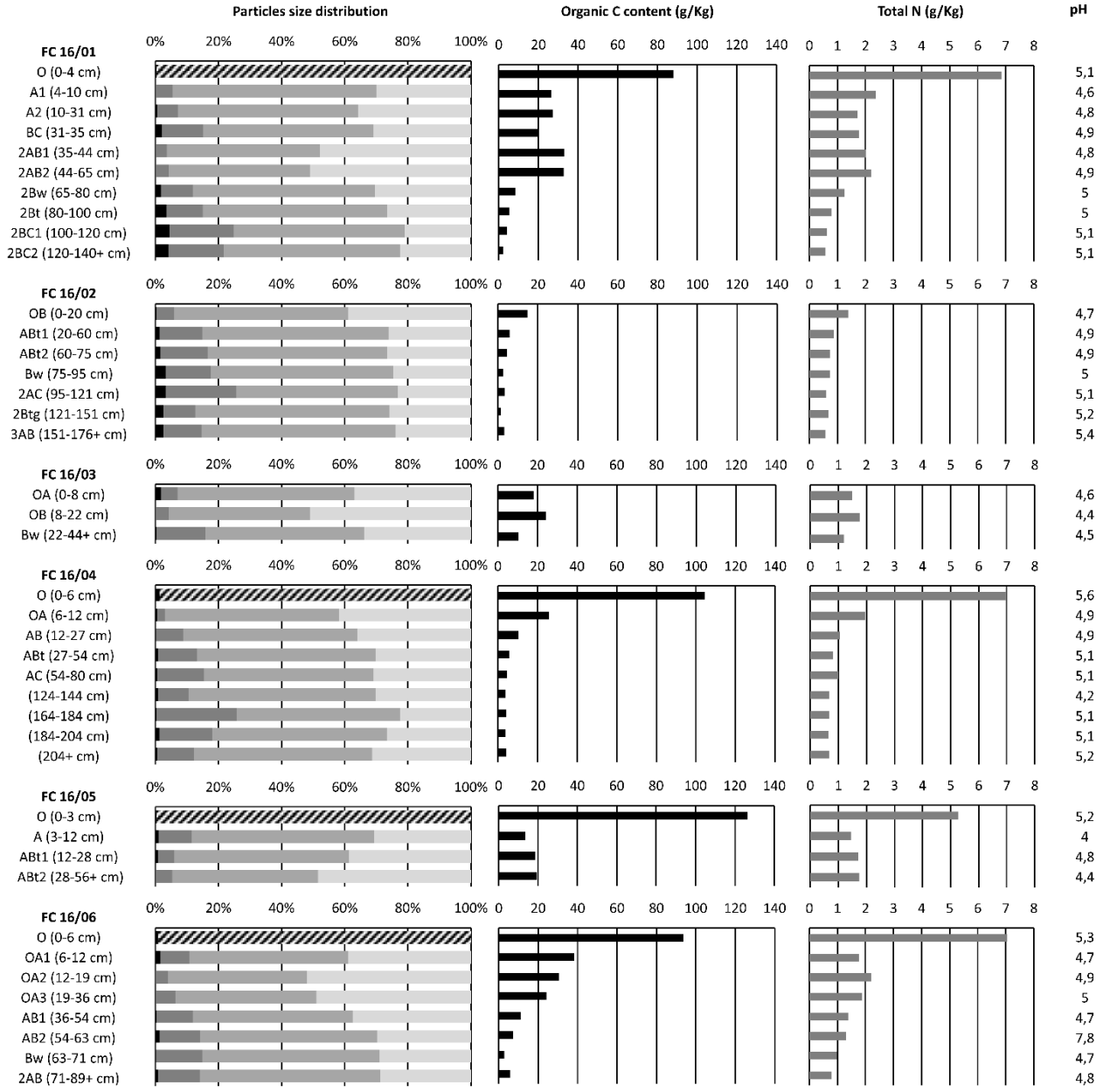

Figure 5.7. Particle size distribution, Organic C content, total Nitrogen content and pH values in the studied profiles. For the particle size distribution plot: in black is depict the gravel content, in dark grey the sand content, in grey the silt content. in light grey the clay content and in black strips the n.d..

Also along the FC 16/02 profile, the coarse component tends to grow up with depth until the 2AC horizon, where sand and gravel represent more than 25% of the material. Below the 2AC horizon, in the 2Btg horizon the coarse component decrease, and in the 3AB horizon rise again (fig. 5.7). Observing the cumulative curves (fig. 5.6), clearly distinguish the curves of the surface horizon (OB), rich in clay, and the deeper 2AC horizon, with more coarse component. The two deepest horizons (2Btg and 3AB) have similar curves to ABt1, ABt2 and Bw horizons, characterized by abundant fine material. Even in this soil profile, there is a discontinuity located at the transition between the 2AC and 2Btg horizons.

In the profile FC 16/04 the content of gravel and sand increases with depth, while the content of clay progressively decreases. The main exceptions to this trend are represented by horizons 124-144 and 204+, which, despite the depth, contain little content of sand (about 10-15%), showing a similar pattern to the more superficial AB and ABt horizons.
In the FC 16/06 profile the content of coarse fraction has a well visible increasing trend with depth, as well as a progressive decreasing trend of the clay. The main anomaly is represented by the OA1 superficial horizon, which contains more sand. Moreover, observing the cumulative curve, the OA1 particles size distribution is very similar to the AB1 horizon one. The deepest horizon 2AB shows a lower sand content than the above horizons (fig. 5.6), and the fine fractions has a slight increase: a granulometric discontinuity can then be identified at the transition between the horizons Bw and 2AB.
The FC 16/03 and FC 16/05 profiles have a few number of horizons, and therefore it is more difficult to recognize a trend.
FC 16/03 shows significantly higher values of sand content in the deepest horizon, while gravels prevail in the most superficial horizon. The variation of the particle size distribution along the profile looks like the FC 16/06 profile. Moreover, the cumulative curves, show that the deeper horizon (Bw) is the horizon with more coarse material, mainly due to the high content of the sand.
On the contrary, in the FC 16/05 profile the gravel and sand content decrease with increasing depth, while clay contents tends to increase.

5.2.3 Organic Carbon Content

The absolute quantities of organic carbon are very variable depending on the type of profile and depth (fig. 5.7). In surface horizons, values ranging between 15 (FC 16/02) and over 100 g/kg (FC 16/04 and FC 16/05) can be found. Usually, the C organic values decrease with depth: the general trend is therefore represented by a decrease of organic carbon content as horizons get deeper: this decrease can be more or less gradual, as in profile FC 16/02, or concentrated as a rapid loss at the transition from the uppermost horizon to the ones those below, such as in profiles FC 16/01, FC 16/04, FC 16/05 e FC 16/06.
Moreover, in the FC 16/03 profile the OB horizon shows a greater C organic content then the surface horizon OA. In the FC 16/05 profile, below the O horizon characterized by a very high organic C values (more than 120 g/Kg), there is a relatively C organic poor horizon (A), that are on top of two horizons with higher C organic content.
There are exceptions to the above described trend: as regards the profiles FC 16/01, FC 16/02 e FC 16/06 a peak in the organic carbon content is often found, corresponding to a specific horizon, while in the horizons underlying it, the values return to decrease.

In FC 16/01, a peak of organic C is observed in the 2AB1 and 2AB2 horizons, which show C values even higher than those recorded for surface horizons A1 and A2 (more than 30 g/Kg). Also in the profile FC 16/06 there is a deep horizon (2AB) richer in organic matter than the above horizon (Bw).
Sometimes, peaks in organic carbon are more than one, like in the profile F16/02 where a slight increase in organic C is recorded at the deep horizons 2AC and 3AC.

5.2.4 Total Nitrogen

The total nitrogen contents have the same trend of the organic C content (fig. 5.7), but with significantly lower values (not exceeding 7 g/Kg). Even the total nitrogen content decreases with depth along the profile, and the same exceptions are be found (profiles FC 16/03 and FC 16/05). The decrease is concentrated as a rapid loss at the transition from the uppermost horizon to the ones those below, while in the underlying horizons the decrease is more gradual.
Among the organic horizons, those belong to the FC 16/01, FC 16/04 and FC 16/06 profiles have the highest N content (about 7 g/Kg), while the lowest values are recorded, as for organic C, in FC 16/02 (about 1.4 g/Kg). Similar trend anomalies may also be recognized to those underlined for organic C content: in the FC 16/01 profile, for example, a significant increase in total N is observed in the 2AB1 and 2AB2 horizons.
Finally, the C/N ratio have a very low values (about 2-3), and generally not exceed 15 (fig. 5.8). Only in FC 16/05 O nd in FC16 / 06 OA1 horizons the C/N ratio is slightly over 20. In general, the C/N ratio is very similar to the C organic content trend. Usually the C/N ratio has higher values in the surface horizons and decreases with depth.

5.2.5 pH

All the soil horizons analyzed have a tendency to acidity, the pH in H_2O never reaches the neutrality and the values of pH in H2O ranging between 4 and 5.6 (fig. 5.7).
Although, the pH values measured in H_2O neither gets large variations between successive horizons nor within the entire depth of profile, in FC 16/01, FC 16/02 and FC 16/04 the pH values progressively increase with the profile depth, approaching to the parent material. In many cases this variation seems very moderate, being rarely more than 1 point of pH and for the FC 16/01 and FC 16/04 profiles the most superficial horizons showing a lower acidity than the immediately underlying horizons, with pH values greater than 5.

Moreover, in the FC 16/01 profile, also, the 2AB1 horizon takes slightly lower values than the horizon above, thus interrupting the generally increasing trend along the profile.

However, in the other profiles, the pH values seem to oscillate independently of the depth, and no well-defined pattern can be recognized.

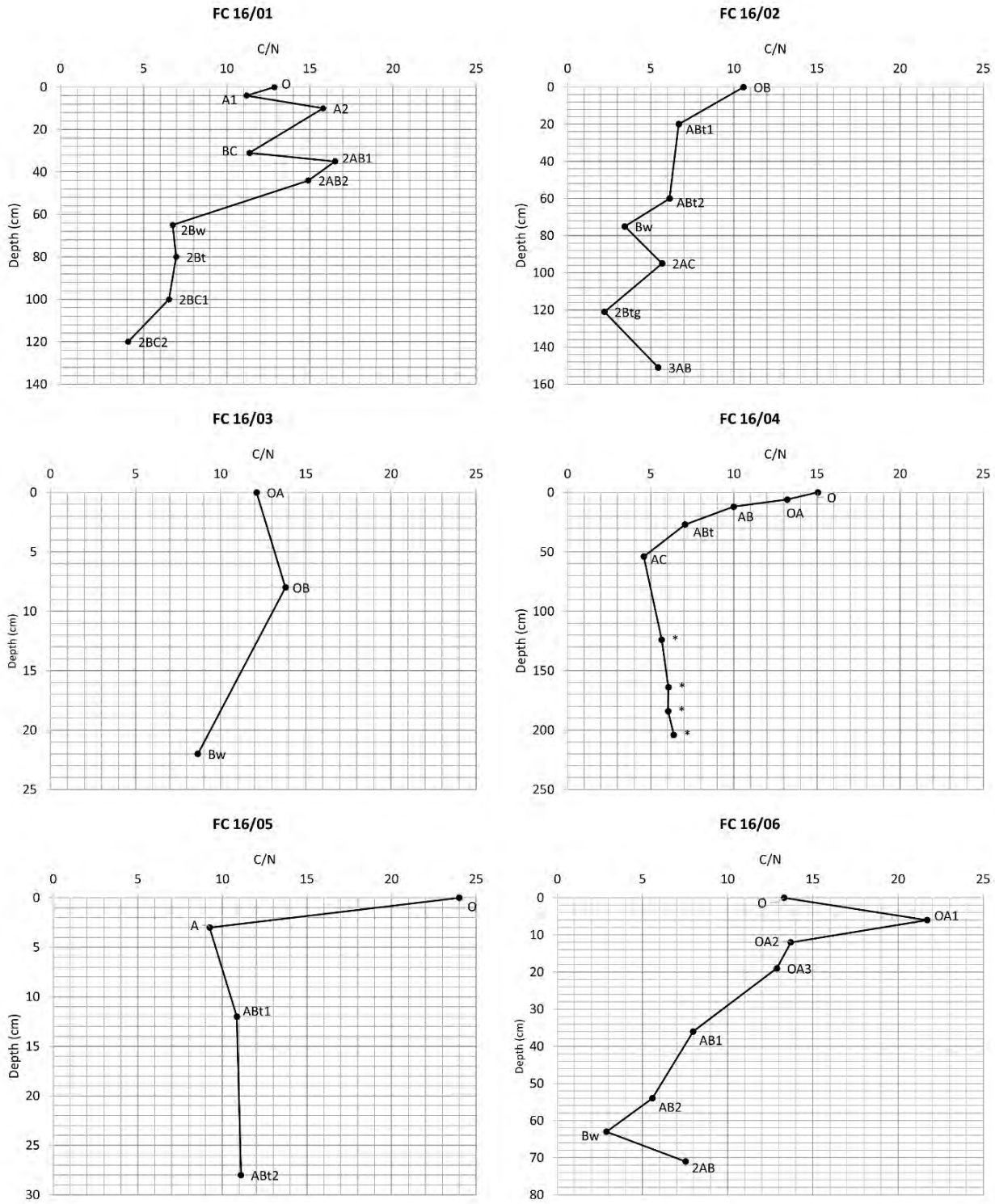

Figure 5.8. C/N ratio in the studied profiles.

5.2.6 Alluminum and Iron extractions

The total content of free iron oxides (Fed) in some horizons can reach 30 g/Kg but generally ranging between 10 and 20 g/Kg. The values of amorphous iron oxides (Feo) tend to be lower, between 0 and 10 g/Kg, as well as iron bound with the organic matter (Fep). For all three of these parameters, particularly high values are observed in FC 16/01 2AB2, FC 16/03 OB, FC 16/05 ABt2, FC 16/06 OA2 and OA3 horizons (fig. 5.9).

As regards the aluminum content, the quantities tend to be inferior to those of iron, and less variable, with the exception of aluminum bound with the organic matter (Alp). Free aluminium oxides (Ald) reaches values between 3 to 5 g/Kg, amorphous aluminium oxides (Alo) between 0 and 5 g/Kg, and the aluminium bound with the organic matter (Alp) between 3 and 10 g/Kg.

Contrary to what has been observed for iron, different types of aluminum do not show similar trends and similar peaks along the profiles. The values of Feo and Alo recorded for FC 16/05 A were not taken into account because they were considered unreliable.

The crystalline iron oxides are mainly concentrated in the B horizons (tab. 5.2), in fact the highest values are found in the FC 16/03 OB (24.4 g/Kg). Instead, the Bw horizons have low value of crystalline iron oxides; the horizons FC 16/01 2Bw, FC 16/02 Bw, FC 16/03 Bw and FC 16/06 Bw rarely exceed 12 g/Kg.

The Feo/Fed index allow us to underline positive peaks that generally occur in the B horizons: in fact, values above 0.5 are observed at FC 16/01 Bw, FC 16/02 Bw and FC 16/03 Bw, in addition to FC 16/04 O and FC 16/04 AB (tab. 5.2). Whereas, in the other B horizons the values are lower and in the FC 16/02 2Btg horizon the iron activity index is very low (0.05 g/Kg).

Finally, the results of the podzolization index Alo + ½ Feo meet the conditions of podzolization processes only in the case of ABt2 and Bw horizons of FC 16/02 (FAO, 2014).

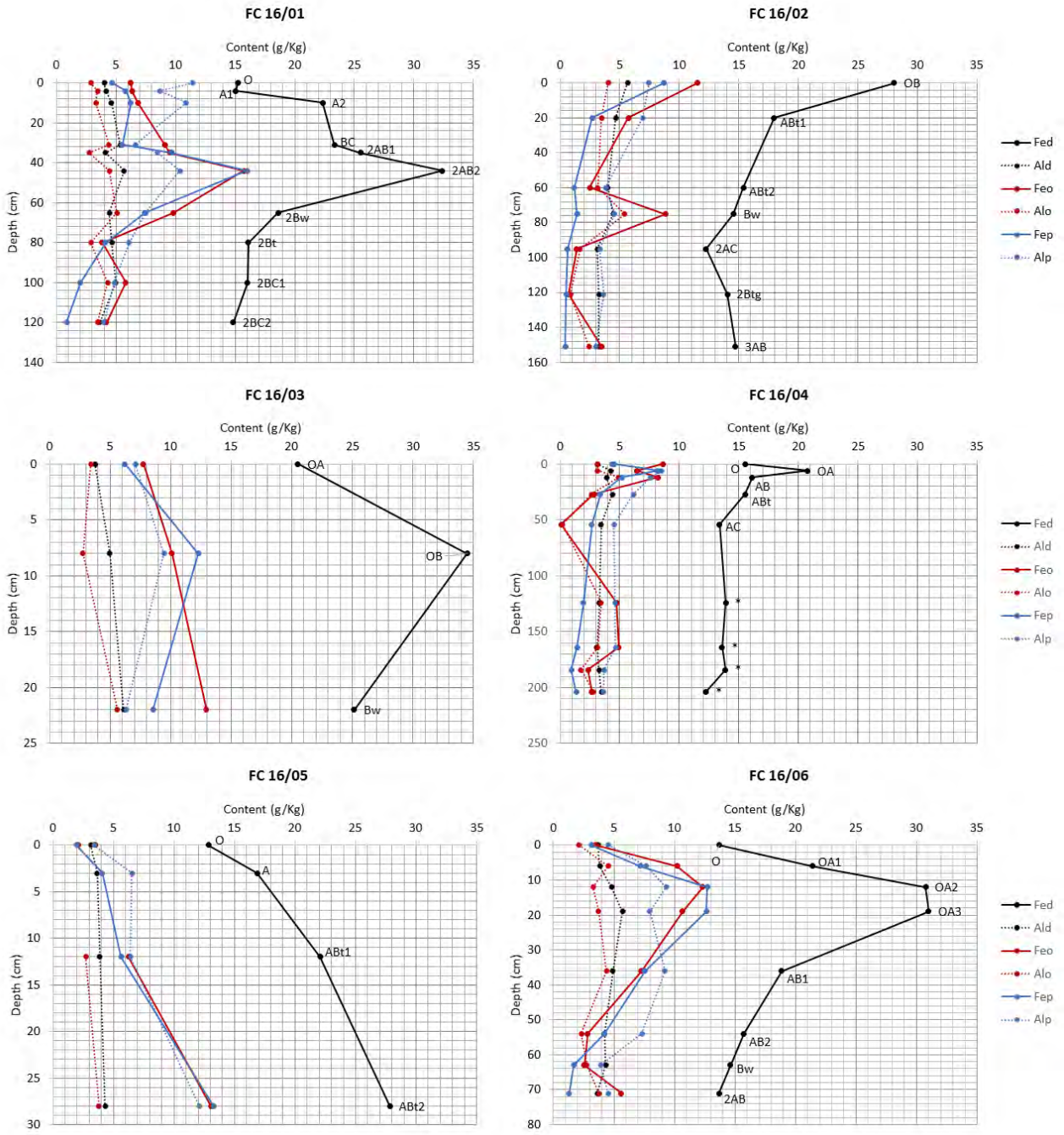

Figure 5.9. Free iron oxides (Fed), amorphous iron oxides (Feo) and iron bound to the organic matter (Fep) content, free aluminum oxides (Ald), amorphous aluminum oxides (Alo) and aluminum bound to the organic matter (Alp) content of the studied profiles The horizons name are close to the Fed curves.

Profile	Horizon	Depth (cm)	Fed - Feo (g/Kg)	Feo/Fed	Alo+1/2Feo (%)
FC 16/01	O	0-4	9.0	0.41	0.6
FC 16/01	A1	4-10	8.7	0.42	0.66
FC 16/01	A2	10-31	15.5	0.31	0.67
FC 16/01	BC	31-35	14.3	0.39	0.89
FC 16/01	2AB1	35-44	16.0	0.37	0.75
FC 16/01	2AB2	44-65	16.7	0.49	1.23
FC 16/01	2Bw	65-80	8.8	0.53	1
FC 16/01	2Bt	80-100	12.3	0.24	0.48
FC 16/01	2BC1	100-120	10.2	0.36	0.72
FC 16/01	2BC2	120-140+	10.6	0.28	0.55
FC 16/02	OB	0-20	16.5	0.41	0.98
FC 16/02	ABt1	20-60	12.2	0.32	0.63
FC 16/02	ABt2	60-75	12.9	0.16	0.44
FC 16/02	Bw	75-95	5.7	0.61	0.98
FC 16/02	2AC	95-121	10.9	0.11	0.24
FC 16/02	2Btg	121-151	13.3	0.05	0.12
FC 16/02	3AB	151-176+	11.2	0.24	0.41
FC 16/03	OA	0-8	12.8	0.38	0.73
FC 16/03	OB	8-22	24.4	0.29	0.78
FC 16/03	Bw	22-44+	12.2	0.51	1.21
FC 16/04	O	0-6	6.9	0.55	0.74
FC 16/04	OA	6-12	14.3	0.31	0.64
FC 16/04	AB	12-27	8.0	0.51	0.9
FC 16/04	ABt	27-54	12.7	0.18	0.4
FC 16/04	AC	54-80	13.3	0.01	0.03
FC 16/04	*	124-144	9.1	0.34	0.58
FC 16/04	*	164-184	8.7	0.36	0.56
FC 16/04	*	184-204	11.5	0.17	0.29
FC 16/04	*	204+	9.6	0.22	0.41
FC 16/05	O	0-3	9.3	0.27	0.39
FC 16/05	A	3-12	n.d.	n.d.	n.d.
FC 16/05	ABt1	12-28	15.8	0.28	0.58
FC 16/05	ABt2	28-56+	14.8	0.47	1.03
FC 16/06	O	0-6	10.2	0.26	0.39
FC 16/06	OA1	6-12	11.2	0.48	0.96
FC 16/06	OA2	12-19	18.4	0.4	0.94
FC 16/06	OA3	19-36	20.3	0.34	0.91
FC 16/06	AB1	36-54	11.6	0.39	0.8
FC 16/06	AB2	54-63	12.9	0.18	0.37
FC 16/06	Bw	63-71	12.1	0.17	0.4
FC 16/06	2AB	71-89+	8.1	0.41	0.66

Table 5.2. Iron and aluminum indeces. Crystalline iron oxides (Fed-Feo), activity iron index (Feo/Fed) and podsolization index (Alo+1/2Feo).

5.2.7 Rock-Eval data

In the I/R diagram the organic horizons have I-index values between 0.2 and 0.3 and a R-index between 0.5 and 0.55. While the OA, AB and OB horizons have I-index values between -0.3 and 0 and a R-index between 0.65 and 0.8. Finally the Bw and 3AB, 2Btg, 2AB, 2AC, 2BC2 horizons have I-index values between 0 and 0.5 and a R-index between 0.65 and 0.8 (fig. 5.10).

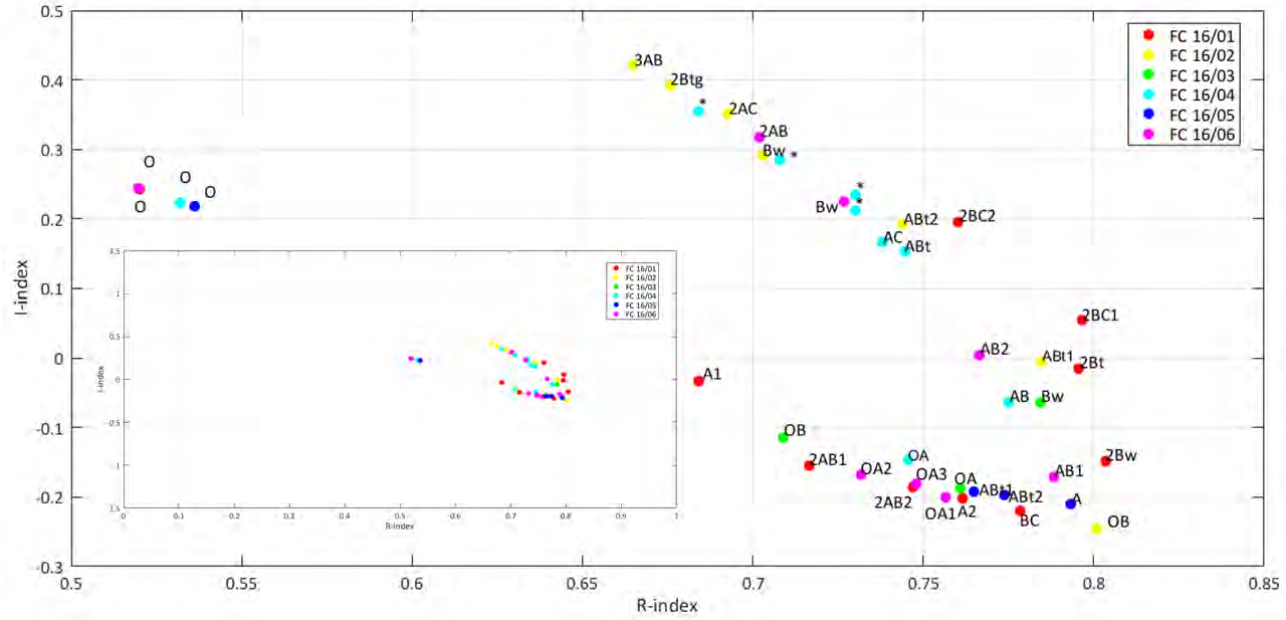

Figure 5.10. I-index/R-index. On the bottom left the data are plotted using the grid value from Sebag et al., 2016 in order to better visualize the trends.

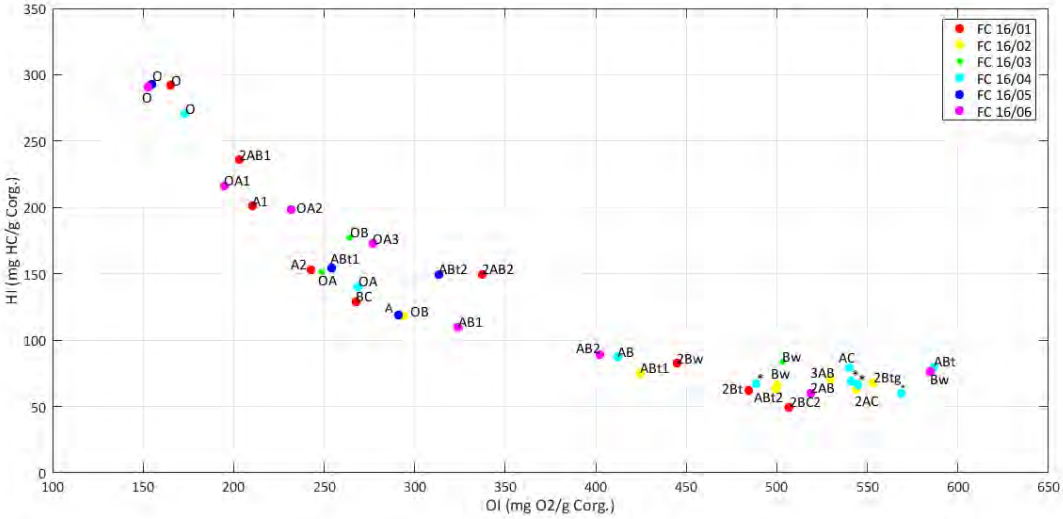

Figure 5.11. HI/OI diagram. The horizon 2BC1 is not plotted due to its out of range value.

The HI/OI index show different values in different horizons typology (fig. 5.11). In fact the O horizons show a high HI values and low OI values, while the Bw and Bt horizons and also the 2Bt, 2AB, 3AB show high OI values and low HI values and finally the A and AB horizons have an intermediate values.

5.2.8 Micromorphological characterization

FC 16/01 29-39 cm

The thin section contain three horizons: A2, BC (for a small thickness) and 2AB1. There are two types of aggregates, crumbs and angular-subangular blocky (fig. 5.12 a,b). The latter, particularly abundant in the horizon BC. Aggregates are easily identifiable, separated from each other and from coarse material by complex packing voids. There are also few linear planes and bioturbation channels. Based on these elements, the microstructure was defined as complex: subangular blocky/crumb.

The amount of fine material (<15 μm) is slightly higher (60%) than the coarse one (40%), therefore the c/f distribution is closed single spaced porphyric. The mineral fragments are mainly composed of claystones and sometimes sandstones, weakly weathered. The fine material, fine clay and fine silt, has a yellowish cloudy speckled b-fabric. Organic and plant tissues (mainly fine roots, less than 3 mm, confirming the presence of bioturbation) were observed among the coarse organic material, rare pieces of partially burnt wood, not larger than 2 mm, and rare phytoliths, that is, amorphous silica structures deposited from the plants inside the cells. The only pedological feautures founded are typical ameboidal Fe/Mn nodules (moderately impregnated), with small size (<300 μm), which are present in the whole thin section, but more commonly in angular and subangular blocky.

FC 16/01 41-51 cm

The thin section is organized into two different types of aggregates: crumbs / granules, with a small size (maximum 1 mm), and angular-subangular blocky, like those found in the previous section (FC 16/01 29-39 cm). These last are the predominant aggregates, and tend to be more abundant in the lower portion of the section. Among the aggregates common compound packing voids, frequent linear planes and very few chambers and channels are present. The different distribution of the aggregates in the thin section determine two different type of microstructure: in the upper part it can be defined as complex, subangular blocky/locally crumb, while in the lower portion is predominantly subangular blocky. This confirms the distinction, made on the field, between the horizons 2AB1 (thin section upper part) and 2AB2 (thin section lower part). The coarse fraction (over 15 μm in size) of mineral material is only 15%, and is composed of fragments of weathered claystones and sandstone (up to 3 mm in size) and quartz (not more than 100 μm). The thin section has an open double spaced porphiric c/f distribution. The micromass, less than 15 μm in size, is composed of fine clay and fine silt, reddish-yellow, and has a speckled-striated b-fabric.

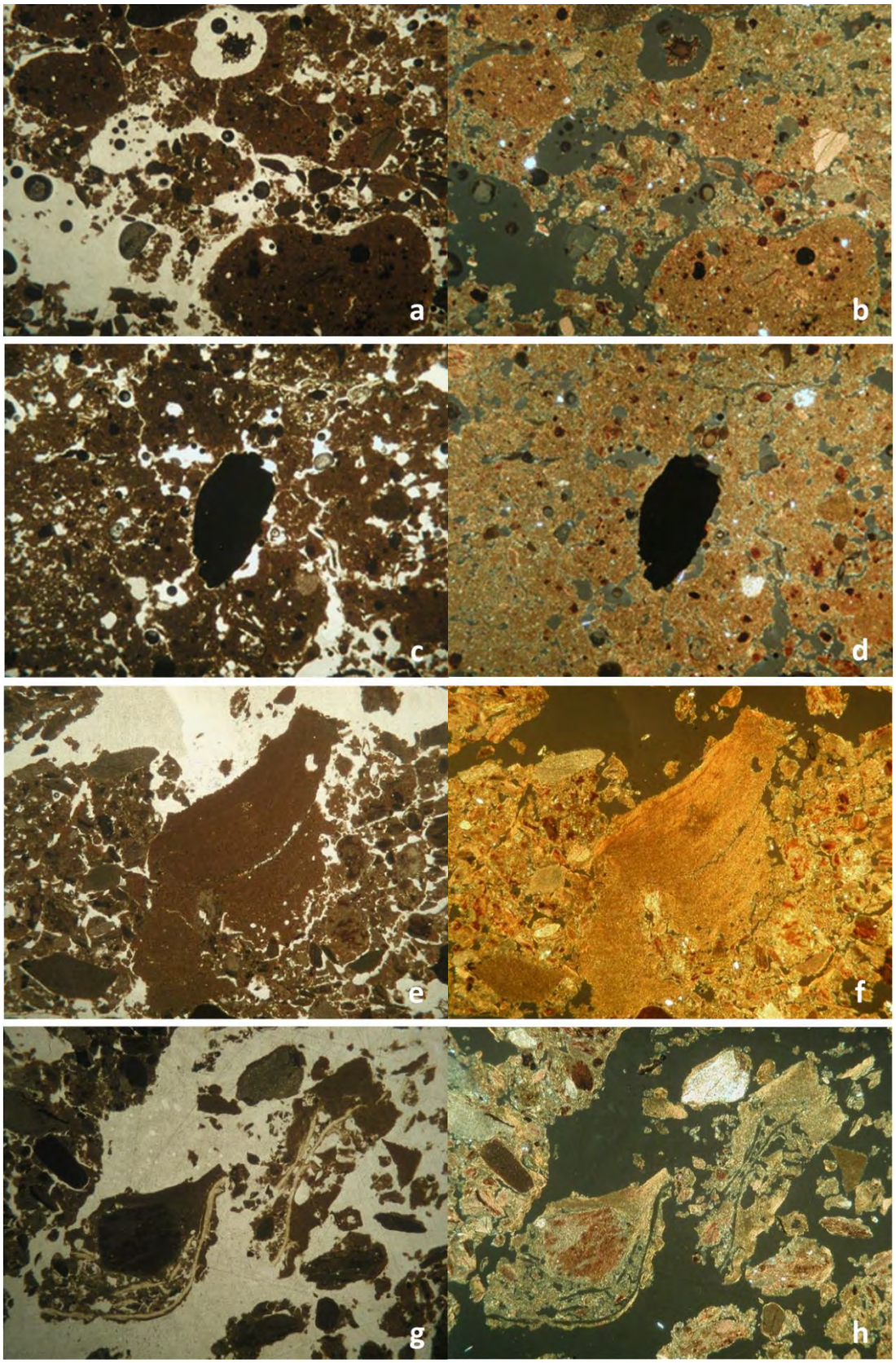

Figure 5.12. a, b) Crumbs and subangular blocky aggregates within the thin section FC 16/01 29-39 cm. In the subangular blocky are visible typical ameboidal Fe-Mn nodules with a different color compared to the micromass. On the right and in the upper part of the thin section bioturbation channels are also visible. 16x, PPL e XPL. c, d) Charcoal fragments partially burnt in the thin section FC 16/01 41-51 cm. In the subangular blocky aggregates are visible typical ameboidal Fe-Mn. 16x, PPL e XPL.e, f) Aggregates composed of fine material in the thin section FC 16/02 20-60 cm. 16x, PPL e XPL. g, h) Filamentous phytoliths in the thin section FC 16/02 20-60 cm. 16x, PPL e XPL. Field length: 8 mm.

Also in this thin section the coarse organic component is represented by roots and plant organs (up to 1 cm in diameter), which together with the channels indicate bioturbation, phytoliths (very scarce, up to 1.5 mm in length) and charcoal fragments (rare, up to 2 mm, fig. 5.12 c, d). Similarly to the previous section, the only pedological features present are small Fe-Mn nodules, which do not exceed 300 μm in diameter.

FC 16/01 86-96 cm

Also in this thin section, there are two types of aggregates: crumbs/granules and angular-subangular blocky. The latter are few, and they do not exceed 600 μm, while the granules can reach the millimeter size. Coarse clasts and aggregates are mainly separated by complex packing voids, very few linear planes and channels. The microstructure, predominantly defined by packing voids and granules, is crumb.

The coarse (> 15 μm) and the fine portions are present in equal quantities, and the distribution is closed single spaced porphiric. The coarse fraction is composed of sandstones (more frequent) and claystones fragments, generally weathered and in size up to 1 cm. The micromass, which includes clay and fine silt, is yellow, and the b-fabric is crumb. The few coarse organic material, not exceeding 1 mm in size, includes roots and plant organs, phytoliths and fragments of charcoal. Even in this case the presence of channels and roots indicates bioturbation. The pedological features founded are few ameboidal typic nodules of Fe-Mn (moderately impregnated) (<200 μm), few typic clay coatings (<300 μm) and rare typic clay yellowish infillings (<100 μm) associated with voids.

FC 16/02 20-60 cm

In this section, belong to the ABt1 horizon, the aggregates are mainly crumbs and granules. There are also rare subangular blocky, up to 2 mm, composed exclusively of fine material (fig. 5.12 e, f). The aggregates and the coarse clasts are separated by complex packing voids, very few linear planes and chambers.

The microstructure, defined by the presence of two types of aggregates, is therefore complex: predominantly granular and locally subangolar blocky. The coarse fraction (c/f limit 15 μm) represents about 40% of the total mineral material, and the relative distribution is open double spaced porphiric.

The clasts are weathered rock fragments (claystones and sandstones). The yellowish micromass has a speckled-striated b-fabric. Among the coarse components of organic origin, few roots with a maximum diameter of 5 mm are observed, and very small phytoliths, concentrated in the upper portion of the section, and no longer than 4 mm (fig. 5.12 g, h). About the pedological features, Very few ameboidal typic nodules of Fe-Mn (moderately impregnated), few typic clay coatings and rare intercalations are found.

FC 16/02 121-151 cm

In this section, belong to 2Btg horizon, the material is very compact, and the few well-isolated aggregates present are granules not exceeding 200 μm. Packing voids between aggregates are very few, while vughs are common (irregular shaped voids). Other types of voids are very few linear planes, channels and chambers. The microstructure, determined by the voids, is defined as vughy.

Coarse fraction (> 15 μm) represents 40% of the mineral material. The c/f distribution is defined as closed single spaced porphiric. The coarse clasts belong to claystone and sandstone and are often weathered. The yellowish micromass has a speckled-striated b-fabric.

No coarse organic material was observed in this thine section. On the other hand, the pedological features are very abundant and developed. In particular, few ameboidal typic nodules of Fe-Mn (moderately impregnated), few typic clay coatings, rare crescent typic clay coatings (often fractured), very few typic clay infillings and rare Fe-Mn hypocoatings are found (fig. 5.13 a,b).

FC 16/04 49-59 cm

The thin section cover the boundary between the ABt (27-54 cm) and BC (54-80 cm) horizons. It has a differentiated microstructure between the upper part, where subangular blocky aggregates dominate with a fissure microstructure (fig. 5.13 c, d), and the lower part where the granular aggregates dominate, with a crumb microstructure (fig. 5.13 e, f). Consequently, among subangular blocky aggregates frequent linear planes prevail, while among granular aggregates the complex packing voids are frequent. Few chambers and channels are also found.

The differences between the two horizons found observing the microstructure confirm what is observed on the field. The distribution of mineral components also highlights the limit between the two horizons: the amount of coarse material (mainly fragments of sandstones and claystones) is higher in the lower part, where it represents 50%, while in the upper portion it does not exceed 30%. On varying the abundance also varies the distribution of coarse components: open double spaced porphiric in the upper part and close single spaced porphiric in the lower part of the thin section. The fine material has a yellowish colour and a speckled-striated b-fabric.

The only coarse organic components are very few fine roots. Among the pedological features, few ameboidal typic nodules of Fe-Mn (moderately impregnated), few typic clay coatings (fig 5.13 g, h), few typic clay infillings and at the top of the section there is an area with clay depletion coatings (recognizable by the color difference of the fine material) (fig. 5.14 a, b).

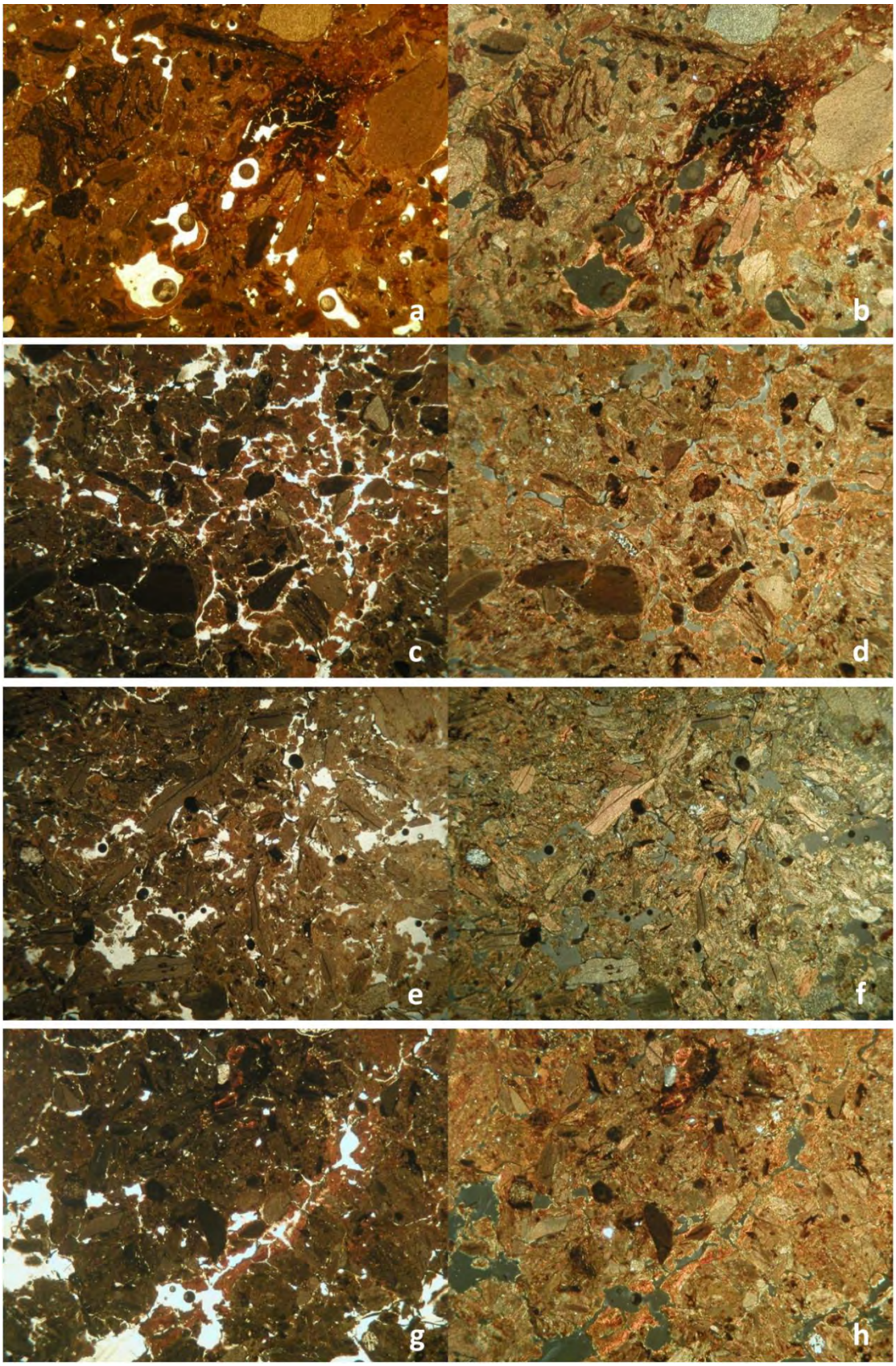

Figure 5.13. a, b) Crescent typic clay coatings and Fe-Mn hypocoatings in the thin section FC 16/02 121-151 cm. The compact microstructure characterized by vughs are also visible. 16x, PPL e XPL. Field lenght: 8 mm. c, d) Fissure microstructure in the thin section FC 16/04 49-59 cm. 16x, PPL e XPL. e, f). Crumb microstructure in the thin section FC 16/04 49-59 cm. 16x, PPL e XPL. g, h) Typic nodules of Fe-Mn, typic clay coatings and clay infillings in the thin section FC 16/04 49-59 cm. 16x, PPL e XPL. Field length: 8 mm.

FC 16/05 21-31 cm

This last thin section includes the boundary between ABt1 (12-28 cm) and ABt2 (28-56+ cm) horizons of FC 16/05. The microstructure, characterized by dominant subangular blocky and granular aggregates is defined complex, subangular blocky/locally crumb. Among granular aggregates, frequent compound packing voids are found, while among subangular blocky aggregates linear planes and channels prevail. Few chambers are also present.

The micromass (less than 15 μm) represents 70% of the mineral material. The distribution is open porphiric, with coarse components (fragments of sandstones and weathered claystones) immersed in the ground mass. The latter, yellow, with a speckled-striated b-fabric, is more red in the subangular blocky aggregates (fig. 5.14 c, d). Among coarse organic components, in addition to the fine roots, there are rarely phytoliths and fragments of partially burnt material. As for the pedological features, there are typical clay coatings, not very developed, and various types of Fe-Mn nodules, which reach 0.5 cm in diameter. The nodules are more abundant within subangular blocky aggregates. In the channels can also be seen passage features, consisting of small aggregates of fine material that fill the void (fig. 5.14 e, f).

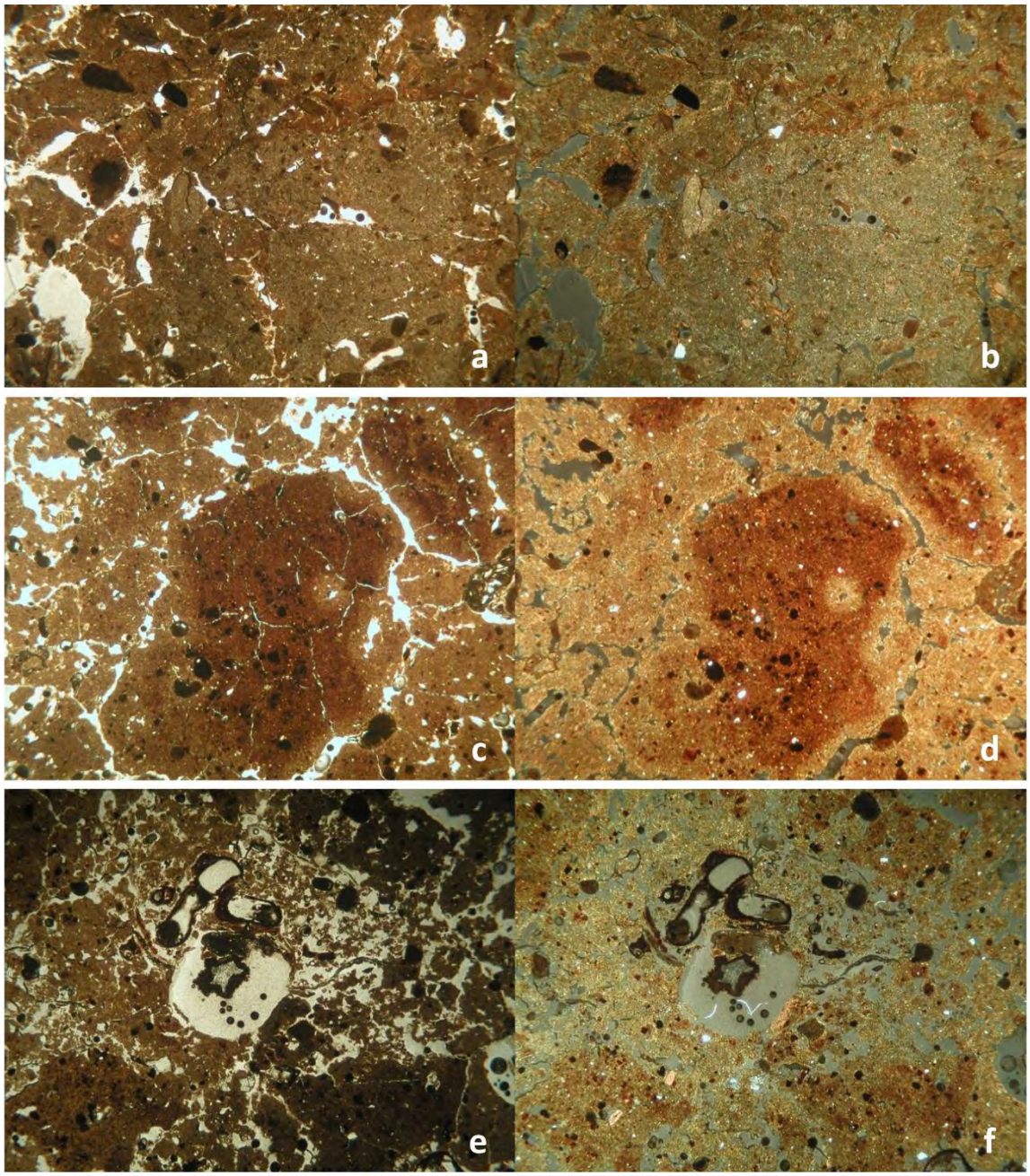

Figure 5.14. a, b) Area with clay depletion coatings in the thin section FC 16/04 49-59 cm. 16x, PPL e XPL. c, d) Aggregates with different colour in the thin section FC 16/05 21-31 cm. It is also visible the higher concentration of Fe-Mn nodules in the subangular blocky aggregates. 16x, PPL e XPL.e, f) Passage features linked to the bioturbation in the thin section FC 16/05 21-31 cm. 16x, PPL e XPL. Field length: 8 mm.

5.3 Discussion

To understand the complex geopedological contest of the study area, different approaches and analyses were used.

First of all the particle size distribution analysis together with the organic C content and the total nitrogen content allow us to identify the presence of different pedological units.

Usually, along a soil profile, the particle size tends to increase with the depth: while in the surface horizons the mineral constituent are disrupted and altered by the pedogenetic processes, in deep horizons the rock fragments from the parent material are preserved. Therefore, in depth, the influence of parent material on soil composition is progressively greater (Atkinson, 2004). Even organic C content and total N content have a specific trend and tend to decrease progressively from the surface, source of organic material, to deep horizons (Soil Survey Staff, 2014). These two parameters are also influenced by the presence and type of vegetation. However, in some cases this trend shows anomalies that may identify the presence of different geopedological units.

In the profile FC 16/01 (between the horizons BC-2AB1), FC 16/02 (between the horizons Bw-2AC and 2Btg-3AB) and FC 16/06 (between the horizons Bw-2AB) the trend anomalies are found.

In particular, in the profiles FC16/01 and FC16/06 a peak in C content and a peak in fine material in deep horizons underline the presence of paleosurfaces, subsequently buried by coarse colluvial deposits, which, due to the contribution of new material, interrupted the pedogenesis. These deep horizons rich in fine material and organic matter are in fact buried by an horizon with a coarse and almost mineral composition. Moreover, on this colluviall material, which became a new parent material, a new pedogenesis was set up.

In profile FC 16/02 the organic C content shows an increase at the 2AC horizon, which is, however, rich in coarse material: therefore, it is not possible to distinguish precisely the paleosurface (underlined by the peak in organic matter) from the colluvial that buried it (signaled by the high percentage of sand and gravel). Since the horizon has a homogeneous aspect during field description and sampling, the distinction between the two units may be difficult due to the material mixing during pedogenesis (fig. 5.7).

The analysis of the organic carbon content and total nitrogen content allowed not only to distinguish this paleosurface but also to identify a deeper paleosurface within the FC profile 16/02. Within this profile, a peak of organic carbon in the deep horizon 3AB is found: this suggests the presence of a paleosurface at a depth of 151 cm.

Therefore, in the profile FC 16/02 it is possible to identify at least three superimposed pedological units: a deep, represented by the 3AB horizon, an intermediate, composed of 2AC and 2Btg horizons, and a superficial, composed of OB, ABt1, ABt2 and Bw horizons.
The anomalies in particle size distribution trend within the profiles FC 16/03, FC 16/04 and FC 16/05 were not attributed to the presence of paleosurfaces or true superimposed pedological units, since C organic peak and total N peak are not found along these profile. In the case of profiles FC 16/03 and FC 16/05, but also FC 16/06, the coarse granulometry of surface horizons could be related to the contribution of coarse material by the higher portion of the slope. This is not in contradiction with the geomorphological context in which the profiles are located, characterized by recurring colluvial phenomena (Panizza, et al., 1982; Compostella et al., 2014; Mariani, 2015).
Finally, in profile FC 16/04 the data of cored samples is difficult to interpret. The sampling modality does not allow to know the depth of origin of the material with absolute precision, and to operate a definite horizons distinction. This makes difficult to compare it with the top of the profile.
In conclusion, thanks to the chemical and physical analyses, different pedological units have been identified in three soil profiles; in particular, in the profiles FC16/01 and FC16/06 two different pedological units are found, while in the profile FC16/02 three different pedological units are found.

The micromorphological analysis allow us to better understand and characterize the above discussed pedological units and also to interpret their relationships.
In the profile FC16/01 also the micromorphological analysis highlights the presence of two distinct units: an older, which affects the deeper material (thin sections 86-96 cm, 41-51 cm and the lower part of 29 - 39 cm), and a superficial, placed on the material deposited above, observable in the upper portion of the thin section 29-39 cm. It is also noted that in the surface units claystones are more abundant while in the deeper one the sandstones are more common, indicating two different parent material. This difference in lithology has also been found in another profile near to the study area (Mariani, 2015).
Regarding the pedological features, Fe-Mn nodules, with blurred contour (redox figures), are present in all the thin section of the FC 16/01 profile, while clay coatings are found only in the deepest thin section (2Bt horizon, presence of clay accumulation for illuviation). In these horizons, the weathering is related to oxidative conditions and water infiltration, as is also evidenced by the tendency of the yellowish color of the ground mass, indicating the presence of goethite (Sauro et al., 2009; Stoops et al., 2010; Compostella et al., 2014; Mariani, 2015). The presence of clay illuviation requires alternating phases of water infiltration into soil and soil drying, in order to allow the clay transportation and deposition in the deep horizons (McCarthy et al., 1998; Stoops et al., 2010). Moreover, the formation of Fe-Mn nodules indicates that, at least for short periods, the soil is waterlogged (McCarthy et al., 1998; Stoops et al.,

2010). The gradual and irregular contours of the nodules test their "in situ" formation, and lead to the exclusion that they have been transported (Fedoroff et al., 1982).

To understand the development of this profile, it is important to interpret the different origins and distribution of aggregates. In the thin section FC 16/01 41-51 cm, the abundance of Fe-Mn nodules and the generally reddish color of the ground mass within blocky aggregates indicate a degree of weathering greater than granules: this has led to the interpretation of these compact aggregates as pedorelicts (sensu Brewer, 1976), or fragments of an older soil, restructured within more superficial horizons (Kemp, 1998; Nicosia, 2006; Rellini et al., 2007; Trombino, 2007; Sauro et al., 2009).

These fragments of paleosol, belonging to the 2AB2 horizon, have been eroded at higher portion of the slope and deposited within the upper BC horizon. As already mentioned, the 29-39 cm section covers the transition between the colluvial unit BC and the more superficial A2: therefore, it proves the contribution of new material, composed mainly of claystoned and pedorelicts (BC), on which the current pedogenesis are developing (A2). Previously micromorphological studies, carried out in the study area, have highlighted the presence of pedorelicts with similar characteristics within colluvial units (Compostella et al., 2014; Mariani, 2015).

In the profile FC16/02 the characteristics of the two observed sections seem to indicate that the past pedogenesis (2Btg horizon) was better developed than the present pedogenensis (ABt1). This is probably due to a greater intensity or duration of the process, or both. A similar result had already been obtained in previous studies, in which the most significant weathering of the M. Cusna paleosol was compared to the present soil (Compostella et al., 2014; Mariani, 2015).

Also in this profile, especially within the ABt1 horizon, there are rare blocky aggregates of fine material, also interpretable as pedorelicts (sensu Brewer, 1976). In fact, they are clearly distinguishable from the other aggregates present, and even these pedorelicts, as to those found in FC 16/01, have been interpreted as fragments of an ancient soil (fragments of internal crusts) eroded at higher portion of the slope and deposited within this horizon. Therefore, this material proves a colluvial phase preceding the formation of the ABt1 horizon, but subsequent to the development of the deep 2Btg horizon, which has not these aggregates.

The pedological features are analogous to those described for profile FC 16/01, and the same considerations are valid for their interpretation. They are more abundant and better developed in deep horizons (section 121-151 cm). In fact, clay coatings are clearly visible, and it is often possible to identify an orientation in the deposition of fine material due to the development of crescent morphology. This corroborate the hypothesis of material transport from more superficial horizons (McCarthy, 1998). Finally, it is the only section presenting the development of Fe-Mn hypocoatings due to the short periods

of waterlogging (McCarthy, 1998; Stoops et al., 2010). Hence, the finding of these pedological features testify the presence of clay illuviation and hydromoprphy (horizon 2Btg).

Hence, it was possible to correlate and characterize the different pedological units depending on the micromorphlogical characteristics.

The thin section FC 16/02 121-151 cm (2Btg) has very few analogies with the other observed thin sections, in fact it is characterized by the presence of well developed pedofeatures and by a vughs microstructure; then a correspondence between the horizon of this thin section and those observed in the other sections was not found. The characteristics of this thin section testify an evolved pedogenetic phase.

The thin sections FC 16/02 20-60 cm (ABt1) and FC 16/01 86-96 cm (2Bw-2Bt), although characterized by a different basic mineral component, are associated with the presence of well-developed pedofeatures of clay illuviation and the same type of aggregates. It has therefore been hypothesized that the two sections belong to horizons affected by the same pedogenesis on different parent materials, due to separate colluvial events, which may explain the differences between the two sections.

The thin sections FC 16/01 41-51 cm (2AB1-2AB2) and FC 16/05 21-31 cm (ABt1-ABt2) show similar aggregates and microstructure. Although in thin section FC 16/05 21-31 cm, there are textural pedological features, which are absent in thin section of profile FC 16/01, the FC 16/05 21-31 cm could be the result of the same pedogenetic processes that affected the 41-51 cm section of profile FC 16/01 on different parent materials. The different source material would therefore be the basis of the different development of the two horizons.

Finally, thin section FC 16/04 49-59 (ABt-AC), in the lower part looks like the section FC 16/01 86-96, while in the upper part seems, for what concern the color of the ground mass and the aggregates the sections FC 16/01 41-51 and FC 16/05 21-31. The presence of pedological features as Fe/Mn nodules and clay illuviation features testify the acting of the same pedogenetic processes of the thin sections FC 16/05 21-31 and those belongs to the profile FC 16/01. The differences found, especially with regard to aggregation and microstructure, may also be justified in this case, assuming the presence of different parent material.

Therefore, the micromorphological analysis allow to distinguish two different pedogenetic phases: the first is represented by the thin section FC 16/02 121-151 and the second is represented by the thin sections FC 16/01 41-51 cm (2AB1-2AB2), FC 16/05 21-31 cm (ABt1-ABt2), FC 16/04 49-59 (ABt-AC), FC 16/02 20-60 cm (ABt1) and FC 16/01 86-96 cm (2Bw-2Bt).

Moreover, further chemical analyses allow to better characterize the pedogenetic processes that characterized the studied profiles.

The analyzed samples have a C/N ratio typically less than 15, these values are related to the type of humus in formation: specifically, this is a mull, typical of acid soils with very low litter, characterized by limited or discontinuous vegetation cover (open deciduous forests and temperate grassland) (Duchaufour, 1983; Barratt, 1964, 1966). As expected, the C/N ratio tends to decrease along the profile, because of the decomposition and mineralization process of the organic matter (Duchaufour, 1983; Egli et al., 2009).

Although the geological substrate of the study area is characterized by the presence of limestones ("Argilliti variegate con calcari"), the soil has an acid pH, which tends to increase progressively moving close to the parent material, previous studies have shown the total absence of carbonates in Mt. Cusna's soils, even at outcrops of marls and limestones (Mariani, 2015). This suggests a strong control by pedogenetic processes in determining the chemical characteristics of the soil. In particular, soil acidity may be caused by the infiltration of water along the profile, causing gradual depletion in cationic form bases (Mariani, 2015; Van Breemen et al., 1983). Previous studies conducted on the paleosols of Mt. Cusna (Mariani, 2015) have shown that pH has a peak of acidity in the presence of buried paleosurfaces, this peak clearly indicates the transition between the colluvial unit and the buried unit. This peak is clearly visible within the FC 16/01 profile, where the 2AB1 horizon shows lower pH values of the above BC horizon.

The content of iron and aluminum oxides within the analyzed horizons shows a good correlation with what emerged in previous studies (Mariani, 2015). The content of crystalline iron oxides increase in the well developed horizons underlined the pedogenetical development. In the Bw horizons, of each profiles, the amorphous iron oxides prevail on crystalline iron oxides, in fact in these horizons, affected by brunification processes, the pedogenesis is not strongly expressed. Finally, although in the FC 16/02 2Btg horizon the iron crystalline oxides has not a low value, the iron activity index has a very low value caused by the illuviation of all amorphous iron oxides. The decrease of the Feo/Fed index within the more mature horizons (Bt, BC) is highlighted, and can be related to the greater alteration of the material and to the translocation of iron from the above horizons. Instead, the Bw horizons (except the FC 16/06 Bw) have a higher iron index value maybe due to a not well-expressed pedogenetic development, in fact these type of horizons are characterized by the development of structure and colour typical of brunification processes but maybe the processes are not so developed. The iron activity index can be used as measure of soil antiquity, indeed this ratio decrease with the soil maturity and alteration degree (Cremaschi & Rodolfi, 1991), hence in this study site the more developed horizons have a lower iron activity index. In particular, very low value are found in the FC 16/02 2AC and 2Btg horizons, which belong to the older paleosols where the pedogenesis was well developed than (FC 16/02 2Btg) the present pedogenensis (FC 16/02 ABt1). With respect to the Alo + ½ Feo index, the values obtained at

ABt2 and Bw horizons of FC 16/02 appear to indicate the presence in this profile of a weakly podzolization, or cryptopodzolization (Do Nascimento et al., 2008; Waroszewski et al., 2013, FAO, 2014), which proves what has already been highlighted in previous studies regarding the current soil of Monte Cusna (Mariani, 2015). This process would begin in the late Holocene, replacing the brunification, started since the end of the last glacial maximum (Mariani, 2015), and could have been favored by the development of low shrub vegetation dominated by *Vaccinium myrtillus* (Duchaufour, 1983; Chersich et al., 2007; Compostella et al., 2012; Mariani, 2015).

The cryptopodozolization trend is also underlined by the Rock-Eval data (fig.5.10). In particular, the O horizons are placed in the range of the box "Litters and Organic Horizons" while the other horizons show different trends (Sebag et al., 2016). The first group of horizons located in the upper part of the graph show an Inherited OM trend. In this group, we can found a lot of horizons belonging to buried paleosols and some well developed and deep horizons of present day soils. This results testify the presence of ancient soil with ancient organic matter. The second group still includes well developed soils and buried paleosols, and has a trend similar to the previous group. Finally the third group located in lower part of the graph show a Spodic trend (Sebag et al., 2016). In this group we found two horizons belonging to FC 16/01 paleosols and the horizons belonging to the superficial (i.e. not buried) soils which are in development now under a vegetation characterized by shrub (*Vaccinium myrtillus*). It should be stresses that in some cases, the parent material of these soils are the exhumed paleosol horizons.

The presence of this trend would strengthen our hypothesis of cryptopodzolization, identified by means of Fe and Al extractions and micromorphology observation.

The Rock-Eval data (fig. 5.11) also provide more information the organic matter maturity. In the HI/OI diagram the horizons are grouped by typology, in fact starting from the top left we find the O horizons, then the OA/A, the B and so on. Is also possible to notice how the horizons belong to the first paleosol (red dots, 2AB1, 2AB2 in fig. 11) are in the same group with the horizons of the soils now in development, while the other peleosols (older) are located at the bottom right.

The relationship between different units of different profiles has been studied with different approaches and in conclusion permit to identify three different units corresponding to three different pedogenetic phases:

- a very old one: observed for the first time exclusively in the FC 16/02 profile (2Btg horizon), which shows the characteristics of a brown soil affected by illuviation and hydromorphy;
- an intermediate one: previously observed in the area, characterized by the development of brown soil characterized by deciduous forest vegetation cover (FC 16/02 ABt1 and FC 16/01 2Bt); which has

probably affected different parent materials. Since FC 16/01 2Bt belongs to a buried paleosol, and FC 16/02 ABt1 is instead rather superficial, it is possible that, in the past, other material could be placed above the FC 16/02 current profile surface, and subsequently be removed from the erosion. Therefore, on the ancient pedogenesis, the current pedogenesis (cryptopodilization, Duchaufour, 1983) could be developed (surface units of the profiles FC 16/01 and FC 16/02). The upper unit of FC 16/02 could be defined as a polycyclic soil (Duchaufour, 1983). As evidenced by the little thickness of the upper unit, the development of current pedogenesis in FC 16/01 is probably too weak to leave traces of podzolization within the profile.

- a recent one, where pedogenesis is still not well evident. Based on micromoprhological evidence, horizons FC 16/01 2AB1-2AB2, FC 16/04 ABt-AC and FC 16/05 ABt1-ABt2 have similar weathering rates and can also be attributed to the same pedogenesis, developed on different parent materials. The FC 16/01 2AB1/2AB2 belong to buried paleososl, while the thin sections belong to profiles FC 16/04 and FC 16/05 belong to superficial horizons. Therefore, also in this case, the current pedogenesis may have been superimposed on the older one.

The same correlation was extended to the profiles FC 16/03 and FC 16/06, located at intermediate points of the study area, and characterized by the same vegetation cover (little shrubs of *Vaccinium myrtillus*). Also in the FC 16/03, FC 16/05 and FC 16/06, similar to FC 16/01, the podzolization process may be too weak to be signaled by the Alo + ½ Feo index.

Finally, the FC 16/04 profile is placed in a forest context incompatible with the development of podzols, but is a forest cover typical of a brown soil: here, in fact, despite the consistent thickness of the profile, the podzolization index did not give positive results.

The recent phase determines the development of different pedogenetic phases in relation to the vegetation cover: in the uppermost areas, with discontinuous vegetation cover (little shrub of *Vaccinium myrtillus*), the formation of cryptopodzolic soils is found, while at lower altitudes, with forested cover, brown soils, less developed than those previously described, are found.

Therefore, the evolution of the study area can be summarized as follows. The first, strongly expressed, pedogenetic phase led to the formation of a brown soil under forest vegetation cover, characterized by intense clay illuviation and hydromorphy, as evidenced by the pedogenic features observed in the thin section. This phase was interrupted by the contribution of colluvial material, mobilized upslope by the water runoff and deposited on the surface of the evolving soil. In this period, the area could not be covered by forest vegetation. This colluvial event provided a new parent material for soil development during the second phase. The pedological characteristics of the second phase indicate the presence of a stable forest cover, which has favored the formation of a brown soil. The soil of the second phase has

pedological features similar to the soil of the first phase but less developed. Therefore, the pedogenetic process is most probably the same (brunification), though less expressed. Afterward, a second colluvial event interrupted this pedogenetic phase. The material, eroded upstream and deposited in the study area, is mainly composed of claystones fragments and pedorelicts, i.e. fragments of the most superficial horizons of the brown paleosol, removed and restructured by the geomorphological processes. Starting from this new material, the actual pedogenesis has been developed, whose characteristics seem to suggest a change in vegetation compared to the previous two phases, in particular at higher altitude the presence of shrub as *Vaccinium myrtillus* promote the cryptopodilization processes.

From this reconstruction the central role of vegetation in guiding the pedological development in the area during the biostasy phases clearly emerges; while, during the phases of instability, characterized by the absence of vegetation cover, deposition of upslope mobilized material caused the interruption of pedogenesis. Locally, the geomorphologic evolution of the slope may have compromised the preservation of the soil, making the scenario even more complex. The finding of paleosol in superficial units testify the hypothesis of superimposing of the present pedogenesis on the ancient one resulting in the formation of polycyclic soils, located next to the soils composed of both the two distinct pedogenetic phases.

The presence of different parent materials is not necessarily the results of several colluvial events, which is difficult to imagine in such a limited area and giving the reduced distance between the studied profiles. It is also possible that the source material comes from a small number of colluvial events, and that it has undergone a differentiated deposition along the slope. In fact, the variable inclination of the slope and the presence of vegetation could have had a significant role on the differentiated deposition of colluvial material, both as a quantity and as composition. In addition, the presence of pedorelicts within the sections FC 16/01 29-39 cm and FC 16/02 20-60 cm seems to indicate that the colluvial material not only includes rock fragments but also fractions of paleosols eroded from soil at higher altitude and deposited in the study area.

Chapter 6

Final discussion and conclusions

This PhD thesis enhances the knowledges of the global change effect on the Alpine environment, analyzing biological and abiological responses to variations in climatic conditions in transitional environments (e.g., treeline ecotone, proglacial area). This project starts from the assumption that the climate plays an important role in every ecosystem, particularly in the mountain transitional environments, where meteorological factors, combined with severe morphological conditions, often show extreme behaviours.

In the first part of the study, the analysis of the treeline position, based on the identification of three main environmental factors (geomorphology, climate, and human impacts) influencing the treeline elevation, show that the treeline elevation in the Upper Valtellina region is primarily limited by geomorphological constraints. In fact, although altitudinal treelines are widely recognized as climatic boundaries, climatic parameters are not the only factor that influence the treeline position. The treeline altitude may be locally influenced by environmental factors, disturbances, and human activities.
Where treelines are limited by geomorphological constraints, these factors may be more important than climate in determining treeline elevation because they directly control tree establishment and growth. Clear evidence of the importance of geomorphological constraints can be found in areas marked by avalanche paths, drainage channels, scree, rock outcrops and rock faces, debris flow channels, and debris flow deposits. Despite rising air temperatures, these treelines are likely driven by the dynamics imposed by geomorphological constraints rather than climate. In particular, where geomorphological processes are dominant, it is their response to climatic triggers that will drive the possibility of tree establishment at any elevation. Treelines under geomorphic control are commonly found at lower elevations than climatic treelines.
Moreover, the analysis on geomorphological constraints reveals that different geomorphological processes and related landforms may have different impacts on the treeline dynamics. Mass movements and deposits due to gravitational processes are the most common in the Alpine environment. Therefore, instability phenomena and erosional and/or depositional processes related to gravity may be considered the most important controlling factors on the treeline position.

However, the main part of the study is focused on the site-scale response of transition environments to climate change. For each site, both the biotic component (i.e., vegetation) and the abiotic component

(i.e., soil and geomorphology) have been analyzed using different techniques based on different purposes.

In particular, where the treeline position is mainly influenced by climatic parameters (Mt. Confinale and Becca di Viou) the response of vegetation to climate change is testified by a treeline upward shift and by a different climate-growth response.

In fact, at Mt. Confinale the results show that the treeline elevation over time increased from 2505 m a.s.l. (period 1990–1999) to 2531 m a.s.l. (period 2000–2009) to 2545 m a.s.l. (in 2013). The altitudinal dynamics are also favoured by the presence of convex and well-exposed rock outcrops where geomorphic gravitational processes are less intense and sporadic, and by ecologic and microtopographic factors (e.g. Holtmeier, 2010). While, at Becca di Viou study site the analysis of the influence of temperature on tree-ring growth shows a decreasing importance of June monthly temperature and an increasing important of May monthly temperature on tree-ring growth. These results, in agreement of other studies attest an extension of the growing season in Europe due to the recent temperature increase.

Although the two study sites (Mt. Confinale and Becca di Viou) show clear vegetation responses to climate change, also the geomorphologic factor plays an important role. In both sites, the geomorphological processes and the slope dynamics influence the soil evolution, which, although showing a good degree of development, does not reach the characteristic of a typical forest soil, due to the instability of the slope. However, the presence of soil, although not particularly developed in the treeline ecotone, suggests that the colonization by the vegetation, favored by ecologic, microtopographic and microclimatic factors, is followed by the development of the soil. Which in turn favors a more active colonization that could lead to a more marked shift to higher altitude of the vegetation belt and the linked soil processes. In fact, a treeline and a consequent timberline upward shift could cause the advance at higher altitudes of the podsolization line, which is related to acidification by coniferous tree litter. The altitudinal rising of podzolization is an evidence of a current and also past global change. In the Becca di Viou study site the presence of “Ranker alpin” (Duchafour, 1995) paleosol in the treeline ecotone highlights that the timberline could reach higher altitude in the past, when the climate was warmer then present. In the same way, if the climate warming persist in the future, we will find the timberline and podsolization at higher altitude. Hence, the “soil memory” is useful not only to reconstruct the past environmental change but also to predict the future scenarios.

Even in the proglacial area of Forni glacier the responses to variations in climatic conditions are particularly evident, in fact in this area the widening of glaciers forelands, followed by ecesis and soil development, is noticeable. However, in this case, the time has a key role in soil development, indeed the soils show different development degree according to the moraines deposition year. All different

environmental components have a peculiar response to climate change with a specific reaction time: after deglaciation, the vegetation starts to colonize the proglacial area, inducing also chemical and physical soil properties transformations. The study of soil chronosequence developed on different regression moraines of Forni glacier allows to identify an age-related trend and better understand the first steps of soil development in the context of climate change responses.

In the other examined sites (Saint Nicolas and Mt. Cusna), contrary to what was presented before, the geomorphological processes and related landforms are the main factor influencing both soil and vegetation responses to climate change at the treeline ecotone.
In particular, at Saint Nicolas study site the colluvial events and the action of water driven processes prevent the vegetation colonization and the soil development. The water driven processes also provoke a soil erosion, as evidenced by the dendrogeomorphological analyses carried out on the exposed roots.
In addition, the presence and the magnitude of geomorphological processes are influenced by the human presence. The anthropic deforestation, carried out since the IV millennium BC on Mt. Fallère to use the area as alpine pasture, has in fact favored the instability of the slope and the soil erosion.
Hence, in Saint Nicolas study site the environmental response to climatic changes is masked to the presence of geomorphological processes.
Also in the Mt. Cusna study area the role of geomorphological factor is evident, but the different environmental conditions of this area may modify the vegetation and soil responses to geomorphological factor. In fact, the Mt. Cusna is the only examined area located in the Apennine and characterized by sedimentary parent material. These two conditions may have favoured the alternation of resistasy phases and biostasy one, which are less common in alpine environments characterized by stronger slope and harsher climatic conditions. Moreover, the central role of vegetation in guiding the pedological development in the area during the biostasy phases clearly emerges; while, during the phases of instability, characterized by the absence of vegetation cover, deposition of upslope mobilized material caused the interruption of pedogenesis. The traces of different phases are recorded in soil as paleosols. The study of paleosols allows to reconstruct the past environmental conditions and understand the evolution of the area. Locally, the geomorphologic evolution of the slope may have compromised the preservation of the soil and the water driven processes bring to light the paleosols.

In the present study, the use of a multidisciplinary approach was crucial in order to make a more complete reconstruction of the environmental changes at the treeline. The use of routine laboratory soil analyses (C organic, total N and pH) beyond to permit soil characterization, provided useful information for the reconstruction of colluvial events and the identification of paleosurfaces. The study of Fe and Al oxides,

and the derived indeces, highlighted the presence in some profiles of processes such as “podzolization”. In the area of Mt. Cusna, the soil processes and the degree of soil development reconstruction, as well as the study of paleosols, have been possible thanks to the micromorphological approach. While the most innovative techniques (Rock-Eval pyrolisis), analyzing the maturity of the organic matter, have allowed to highlight trends in soil development and, in addition to the stable isotope analyses, to support the hypothesis of the presence of buried pedological units. Lastly, dendrochronological and dendroclimatic analyses have allowed to understand the trees responses to climate change, while in dendrogeomorphologic analyses the trees have been revealed to be a useful instrument for detecting the soil erosion.

The multidisciplinary approach used in the present PhD project clarifies some common traits: first of all, the geomorphological processes and related landforms are the most important factor influencing the treeline position. However, in the areas dominated by a climatic constraint (i.e., Mt. Confinale, Progracial area of the Forni glacier and Becca di Viou) an upward shift of vegetation belt, together with related soil types, has been identified. On the contrary, in the areas with geomorphological constraints (i.e., Saint Nicolas and Mt. Cusna) the vegetation and soil responses to climate change are rather masked by the effects of geomorphological processes.

In conclusion, the study underlines that the comprehension of the response of sensitive environment to climate change requires a particular knowledge of all the biotic and abiotic elements and of the interactions occurring among these.

Hence, the soil may play a key role in the study of the response of sensitive environments to climate change, in fact its formation and developments are closely linked to important environmental parameters as climate, organic activity (e.g., vegetation, human impact), relief, parent material, time (Jenny, 1941).

Chapter 7

References

Alestalo J. (1971). Dendrochronological interpretation of geomorphic processes. Fennia, 105, 1-139.

Akhalkatsi M., Abdaladze O., Nakhutsrishvili G. & Smith W. K. (2006). Facilitation of seedling microsites by Rhododendron caucasicum extends the Betula litwinowii alpine treeline, Caucasus Mountains, Republic of Georgia. Arctic, Antarctic and Alpine Research, 38, 481–488.

Anderson R. S., Jiménez-Moreno G., Carrión J. S. & Pérez–Martínez C. (2011). Postglacial history of alpine vegetation, fire, and climate from Laguna de Río Seco, Sierra Nevada, southern Spain. Quaternary Science Reviews, 30, 1615–1629.

Andreis C., Armiraglio S., Caccianiga M. & Cerabolini B. (2009), La vegetazione forestale dell'ordine Piceetalia excelsae Pawl. in Pawl. et al. 1928 nelle Alpi Lombarde. Fitosociologia, 46(1), 49-74.

Angelucci D., Cremaschi M., Negrino F. & Pelfini M. (1993). Il sito mesolitico di Dosso Gavia - Val di Gavia (Sondrio - Italia): evoluzione ambientale e popolamento umano durante l'Olocene antico nelle Alpi Centrali. Preistoria Alpina, Museo Tridentino di Scienze Naturali, 28, 19-32.

Arduino E., Barberis E., Carraro F. & Forno M.G. (1984). Estimating relative ages from iron-oxide/total-iron ratios of soils in the Western Po valley, Italy. Geoderma, 33, 39-52.

Astori C., Ciavatta C., Satanassi A. & Sequi P. (1994). Carbonio Organico. In: Metodi ufficiali di analisi chimica del suolo. Ministero delle Risorse Agricole Alimentari e Osservatorio Nazionale Pedologico per la Qualità del Suolo, Roma.

Atkinson D. (2004). Weathering, slopes and landforms. Hodder & Stoughton, London, 55-78

Auer I., Böhm R., Jurkovic A., Lipa W., Orlik A., Potzmann R. & Nieplova E. (2007). HISTALP – historical instrumental climatological surface time series of the Greater Alpine Region. International Journal of Climatology, 27, 17–46.

Avery B.W. & Bascomb C.L. (1974). Soil Survey Laboratory Methods. Soil Survey Technical Monograph, 6, Harpenden.

Azzoni R. S., Senese A., Zerboni A., Maugeri M., Smiraglia C. & Diolaiuti G. A. (2014). A novel integrated method to describe dust and fine supraglacial debris and their effects on ice albedo: the case study of Forni Glacier, Italian Alps, The Cryosphere Discuss., 8, 3171–3206, doi:10.5194/tcd-8-3171-2014, 2014.

Balesdent, J., Girardin, C., & Mariotti, A. (1993). Site-Related^(13) C of Tree Leaves and Soil Organic Matter in a Temperate Forest. Ecology, 74(6), 1713-1721.

Balestrieri M.L., Bernet M., Brandon M.T., Picotti V., Reiners P. & Zattin M. (2003). Pliocene and Pleistocene exhumation and uplift of two key areas of the Northern Apennines. Quaternary International, 101-102, 67–73.

Ballesteros-Cánovas J. A., Bodoque J. M., Lucía A., Martín-Duque J. F., Díez-Herrero A., Ruiz-Villanueva V., Rubiales J.M. & Genova M. (2013). Dendrogeomorphology in badlands: methods, case studies and prospects.Catena, 106, pp 113-122.

Barker G. (1985). Prehistoric farming in Europe. CUP Archive.

Barratt B.C. (1964). A classification of humus forms and micro-fabrics of temperate grasslands. European Journal of Soil Science, 15 (2), 342-356.

Barratt B.C. (1966). Factors of mull and mor development in temperate grasslands. Proceedings (New Zealand Ecological Society), 13 (13), 24-29.

Bartolini C., Bernini M., Carloni G.C., Costantini A., Federici P.R., Gasperi G., Lazzarotto A., Marchetti G., Mazzanti R., Papani G., Pranzini G., Rau A., Sandrelli F., Vercesi P.L., Castaldini D. & Francavilla F. (1982). Carta neotettonica dell'Appennino Settentrionale. Note illustrative. 101, 523–549.

Bascomb C. L. (1968). Distribution of pyrophosphate-extractable iron and organic carbon in soils of various groups. European Journal of Soil Science, 19(2), 251-268.

Bellotti B., D'Orefice M. & Graciotti R. (1995). Saggio di rilevamento geomorfologico in Alta Valtellina (Vedretta de' Piazzi): esempio di applicazione della normativa per la Carta geomorfologica d'Italia in scala 1:50000. Bollettino del Servizio Geologico d'Italia, 114, 3-26.

Beniston M. (2006). Mountain weather and climate: A general overview and a focus on climatic change in the Alps. Hydrobiologia, 562, 3–16.

Bertolani Marchetti D., Dallai D., Mori Secci M. & Trevisan Grandi G. (1994). Palynological evidence and forest events in the upper Tuscan/Emilian Apennines in the context of the whole Apennines Holocene history. Fisotociologia, 26, 145-164.

Beckage B., Osborne B., Gavin D. G., Pucko C., Siccama T. & Perkins T. (2008). A rapid upward shift of a forest ecotone during 40 years of warming in the Green Mountains of Vermont. Proceedings of the National Academy of Sciences, 105, 4197–4202.

Biondi F. & Waikul K. (2004). Dendroclim 2002: a C++ program for statistical calibration of climate signals in tree-ring chronologies. Computers and Geosciences 30, 303–311.

Boccaletti M., Elter P. & Guazzone G. (1971). Plate tectonic model for the development of the Western Alps and Northern Apennines. Nature, 234, 108–110.

Bodoque J. M., Ballesteros-Cánovas J. A., Lucía A., Díez-Herrero A. & Martín-Duque J. F. (2015). Source of error and uncertainty in sheet erosion rates estimated from dendrogeomorphology. Earth Surface Processes and Landforms, 40, 1146-1157.

Bodoque J.M., Lucía A., Ballesteros J.A., Martín-Duque J.F., Rubiales J.M. & Genova M. (2011). Measuring medium-term sheet erosion in gullies from trees: a case study using dendrogeomorphological analysis of exposed pine roots in central Iberia. Geomorphology 134, 417–425.

Bollati I., Della Seta M., Pelfini M., Del Monte M., Fredi P. & Lupia Palmieri E. (2012). Dendrochronological and geomorphological investigations to assess water erosion and mass wasting processes in the Apennines of Southern Tuscany (Italy). Catena, 90, 1–17.

Bollati I., Reynard E., Lupia Palmieri E. & Pelfini M. (2016). Runoff Impact on Active Geomorphosites in Unconsolidated Substrate. A Comparison Between Landforms in Glacial and Marine Clay Sediments: Two Case Studies from the Swiss Alps and the Italian Apennines. Geoheritage DOI 10.1007/s12371-015-0161-0

Bonetti A. (2013). Ritiro glaciale recente ed ecesi nella valle dei Forni (Valtellina, SO): analisi dendroglaciologiche e gis. Unpublished master degree thesis, University of Milan.

Bonsignore G., Borgo A., Gelati R., Montrasio A., Potenza R., Pozzi R., Ragni U. & Schiavianto G. (1969). Note illustrative della Carta Geologica d'Italia alla scala 1 :100000 : Foglio 8 – Bormio. Serv. Geol. d'It, 123p.

Bonsignore G., Bravi C.E., Nangeroni G. & Ragni U. (1970). La geologia del territorio della provincia di Sondrio, con carta geologica 1:200000. Ed. Amministr. Prov. Sondrio.

Bortolotti V. (1992), Guide Geologiche Regionali: Appennino Tosco-Emiliano. Società Geologica Italiana. BE-MA Editrice, Milano.

Brewer R. (1976). Fabric and Mineral Analysis of Soils. Huntington, NY: Krieger

Briffa K. R., Shishov V. V., Melvin T. M., Vaganov E. A., Grudd H., Hantemirov R. M. & Naurzbaev M. M. (2008). Trends in recent temperature and radial tree growth spanning 2000 years across northwest Eurasia. Philosophical Transactions of the Royal Society B-Biological Sciences, 363, 2271–2284.

Burga C. A. (1999). Vegetation development on the glacier forefield Morteratsch (Switzerland). Applied Vegetation Science, 2(1), 17-24.

Burga C. A. (1991). Vegetation history and palaeoclimatology of the Middle Holocene: Pollen analysis of alpine peat bog sediments, covered formerly by the Rutor Glacier, 2510 m (Aosta Valley, Italy). Global Ecology and Biogeography Letters, 1, 43–150.

Burga C. A., Frauenfelder R., Ruffet J., Hoelzle M. & Kääb A. (2004). Vegetation on Alpine rock glacier surfaces: a contribution to abundance and dynamics on extreme plant habitats. Flora-Morphology, Distribution, Functional Ecology of Plants, 199(6), 505-515.

Burga C. A., Krüsi B., Egli M., Wernli M., Elsener S., Ziefle M., Fischer T. & Mavris C. (2010). Plant succession and soil development on the foreland of the Morteratsch glacier (Pontresina, Switzerland): Straight forward or chaotic?. Flora (2010) 205(9), pp 561-576.

Butler D. R. & Walsh S. J. (1994). Site characteristics of debris flows and their relationship to alpine treeline. Physical Geography, 15, 181–199.

Butler D. R., Malanson G. P., Bekker M. F. & Resler L. M. (2003). Lithologic, structural, and geomorphic controls on ribbon forest patterns in a glaciated mountain environment. Geomorphology, 55, 203–217.

Butler D. R., Malanson G. P., Resler L. M., Walsh S. J., Wilkerson F. D., Schmid G. L. & Sawyer C. F. (2009). Geomorphic patterns and processes at alpine treeline. Developments in Earth Surface Processes, 12, 63-84.

Butler D. R., Malanson G. P., Walsh S. J. & Fagre D. B. (2007). Influences of geomorphology and geology on alpine treeline in the American west—more important than climatic influences?. Physical Geography, 28(5), 434-450.

Caccianiga M., Andreis C., Armiraglio S., Leonelli G., Pelfini M. & Sala D. (2008). Climate continentality and treeline species distribution in the Alps. Plant Biosystems, 142 (1), 66 – 78.

Carlini M., Artoni A., Aldega L., Balestrieri M.L., Corrado S., Vescovi P., Bernini M. & Torelli L. (2013). Exhumation and reshaping of far-travelled/allochthonous tectonic units in mountain belts. New insights for the relationships between shortening and coeval extension in the western Northern Apennines (Italy). Tectonophysics, 608, 267–287.

Carnelli A. L., Theurillat J. P., Thinon M., Vadi G. & Talon B. (2004). Past uppermost tree limit in the Central European Alps (Switzerland) based on soil and soil charcoal. *The Holocene*, *14*(3), 393-405.

Carrer M. & Urbinati C. (2006). Long-term change in the sensitivity of tree-ring growth to climate forcing in Larix decidua. New Phytologist 1 (70), 861–872.

Case B. S. & Duncan R. P. (2014). A novel framework for disentangling the scale-dependent influences of abiotic factors on alpine treeline position. Ecography, 37, 838–851.

Castelletti L., Cremaschi M. & Notini P. (1976), L'insediamento di Lama Lite sull'Appennino Tosco-Emiliano. Preistoria Alpina, Museo Tridentino di Scienze Naturali, 12, 7-32.

Catoni M., D'Amico M. E., Zanini E. & Bonifacio E. (2016). Effect of pedogenic processes and formation factors on organic matter stabilization in alpine forest soils. Geoderma, 263, 151-160.

Cattaneo A. (2014). I geomorfositi attivi nel catalogo nazionale dei geositi. Analisi di geomorfositi italiani in differenti contesti morfoclimatici con strumenti open source. Unpublished master degree thesis, University of Milan.

Cavallin A., Baroni C., Bini A., Carton A., Marchetti M., Orombelli G., Pelfini M. & Zanchi A. (1997). Geomorphology of the central and southern Alps (Fourth international conference on geomorphology, guide for the excursion). Suppl. Geogr. Fis. Dinam. Quat., III, T. 2 (1997), 13-47.

Centro Funzionale della Valle d'Aosta (2017). http://cf.regione.vda.it/.

Chauchard S., Beilhe F., Denis N. & Carcaillet C. (2010). An increase in the upper tree-limit of silver fir (Abiesalba Mill.) in the Alps since the mid-20th century: A land-use change phenomenon. Forest Ecology and Management, 259(8), 1406-1415.

Chauchard S., Carcaillet C. & Guibal F. (2007). Patterns of land-use abandonment control tree-recruitment and forest dynamics in Mediterranean mountains. Ecosystems, 10(6), 936-948.

Chersich S., Galvan P., Frizzera L. & Scattolin L. (2007). Variabilità delle forme di humus in due siti campione di pecceta altimontana trentina. Forest@-Journal of Silviculture and Forest Ecology, 4 (2), 220-226.

Clague J. J., Wolhfarth B., Ayotte J., Eriksson M., Hutchinson I., Mathewes R. W. & Walker L. (2004). Late Holocene environmental change at treeline in the northern Coast Mountains, British Columbia, Canada. Quaternary Science Reviews, 23, 2413–2431.

Clemenzi L., Molli G., Storti F., Muchez P., Swennen R & Torelli L. (2014). Extensional deformation structures within a convergent orogen: The Val di Lima low-angle normal fault system (Northern Apennines, Italy). J. Structural Geology 66, 205-222.

Compostella C. (2011). Paleosuoli ed altri archivi paleoambientali per la ricostruzione delle fluttuazioni oloceniche della treeline alpina e appenninica. Phd Thesis, University of Milan.

Compostella C., Mariani G.S. & Trombino L. (2014), Holocene environmental history at the treeline in the Northern Apennines, Italy: A micromorphological approach. The Holocene, 24(4), 393–404.

Compostella C., Trombino L. & Caccianiga M. (2013). Late Holocene soil evolution and treeline fluctuations in the Northern Apennines. Quaternary International, 289, 46–59.

Cook E.R. & Briffa K.R. (1990). A comparison of some tree-ring standardization methods. In: Cook, E.R., Kairiukstis, L.A. (Eds.), Methods of Dendrochronology. Kluwer, Dordrecht, pp. 104–123.

Cook E.R., Briffa K.R., Shiyatov S. & Mazepa V. (1990). Tree-ring standardization and growth-trend estimation. In: Cook ER, Kairiukstis LA (eds) Methods of dendrochronology. Applications in the environmental sciences. Kluwer, Boston, pp 104–123.

Coppola A., Leonelli G., Salvatore M. C., Pelfini M, & Baroni C. (2012). Weakening climatic signal since mid-20th century in European larch tree-ring chronologies at different altitudes from the Adamello-Presanella Massif (Italian Alps). Quaternary research, 77(3), 344-354.

Cremaschi M. (2000). Manuale di geoarcheologia. Laterza.

Cremaschi M. & Rodolfi G. (1991). Il suolo - Pedologia nelle scienze della Terra e nella valutazione del territorio. La Nuova Italia Scientifica, Roma.

Cremaschi M., Biagi P., Accorsi C.A., Bandini Mazzanti M., Rodolfi G., Castelletti L. & Leoni L. (1984). Il sito mesolitico di Monte Bagioletto (Appennino Reggiano) nel quadro delle variazioni ambientali oloceniche dell'Appennino Tosco-Emiliano. Emilia Preromana, 9/10, 11-46.

Cunill R., Soriano J. M., Bal M. C., Pèlachs A., Rodriguez J. M. & Pérez-Obiol R. (2013). Holocene high altitude vegetation dynamics in the Pyrenees: A pedoanthracology contribution to an interdisciplinary approach. Quaternary International, 289, 60–70.

D'Agata C., Bocchiola D., Maragno D., Smiraglia C. & Diolaiuti G. (2014): Glacier shrinkage driven by climate change in The Ortles-Cevedale group (Stelvio National Park, Lombardy, Italian Alps) during half a century (1954–2007), Theor. Appl. Climatol., 116, 169–190, 2014.

D'Amico M. E., Calabrese F. & Previtali F. (2009). Suoli di alta quota ed ecologia del Parco Naturale del Mont Avic (Valle d'Aosta). Studi Trentini di Scienze Naturali, 85, 23-37.

D'Amico M. E., Freppaz M., Leonelli G., Bonifacio E. & Zanini E. (2015). Early stages of soil development on serpentinite: the proglacial area of the Verra Grande Glacier, Western Italian Alps. Journal of Soils and Sediments, 15(6), 1292-1310.

Dal Piaz G.V. (ed.) (1992). Le Alpi dal Monte Bianco al Lago Maggiore. Guide Geologiche Regionali, 3 (1): pp. 311, 3 (2): pp. 209, Società Geologica Italiana, BE.MA, Milano

Dal Piaz G. V., Bistacchi A. & Massironi M. (2003). Geological outline of the Alps. Episodes, 26(3), 175-180.

Dal Piaz G. V., Gianotti F., Monopoli B., Pennacchioni G., Tartarotti P. & Schiavo A. (2010). Note illustrative della Carta Geologica d'Italia alla scala 1: 50.000, Foglio 091 Chatillon. Servizio Geologico d'Italia, Foglio, 91, 5-152.

De Giusti F., Dal Piaz G. V., Massironi M. & Schiavo A. (2003). Carta geotettonica della Valle d'Aosta. Memorie di Scienze Geologiche, 55, 129-49.

Derbyshire E., Gregory K. J. & Hails J. R. (1979). Patterns of process. In E. Derbyshire, K. J. Gregory, J. R. Hails, & K. J. Gregory (Eds.), Geomorphological processes: Studies in physical geography (pp.89–104). Folkestone, Kent (UK): Dawson Publishing.

Diolaiuti G. & Smiraglia C. (2010). Changing glaciers in a changing climate: how vanishing geomorphosites have been driving deep changes in mountain landscapes and environments, Géomorphologie, 2, 131–152, 2010.

Diolaiuti G., Bocchiola D., D'Agata C. & Smiraglia C. (2012): Evidence of climate change impact upon glaciers' recession within the Italian Alps: the case of Lombardy glaciers, Theor. Appl. Climatol., 109, 429–445, doi:10.1007/s00704-012-0589-y, 2012.

Disnar J. R., Guillet B., Kéravis D., Di-Giovanni C. & Sebag D. (2003). Soil organic matter (SOM) characterization by Rock-Eval pyrolysis: scope and limitations. Organic geochemistry, 34(3), 327-343.

Do Nascimento N. R., Fritsch E., Bueno G. T., Bardy M., Grimaldi C. & Melfi A. J. (2008). Podzolization as a deferralitization process: dynamics and chemistry of ground and surface waters in an Acrisol–Podzol sequence of the upper Amazon Basin. European Journal of Soil Science, 59(5), 911-924.

Dyurgerov M.B. & Meier M.F. (2000). Twentieth Century Climate Change: Evidence from Small Glaciers. Proceedings of the National Academy of Sciences, 97, 1406-1411.

Duchaufour P. (1983). Pedologie 1: Pedogenese et classification, Masson, Paris.

Duchaufour P. (1995). Pedology. Soil, vegetation, environment. Pedology. Soil, vegetation, environment., (Ed. 4).

Egli M., Fitze P. & Mirabella A. (2001).Weathering and evolution of soils formed on granitic, glacial deposits: results from chronosequences of Swiss alpine environments. Catena 45, 19–47.

Egli M., Sartori G., Mirabella A., Favilli F., Giaccai D. & Delbos E. (2009). Effect of north and south exposure on organic matter in high Alpine soils. Geoderma, 149 (1), 124-136.

Egli M., Wernli M., Kneisel C. & Haeberli W. (2006). Melting glaciers and soil development in the proglacial area Morteratsch (Swiss Alps): I. Soil type chronosequence. Arctic, Antarctic, and Alpine Research, 38(4), 499-509.

Ellenberg, H. (1963). Vegetation Mitteleuropas mit den Alpen: in kausaler, dynamischer und historischer Sicht [Vegetation of Central Europe with the Alps: In a more causal, dynamic and historical view]. Stuttgart: Ulmer.

Elliott G. P. & Kipfmueller K. F. (2010). Multi–scale influences of slope aspect and spatial pattern on ecotonal dynamics at upper treeline in the Southern Rocky Mountains, U.S.A. Arctic, Antarctic & Alpine Research, 42, 45–56.

Elter G. (1960). La Zona Pennidica dell'alta e media Valle d'Aosta e le unita limitrofe.

ERSAF, Ente Regionale per i Servizi all'agricoltura e alle Foreste (2012). Map available at: http://www.geoportale.regione.lombardia.it/.

Evans S. G. & Clague J. J. (1994). Recent climatic change and catastrophic geomorphic processes in mountain environments. Geomorphology, 10(1), 107-128.

Fellin M.G., Reiners P.W., Brandon M.T., Wüthrich E., Balestrieri M.L. & Molli G. (2007). Thermochronologic evidence for the exhumational history of the Alpi Apuane metamorphic core complex, northern Apennines, Italy. Tectonics 26, doi:10.1029/2006TC002085.

Fedele F. (1981). Il popolamento delle Alpi nel Paleolitico. Le Scienze, 27(160), 22-39.

Fedele F. (1990). Terminal Palaeolithic hunters within the Alps. Discoveries near the Splugen Pass, Italy. In: Moe D, Hicks S (eds), Impact of prehistoric and medieval man on the vegetation: man at the forest limit. Pact, 31, 81-85.

Fedoroff N. & Goldberg P. (1982). Comparative micromorphology of two late Pleistocene paleosols (in the Paris Basin). Catena, 9, 227-251.

Filippi M.L., Heiri O., Arpenti E., Angeli N., Bortolotti M., Lotter A.F. & Van der Borg K. (2005). Studio paleolimnologico del Lago Nero di Cornisello (Parco Naturale Adamello-Brenta, Trentino). Studi Trent Sci Nat, Acta Geol, 82, 261-278.

Food and Agriculture Organization (FAO) (2014). World reference base for soil resource 2014. International soil classification system for naming soils and creating legends for soil maps. World Soil Resources Reports. N°106. FAO, Rome.

Forno M. G., Comina C., Gattiglio M., Gianotti F., Lo Russo S., Raiteri L., Sambuelli L., Taddia G. (2016). Preservation of quaternary sediments in DSGSD environments: The Mont Fallère case study (Aosta Valley, NW Italy). Alpine and Mediterranean Quaternary, 29 (2), 2016, 1 - 11

Forno M. G., Gattiglio M. & Gianotti F. (2012). Geological context of the Becca France historical landslide (Aosta Valley, NW Italy) Alpine and Mediterranean Quaternary, 25 (2), 125-140.

Forno M. G., Gattiglio M., Gianotti F., Guerreschi A. & Raiteri L. (2013). Deep-seated gravitational slope deformations as possible suitable locations for prehistoric human settlements: An example from the Italian Western Alps. Quaternary international, 303, 180-190.

Fritts H. C. (1976). Tree rings and climate, 567 pp. Academic, San Diego, Calif.

Frezzotti M. & Orombelli G. (2014). Glaciers and ice sheets: current status and trends. Rendiconti Lincei, 25 (1), 59-70.

Gale S.J. & Hoare P.G. (1991). Quaternary Sediments. Belhaven Press, London.

Garavaglia V., Diolaiuti G., Smiraglia C., Pasquale V. & Pelfini M. (2012). Evaluating tourist perception of environmental changes as a contribution to managing natural resources in glacierized areas: A case study of the Forni Glacier (Stelvio National Park, Italian Alps). Environmental management, 50(6), 1125-1138.

Garavaglia V., Pelfini M. & Bollati I. (2010). The influence of climate change on geodiversity: the case of two italian glacial geomorphosites investigated through dendrochronology - Influence du changement climatique sur la géodiversité: l'example de deux géomorphosites glaciales italiens enquêtés avec la dendrocronologie. Géomorphologie: relief, processus, environment, 2, 153-164

Gärtner H. (2007).Tree roots — methodological review and new development in dating and quantifying erosive processes. Geomorphology,86, 243–251.

Gehrig–Fasel J., Guisan A. & Zimmerman N.E. (2007). Treeline shifts in the Swiss Alps: climate change or land abandonment?. Journal of Vegetation Science, 18, 571–582.

Gehrig-Fasel J., Guisan A. & Zimmermann N. E. (2008). Evaluating thermal treeline indicators based on air and soil temperature using an air-to-soil temperature transfer model. Ecological modelling, 213(3), 345-355.

Geoportale Nazionale (2013). Carta Ecopedologica d'Italia 1:250000. Servizi WMS, http://wms.pcn.minambiente.it/ogc?map=/ms_ogc/WMS_v1.3/Vettoriali/Carta_ecopedologica.map.

Geoportale della Valle d'Aosta (2013). Forestazione – Foreste di protezione. http://geonavsct.partout.it/pub/GeoForeste/index.html?funzione=GF_PROTE

Gianotti F., Forno M.G., Ivy-Ochs S. & Kubik P.W. (2008). New chronological and stratigraphical data on the Ivrea Amphitheatre (Piedmont, NW Italy). Quaternary International, 190, 123-135.

Giordano A. (1999). Pedologia. Edizioni UTET, Torino.

Gobet E., Tinner W., Hochuli P.A., van Leeuwen J.F.N. & Ammann B. (2003). Middle to Late Holocene vegetation history of the Upper Engadine (Swiss Alps): the role of man and fire. Veget Hist Archaeobot, 12,143-163.

Grafius D. R., Malanson G. P. & Weiss D. (2012). Secondary controls of alpine treeline elevations in the Western USA. Physical Geography, 33, 146–164.

Grissino-Mayer H.D. (2001). Evaluating crossdating accuracy: A manual and tutorial for the computer program COFECHA. Tree-Ring Research 57(2):205-221.

Guida D., Pelfini M. & Santilli M. (2008). Geomorphological and dendrochronological analyses of a complex landslide in the Southern Apennines. Geografiska Annaler A 90 (3), 211–226.

Haeberli W., Wegmann M. & Vonder Muhll D. (1997). Slope stability problems related to glacier shrinkage and permafrost degradation in the Alps. Eclogae Geologicae Helvetiae, 90 (3), 407-414.

Halpin P. N. (1994). Latitudinal variation in the potential response of mountain ecosystems to climatic change. In Mountain environments in changing climates, ed. M. Beniston, 180-203. London: Routledge Publishing Co.

Helama S., Seppä H., Birks H. J. B. & Bjune A. E. (2010). Reconciling pollen-stratigraphical and tree-ring evidence for high- and low-frequency temperature variability in the past millennium. Quaternary Science Reviews, 29, 3905–3918.

Hofgaard A., Tardif J. & Bergeron Y. (1999). Dendroclimatic response of Picea mariana and Pinus banksiana along a latitudinal gradient in the eastern Canadian boreal forest. Can J For Res 29:1333–1346

Holmes R.L., Adams R.K. & Fritts H.C. (1986). Tree-ring chronologies of North America: California, Eastern Oregon and Northern Great Basin with procedures used in the chronology development work including user manual for computer program COFECHA and ARSTAN. Chronology Series VI. University of Arizona, Laboratory of Tree-Ring Research, Tucson, USA.

Holtmeier F. K. (2010). Mountain timberlines: Ecology, patchiness, and dynamics. New York, NY: Springer Science.

Holtmeier F. K. & Broll G. (2005). Sensitivity and response of northern hemisphere altitudinal and polar treelines to environmental change at landscape and local scales. Global ecology and Biogeography, 14(5), 395-410.

Holtmeier F. K. & Broll G. (2007). Treeline advance–driving processes and adverse factors. Landscape Online, 1, 1-33.

Holtmeier F. K. & Broll G. (2012). Landform influences on treeline patchiness and dynamics in a changing climate. Physical Geography, 33(5), 403-437.

Hughes N. M., Johnson D. M., Akhalkatsi M. & Abdaladze O. (2009). Characterizing Betula litwinowii seedling microsites at the alpine–treeline ecotone, Central Greater Caucasus Mountains, Georgia. Arctic, Antarctic and Alpine Research, 41, 112–118.

Hupp C. & Carey W.P. (1990). Dendrogeomorphic approach to estimating slope retreat. Maxey Flats, Kentucky. Geology 18 (7), 658–661.

Jenny H. (1941). Factors of soil formation: a system of quantitative pedology. McGraw-Hill book company inc., New York.

Kabala C. & Zapart J. (2012). Initial soil development and carbon accumulation on moraines of the rapidly retreating Werenskiold Glacier, SW Spitsbergen, Svalbard archipelago. Geoderma, 175, 9-20.

Kemp R.A. (1998). Role of Micromorphology in paleopedological research. Quaternary International 51-52, 133-141.

Kligfield R. (1979). The Northern Apennines as a collisional orogen. American Journal of Science, 279, 676–691.

Klasner F. L. (2002). A half century of change in alpine treeline patterns at Glacier National Park, Montana, USA. Arctic, Antarctic, and Alpine Research, 34, 49–56.

Körner C. (1999). Alpine Plant Life. Springer, Berlin.

Körner C. (2002). Mountain biodiversity, its causes and function: An overview. In C. Körner & E. M. Spehn (Eds.), Mountain biodiversity: A global assessment (pp. 3–20). London: Parthenon Publishing.

Körner C. (2003). Alpine plant life: functional plant ecology of high mountain ecosystem. Springer Science & Business Media.

Körner C. (2012). Alpine treelines: functional ecology of the global high elevation tree limits. Springer Science & Business Media.

Körner C. & Paulsen J. (2004). A world-wide study of high altitude treeline temperatures. Journal of Biogeography, 31(5), 713-732.

Krasilnikov P. & Calderón N. E. G. (2006). A WRB-based buried paleosol classification. Quaternary International, 156, 176-188.

Kubiëna W.L. (1953). Bestimmungsbuch und Systematik der Böden Europas. F. Enke Verlag, Stuttgart.

Küfmann C. (2003). Soil types and eolian dust in high-mountainous karst of the Northern Calcareous Alps (Zugspitzplatt, Wetterstein Mountains, Germany). Catena, 53(3), 211-227.

Kullman L. (2001). 20th century climate warming and tree-limit rise in the southern Scandes of Sweden. Ambio, 30, 72–80.

Kullman L. (2002). Rapid recent range-margin rise of tree and shrub species in the Swedish Scandes Journal of Ecology, 90, 68–77.

Kullman L. & Öberg L. (2009). Post-Little Ice Age tree line rise and climate warming in the Swedish Scandes: A landscape ecological perspective. Journal of Ecology, 97, 415–429.

Leonelli G., Masseroli A. & Pelfini M. (2016). The influence of topographic variables on treeline trees under different environmental conditions. Physical Geography, 37(1), 56-72.

Leonelli G., Pelfini M. & Morra di Cella U. (2009a). Detecting climatic treelines in Italian Alps: the influence of geomorphological factors and human impacts. Physical Geography, 30(4), 338– 352.

Leonelli G., Pelfini M., Battipaglia G. & Cherubini P. (2009b). Site-aspect influence on climate sensitivity over time of a high-altitude Pinus cembra tree-ring network. Climatic Change 96, 185–201. doi:10.1007/s10584-009-9574-6.

Leonelli G., Pelfini M., Morra di Cella U. & Garavaglia V. (2011a). Climate warming and the recent treeline shift in the European Alps: the role of geomorphological factors in high–altitudes sites. Ambio, 40, 264–273.

Leonelli G., Pelfini M., D'Arrigo R., Haeberli W. & Cherubini P. (2011b). Non-stationary responses of tree-ring chronologies and glacier mass balance to climate in the European Alps. Arctic, Antarctic, and Alpine Research 43 (1), 56–65.

Losacco U. (1949). La glaciazione quaternaria dell'Appennino Settentrionale. Rivista Geografica Italiana, 56(2), 90-152.

Luckman, B. & Kavanagh T. (2000). Impact of climate fluctuations on mountain environments in the Canadian Rockies. Ambio, 29, 371–380.

MacDonald G. M., Kremenetski K. V. & Beilman D. W. (2008). Climate change and the northern Russian treeline zone. Philosophical Transactions of the Royal Society of London B: Biological Sciences, 363(1501), 2283-2299.

Macias-Fauria M. & Johnson E.A. (2013) - Warming-induced upslope advance of subalpine forest is severely limited by geomorphic processes. PNAS, 110, 8117–8122.

Magaldi D., Bazzoffi P., Bidini D., Frascati F., Gregori E., Lorenzoni P., Miclaus N. & Zanchi C. (1981). Studio interdisciplinare sulla classificazione e la valutazione del territorio: un esempio nel Comune di Pescia (Pistoia). Istituto Sperimentale Studio e Difesa del Suolo, Firenze, Italy. Annali, 12, 31-114.

Malanson G. P., Butler D. R., Fagre D. B., Walsh S. J., Tomback D. F., Daniels L. D., Resler L. M., Smith W. K., Weiss D. J., Peterson D. L., Bunn A. G., Hiemstra C. A., Liptzin D., Bourgeron P. S., Shen Z. & Millar C. I. (2007). Alpine treeline of western North America: linking organism-to-landscape dynamics. Physical Geography, 28(5), 378-396.

Malanson G. P., Resler L. M., Bader M. Y., Holtmeier F. K., Butler D. R., Weiss D. J. & Daniels L. D. (2011). Mountain treelines: A roadmap for research orientation. Arctic, Antarctic and Alpine Research, 43, 167–177.

Maugeri M., Sancrotti M., Smiraglia C., Rosso R., Notarpietro A. & Tagliaferri A. (2008). Climatologia. In Regione Lombardia (Ed.), Progetto Kyoto Lombardia: per vincere la sfida dei cambiamenti climatici e del controllo dei gas serra nella regione più industrializzata d'Italia [Kyoto Project - Lombardy: For winning the challenge of climate change and of the greenhouse gases control in the most industrialized region of Italy] (277 pp.). Milano: Fondazione Lombardia per l'Ambiente.

Mariani G. S. (2015). The role of paleosols in paleoenvironmental studies: genesis and development of Apennine mountain soils during the Holocene. Phd Thesis, University of Milan.

Masseroli A., Leonelli G., Bollati I., Trombino L. & Pelfini M. (2016). The influence of geomorphological processes on the treeline position in Upper Valtellina (Central Italian Alps). Geografia Fisica e Dinamica Quaternaria, 39(2), 171-182.

Mazepa V. S. (2005). Stand density in the last millennium at the upper tree-line ecotone in the Polar Ural Mountains. Canadian Journal of Forest Research, 35, 2082–2091.

McCarthy P.J., Martini I.P. & Leckie D.A. (1998). Use of micromorphology for paleoenvironmental interpretation of complex alluvial paleosols: an example from the Mill Creek Formation (Albian), southwestern Alberta, Canada. Palaeogeography, Palaeoclimatology, Palaeoecology 143, 87-110

McRae S.G. (1991). Pedologia pratica - Come studiare i suoli sul campo, Zanichelli, Bologna.

Menzel A. & Fabian P. (1999). Growing season extended in Europe. Nature 397, 659.

Menzel A., Sparks T.H., Estrella N., Koch E., Aasa A., Ahas R., Alm-Kübler K., Bissolli P., Braslavska O., Briede A., Chmielewski F.M., Crepinsek Z., Curnel Y., Dahl A., Defila C., Donnelly A., Filella Y., Jatczak K., Mage F., Mestre A., Nordli Ø., Penuelas J., Pirinen P., Remisova V., Scheifinger H., Striz M., Susnik A., Van Vliet A.J.H., Wielgolaski F.-E., Zach S. & Zust A. (2006). European phonological response to climate change matches the warming pattern. Global Change Biology 12 (10), 1969–1976.

Mercalli L., Cat Berro D. & Montuschi S. (2003). Atlante climatico della Valle d'Aosta, 416 pp. Turin: Società Meteorologica Subalpina.

Merkli C., Sartori G., Mirabella A., Egli M., Mancabell A. & Plotze M. (2009). The soils in the Brenta region: chemical and mineralogical characteristics and their relation to landscape evolution. Studi Trentini di Scienze Naturali, 85, 7-22.

Milisauskas S. (2002). European prehistory: A survey. New York. NY: Springer.

Ministero per le Politiche Agricole (1999). Approvazione dei "Metodi ufficiali di analisi chimica del suolo", Decreto Ministeriale del 13/09/1999, Gazz. Uff. Suppl. Ordin. n° 248 del 21/10/1999.

Moe D., Fedele F.G., Maude A.E. & Kvamme M. (2007). Vegetational changes and human presence in the low-alpine and subalpine zone in Val Febbraro, upper Valle di Spluga (Italian central Alps), from the Neolithic to the Roman period. Veget Hist Archaeobot, 16, 431-451.

Montrasio A., Berra F., Cariboni M., Ceriani M., Deichman N., Ferliga C., Gregnanin A., Guerra S., Guglielmin M., Jadoul F., Longhin M., Mair V., Mazzoccola D., Sciesia E. & Zappone A. (2012). Foglio 024 Bormio. Carta Geologica d'Italia alla scala 1: 50.000.

Motta R. & Garbarino F. (2003). Stand history and its consequences for the present and future dynamic in two silver fir (Abies alba Mill.) stands in the high Pesio Valley (Piedmont, Italy). Annals of Forest Science, 60(4), 361-370.

Motta R. & Nola P. (2001). Growth trends and dynamics in sub-alpine forest stands in the Varaita Valley (Piedmont, Italy) and their relationships with human activities and global change. Journal of Vegetation Science, 12, 219–230.

Munsell® Color (1994). Munsell Soil Color Charts, Revised edition. Macbeth Division of Kollmorgen Instruments Corporation, New Windsor, NY.

Nagy L. & Grabherr G. (2009). The biology of alpine habitats. Oxford: University of Oxford Press.

Nakhutsrishvili G. (2003). High-mountain vegetation of the Caucasus Region. In L. Nagy, G. Grabherr, C. Körner, & D. B. A. Thompson (Eds.), Alpine biodiversity in Europe (pp. 93–103).Berlin: Springer.

Nicolussi K., Kaufmann M., Patzelt G., Plicht van der J. & Thurner A. (2005). Holocene tree-line variability in the Kauner Valley, Central Eastern Alps, indicated by dendrochronological analysis of living trees and subfossil logs. Vegetation History and Archaeobotany, 14, 221–234.

Nicosia C. (2006). Indicatori micromorfologici di erosione dei suoli nel settore settentrionale delle Valli Grandi Veronesi durante l'età del Ferro. Padusa, 62, 108-112.

Nigrelli G. (2008). Inquadramento climatico della Valtellina e della Val Camonica. Definizione delle soglie pluviometriche d'innesco di frane superficiali e colate torrentizie: accorpamento per aree omogenee. Progetto di Ricerca IReR n 2007B023, Rapporto finale, Milano, 73-80.

Orombelli G. & Porter S.C. (1982), Late Holocene fluctuations of Brenva Glacier. Geografia Fisica e Dinamica Quaternaria, 5, 14-37.

Panizza M., Bettelli G., Bollettinari G., Carton A., Castaldini D., Piacente S., Bernini M., Clerici A., Tellini C., Vittorini S., Canuti P., Moisello U., Tenti G., Dramis F., Gentili B., Pambianchi G., Bidini D., Lulli L., Rodolfi G., Busoni E., Ferrari G., Cremaschi M., Marchesini A., Accorsi C.A., Mazzanti M., Francavilla F., Marchetti G., Vercesi P.L., Di Gregorio F. & Marini A. (Gruppo Ricerca Geomorfologia CNR) (1982), Geomorfologia del territorio di Febbio tra il M.Cusna e il F.Secchia (Appennino Emiliano). Geografia Fisica Dinamica Quaternaria, 5, 285-360.

Paulsen J. & Körner C. (2001). GIS – analysis of tree-line elevation in the Swiss Alps suggests no exposure effect. Journal of Vegetation Science, 12, 817–824.

Pelfini M. (1988). Contributo alla conoscenza delle fluttuazioni oloceniche del Ghiacciaio dei Forni. Natura Bresciana, 24, 237-257.

Pelfini M. & Gobbi M. (2005). Enhancement of the ecological value of Forni Glacier as a possible new geomorphosite: new data from arthropods communities. Geog. Fis. Dinam. Quat., 28, 211 -217.

Pelfini M. & Santilli M. (2006). Dendrogeomorphological analyses on exposed roots along two mountain hiking trails in the Central Italian Alps. Geografiska Annaler, Series A: Physical Geography, 88, 223-236.

Pelfini M. & Santilli M. (2008). Frequency of debris flows and their relation with precipitation: A case study in the Central Alps, Italy. Geomorphology, 101, 721–730.

Pelfini M., Diolaiuti G., Leonelli G., Bozzoni M., Bressan N., Brioschi D. & Riccardi A. (2012). The influence of glacier surface processes on the short-term evolution of supraglacial tree vegetation: The case study of the Miage Glacier, Italian Alps. The Holocene, 22 (8), 847 – 857.

Pelfini M., Leonelli G. & Santilli M. (2006). Climatic and environmental influences on Mountain pine (Pinus Montana Miller) growth in the Central Italian Alps. Arctic, Antarctict, and Alpine Research, 38 (4), 614 – 623.

Pelfini M., Leonelli G., Trombino L., Zerboni A., Bollati I., Merlini A., Smiraglia C. & Diolaiuti G. (2014). New data on glacier fluctuations during the climatic transition at~ 4,000 cal. year BP from a buried log in the Forni Glacier forefield (Italian Alps). Rendiconti Lincei, 25(4), 427-437.

Pellegrini M. (2016). Erosione pseudocalanchiva sul versante sud del monte Fallére (Valle D'aosta) in rapporto alla dinamica dei suoli e della vegetazione arborea. Unpublished master degree thesis, University of Milan.

Persicani D. (1989). Elementi di scienza del suolo, Casa Editrice Ambrosiana, Milano.

Pignatti S. (1979). I piani di vegetazione in Italia. Giornale Botanico Italiano, 113, 411-428.

Pignatti S. (1995). Ecologia vegetale, UTET.

Pini G.A. (1999). Tectonosomes and olistostromes in the Argille Scagliose of the Northern Apennines, Italy. Geol. Soc. of America Special Publ. 335, 73. Pini R., Aceti A., Maggi V., Orombelli G.,

Raiteri L. & Ravazzi C. (2012). Holocene forest history and timberline fluctuations in the Western and Central Alps: the role of climatic factors and men. In: Abstracts of AIQUA Congress "The transition from natural to anthropogenic-dominated environmental change in Italy and the surrounding regions since the Neolithic", February 15-17, 2012, Pisa (Italy).

Plesi G., Daniele G., Chicchi S., Bettelli G., Catanzariti R., Feroni C., De Nardo M.T., Martinelli P., Ottria G. & Panini F. (2002). Note illustrative della Carta Geologica d'Italia alla scala 1: 50.000, Foglio 235 "Pievepelago". Servizio Geologico d'Italia-Regione Emilia Romagna, Roma Pliny the Elder (77–78 AD). Historia mundi naturalis, II.

Polino R., Bonetto F., Carraro F., Gianotti F., Gouffon Y., Malusà M.G., Martin S., Perello P. & Schiavo A. (2015). Note Illustrative della Carta Geologica d'Italia. Foglio 90 "Aosta". Serv. Geol. It., ISPRA, 148 pp.

Porter S. C. & Orombelli G. (1985). Glacier contraction during the middle Holocene in the western Italian Alps: Evidence and implications. Geology, 13, 296–298.

Pozzi R., Bollettinari G. & Clerici A. (1990). Studio geomorfologico e geologico applicato dell'Alta Valtellina. Milano: Quaderni AEM, 151 p.

Qi Z., Liu H., Wu X. & Hao Q. (2015). Climate-driven speedup of alpine treeline forest growth in the Tianshan Mountains, Northwestern China. Global Change Biology, 21, 816–826.

Rabasa S. G., Granda E., Benavides R., Kunstler G., Espelta J. M., Ogaya R. & Valladares F. (2013). Disparity in elevational shifts of European trees in response to recent climate warming. Global Change Biology, 19, 2490–2499.

Redondi A. (2009). La vegetazione attuale al limite degli alberi nel Parco dell'Appennino Tosco-Emiliano e confronti con le evidenze paleobotaniche. Tesi di Laurea Triennale in Scienze Naturali, Università degli Studi di Milano.

Regione Lombardia (2013). Carta pedologica 1:250000 in Basi informative dei suoli. Retrieved from http://www.geoportale. regione.lombardia.it/

Regione Lombardia (2004). Geoiffi, Inventario delle frane e dei dissesti idrogeologici della Regione Lombardia. Retrieved from http://www.cartografia.regione.lombardia.it/rlregisdownload/

Regione Lombardia (2014). DTM 20 – ESRI GRID format. Retrieved from http://www.geoportale. regione.lombardia.it/

Rellini I., Trombino L., Firpo M. & Piccazzo M. (2007). Geomorphological context of "plinthitic paleosols" in the Mediterranean region: examples from the coast of western Liguria (northern Italy).Rev. C. & G., 21 (1-2), 27-40.

Remaury M., Oliva P., Guillet B., Martin F., Toutain F., Dagnac J., Bellet J.M., Dupré B. & Gauquelin T. (2002). Nature and genesis of spodic horizons characterized by inverted color and organic content in a subalpine podzolic soil (Pyrenees Mountains, France). Bulletin de la Société Géologique de France, 173(1), 77-86.

Resler L. M. (2006). Geomorphic Controls of Spatial Pattern and Process at Alpine Treeline∗. The Professional Geographer, 58(2), 124-138.

Resler L. M., Butler D. R. & Malanson G. P. (2005). Topographic shelter and conifer establishment and mortality in an alpine environment, Glacier National Park, Montana. Physical Geography, 26(2), 112-125.

Rhodes E.R. & Sutton P.N. (1978). Active iron ratio of some soils from three physiographic units in Sierra Leone, in "Soil Science", 125(5), pp.326-8.

Ricci Lucchi F. (1986). The Oligocene to Recent foreland basins of the northern Apennines. In: Allen, P.A., Homewood, P. (Eds.), Foreland Basins. Blackwell, Freiburg, 105-140.

Righi D., Huber K. & Keller C. (1999). Clay formation and podzol development from postglacial moraines in Switzerland. Clay Minerals 34, 319–332.

Rossi G. (1989). Déneigement, temperature et répartition de la végétation dans le cirque glaciale du Mont Prado (Apennin septentrional, Italie). Première contribution. Publications de l'Association Internationale de Climatologie, 2, 271-275.

Salzer M. W., Hughes M. K., Bunn A. G. & Kipfmueller K. F. (2009). Recent unprecedented treering growth in bristlecone pine at the highest elevations and possible causes. Proceedings of the National Academy of Sciences, 106, 20348–20353.

Sanesi G. (1977). Guida alla descrizione del suolo. C.N.R. Progetto finalizzato alla Conservazione del suolo.

Sanesi G. (2000). Elementi di pedologia - I suoli, loro proprietà, gestione e relazioni con l'ambiente, Edagricole, Edizioni Agricole Calderini s.r.l., Bologna.

Sauro U., Ferrarese F., Francese R., Miola A., Mozzi P., Rondo G.Q., Trombino L. & Valentini G. (2009). Doline fills- case study of the Faverghera Plateau (Venetian Pre-Alps, Italy). Acta Carsologica, 38 (1), 51-63

Scapozza C., Lambiel C., Reynard E., Fallot J. M., Antognini M. & Schieneich P. (2010). Radiocarbon dating of fossil wood remains buried by the Piancabella rock glacier, Blenio Valley (Ticino, Southern Swiss Alps): implications for rock glacier, treeline and climate history. Permafrost and Periglacial Processes, 21, 90–96.

Schweingruber F. H. (1988). Tree Rings: Basics and Application of Dendrochronology. Dordrecht: Kluwer Academic Publishers, 402 pp.

Schwörer C., Kaltenrieder P., Glur L., Berlinger M., Elbert J., Frei S. & Tinner W. (2014). Holocene climate, fire and vegetation dynamics at the treeline in the Northwestern Swiss Alps. Vegetation History and Archaeobotany, 23, 479–496.

Scotti R., Brardinoni F., Alberti S., Frattini P. & Crosta G.B. (2013). A regional inventory of rock glaciers and protalus ramparts in the central Italian Alps. Geomorphology, 186, 136–149.

Sebag D., Verrecchia E. P., Cécillon L., Adatte T., Albrecht R., Aubert M., Bureau F., Cailleau G., Copard Y., Decaens T., Disnar J. R., Hetényi M., Nyilas T. & Trombino L. (2016). Dynamics of soil organic matter based on new Rock-Eval indices. Geoderma, 284, 185-203.

Senese A., Diolaiuti G., Mihalcea C. & Smiraglia C. (2012). Energy and mass balance of Forni Glacier (Stelvio National Park, Italian Alps) from a four-year meteorological data record. Arctic, antarctic, and alpine research, 44(1), 122-134.

Senese A., Maugeri M., Vuillermoz E., Smiraglia C. & Diolaiuti,G. (2014). Using daily air temperature thresholds to evaluate snow melting occurrence and amount on Alpine glaciers by T-index models: the case study of the Forni Glacier (Italy). The Cryosphere, 8(5), 1921-1933.

Servizio Geologico d'Italia (2002). Carta geologica d'Italia, scala 1:50.000. Foglio 235 "Pievepelago". S.EL.CA., Firenze

Servizio Geologico, Sismico e dei Suoli della Regione Emilia Romagna (2007). Carta geologica dell'Appennino Emiliano-Romagnolo, scala 1:10 000. Sezione 235090: Monte Cusna. Bologna, SGSS.

Shiyatov S. G., Terent'ev M. M. & Fomin V. V. (2005). Spatiotemporal dynamics of forest-tundra communities in the Poral Urals. Russian Journal of Ecology, 36, 69–75.

Smiraglia C., Azzoni R. & Diolaiuti G. (2015). Il nuovo catasto dei ghiacciai italiani. Eds. EvK2CNR.

Soil Survey Staff (1975). Soil taxonomy (a basic system of soils survey). Handbook n. 436. Washington, USDA.

Soil Survey Staff (2014). Keys to Soil Taxonomy. 12th ed. USDA-Natural Resources Conservation Service, Washington, DC.

Sparks T.H. & Menzel A. (2002). Observed changes in the seasons: an overview. International Journal of Climatology 22, 1715–1725.

Stahr K., Jahn R., Hurth A. & Gauer J. (1989). Influence of eolian sedimentation on soil formation in Egypt and Canary Island deserts. Catena, Suppl. 14, 127 – 144.

Stoffel M., Corona C., Ballesteros-Cànovas J.A. & Bodoque J.M. (2013). Dating and quantification of erosion processes based on exposed roots. Earth-Science Reviews 123, 18-34.

Stoops G. (2003). Guidelines for analysis and description of soil and regolith thin sections. Soil Science Society of America, Inc., Madison, Wisconsin, USA.

Stoops G., Marcelino V. & Mees F. (2010). Interpretation of micromorphological features of soils and regoliths. Elsevier.

Stueve K. M., Isaacs R. E., Tyrrell L. E. & Densmore R. V. (2011). Spatial variability of biotic and abiotic tree establishment constraints across a treeline ecotone in the Alaska Range. Ecology, 92, 496–506.

Theurillat J. P., Felber F., Geissler P., Gobat J. M., Fierz M., Fischlin A., Küpfer P., Schlüssel A., Velluti C., Zaho G.F. & Williams J. (1998). Sensitivity of plant and soil ecosystems of the Alps to climate change. Views from the Alps: regional perspectives on climate change, 225-308.

Thomson S.N., Brandon M.T., Reiners P.W., Zattin M., Isaacson P.J. & Balestrieri M.L. (2010). Thermochronologic evidence for orogen-parallel variability in wedge kinematics during extending convergent orogenesis of the northern Apennines, Italy. Geol. Soc. Am. Bull. 122, 1160–1179.

Thornes J. B. (1985). The ecology of erosion. Geography, 70 (3), pp 222-235.

Tinner W. & Theurillat J. (2003). Uppermost limit, extent, and fluctuations of the timberline and treeline ecocline in the Swiss Central Alps during the past 11,500 years. Arctic, Antarctic, and Alpine Research, 35, 158–169.

Tomaselli M. (1994). The vegetation of summit rock faces, talus slopes and grasslands in the northern Apennines (N Italy). Fitosociologia, 26, 35-50.

Tomaselli M. (1997). Guida alla vegetazione dell'Emilia Romagna. Collana Annali Facoltà di Scienze Matematiche Fisiche e Naturali, Università di Parma.

Tomaselli M., Manzini M.L. & Del Prete C. (1994). Vegetation map of the Regional Park of the Modena High Apennines (N Italy). Fisotociologia, 26, 165-169.

Trombino L. (1998). Il suolo come memoria storica dei mutamenti paleoambientali. Genesi e significato paleoclimatici delle "terre rosse" plio-pleistoceniche. Tesi di Dottorato in Scienze Naturalistiche e Ambientali. Dipartimento di Scienze della Terra, Università degli Studi di Milano.

Trombino L. (2007). Micromorphological reconstruction of the archaeological land use and palaeoenvironment of Tell Mishrifeh: Evidence from the sinkhole south of the site. Forum Editrice

Vai G.B. & Martini I.P. (2001). Anatomy of an orogen: the Apennines and adjacent Mediterranean basins. Kluver Academic Publisher, Dordrecht/Boston/London.

Van Breemen N., Mulder J. & Driscoll C.T. (1983). Acidification and alkalinization of soils. Plant and Soil, 75, 283-308

Virtanen R., Luoto M., Rämä T., Mikkola K., Hjort J., Grytnes J. A. & Birks H. J. B. (2010). Recent vegetation changes at the high-latitude tree line ecotone are controlled by geomorphological disturbance, productivity and diversity. Global Ecology and Biogeography, 19(6), 810-821.

Vittoz P., Rulence B., Largey T. & Freléchoux F. (2008). Effects of climate and land-use change on the establishment and growth of Cembran pine (Pinus cembra L.) over the altitudinal treeline ecotone in the Central Swiss Alps. Arctic, Antarctic, and Alpine Research, 40, 225–232.

Walker L. R., Wardle D. A., Bardgett R. D. & Clarkson B. D. (2010). The use of chronosequences in studies of ecological succession and soil development. Journal of Ecology, 98(4), 725-736.

Walkley A. & Black I.A. (1934). An examination of the Degtjareff method for determining soil organic matter, and proposed modification of the chromic acid titration method. Soil Sci, 37(1), 29-38.

Walsh S. J., Butler D. R., Allen T. R. & Malanson G. P. (1994). Influence of snow patterns and snow avalanches on the alpine treeline ecotone. Journal of Vegetation Science, 5(5), 657-672.

Walther G.R., Post E., Convey P., Menzel A., Parmesan C., Beebee T.J.C., Fromentin O., Hoegh-Guldberg J.-M. & Bairlein F. (2002). Ecological responses to recent climate change. Nature 416, 389–395.

Wang W., Körner C., Zhang Z., Wu R., Geng Y., Shi W. & Ou X. (2013). No slope exposure effect on alpine treeline position in the Three Parallel Rivers Region, SW China. Alpine Botany, 123, 87–95.

Waroszewski J., Kalinski K., Malkiewicz M., Mazurek R., Kozlowski G. & Kabala C. (2013). Pleistocene–Holocene cover-beds on granite regolith as parent material for Podzols—an example from the Sudeten Mountains. Catena, 104, 161-173.

Wick L. & Tinner W. (1997). Vegetation changes and timberline fluctuations in the Central Alps as an indicators of Holocene climatic oscillations. Arctic and Alpine Research, 29, 445–458.

Wigley T.M.L., Briffa K.R. & Jones P.D. (1984). On the average value of correlated time series, with applications in dendroclimatology and hydrometeorology. Journal of Climate and Applied Meteorology 23, 201–213.

Wipf S., Stockli V., Herz K. & Rixen C. (2013). The oldest monitoring site of the Alps revisited: Accelerated increase in plant species richness on Piz Linard summit since 1835. Plant Ecology & Diversity, 6, 447–455.

Zald H. S., Spies T. A., Huso M. & Gatziolis D. (2012). Climatic, landform, microtopographic, and overstory canopy controls of tree invasion in a subalpine meadow landscape, Oregon Cascades, USA. Landscape ecology, 27(8), 1197-1212.

Acknowledgments

At the end of this intense journey, I would like to thank those people who supported me in this adventure.

First, I would like to thank my supervisor Prof. Luca Trombino, for his expertise and attention. I am also grateful to him for his teachings and for all the opportunities he gave to me.

My appreciation goes to Prof. Manuela Pelfini for her personal support and for all her good advice.

Special thanks go to Dr. Giovanni Leonelli and Dr. Irene Bollati, who, besides being irreplaceable guides throughout my academic career, showed me the passion for the research and the desire to discover new things.

I gratefully acknowledge Prof. Eric Verrecchia for the helpful and kind hospitality at the University of Lausanne, and for the opportunity he gave me to experiment new analyses in their laboratory.

Thanks to Dr. Chiara Compostella and Dr. Elena Ferrari for their precious help in the soil analyses.

Thanks also to Prof. Fulvia Tambone and Dr. Roberto Comolli, that hosted me in their laboratory.

A great thank to my colleagues Andrea, Chiara, Cinzia, Claudia, Cristina, Francesca, Francesco, Gaia, Giulia, Guido, Marco, Roberto, Silvia, Stefano for the time we spent together.

I am very grateful to all the people that I met in Lausanne for their warm welcome.

Special thanks go to the master students Marco, Sara, Emanuele and Enrico who proved to be a precious help.

To my precious friends a sincere thank.

I heartily thank my mum and dad and my sister for their support, their presence and good advice.

And lastly, I do thank Mattia for his patience and his continuous loving support.